Modeling and Behavior of the Beam/Column Joint Region of Steel Moment Resisting Frames

by:

William M. Downs

Thesis submitted to the Faculty of the
Virginia Polytechnic Institute and State University
In partial fulfillment of the requirements for the degree of

Master of Science
in
Civil Engineering

Approvals

Finley A. Charney — Committee Chairman

Thomas M. Murray — Committee Member

Raymond H. Plaut — Committee Member

December 6, 2002
Blacksburg Virginia

Keywords: steel moment resisting frame (SMRF), panel zone, computer modeling

Modeling and Behavior of the Beam/Column Joint Region of Steel Moment Resisting Frames

William M. Downs

(Abstract)

The effect of panel zone (PZ) flexibility and yielding on the stiffness and strength of steel moment resisting frames (SMRF) has been the topic of numerous papers over the past thirty years. When properly detailed, the PZ is an excellent source of energy dissipation, even under large inelastic deformations. Due to these large inelastic deformations, the PZ region may also be a weak link in steel moment frame behavior. Because of the importance of PZ deformation in the behavior of steel frames, accurate modeling of this region is critical. Two of the most commonly used mathematical models for representing PZ behavior are investigated. They are referred to herein as the Krawinkler model and the Scissors model. From the literature review conducted at the beginning of this study, it was determined that there were no PZ models available that accounted for the elastic drift associated with PZ flexure which could be used in computer representations using commercial software that is currently available. This thesis details the analytical work used to establish the estimated elastic drift associated with PZ flexure and a method to include this estimated drift and the contribution of continuity plates in the Krawinkler and Scissors models.

This study is initially focused on elastic deformations of individual structural subassemblages. First, formulas are derived to account for each major elastic component of drift in an individual subassemblage. The results from these derivations were implemented into a computer program named PANELS to allow for rapid calculation of the estimated drifts. Then, the properties (elastic and inelastic) for the Krawinkler and Scissors models are derived in their entirety. The Krawinkler model's results are compared to the results from PANELS, neglecting the PZ flexural component in PANELS and any inelastic contributions in the Krawinkler model. Since the Krawinkler

model does not include PZ flexure, this established that the derived formulas accounted for all the remaining sources of elastic strain energy, assuming that the Krawinkler model is accurate. The results from PANELS are compared to those from finite element models developed using ABAQUS. Using the ABAQUS results, a method for determining the elastic drift associated with PZ flexure in PANELS is presented.

A detailed inelastic study of the Krawinkler and Scissors models is then conducted both on the subassemblage level and on full structural frames to determine any differences associated with them. First, the two models are compared to each other on a subassemblage level to ensure that they both give the same results. Then, both PZ models are included in multiple full structural frames using various design configurations and loading conditions to ascertain their differences. Initially it was believed that there would be a large disparity between the two models. This study shows that there is actually little difference between the two models, although the kinematics of the Scissors model is still questionable.

Elastic and inelastic comparisons between the PANELS formulas (elastic) and the ABAQUS models (elastic and inelastic) and data collected from tests performed at Lehigh University by Dr. James Ricles are then presented. This was done to show that the ABAQUS models and the PANELS formulas (including the PZ flexural component) give an accurate estimation of the drift of a subassemblage. The results from these comparisons show that the modeling techniques used are accurate and not including PZ flexural component of drift will cause the overall drift estimate to be unconservative. Finally, a method of including the elastic component of drift attributed to PZ flexure and continuity plates in both models is presented. The Ricles' Lehigh test data is again used in an inelastic comparison between the original Krawinkler and Scissors models and their updated counterparts. These comparisons show that including this component enables both the Krawinkler and Scissors models to more accurately estimate the total drift of an individual subassemblage.

Acknowledgements

The author would like to thank the following people for their contribution and support in the work required for this thesis.

- **Pam Downs-** For the last six years, my wife has been first in my life and due to her patience, love and support she demonstrated during my two years here at Virginia Tech she deserves to be the first person in these acknowledgements. I will not say that I could not have done this without her, but having her made the process of writing this thesis far easier. My experiences in and outside of Virginia Tech have been immensely more pleasurable than they would have been without her.

- **Dr. Finley Charney-** Not only are all the ideas presented in this document based on his guidance and previous research, Dr. Charney's experience in structural behavior and analysis was crucial to the completion of this thesis. Thank you for your time and the patience you demonstrated over the past year and a half while serving as my advisor. I consider myself very fortunate to have had this opportunity to work with you.

- **Faculty of Virginia Tech-** The instructors here provided an excellent learning environment. Their in-depth knowledge of the subjects they presented allowed me to develop a solid foundation in both structural design and analysis. I was continuously amazed at the amount of time outside of the classroom which the instructors here were willing to provide. I firmly believe that there is no other top tier university in the country where the faculty is willing to provide this additional support to their students. Finally, a special thanks goes out to both Dr. Plaut and Dr. Murray for taking the time out of their busy schedules to serve on my thesis committee.

- **CEE Department-** Without the initial financial assistance provided to me by the CEE department, obtaining my degree would not have been possible. Being provided with an employment opportunity as well as not having to pay out-of-

state tuition alleviated the financial stresses associated with moving across the country to attend this institution. I am indebted to the CEE department for this.

- **Family-** I would like to thank my Father (Bill Downs), my Mother (Mary Downs) and my brother (Matt Downs) for the love and encouragement they have given me thoughout the years. Even during a long immature period of my life when the possibility of seeing me attending college was only a fleeting hope, they were still there providing me unconditional support in all my endeavors. The "never give up" attitude my parents instilled in me throughout my youth enabled me to stay the course and complete this long journey. Finally, I want to give a big thank you to my grandmother (Betty Whipkey). She is the person who gave me the money to purchase the computer on which all of the analysis and word processing for this entire project was performed. Without a computer, none of this work presented could have been accomplished.

Table of Contents

List of Tables

List of Figures

1 Introduction

1.1 History of the Panel Zone Phenomenon

The behavior of the panel zone (PZ) region of steel moment resisting frames (SMRF) has been the subject of various tests, both experimental and analytical, in order to obtain an in-depth understanding of the complex interaction between column and girder components. A typical interior beam/column joint is shown with the common PZ components detailed in Figure 1.1-1. Throughout this document the term *joint* and/or *beam/column joint* refers to the entire assembly at the intersection of the beam and column. *Doubler plates* are steel plates placed parallel to the column web between the column flanges and held in place by fillet welds, full penetration welds and/or plug welds along the column flanges and column web. *Continuity plates* (also known as *stiffeners*) are steel plates placed horizontally across the column web and in line with the girder flanges. They are held in place with fillet welds or full penetration welds at the inside faces of the column flanges and along the column web. The *panel zone* (*PZ*) is the part of the column web forming the joint including the doubler plate if present (Popov 1988).

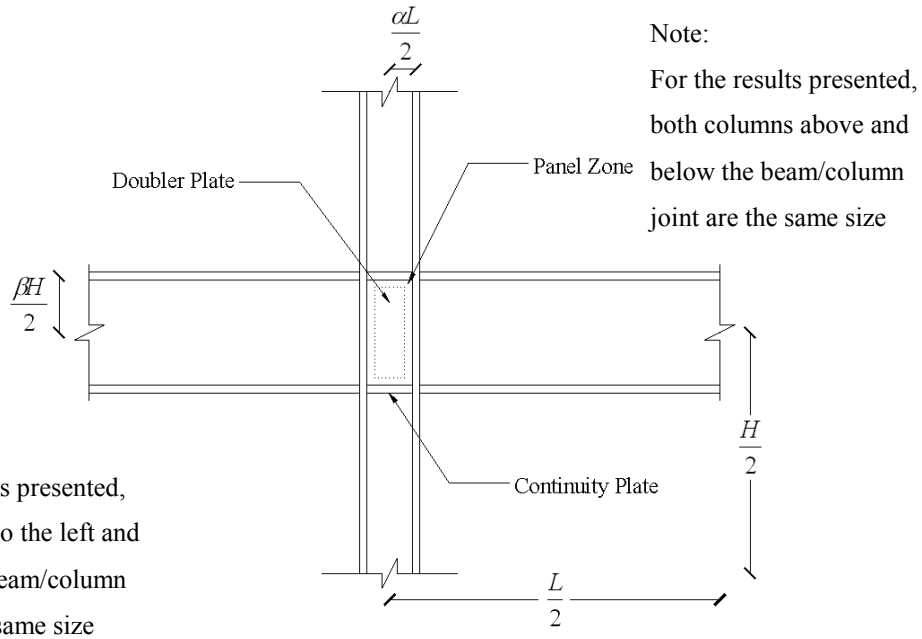

Figure 1.1-1: Typical Beam/Column Joint Components

In the 1970's, the intent of the experimental tests was to demonstrate not only the strength of the system but to determine its ductility. In these early experiments (Fielding and Huang 1971; Betero et al. 1972; Krawinkler et al. 1975; Becker 1975), testing revealed that the PZ of a beam/column joint has a very stable hysteretic behavior when subjected to large deformations, and the overall behavior and the failure mechanism was very dependent on the section properties of the joint. The beam/column joint has high reserve strength well beyond first yield, and the decrease in stiffness after first yield is small and gradual. The experimental research of the 1980's focused on gaining a thorough understanding of the mechanics involved in the distribution of forces in the PZ region and on expanding the previous decade's research into studying the behavior of larger beam/column joints (Popov et al. 1985, Popov and Tsai 1989). From the mid-1990's to date, the SAC steel project has focused on SMRF research, devoting a tremendous amount of time and resources to studying the PZ phenomena. The SAC experimental research associated with it is discussed in detail in Chapter 6.

In the early experiments, the effects of doubler plates and continuity plates were also examined to determine their contribution to the strength and stiffness in the PZ region and to investigate the stress distributions associated with these additional components. The continuity plates were shown to perform quite favorably even when stressed well beyond their elastic limits. Tests revealed that, when properly detailed, they do an excellent job transferring additional forces from the girder flanges into the column web (Fielding and Huang 1971). Doubler plates were deemed very effective at increasing the shear capacity of the PZ region. This increased shear capacity was shown to correlate directly to a decrease in the overall drift in the structure. However, there was little relationship between the stress distribution in the doubler plate and the column web before the column web experienced a considerable level of yielding. The percentage of stress that the doubler plate was subjected to, as compared to the column web, was much less. This was attributed to the complex force interaction between the welds and the doubler plate and there not being any continuous interface to efficiently transfer forces between the two plates. This disparity in stresses continued until the column web was

stressed at three to four times its yield capacity. At that point, the strain in the plate and the web could be equated via their relative areas. One interesting point of note is that once the PZ yielded all of the axial force, which was applied during testing, was transferred to the flanges of the column. This implies that at an ultimate strength level, the shear strength of the PZ is independent of the applied axial load (Krawinkler et al. 1975).

With the discovery of the PZ phenomena, the design codes have switched back and forth on various ways to handle it. One method was to attempt to alleviate any yielding in the PZ region altogether by detailing it with very thick doubler plates and stiffeners to ensure that all of the yielding occurred in the girders following the strong column/weak beam approach (strong panel zone). Another method was to allow all of the yielding to occur in the PZ region (weak panel zone). The third option was to balance the plastic rotation between the two, utilizing the deformations in the PZ as well as developing plastic hinges in the girders (balanced panel zone). The most conservative approach of limiting the plastic rotation of the PZ using doubler plates and stiffeners was the design procedure initially adopted. This method was a very expensive way to eliminate the PZ variable from the design, making it economically advantageous for designers to eliminate these additional members by reducing the number of seismic resisting frames through the use of larger beam and column sections.

The moment resisting frames of the 1960's and 1970's were designed as multiple bay systems, allowing the designers to use smaller columns. As the importance of proper weld detailing became apparent, inspections of all SMRF joints in a structural system were required. With the increase in the cost of labor, it became more cost effective to minimize the number of joints to be inspected by reducing the number of seismic resisting bays and increasing the column and beam sizes of the remaining moment resisting bays. Unfortunately, the experimental data on which the design equations were based was collected on the smaller beam/column subassemblages (Whittaker et al. 1998).

Experiments (Popov et al. 1985, Popov 1987, Popov 1988, Popov and Tsai 1989) were performed to examine the advantages and disadvantages of different approaches

used to detail the beam/column joint, i.e., strong, balanced and weak panel zones. Various beam/column assemblies were detailed which include and exclude doubler plates and stiffeners of different sizes in order to evaluate the differences in behavior created by these additional members. From these results, it was shown that the plastic hinge rotation in the beam/column joint of members with thin webs designed without doubler plates was comprised of only plastic rotation in the PZ region, with high stress concentrations at the girder flange/column flange interface causing plastic hinges to form in the column flanges (Figure 1.1-2). The decreased overall thickness due to the omission of a doubler plate significantly reduced the strength above nominal capacity when compared to the other test configuration. Even though the PZ had been shown to be very ductile, limiting all of the rotation to the PZ region reduces the overall ductility of the sub-assemblage when compared to a design allowing for rotation in both the PZ and girder. This loss in ductility was attributed to brittle failures of the welds at the interface of the girder and column in the joint. The failures were caused by high stresses in the PZ at the girder flange/column flange interface.

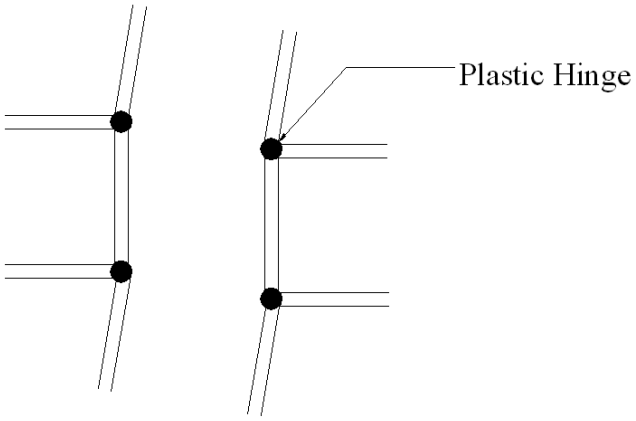

Figure 1.1-2: Column Flange Plastic Hinging

The occurrence of these plastic hinges in the column flanges can have an adverse effect on the response of a SMRF. Considering static plastic analysis, the occurrence of these plastic hinges in the column flanges results in a significant loss of the strength and stiffness at this region of the column, forming a local collapse mechanism. As more collapse mechanisms develop in the columns of the structure, the frame's stability

becomes a concern. Once plastic hinges have developed at each end of each column on the same story level, a story mechanism has formed in the frame and its structural integrity has been compromised. This is the reasoning behind the concept of strong column/weak beam design. By allowing for the plastic hinging to be concentrated in the girders and PZ of the SMRF, the possibility of a story mechanism developing is greatly reduced.

Even with a significantly over-designed PZ region, none of the test specimens were capable of limiting all of the plastic hinge formation to the girders. Nevertheless, these tests showed that there is a very delicate balance between the size of the doubler plate and the ability to develop plastic hinges in the girders. A small increase in the thickness of the doubler plate made a large difference in the amount of plastic deformation that the panel zones experienced. The benefit of a reduction in PZ deformation is twofold. First, it lessens the possibility of the development of a story mechanism and second, the overall story drift is much less. This implies that for seismic design, the more significant portion of the frame ductility should be developed in the girders, with the rest being contributed by the PZ region.

Currently, the most commonly used method in design practice to model a SMRF is to generate the model as line elements, treating the PZ as an infinitely rigid point (IRP). By using this representation, the designer is assuming that there are no relative changes in the angle of rotation between the beam and column centerlines. This assumption will cause the model to overestimate the flexural deformations and underestimate the shear deformations within the PZ region. Although these potential sources of error can cancel each other out, it is felt that a better approach is to use a more accurate representation of the PZ region. Another shortcoming of the IRP model is that there is no way to include yielding within the beam/column joint region. It is the author's belief that the rationales behind ignoring the limitations of the IRP model are that the current PZ models presented in the literature are either too complicated for daily design office analysis or have not been adequately explained. There is also a general lack of understanding of how PZ

deformations affect the overall structural behavior and how to adapt these PZ models for use in computer simulations (Charney 1990).

1.2 Project Scope

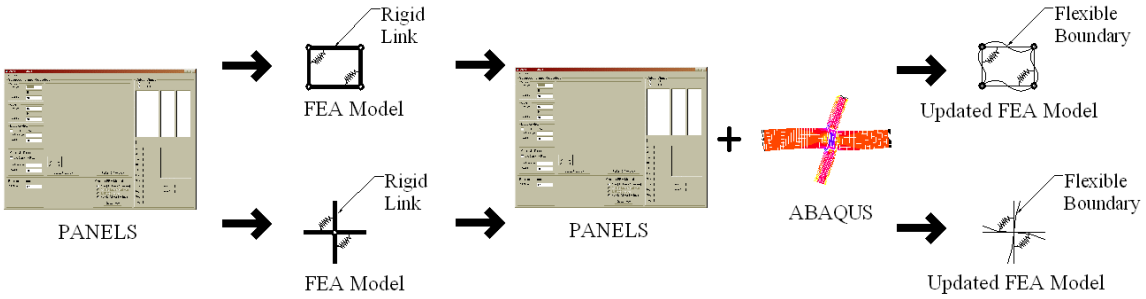

Figure 1.2-1: Research Flow Chart

In an attempt to address these concerns, the following research was conducted and is pictorially illustrated by the flow chart shown in Figure 1.2-1. First, properties for elastic subassemblage models were developed using the principle of virtual work (Chapter 2). This was done to estimate the elastic response of a beam/column subassembly and to quantify the individual components of drift to determine the PZ's contribution to the overall subassemblage's drift. A computer program, named PANELS, was developed to calculate these results using the derived equations. The strength and stiffness properties for two inelastic subassemblage models, referred to herein as Krawinkler and Scissors, were then derived (Chapter 3). These models were developed to be included in structural analysis software to explicitly model the PZ region of the beam/column joint. Adjusting its strength properties to ensure that no yielding would occur, a series of elastic analyses was conducted to compare the overall drift of the Krawinkler model to PANELS results (Chapter 4). This ensured that the total drift determined using the PANELS formulas and the drift from a Krawinkler subassemblage modeled in Drain-2DX (Prakash et al. 1993) were identical. Since the Krawinkler model does not include PZ flexure and PANELS does not include column flange hinging, these drift components were not included in this comparison. Another elastic drift comparison was performed using subassemblages modeled using ABAQUS (Hibbitt et al. 2001).

This was performed to quantify the drift solely due to PZ flexure and to determine how to properly account for this drift component in PANELS. Once the elastic model contrasts were completed and deemed accurate, inelastic static pushover analyses were performed comparing the Krawinkler and Scissors models using both subassemblies and full structural frames. The intent of these analyses was to demonstrate the behavioral similarities and differences between the two models (Chapter 5) and to determine which model to make adjustments to for inclusion of panel zone flexure. Next, the PANELS formulas, the Krawinkler model and the ABAQUS model were compared to test data from the SAC project to ensure that the models' results are reasonable (Chapter 6). With PANELS, this was an elastic evaluation. For the Krawinkler and ABAQUS models, it was inelastic. Finally, updates to the Krawinkler and Scissors model are proposed (Chapter 7) that will account for the PZ flexure component of drift currently not included in either model. The purpose of this thesis is not to recreate the work done by previous authors on this subject, but to examine the accuracy and limitations of two current models (Krawinkler and Scissors) used by the design community and propose a new model that includes flexure in the panel zone region.

1.3 Modeling Assumptions and Nomenclature

Using the portal method of analysis, a 2-D steel moment resisting frame (SMRF), can be modeled as a series of individual subassemblages, with each subassemblage providing its own contribution to the overall drift of a structure. Following this method's assumptions, the subassemblages are given a pin-pin support condition, implying that there is zero moment at the midspans of the girders and mid-height of the columns in the real structure. While the shear in the column above and below a particular floor level is typically different, the analyses described herein use the same shear in the column both above and below, with this value being the average of the true shears in the columns. Since the same amount of total force is being applied to the same elastic structural system, there is an equivalent total of strain energy which suggests that this deviation should not cause an error in the derivations presented.

In this research, the four possible subassemblage configurations (Figure 1.3-1) are referred to as:

1. Cruciform sections- in the interior of the structure
2. Corner sections- at the top right and top left of the model
3. End section- make up the left or right sides of the model.
4. Tee section- the remaining assemblies on the top floor of the structure

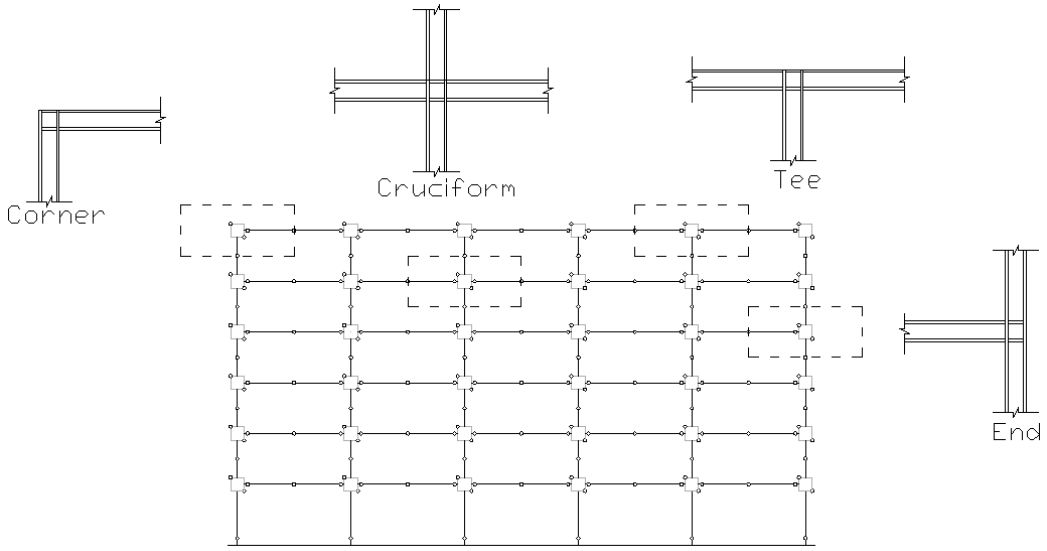

Figure 1.3-1: Structural Subassemblies

For the formulas and relationships which will be developed, d_c is the depth of the column, t_{cf} is the thickness of the column flange, b_{cf} is the width of the column flange, d_b is the depth of the girder, t_p represents the total thickness of the PZ, including the doubler plate, if present, E, G, and F_y are Young's modulus, the shear modulus and yield strength of the steel, respectively. It should also be noted that the analytical results presented are based on models developed using the following definitions for the effective depth of the design sections. This was done to be consistent with the assumption made in Chapters 2 and 3 that the forces which are present within these sections act through the centers of the flanges.

$$d_c = d_{c,nom} - t_{cf} \quad \text{.....(1.3-1)}$$

$$d_b = d_{b,nom} - t_{bf} \quad \text{.....(1.3-2)}$$

where

$d_{c,nom}$ and $d_{b,nom}$ are the tabulated depth values in the current AISC-LRFD manual (2001).

Throughout this document, one-half of the effective depth of the column (d_c) will be equivalent to ½ αL and ½ the effective depth of the girder (d_b) to ½ βH where ½ L is the distance from the center of the PZ to the end of the girder and ½ H is the distance from the center of the PZ to the end of the column (Figure 1.1-1). This was done to develop the following mathematical relationships:

$$\alpha = \frac{d_c/2}{L/2} = \frac{d_c}{L} \quad \text{.....(1.3-3)}$$

$$\beta = \frac{d_b/2}{H/2} = \frac{d_b}{H} \quad \text{.....(1.3-4)}$$

which would relate the dimensions of the PZ to the overall dimensions of the individual subassemblage. The significance of these relationships is shown in Chapter 3 where the use of α and β significantly simplify the expressions that are derived.

The overall drift of the Corner, Cruciform, End and Tee subassemblages are defined in Figure 1.3-2. This definition of drift is used throughout this document for all the analytical model development and comparisons with the exception of the comparison with the SAC test data. Due to the boundary conditions used in these experiments, this definition is redefined. These changes are addressed in Chapter 6 when comparisons with this data are made.

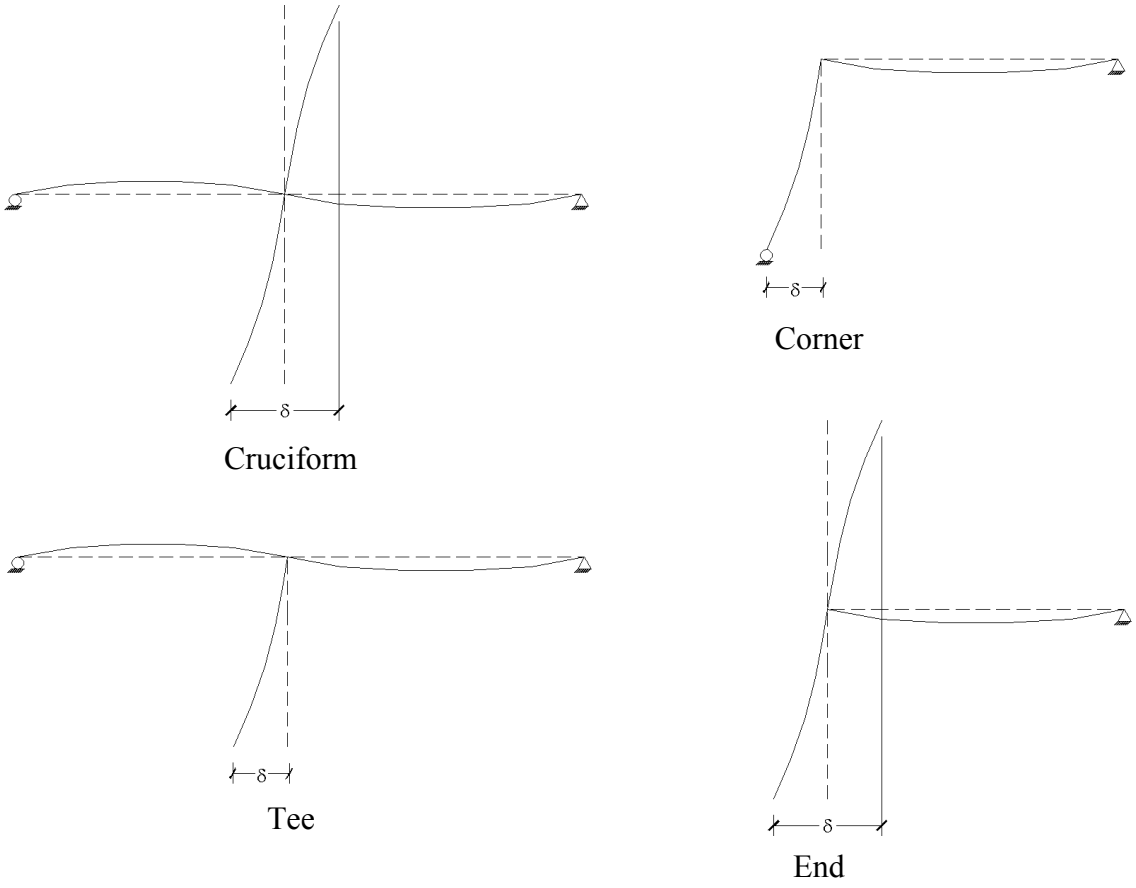

Figure 1.3-2: Subassemblage Deflection Diagrams

2 Development of Elastic Subassemblage Models (PANELS Approach)

2.1 Introduction and Scope

In order to derive the mathematical relationships for computing the contribution of Panel Zone (PZ) deformation to overall structural displacement, the structure will be subdivided into an assemblage of statically determinate subassemblages. These subassemblages facilitate a better understanding of the PZ behavior, and simplify the development of the PZ model. This is particularly important when determining the effects of doubler plates and continuity plates when they are included in the beam/column joint region. These additional components add even more uncertainties to the one area of the subassemblage that is already highly indeterminate.

Following the principle of virtual work, the displacement of a structure at the point of application and in the direction of a virtual unit force is the sum of the individual strain energy contributions from beam/column flexure, beam/column shear, beam/column axial forces, and shear and flexure in the PZ region of the individual subassemblies. This displacement is determined by equating the external work (WE) to the internal work (WI) of each element. Assuming that these systems are statically loaded, linear elastic and conservative, WE and WI are given by

$$WE = 1 * \delta \quad \text{.....(2.1-1)}$$

$$WI = \sum_{i=1}^{nsub} \sum_{j=1}^{nelem} \sum_{k=1}^{source} \int_{V} \sigma \varepsilon \, dV \quad \text{.....(2.1-2)}$$

where

δ is the real displacement in the direction of the virtual force

nsub is the number of subassemblies in the structure

nelem is the number of elements in a subassemblage (e.g., beam, column, PZ)

source is the number of individual strain energy sources in the element

σ is the virtual stress

ε is the resulting real strain

V is the volume over which the strain energy source is applicable

These equations are valid for 2D frame analysis in which both the real and virtual forces can be determined. For the purpose of the analyses contained herein, the determination of these forces is facilitated by the analysis of the statically determinate subassemblages.

Looking at Equation 2.1-2, the reader can observe that any strain energy source which is not included in the summation will cause the overall true drift of the subassemblage to be underestimated. However, as more sources of energy are included in the summation, the drift will approach its upper bound solution assuming that one has accurately represented all the forces within the region.

Setting the Equation 2.1-1 equal to Equation 2.1-2, the following formulas for displacement due to the individual strain energy sources can be derived:

$$\delta_{Flex} = \int_0^L \frac{M_R M_V}{EI} dx \quad \text{.....(2.1-3)}$$

$$\delta_{Shear} = \int_0^L \frac{V_R V_V}{A^* G} dx \quad \text{.....(2.1-4)}$$

$$\delta_{Axial} = \int_0^L \frac{F_R F_V}{EA} dx \quad \text{.....(2.1-5)}$$

where

M_R = Moment due to the applied real force

M_V = Moment due to an applied virtual force

E = Young's Modulus (29000 ksi)

I = Moment of inertia about the bending axis

V_R = Shear force due to the applied real force

V_V = Shear force due to the applied virtual force

A^* = Effective Shear area $(d - t_f)t_w$ .....(2.1-6)

G = Shear Modulus $\dfrac{E}{2(1+v)}$ .....(2.1-7)

where v = 0.3 for all analysis herein

F_R = The applied real axial force

F_V = The applied virtual axial force

A = Section area

L = The length of the element over which the strain energy source is considered, and is component dependent. A specific definition is given when each formula is derived.

These three relationships will be used to develop the mathematical models utilized herein to quantify the elastic displacements of the individual subassemblages. To allow for rapid calculation of these interstory drift values, a computer program was also developed. The term PANELS is a reference to this computer program. Originally developed by Dr. Finley Charney, it was enhanced for use in this research to include all four subassemblage models that will be derived using Equations 2.1-3 through 2.1-5. A complete explanation of the capabilities of PANELS is provided in Appendix A.

2.2 Literature Review

Practically all the work found related to elastic modeling of PZ deformation was performed by Dr. Finley Charney and his colleagues. The method employed in this research uses a work-based approach (Charney and Johnson 1986; Horvilleur and Charney 1993). The sources of deformation in the analysis of the cruciform subassemblages were:

- Beam Flexure
- Beam Shear Force
- Column Flexure
- Column Shear Force
- PZ Flexure due to Beam Forces
- PZ Flexure due to Column Forces
- PZ Shear Force

These individual components are then combined using Equation 2.1-2 to estimate the overall drift of the subassemblage illustrated in Figure 1.3-2. While the beam and column drift components are systematically included in finite element analysis computer programs, the PZ components are dependent on the dimensions of the PZ region and are not accounted for without explicitly modifying the PZ region to account for their contribution to the overall subassemblage's deflection.

All the subsequent derivations for the Cruciform subassemblages are a repeat of those found within the Charney-Johnson and Horvilleur-Charney papers. The formulas presented for the Corner, End and Tee models were not found in the literature search. Due to the symmetry of the resulting forces in the Cruciform model, no axial forces are present in the column or girder components of the subassemblages. This is not true for the Corner, End and Tee subassemblage models. To account for the additional elastic strain energy which will occur in the finite element models of these three

subassemblages, the axial component of drift must be included. This results in the last two sources of drift which will be considered in this thesis:

- Beam Axial Force
- Column Axial Force

2.3 Model Derivation Using Virtual Work

One method of treating the beam/column subassembly is to ignore the presence of the PZ region by treating it as a point. While there will be no strain energy associated with this point, there will be axial, flexural and shear strain energy associated with the portion of the column located within the beam/column joint region. Following the assumptions of this model, the length used in Equations 2.1-3 through 2.1-5 is either ½ the height (H) of the column or ½ the span (L) of the girder, respectively. Using these values for the upper limits of integration, the shear and bending moment diagrams in Figure 2.3-1 and Figure 2.3-2, and doubling the results to account for dividing the integration limits in half, the following mathematical relationships (Equations 2.3-1 through 2.3-4) are derived. They will be referred to as Centerline models. In both figures, the bold lines located at the intersection of the column and girder represent the height (βH) and the width (αL) of the PZ boundary and are shown in this manner to enhance the clarity of the figures.

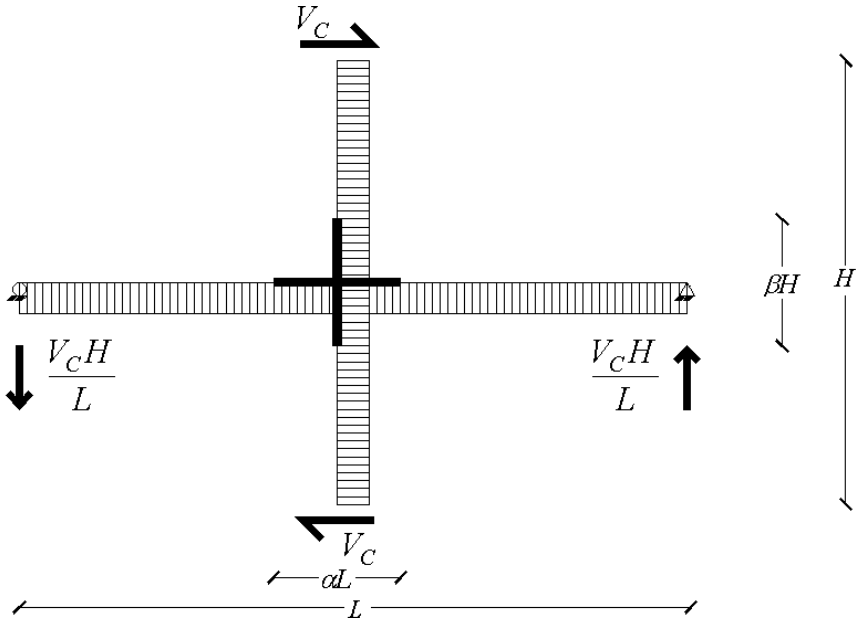

Figure 2.3-1: Cruciform Shear Diagram

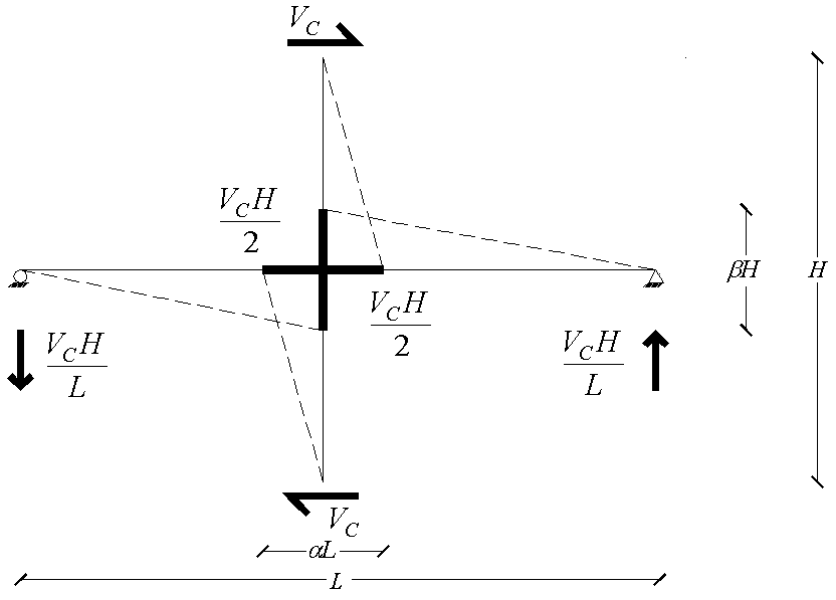

Figure 2.3-2: Cruciform Moment Diagram

$$\hat{\delta}_{C,F} = \frac{VH^3}{12EI_C} \quad \text{.....(2.3-1)}$$

$$\hat{\delta}_{G,F} = \frac{VH^2L}{12EI_G} \quad \text{.....(2.3-2)}$$

$$\hat{\delta}_{C,V} = \frac{VH}{A_C^* G} \quad \text{.....(2.3-3)}$$

$$\hat{\delta}_{G,V} = \frac{VH^2}{A_G^* GL} \quad \text{.....(2.3-4)}$$

where

$\hat{\delta}_{C,F}$ = the component of drift due to column flexure

$\hat{\delta}_{G,F}$ = the component of drift due to girder flexure

$\hat{\delta}_{C,V}$ = the component of drift due to column shear

$\hat{\delta}_{G,V}$ = the component of drift due to girder shear

Another method of treating the beam/column joint is to assume that the PZ region is completely rigid. Looking again at Figure 2.3-1 and Figure 2.3-2, it is observed that this will alter the limits of integration from $\frac{1}{2} H$ and $\frac{1}{2} L$, used in the Centerline models, to the clear-span dimensions of $\frac{1}{2} H(1-\beta)$ and $\frac{1}{2} L(1-\alpha)$. Using these new upper limits and again doubling the results will give the "Rigid" models the following mathematical relationships:

$$\delta_{C,F} = \frac{VH^3}{12EI_C}(1-\beta)^3 \quad \text{.....(2.3-5)}$$

$$\delta_{G,F} = \frac{VH^2L}{12EI_G}(1-\alpha)^3 \quad \text{.....(2.3-6)}$$

$$\delta_{C,V} = \frac{VH}{A_{V,C}^{*} G}(1-\beta) \quad \text{.....(2.3-7)}$$

$$\delta_{G,V} = \frac{VH^{2}}{A_{V,G}^{*} GL}(1-\alpha) \quad \text{.....(2.3-8)}$$

A third treatment of the beam/column joint is a continuation of the Rigid models approach. But, instead of ignoring the strain energy sources within the beam/column joint region, these "Flexible" models include the PZ effects by determining the resultant shear forces and moments at the PZ interface and using virtual work to develop their contribution to the subassembly's displacement. To compute the shear force in the panel, the force transferred from the girder flanges ($F_{Flange,G}$) into the PZ region needs to be determined. Using Figure 2.3-3 and summing the moments at the interface of the girder flange and the column web, the moment in the girder (M_{Girder}) at the face of the column is equal to

$$M_{Girder} = \frac{V_C H}{L}\frac{L-\alpha L}{2} = \frac{V_C H(1-\alpha)}{2} \quad \text{.....(2.3-9)}$$

This moment can be converted into an equivalent force couple over the depth of the girder. The force ($F_{Flange,G}$) can then be determined:

$$F_{Flange,G} = \frac{M_{Girder}}{\beta H} = \frac{V_C H(1-\alpha)}{2}\frac{1}{\beta H} = \frac{V_C(1-\alpha)}{2\beta} \quad \text{.....(2.3-10)}$$

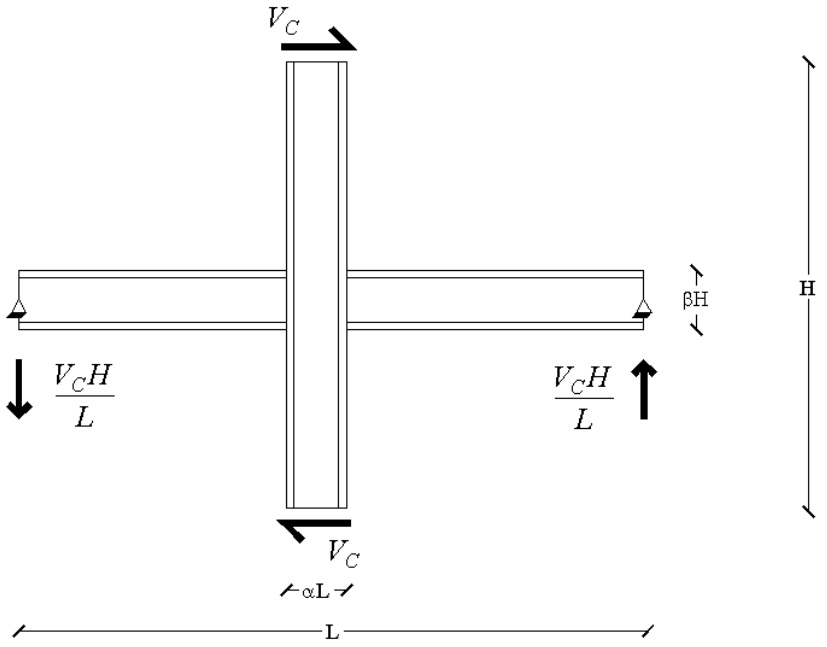

Figure 2.3-3: Cruciform Subassembly

This force, $F_{Flange,G}$, is only an approximation since the actual stress is linearly distributed through the depth of the girder as shown in Figure 2.3-4.

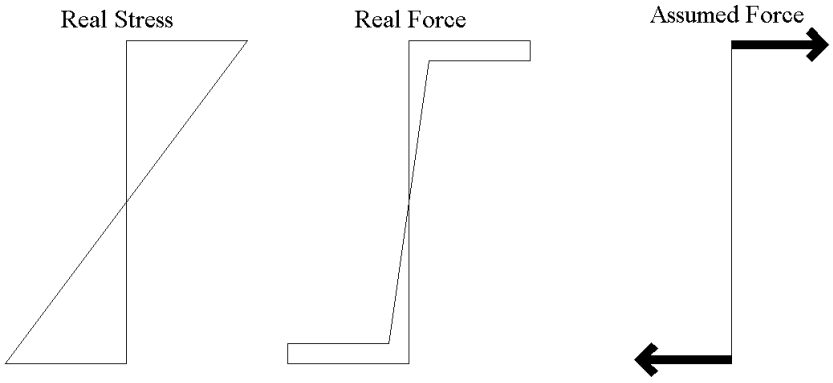

Figure 2.3-4: Girder Flange Force Assumption

Knowing $F_{Flange,G}$, the shear force in the panel (V_{Panel}) is then calculated by summing the forces in Figure 2.3-5.

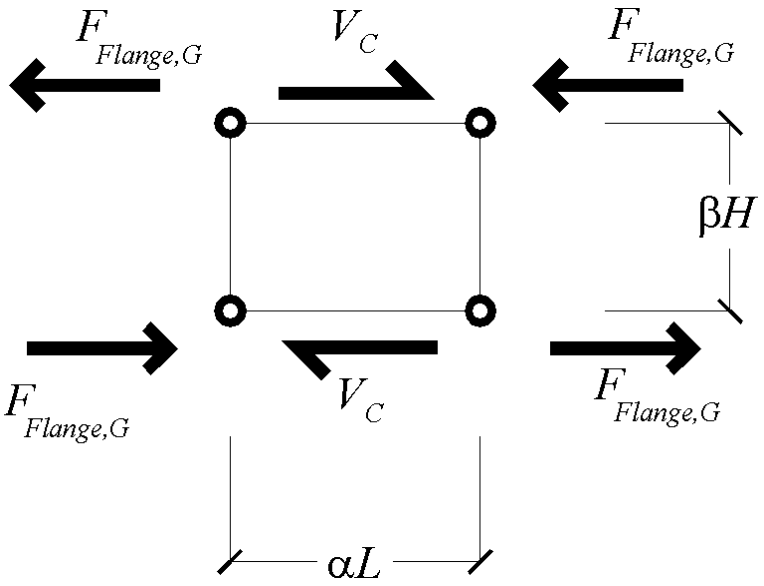

Figure 2.3-5: Resultant Panel Zone Forces

$$V_{Panel} = V_C - 2F_{Flange,G} = V_C - \frac{V_C(1-\alpha)}{\beta} = -\frac{V_C(1-\alpha-\beta)}{\beta} \quad \text{.....(2.3-11)}$$

To determine the drift ($\delta_{PZ,V}$) associated with V_{Panel} from Equation 2.3-11, the shear Equation 2.1-4 can be employed and will produce the following relationship:

$$\delta_{PZ,V} = \frac{VH(1-\alpha-\beta)^2}{\beta A_{PZ}{}^{*} G} \quad \text{.....(2.3-12)}$$

The panel shear is not included again since the effect of the applied force V to this region has already been accounted for. To do so would be doubling its effect. A different expression for PZ shear would be determined if one worked with the column flange forces instead of the beam forces. However, the shear stress computed in each "direction" is the same, and the contribution of PZ shear will be the same as shown in Equation 2.3-12.

The flexural component of drift in the PZ region ($\delta_{PZ,CF}$) is by far the most complex portion to the overall drift of the subassembly. Due to the highly indeterminate stress conditions inside this region, determining the moment variation throughout the PZ

is very problematic and must be simplified for use in Equation 2.1-3. There are two simplified moment diagrams examined in this thesis. Both assume a linear stress distribution through the PZ, the maximum moment is at the face of the beam/column joint and the moment is equal to zero at the center of the PZ. But, the first ($Actual\ \delta_{PZ,CF}$) includes a better static account of the resultant forces in Figure 2.3-5. Both moment diagrams are shown in Figure 2.3-6.

$$Actual\ \delta_{PZ,CF} = \frac{VH^3\beta}{4EI_{Col}}\left[\alpha(1-\beta)+\frac{(1-\alpha-\beta)^2}{3}\right] \quad \text{.....(2.3-13)}$$

$$Simplified\ \delta_{PZ,CF} = \frac{VH^3\beta(1-\beta)^2}{12EI_{Col}} \quad \text{.....(2.3-14)}$$

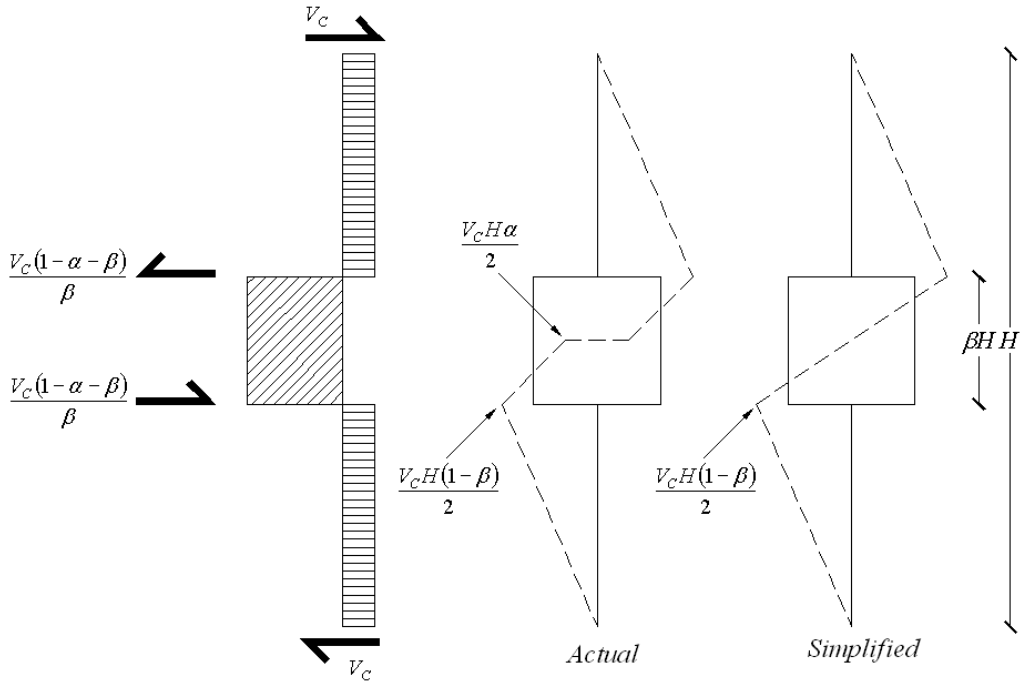

Figure 2.3-6: Shear and Bending Moment Diagrams from Column Forces

This procedure is then repeated to determine the PZ deflection contribution from the girder moment ($\delta_{PZ,GF}$) shown in Figure 2.3-7. The flexure component is:

$$Actual\ \delta_{PZ,GF} = \frac{VH^2 \alpha L}{4EI_{PZ}}\left[\beta(1-\alpha) + \frac{(1-\alpha-\beta)^2}{3}\right] \quad \text{.....(2.3-15)}$$

$$Simplified\ \delta_{PZ,GF} = \frac{VH^2 \alpha L(1-\alpha)^2}{12EI_{PZ}} \quad \text{.....(2.3-16)}$$

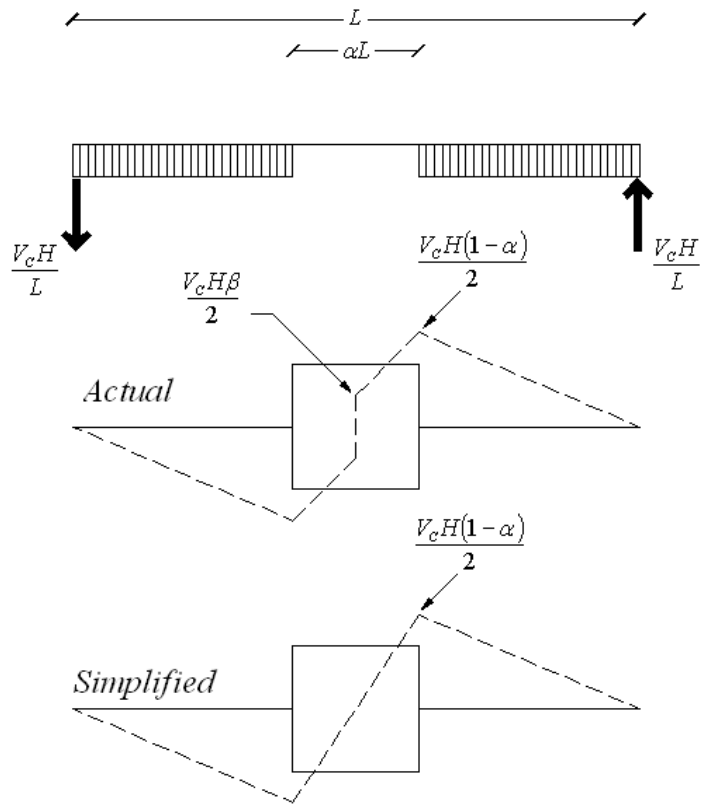

Figure 2.3-7: Shear and Bending Moment Diagrams from Girder Forces

For comparison purposes, the effect of using Equation 2.3-13 versus Equation 2.3-14 and Equation 2.3-15 and Equation 2.3-16 based on typical α and β values was performed. In the tables below, the values shown are based only on α and β since the remaining variables will cancel out when the equations are set equal to each other.

Table 2.3-1: α and β Factors From Equation 2.3-13: $\left[\alpha(1-\beta)+\frac{(1-\alpha-\beta)^2}{3}\right]$

	β	0.02	0.04	0.06	0.08	0.10	0.12	0.14	0.16	0.18	0.20	0.22	0.24	0.26
α														
0.02		0.33	0.31	0.30	0.29	0.28	0.26	0.25	0.24	0.23	0.22	0.21	0.20	0.19
0.04		0.33	0.32	0.31	0.29	0.28	0.27	0.26	0.25	0.24	0.22	0.21	0.20	0.19
0.06		0.34	0.33	0.31	0.30	0.29	0.28	0.26	0.25	0.24	0.23	0.22	0.21	0.20
0.08		0.35	0.33	0.32	0.31	0.30	0.28	0.27	0.26	0.25	0.24	0.23	0.21	0.20
0.10		0.36	0.34	0.33	0.32	0.30	0.29	0.28	0.27	0.25	0.24	0.23	0.22	0.21
0.12		0.36	0.35	0.34	0.32	0.31	0.30	0.29	0.27	0.26	0.25	0.24	0.23	0.22
0.14		0.37	0.36	0.34	0.33	0.32	0.31	0.29	0.28	0.27	0.26	0.25	0.23	0.22
0.16		0.38	0.37	0.35	0.34	0.33	0.31	0.30	0.29	0.28	0.26	0.25	0.24	0.23
0.18		0.39	0.38	0.36	0.35	0.33	0.32	0.31	0.30	0.28	0.27	0.26	0.25	0.24
0.20		0.40	0.38	0.37	0.36	0.34	0.33	0.32	0.30	0.29	0.28	0.27	0.26	0.25
0.22		0.41	0.39	0.38	0.37	0.35	0.34	0.33	0.31	0.30	0.29	0.28	0.26	0.25
0.24		0.42	0.40	0.39	0.37	0.36	0.35	0.33	0.32	0.31	0.30	0.28	0.27	0.26
0.26		0.43	0.41	0.40	0.38	0.37	0.36	0.34	0.33	0.32	0.31	0.29	0.28	0.27

Table 2.3-2: β Factors From Equation 2.3-14: $\frac{(1-\beta)^2}{3}$

	β	0.02	0.04	0.06	0.08	0.10	0.12	0.14	0.16	0.18	0.20	0.22	0.24	0.26
α														
0.02		0.32	0.31	0.29	0.28	0.27	0.26	0.25	0.24	0.22	0.21	0.20	0.19	0.18
0.04		0.32	0.31	0.29	0.28	0.27	0.26	0.25	0.24	0.22	0.21	0.20	0.19	0.18
0.06		0.32	0.31	0.29	0.28	0.27	0.26	0.25	0.24	0.22	0.21	0.20	0.19	0.18
0.08		0.32	0.31	0.29	0.28	0.27	0.26	0.25	0.24	0.22	0.21	0.20	0.19	0.18
0.10		0.32	0.31	0.29	0.28	0.27	0.26	0.25	0.24	0.22	0.21	0.20	0.19	0.18
0.12		0.32	0.31	0.29	0.28	0.27	0.26	0.25	0.24	0.22	0.21	0.20	0.19	0.18
0.14		0.32	0.31	0.29	0.28	0.27	0.26	0.25	0.24	0.22	0.21	0.20	0.19	0.18
0.16		0.32	0.31	0.29	0.28	0.27	0.26	0.25	0.24	0.22	0.21	0.20	0.19	0.18
0.18		0.32	0.31	0.29	0.28	0.27	0.26	0.25	0.24	0.22	0.21	0.20	0.19	0.18
0.20		0.32	0.31	0.29	0.28	0.27	0.26	0.25	0.24	0.22	0.21	0.20	0.19	0.18
0.22		0.32	0.31	0.29	0.28	0.27	0.26	0.25	0.24	0.22	0.21	0.20	0.19	0.18
0.24		0.32	0.31	0.29	0.28	0.27	0.26	0.25	0.24	0.22	0.21	0.20	0.19	0.18
0.26		0.32	0.31	0.29	0.28	0.27	0.26	0.25	0.24	0.22	0.21	0.20	0.19	0.18

Table 2.3-3: α and β Factors From Equation 2.3-15: $\left[\beta(1-\alpha)+\frac{(1-\alpha-\beta)^2}{3}\right]$

	β	0.02	0.04	0.06	0.08	0.10	0.12	0.14	0.16	0.18	0.20	0.22	0.24	0.26
α														
0.02		0.33	0.33	0.34	0.35	0.36	0.36	0.37	0.38	0.39	0.40	0.41	0.42	0.43
0.04		0.31	0.32	0.33	0.33	0.34	0.35	0.36	0.37	0.38	0.38	0.39	0.40	0.41
0.06		0.30	0.31	0.31	0.32	0.33	0.34	0.34	0.35	0.36	0.37	0.38	0.39	0.40
0.08		0.29	0.29	0.30	0.31	0.32	0.32	0.33	0.34	0.35	0.36	0.37	0.37	0.38
0.10		0.28	0.28	0.29	0.30	0.30	0.31	0.32	0.33	0.33	0.34	0.35	0.36	0.37
0.12		0.26	0.27	0.28	0.28	0.29	0.30	0.31	0.31	0.32	0.33	0.34	0.35	0.36
0.14		0.25	0.26	0.26	0.27	0.28	0.29	0.29	0.30	0.31	0.32	0.33	0.33	0.34
0.16		0.24	0.25	0.25	0.26	0.27	0.27	0.28	0.29	0.30	0.30	0.31	0.32	0.33
0.18		0.23	0.24	0.24	0.25	0.25	0.26	0.27	0.28	0.28	0.29	0.30	0.31	0.32
0.20		0.22	0.22	0.23	0.24	0.24	0.25	0.26	0.26	0.27	0.28	0.29	0.30	0.31
0.22		0.21	0.21	0.22	0.23	0.23	0.24	0.25	0.25	0.26	0.27	0.28	0.28	0.29
0.24		0.20	0.20	0.21	0.21	0.22	0.23	0.23	0.24	0.25	0.26	0.26	0.27	0.28
0.26		0.19	0.19	0.20	0.20	0.21	0.22	0.22	0.23	0.24	0.25	0.25	0.26	0.27

Table 2.3-4: α Factors From Equation 2.3-16: $\frac{(1-\alpha)^2}{3}$

	β	0.02	0.04	0.06	0.08	0.10	0.12	0.14	0.16	0.18	0.20	0.22	0.24	0.26
β														
0.02		0.32	0.32	0.32	0.32	0.32	0.32	0.32	0.32	0.32	0.32	0.32	0.32	0.32
0.04		0.31	0.31	0.31	0.31	0.31	0.31	0.31	0.31	0.31	0.31	0.31	0.31	0.31
0.06		0.29	0.29	0.29	0.29	0.29	0.29	0.29	0.29	0.29	0.29	0.29	0.29	0.29
0.08		0.28	0.28	0.28	0.28	0.28	0.28	0.28	0.28	0.28	0.28	0.28	0.28	0.28
0.10		0.27	0.27	0.27	0.27	0.27	0.27	0.27	0.27	0.27	0.27	0.27	0.27	0.27
0.12		0.26	0.26	0.26	0.26	0.26	0.26	0.26	0.26	0.26	0.26	0.26	0.26	0.26
0.14		0.25	0.25	0.25	0.25	0.25	0.25	0.25	0.25	0.25	0.25	0.25	0.25	0.25
0.16		0.24	0.24	0.24	0.24	0.24	0.24	0.24	0.24	0.24	0.24	0.24	0.24	0.24
0.18		0.22	0.22	0.22	0.22	0.22	0.22	0.22	0.22	0.22	0.22	0.22	0.22	0.22
0.20		0.21	0.21	0.21	0.21	0.21	0.21	0.21	0.21	0.21	0.21	0.21	0.21	0.21
0.22		0.20	0.20	0.20	0.20	0.20	0.20	0.20	0.20	0.20	0.20	0.20	0.20	0.20
0.24		0.19	0.19	0.19	0.19	0.19	0.19	0.19	0.19	0.19	0.19	0.19	0.19	0.19
0.26		0.18	0.18	0.18	0.18	0.18	0.18	0.18	0.18	0.18	0.18	0.18	0.18	0.18

As seen in the above tables, the simplified equations will give an equivalent value for drift when α and β are small. However, as α and β get larger, the resulting PZ flexural drift contribution will be different depending on which formula is used.

These derivations were then repeated for the Corner, End and Tee subassemblages. The individual results are not repeated but the representative figures used to develop the formulas are shown. In all three models, the axial component of drift is now included and was determined using Equation 2.1-5 with the upper limits of integration being equal to either ½ L or ½ H. Again, this was done to ensure that all the sources of elastic strain energy were accounted for when making comparisons with the FEA models. By placing the roller at the center of the PZ region instead of the end of the column, different boundary conditions would have eliminated the need to account for axial forces in the Corner and End models. This was not done to avoid stress concentrations in the PZ region of the finite element models. The final results from these derivations are found in Table 2.3-5 below.

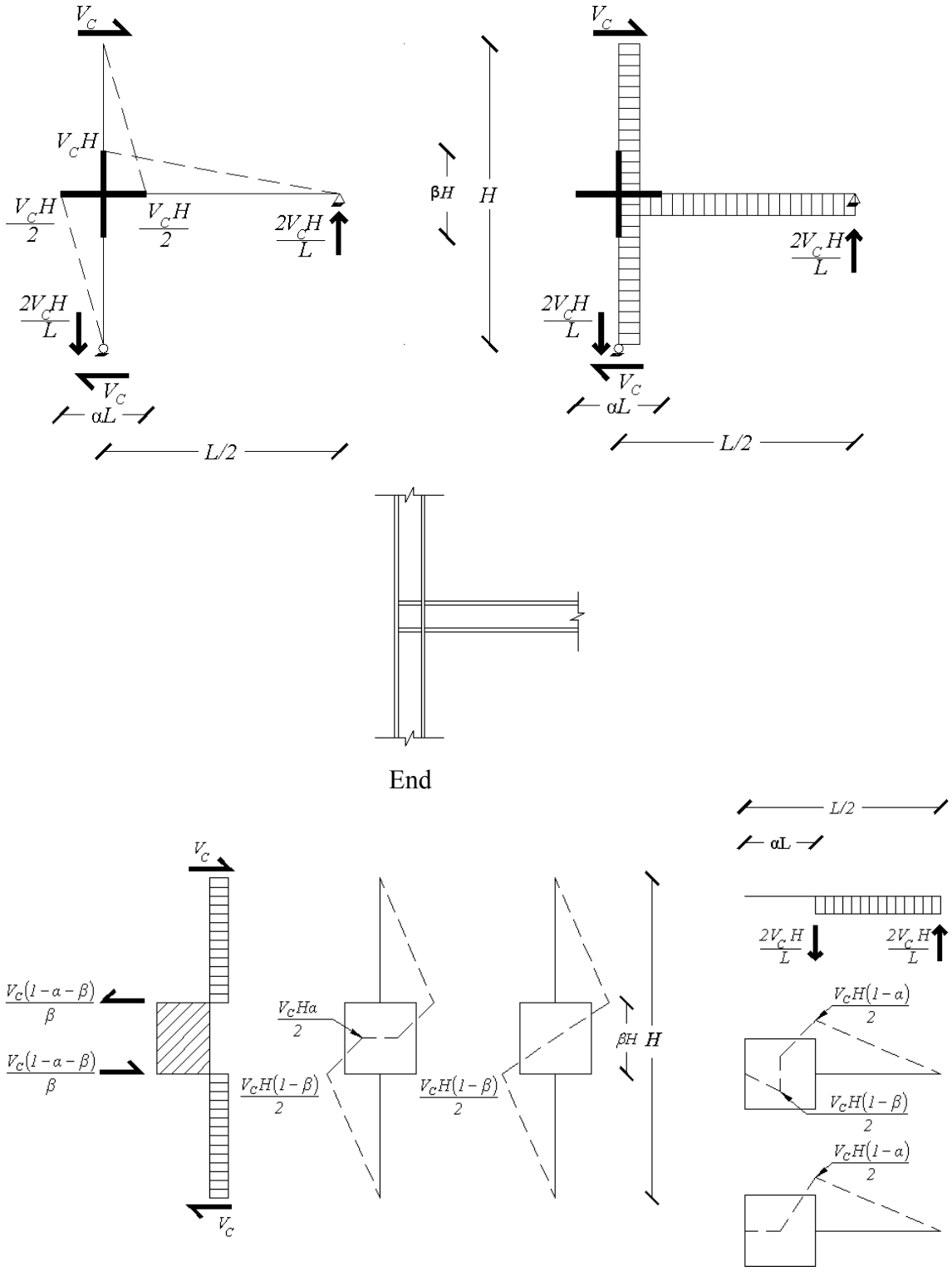

Figure 2.3-8: End Subassembly Resultant Shear and Moment Diagrams

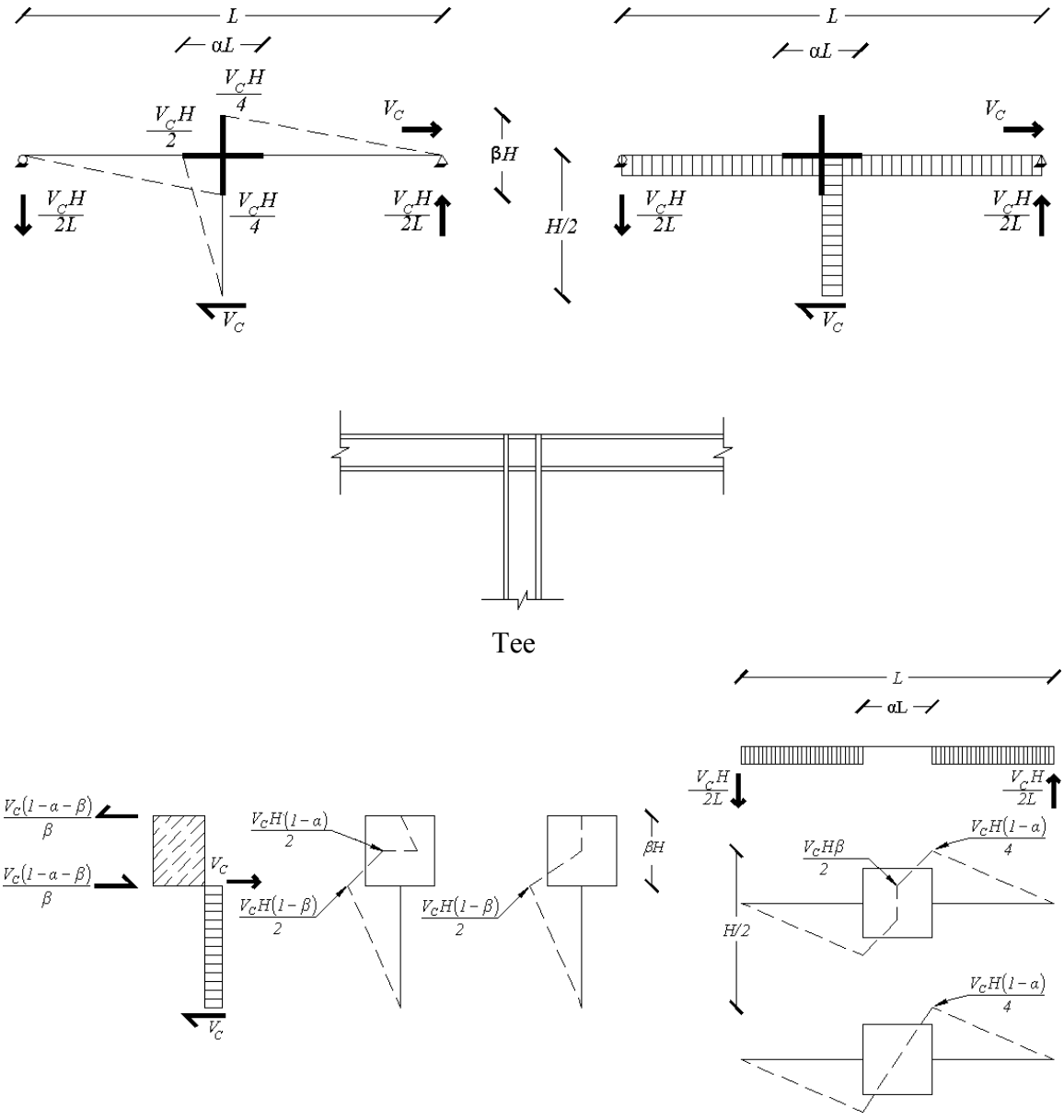

Figure 2.3-9: Tee Subassembly Shear and Moment Diagram

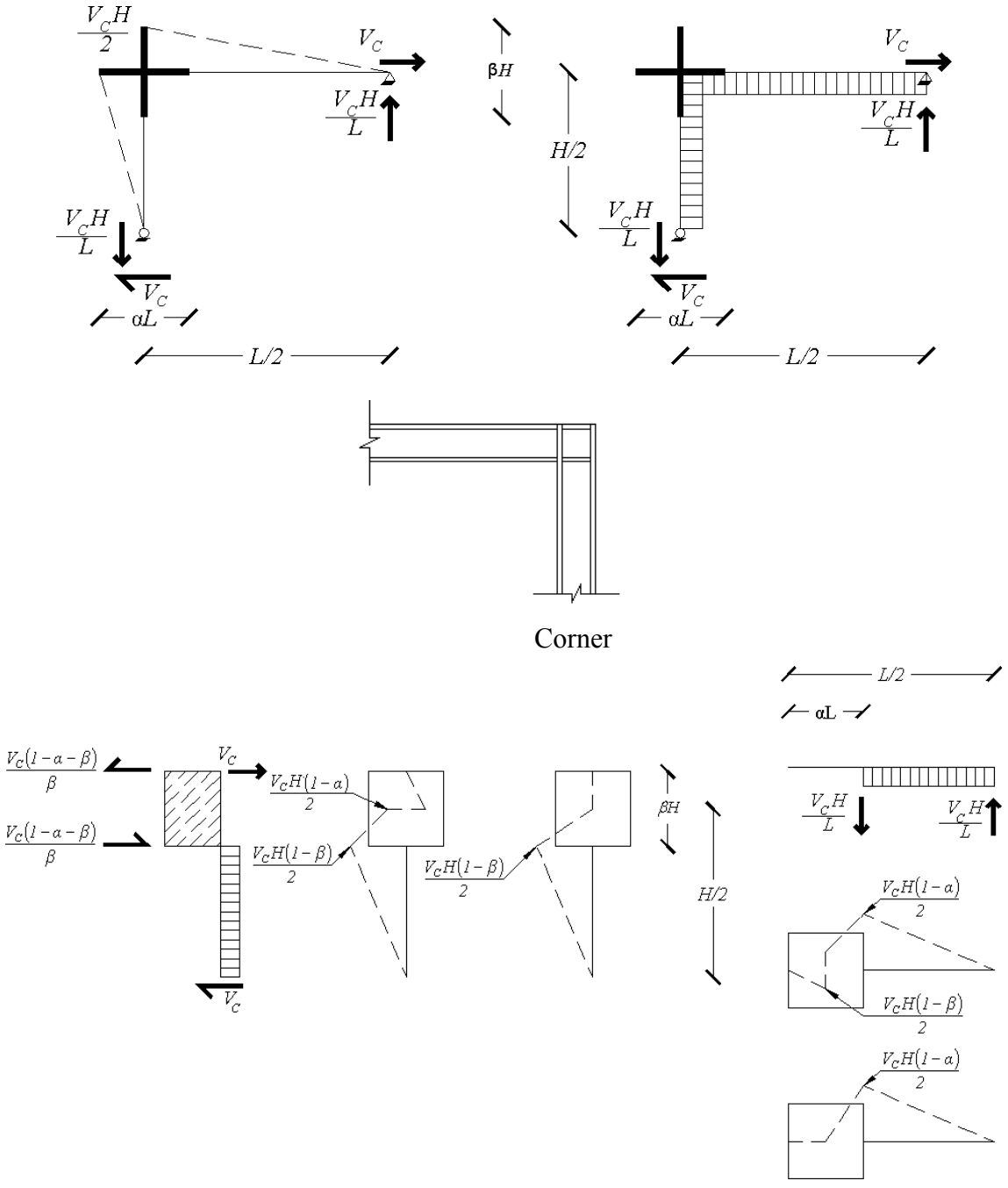

Figure 2.3-10: Corner Subassembly Resultant Shear and Moment Diagrams

The formulas for the Corner, End and Tee models are reported in relation to the results from the Cruciform model derivations, which is the way they were implemented into the PANELS program. The constants C' and C'' which were derived for the PZ flexure formulas using the Corner, End and Tee subassemblages are included for mathematical consistency. They were included in the PANELS program and their contribution can be seen in the example problem located in Appendix A, which is the "User's Manual" for the PANELS program. Two example problems are given to provide a detailed illustration of the formulas shown in Table 2.3-5.

Table 2.3-5: PANELS Equations for the Four Different Subassemblages

Deflection	Cruciform (Cru)	End	Corner	Tee
$\delta_{C,F}$	$\frac{VH^3}{12EI_C}(1-\beta)^3$	Cru	½*Cru	½*Cru
$\delta_{G,F}$	$\frac{VH^2L}{12EI_G}(1-\alpha)^3$	2*Cru	½*Cru	¼*Cru
$\delta_{C,V}$	$\frac{VH}{A_{V,C}^{*}G}(1-\beta)$	Cru	½*Cru	½*Cru
$\delta_{G,V}$	$\frac{VH^2}{A_{V,G}^{*}GL}(1-\alpha)$	2*Cru	½*Cru	¼*Cru
$\delta_{C,A}$	0	$\frac{2VH^3(1-\beta)}{EL^2A_C}$	$\frac{VH^3(1-\beta)}{2EL^2A_C}$	0
$\delta_{G,A}$	0	0	$\frac{VL(1-\alpha)}{2EA_G}$	$\frac{VL(1-\alpha)}{2EA_G}$
$\delta_{PZ,V}$	$\delta_{PZ,V}=\frac{VH(1-\alpha-\beta)^2}{\beta A_{PZ}^{*}G}$	Cru	¼*Cru	¼*Cru
Actual $\delta_{PZ,CF}$	$\frac{VH^3\beta}{4EI_{Col}}\left[\alpha(1-\beta)+\frac{(1-\alpha-\beta)^2}{3}\right]$	Cru+ C’	½*Cru + C’	½*Cru + C’
Simplified $\delta_{PZ,CF}$	$\frac{VH^3\beta(1-\beta)^2}{12EI_C}$	Cru	½*Cru	½*Cru
Actual $\delta_{PZ,GF}$	$\frac{VH^2\alpha L}{4EI_{PZ}}\left[\beta(1-\alpha)+\frac{(1-\alpha-\beta)^2}{3}\right]$	2*Cru+ C’	½*Cru + C’’	¼*Cru + C’’
Simplified $\delta_{PZ,GF}$	$\frac{VH^2\alpha L(1-\alpha)^2}{12EI_{PZ}}$	2*Cru	½*Cru	¼*Cru

where C’ = $\frac{V(1-\alpha)^2\beta H^3}{24EI_C}$ and C’’= $\frac{V(1-\beta)^2H^2\alpha L}{24EI_{PZ}}$

The reader is reminded that the drift values calculated using this table follow the definition of drift for each subassemblage shown in Figure 1.3-2

2.4 Summary and Discussion

The differences between the Centerline, Rigid and Flexible models were not the focus of this thesis. An in-depth study was completed by Charney and Johnson (1986), which showed the limitations and inaccuracies of the Centerline and Rigid models. In that paper, the authors determined that in all instances, the Rigid model grossly underestimates the interstory drift of a subassembly. The Centerline model either overestimated or underestimated the total drift depending on the geometry of the beam/column joint. The reason for the variability in the Centerline model is that it overestimates the flexural deformations and underestimates the shear deformations within the PZ region. Following the recommendations of that paper, the Flexible models, which explicitly account for deformation due to strain energy within the PZ region, will be used for the comparisons contained within this thesis. If the ability to model the PZ region is not possible due to software constraints, the use of the "Centerline" model is the best choice.

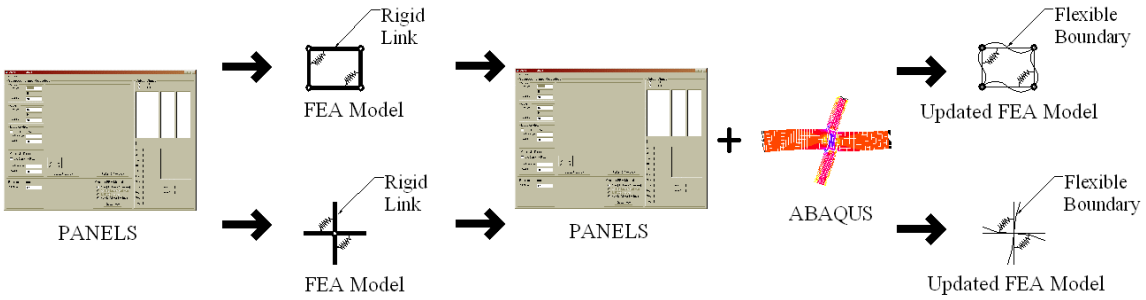

Figure 2.4-1: Research Flow Chart

Looking at Figure 2.4-1, the PANELS component has now been presented. To verify the Flexible model derivations, they will be compared to finite element analysis (FEA) models. One of the major focuses will be how to determine the effective moment of inertia used in Equations 2.3-13, I_{Col}, and 2.3-15, I_{PZ}. Chapter 4 contains this additional Flexible development based on elastic FEA comparisons using ABAQUS.

3 Development of Inelastic Subassemblage Models

3.1 Introduction and Scope

With the recent increase in computer processor speed and the development of more robust computer programs, explicit modeling of the PZ region has become more common. To accomplish this, different modeling approaches have been developed. A literature search was conducted to determine which models are currently available. This search resulted in the discovery of two models, both based on theoretical and experimental work performed by Dr. Helmut Krawinkler of Stanford University, that explicitly model both the elastic and inelastic deformations within the PZ region. The first model, referred to as the Krawinkler model, was originally developed in 1978, will be rederived in its entirety. The second, named the Scissors model, is used extensively for PZ modeling because of its simplicity. Unfortunately, as determined in the review of the literature, it is commonly used incorrectly. A complete explanation of how the properties of this model are developed is also included. Both models are included in the PANELS program, which has the capabilities to create the Drain-2DX (Prakash at al. 1993) input files for each. See Appendix A for details on PANELS and the options associated with creating the Drain-2DX models.

3.2 Literature Review

The establishment of PZ design models has gone through various stages. One of the first and by far the most documented (Krawinkler 1978), shown in Figure 3.2-1, treats the boundary of the PZ as infinitely rigid links connected at the corners by compound nodes.

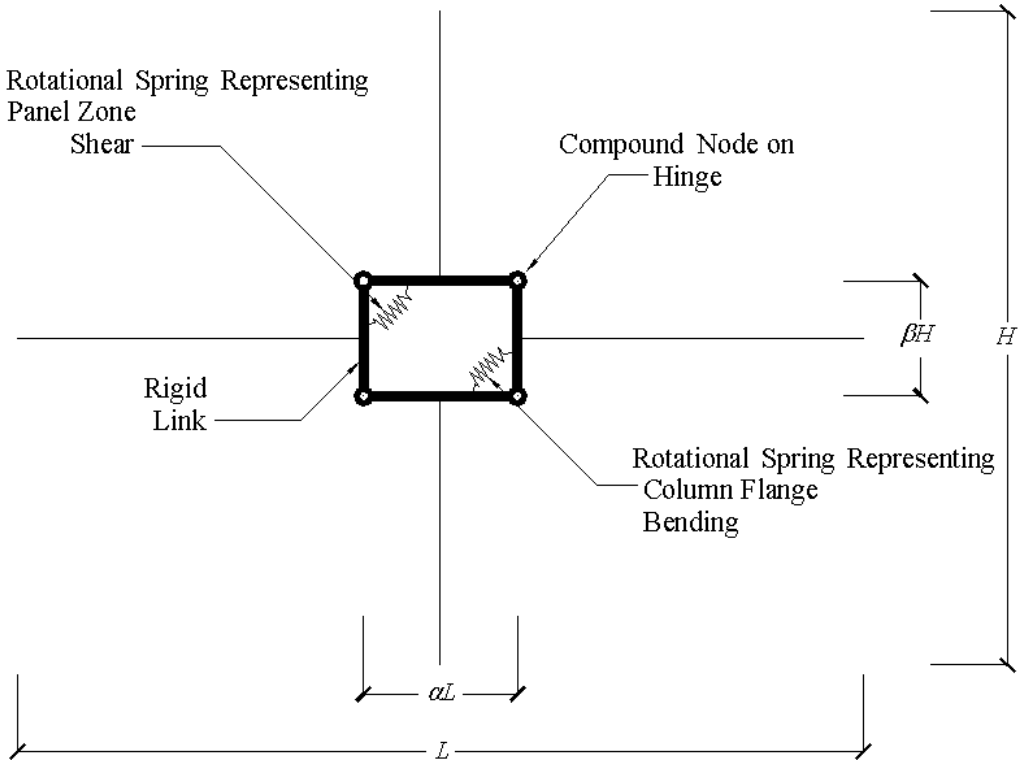

Figure 3.2-1: Krawinkler Model

These compound joints are created by placing two nodes at the same X and Y coordinates and constraining their translational degrees of freedom. At two diagonally opposite corners of the panel, rotational springs are used to represent the resistance to panel zone shear and column flange bending. These rotational springs are derived from the shear force versus shear strain behavior idealized in Figure 3.2-2.

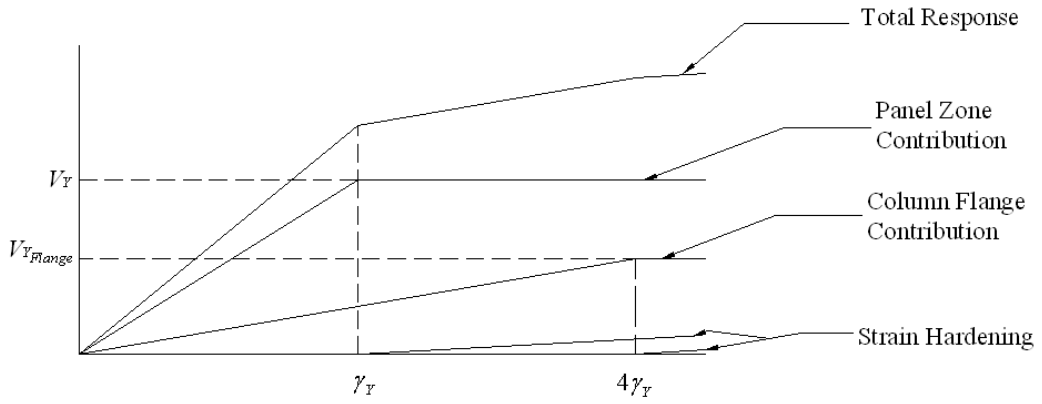

Figure 3.2-2: Krawinkler Shear Force vs. Shear Strain Relationship

The two stiffnesses, shear resistance of the PZ and the flexural resistance of the column flange, act in parallel. For this model, γ_Y is the strain which the elastic spring associated with the shear resistance of the PZ yields. According to Krawinkler's assumption, the post-elastic strength and stiffness are effective until an overall strain of $4\gamma_Y$ is achieved. By accounting for strain hardening, the complete trilinear relationship seen in Figure 3.2-2 is created. The two additional corners of the PZ region seen in Figure 3.2-1 are modeled as hinges by using two nodes at the intersection of the rigid links but no spring. If parallel constraints are ignored, there are a total of twelve nodes, eight rigid elements and two rotational springs with 28 degrees of freedom in the Krawinkler model. Although this large number of degrees of freedom can be very taxing on a computer's resources, this model has the advantage of physically representing the PZ distortion and, as will be seen, its properties are completely independent of the structural geometry outside the PZ region. This model can be reduced to four independent degrees of freedom if the proper constraints (not available in all commercial software) are used.

A second representation of the PZ (Krawinkler and Mohasseb 1987, Kim and Engelhardt 1995 and 2002, Schneider and Amidi 1998, Foutch and Yun 2002) is four infinitely rigid links attached by springs located at the center of the PZ. Referred to as the Scissors model, it is shown in Figure 3.2-3.

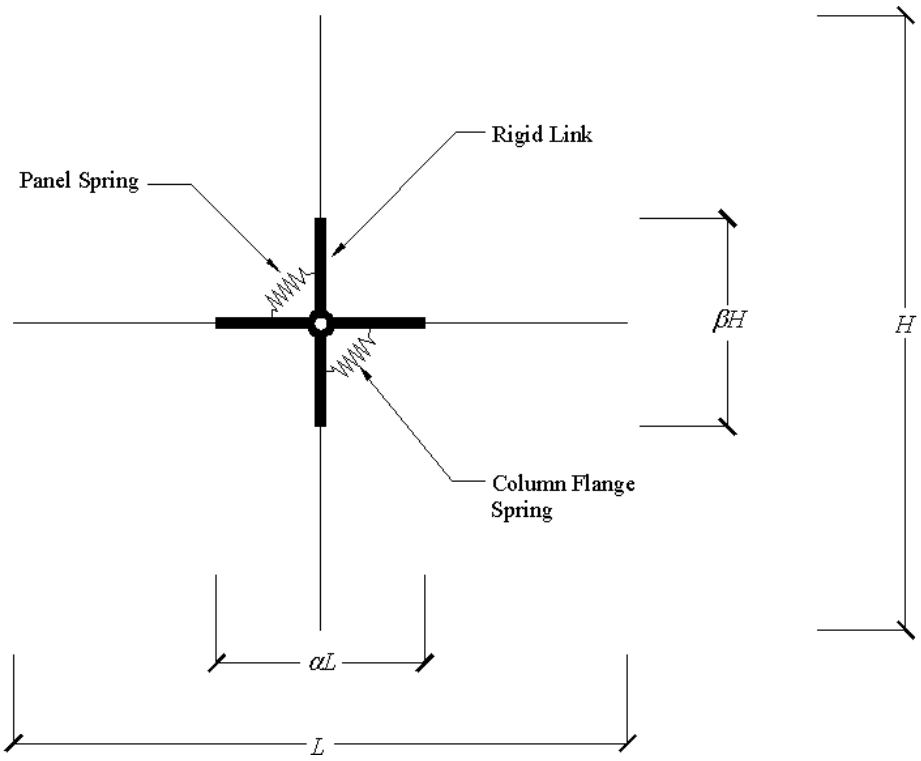

Figure 3.2-3: Scissors Model

These springs represent both the inelastic PZ contribution and inelastic column flange contribution to the overall stiffness. They are also modeled using a compound joint at the intersection of the rigid links in the center of the model and utilize the same definition for γ_Y as in the Krawinkler model. Employing Krawinkler's assumption, the Scissors model considers the column flange spring effective until a rotation of $4\theta_Y$ is achieved and includes the effects of strain hardening, shown in Figure 3.2-2. The difference between the two models is in their respective geometric properties, the number of components used to create the model and the kinematics of the models' deformation. All of these differences are addressed in detail in this chapter.

In a continuation of their PZ research, Krawinkler and Mohasseb (1987) investigated the overall drift of structural frames using computer analysis. This research showed the significance of proper PZ modeling but, more importantly, appears to be the first published usage of the Scissors model, Figure 3.4-1, using the properties derived

using the 1978 Krawinkler model. Considering the limited processor speed of computers in the 1980's, it is not surprising that the Scissors model was used. The Scissors model requires only six nodes for its four elements, adding only four degrees of freedom per joint. If the program includes rigid end zones, only two nodes are required. This makes the Scissors model much less demanding on a computer's resources, greatly reducing the amount of time required to generate the final results. However, as will be seen, the Scissors model is hampered by its dependence on the geometry outside the PZ region and its inability to mimic the PZ true behavior. Unfortunately, no article was found which directly addressed the differences in the Krawinkler and Scissors models.

In the papers by Kim and Engelhardt (1995 and 2002), the spring properties developed for this version of the Scissors model appear to be based on the previous derivations used to develop the Krawinkler model (1978) but are scaled by a factor ρ to account for the geometric differences between it and the Krawinkler model:

$$\rho = \frac{d_b - t_{bf}}{H_c} \approx \beta \quad \text{.....(3.2-1)}$$

A clear definition of how the factor ρ was derived was not evident, and by observation the definition of ρ appears to be inconsistent with the model's geometry. While the subsequent Scissors model derivations also result in a scaling factor that is used with the Krawinkler model properties, there is an obvious difference in the definition of the ρ and the combination of the α and β scaling factors that will be derived herein. It is also not completely clear whether or not the geometric differences were accounted for. Two different figures are shown in the 1995 Kim and Engelhardt document, one Krawinkler and one Scissors, with only the Krawinkler model properties actually being published. The authors also imply that this scaling factor was used in Krawinkler's derivations. It is true that a scaling factor was used in an earlier publication of Krawinkler's derivations (Krawinkler et al. 1975) but was dropped in his 1978 paper. In the 1975 paper, Krawinkler arbitrarily included this factor in his analytical models to account for "the

beneficial effect of column shear above and below the column." Since no derivations are given, determining which model and property combination were used is difficult at best.

Two other models, Fielding (1971) and Wang (1988), were redeveloped in detail and compared to the Krawinkler model by Kim and Engelhardt (1995 and 2002). For these two models the strength and stiffness in the elastic region is determined in an identical manner as in the Krawinkler model. The major difference between the Fielding, Wang and Krawinkler models is that each uses a different empirical relationship for the inelastic strength and stiffness properties. The Fielding model also ignores the effects of strain hardening in the inelastic region. The Wang model is very similar to the Krawinkler model except for the definition of the shear area being equal to $(d_c - 2t_{cf})t_{cw}$ instead of $(d_c - t_{cf})t_{cw}$ and the strain hardening beginning at a rotation of $3.5\theta_Y$. The results from the Kim and Engelhardt comparison showed that of the three models, the Krawinkler model compared most favorably to test data. The bilinear Fielding model and the trilinear Wang model were then modified by Kim and Engelhardt in an attempt to enhance the performance and were again compared to test data. These modified models did not appear to perform any better than the Krawinkler model so were not included in this thesis. The reader is encouraged to refer to the above references for the development of the updated inelastic properties and results for these modified models.

Very detailed finite element analysis models have also been developed (Lui and Chen 1986; Leger, Paultre and Nuggihalli 1991; Challa and Hall 1994; El-Tawil et al. 1999). While this approach is an excellent way to model the contribution of the PZ to the system model, the techniques involved in developing this type of model are too elaborate for day-to-day use in a design firm and typically do not result in a PZ model that can be efficiently integrated into analysis programs.

3.3 The Krawinkler Model

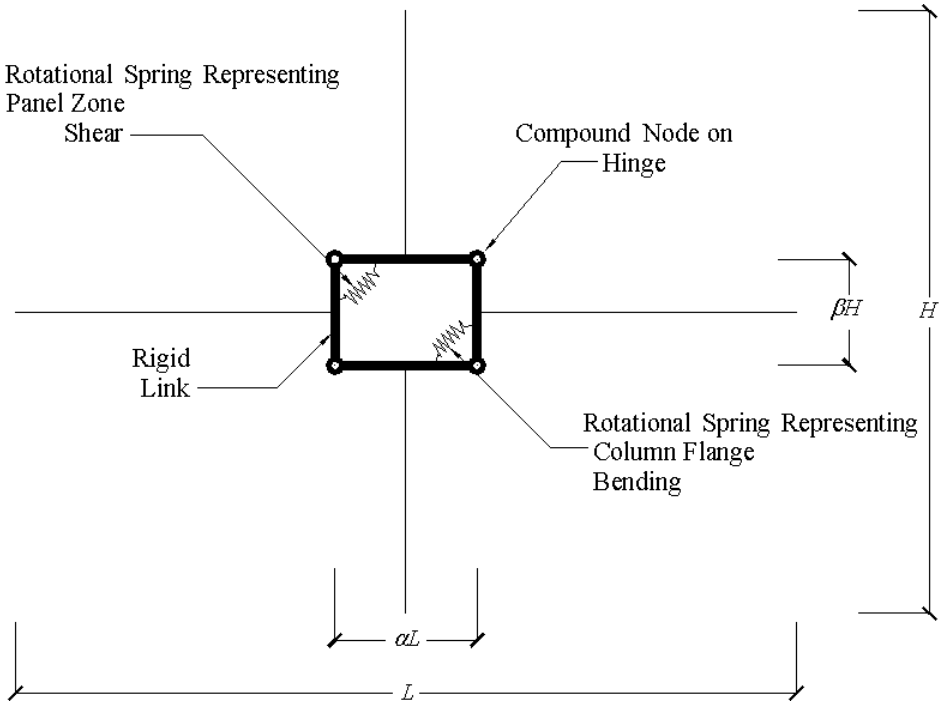

Figure 3.3-1: Krawinkler Model

As was discussed in Section 3.2, the Krawinkler model includes two different rotational springs to represent the strength and stiffness properties of the PZ region. In his derivations, Krawinkler (1978) assumes that the first spring, which represents the elastic contribution of the PZ, yields at a shear force determined using Von Mises' yield criterion. The second spring represents the inelastic component of drift attributed to plastic hinges forming in the column flanges. These hinges are assumed to occur at a strain that is four times the drift associated with the PZ hinge yielding. This relationship, shown in Figure 3.2-2, is then made trilinear by including the contribution of strain hardening. To develop the Krawinkler model's properties, this $V-\gamma$ diagram, Figure 3.2-2, must be converted to an equivalent $M-\theta$ relationship shown in Figure 3.3-2.

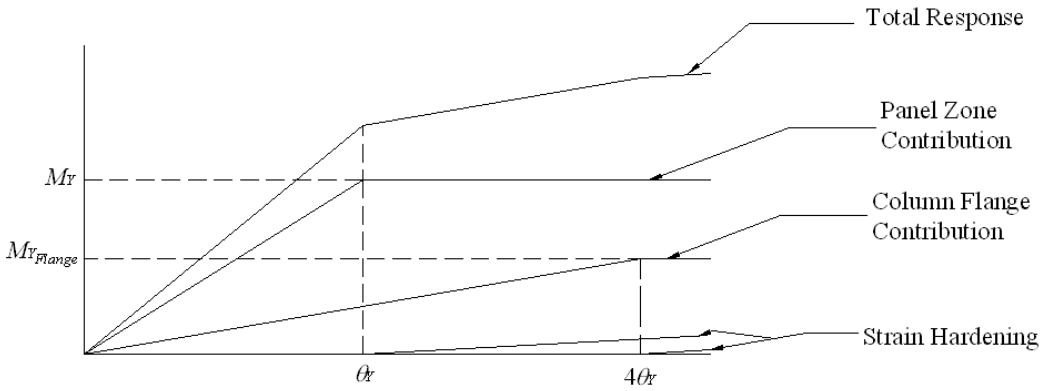

Figure 3.3-2: Krawinkler Model Component Moment-Curvature Relationship

3.3.1 Derivation of the Elastic Stiffness Properties of the Panel Zone Region

To compute the shear force in the panel, the force transferred from the girder flanges ($F_{Flange,G}$) needs to be determined. Using Figure 3.3-3, the moment in the girder (M_{Girder}) at the interfaces of the midpoint of girder flange and column flange is equal to

$$M_{Girder} = \frac{V_C H}{L}\frac{L-\alpha L}{2} = \frac{V_C H(1-\alpha)}{2} \quad \text{.....(3.3-1)}$$

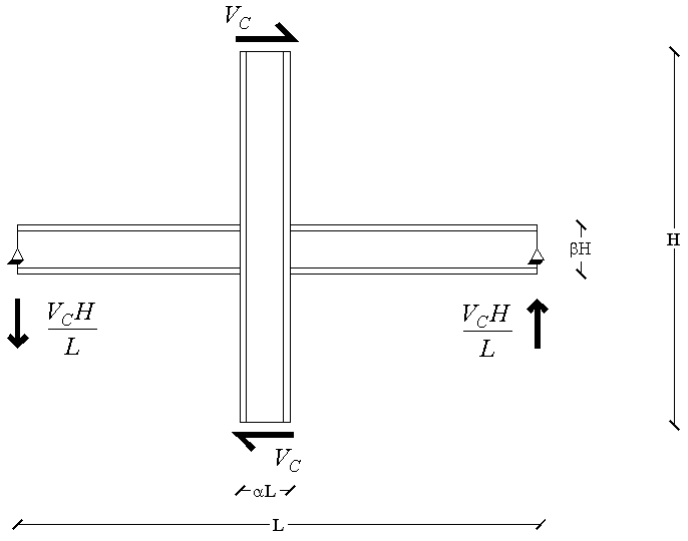

Figure 3.3-3: Cruciform Subassembly Resultant Forces

This moment can be converted into an equivalent force-couple over the depth of the girder. The force ($F_{Flange,G}$) can then be determined by:

$$F_{Flange,G} = \frac{M_{Girder}}{\beta H} = \frac{V_C H(1-\alpha)}{2}\frac{1}{\beta H} = \frac{V_C(1-\alpha)}{2\beta} \quad \text{.....(3.3-2)}$$

Again, this force is only an approximation since the actual stress is linearly distributed through the depth of the girder (Figure 2.3-4). Knowing $F_{Flange,G}$, the shear force in the panel (V_{Panel}) is then calculated by summing the forces in Figure 3.3-4.

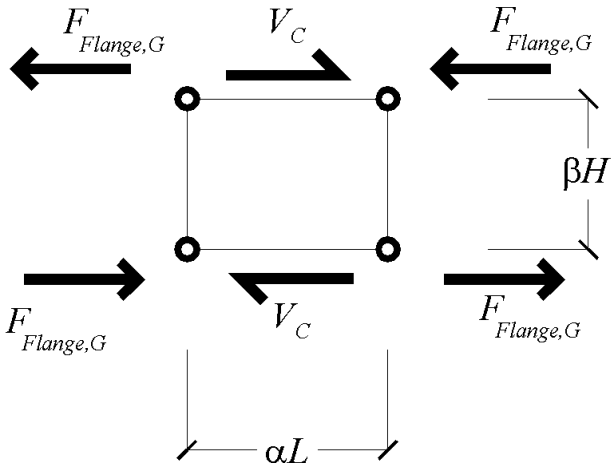

Figure 3.3-4: Krawinkler Panel Zone Shear Forces

$$V_{Panel} = V_C - 2F_{Flange,G} = V_C - \frac{V_C(1-\alpha)}{\beta} = -\frac{V_C(1-\alpha-\beta)}{\beta} \quad \text{.....(3.3-3)}$$

Now, using Figure 3.3-5, the stiffness of the PZ model (K_{Panel}) can be determined for the $M-\theta$ relationship based on the actual $V-\delta$ behavior.

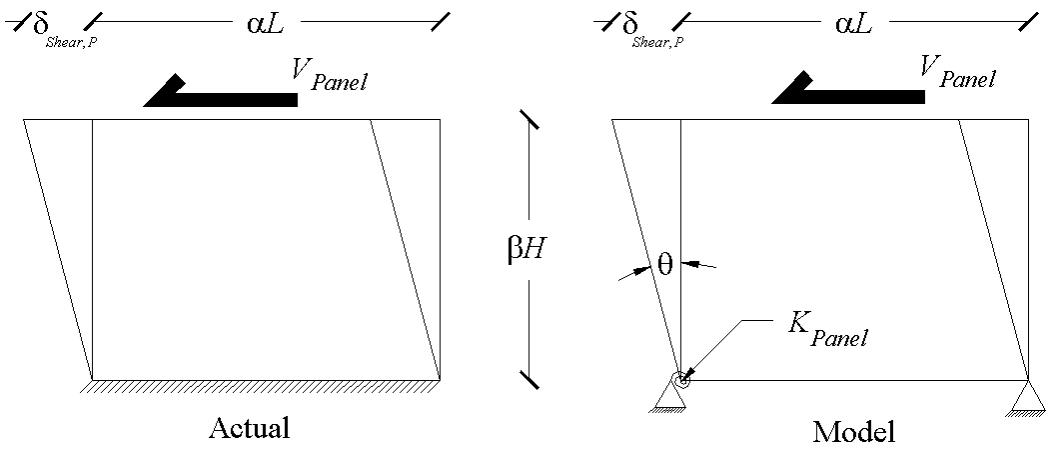

Figure 3.3-5: Krawinkler Panel Zone Stiffness

Applying the virtual work equation (3.3-4)

$$U_{Shear} = \int_0^{\beta H} \frac{V_{R,Panel} V_{V,Panel}}{G A} dx \quad \text{.....(3.3-4)}$$

to the actual $V-\delta$ relationship shown on the left side of Figure 3.3-5, the displacement ($\delta_{Shear,P}$) of the panel due to the shear force (V_{Panel}) is equal to

$$\delta_{Shear,P} = \frac{V_{Panel}\,\beta H}{G\,t_p\,\alpha L} \quad \text{.....(3.3-5)}$$

Organizing this relationship in terms of horizontal stiffness gives:

$$\frac{V_{Panel}}{\delta_{Shear,P}} = \frac{G\,t_p\,\alpha L}{\beta H} \quad \text{.....(3.3-6)}$$

Looking at the right side of Figure 3.3-5, the moment in the model spring due to V_{Panel} is:

$$M_{Panel} = V_{Panel}\,\beta H = K_{Panel}\,\theta \quad \text{.....(3.3-7)}$$

From small angle theory, the rotation angle θ can be approximated by:

$$\theta = \frac{\delta_{Shear,P}}{\beta H} \quad \text{.....(3.3-8)}$$

Substituting for θ in Equation 3.3-7 gives:

$$K_{Panel}\frac{\delta_{Shear,P}}{\beta H} = V_{Panel}\,\beta H \quad \text{.....(3.3-9)}$$

Rewriting this equation in terms of stiffness and setting it equal to the stiffness determined using the $V-\delta$ relationship (Equation 3.3-6), the stiffness contribution of the PZ based on the model $M-\theta$ relationship equals:

$$K_{Panel} = Gt_p\alpha L\,\beta H = G\,Vol_{Panel} \text{ .....(3.3-10)}$$

where Vol_{Panel} is the volume of material in the PZ region, including doubler plates.

3.3.2 Derivation of the Inelastic Strength Properties of the Panel Zone Region

From Von Mises' Yield Criterion

$$\left(\frac{F_Y}{\sqrt{3}}\right) \cong 0.6F_Y \quad \text{.....(3.3-11)}$$

the maximum shear force ($V_{Y,Panel}$) that can be obtained in the panel is:

$$V_{Y,Panel} = 0.6F_Y d_c t_p = 0.6F_Y \alpha L t_p \quad \text{.....(3.3-12)}$$

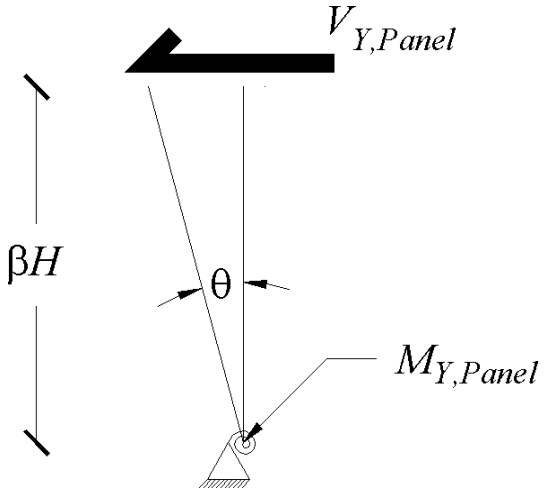

Figure 3.3-6: Krawinkler Yield Moment in the Panel Zone

Applying this force in Figure 3.3-6 results in a moment equal to

$$M_{Y,Panel} = V_{Y,Panel}\,\beta H = 0.6F_Y\,\alpha L\,\beta H\,t_p = 0.6F_Y\,Vol_{Panel} \quad \text{.....(3.3-13)}$$

3.3.3 Derivation of the Inelastic Strength Properties of the Column Flanges

The column flange spring properties can then be derived, using Figure 3.3-7 and Figure 3.3-8, in the same manner that the panel spring properties were developed. The flexural resistance of the column flanges is based on Krawinkler's assumption that the column flanges yield at a deformation that is four times larger than the yield deformation (θ_Y) of the panel. When exposed to this level of deformation, the flanges are assumed to develop kinks in them that can be represented as plastic hinges, which develop a plastic moment capacity of:

$$M_P = F_Y Z = \frac{F_Y b_{cf}\,t_{cf}^{\,2}}{4} \quad \text{.....(3.3-14)}$$

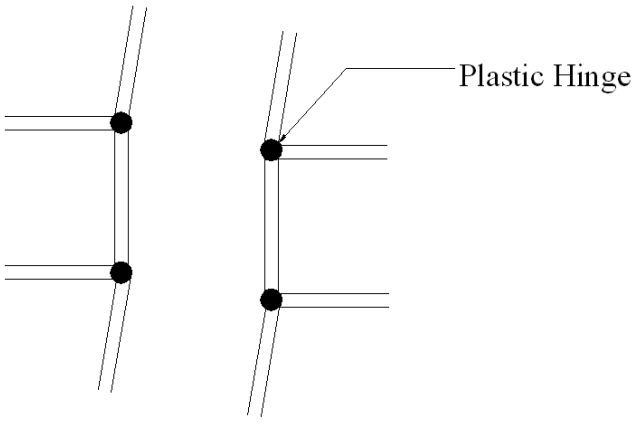

Figure 3.3-7: Plastic Hinges in the Column Flanges

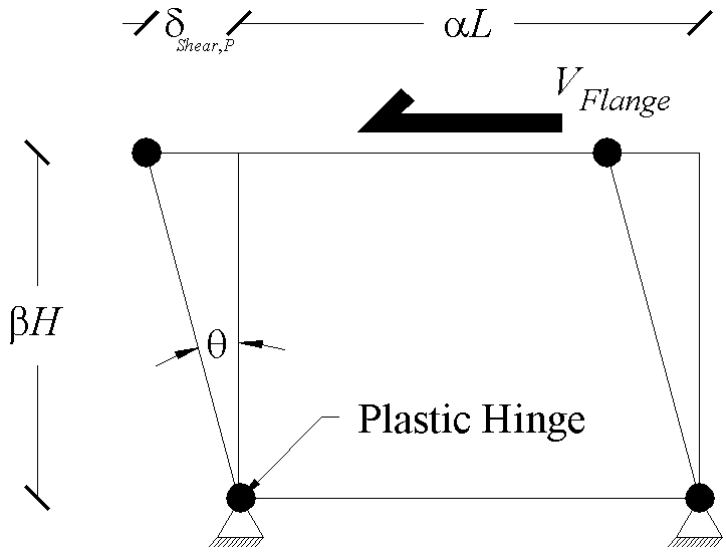

Figure 3.3-8: Krawinkler Plastic Hinges in the Column Flanges

Using the principle of virtual work with Figure 3.3-8,

$$V_{Flange}\,\delta_{Shear,F} = 4M_P\theta \quad \text{.....(3.3-15)}$$

Substituting the plastic moment capacity given from Equation 3.3-14 into Equation 3.3-15 and rewriting it in terms of the shear force V_{Flange} gives:

$$V_{Flange} = \frac{4M_P}{\beta H} = \frac{F_Y b_{cf}\, t_{cf}^{\,2}}{\beta H} \quad \text{.....(3.3-16)}$$

With this shear force, the rotational properties of the flanges can then be determined using statics. Looking at Figure 3.3-8, the moment is equal to the V_{Flange} multiplied by the moment arm βH. Substituting for V_{Flange} with the results from Equation 3.3-16, the yield moment of the flanges ($M_{Y_{Flange}}$) equals:

$$M_{Y_{Flange}} = V_{Flange}\,\beta H = F_Y b_{cf}\, t_{cf}^{\,2} \quad \text{.....(3.3-17)}$$

Including the 1.8 multiplier developed from experimental data (Krawinkler 1978), the yield moment of the four plastic hinges that develop in the column flanges is equal to

$$M_{Y_{Flange}} = 1.8\,V_{Flange}\,\beta H = 1.8F_Y b_{cf}\, t_{cf}^{\,2} \quad \text{.....(3.3-18)}$$

3.3.4 Derivation of the Inelastic Stiffness Properties of the Column Flanges

Using small angle theory, the yield rotation of the panel is equal to

$$\theta_Y = \frac{M_{Panel}}{K_{Panel,\theta}} = \frac{0.6F_Y}{G} \quad \text{.....(3.3-19)}$$

Accounting for Krawinkler's $4\theta_Y$ assumption, the flange stiffness ($K_{Flanges}$) can be determined using Equations 3.3-18 and 3.3-19 and writing them in terms of stiffness:

$$K_{Flanges} = \frac{M_{Y_{Flange}}}{4\theta_Y} = 0.75\, Gb_{cf} t_{cf}^{\ 2} \quad \text{.....(3.3-20)}$$

3.4 The Scissors Model

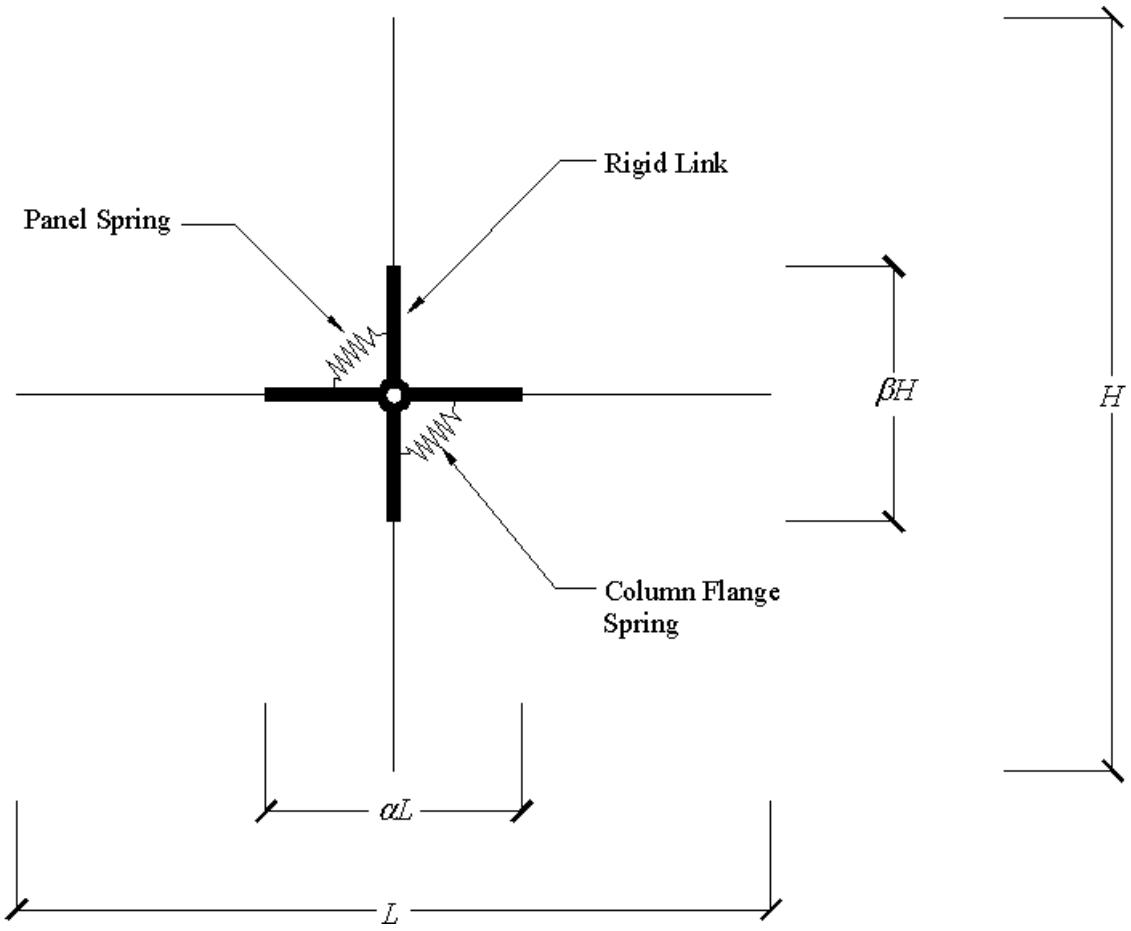

Figure 3.4-1: Scissors Model

Using the same value for the PZ shear, Equation 3.3-3, which was previously derived for the Krawinkler model and Figure 3.4-2, the contribution of the Scissors model to the total story drift will be determined.

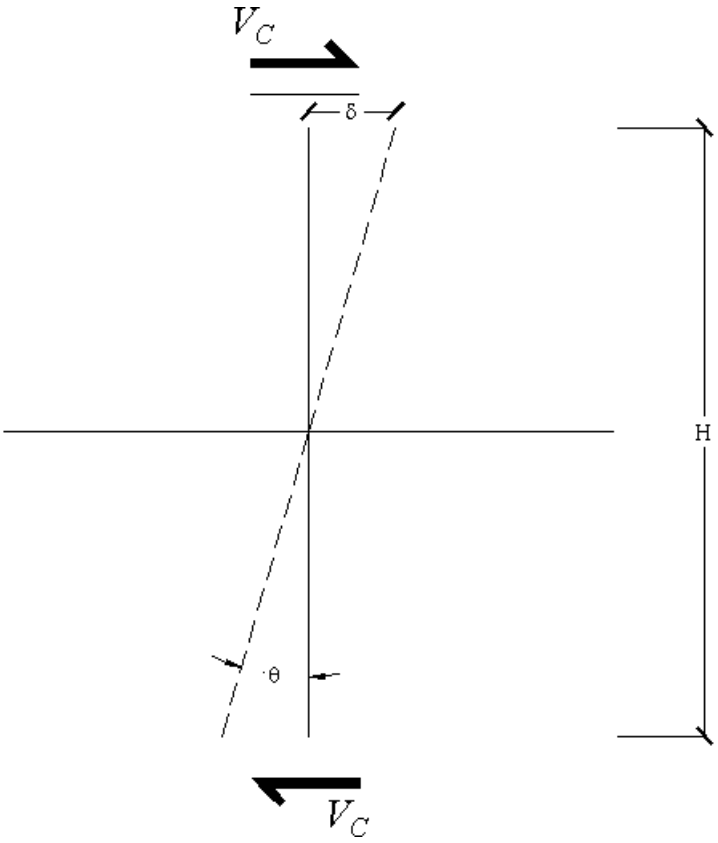

Figure 3.4-2: Scissors Model Shear Rotation Diagram

From the work equation

$$U_{Shear} = \int_0^{\beta H} \frac{V_{R,Panel} V_{V,Panel}}{GA} dx \quad \text{.....(3.4-1)}$$

the deflection due to the shear in the PZ is equal to

$$\delta_{shear,P} = \frac{V_{R,Panel} V_{V,Panel} \beta H}{G t_p \alpha L} \quad \text{.....(3.4-2)}$$

The internal virtual shear in the panel ($V_{V,Panel}$) is represented by:

$$V_{V,Panel} = \frac{-V_{V,C}(1-\alpha-\beta)}{\beta} \quad \text{.....(3.4-3)}$$

Substituting for $V_{R,Panel}$, setting the internal virtual column shear equal to unity and plugging these results into Equation 3.4-3 reveals that the portion of the overall drift due to PZ deformation is equal to

$$\delta_{Shear,P} = \frac{V_C(1-\alpha-\beta)}{\beta}\frac{(1-\alpha-\beta)}{\beta}\frac{\beta H}{Gt_p \alpha L} = \frac{V_C(1-\alpha-\beta)^2 H}{\alpha L \beta G t_p} \quad \text{.....(3.4-4)}$$

Using Figure 3.4-2, a rotational spring that will result in the same deflection can be determined. From statics, the moment (M_{Spring}) is:

$$M_{Spring} = \frac{V_C H}{2} + \frac{V_C H}{2} = V_C H \quad \text{.....(3.4-5)}$$

Since the deflections are considered small, small angle theory applies. Through observation, the reader can observe that the total story drift (δ_{Story}) is equal to 2δ, which results in θ_{Spring} being equal to

$$\theta_{Spring} = \frac{2\delta}{H} = \frac{\delta_{Story}}{H} \quad \text{.....(3.4-6)}$$

By setting the stiffness of the spring (K_{Spring}) equal to the moment from Equation 3.4-6 divided by the rotation derived in Equation 3.4-7, it is shown that:

$$K_{Spring} = \frac{M_{Spring}}{\theta_{Spring}} = \frac{V_C H^2}{\delta_{Story}} \quad \text{.....(3.4-7)}$$

If the story shear δ_{Story} is substituted for $\delta_{Shear,P}$ in Equation 3.4-5 and it is assumed that $K_{Panel} = K_{Spring}$, the panel stiffness K_{Panel} is equal to

$$K_{Panel} = \frac{\beta H \alpha L t_p G}{(1-\alpha-\beta)^2} = \frac{Vol_{Panel}\, G}{(1-\alpha-\beta)^2} \quad \text{.....(3.4-8)}$$

Using the Equation 3.3-10 and the PZ shear force derived in Equation 3.3-3, the shear in the column (V_C) is:

$$V_C = \frac{0.6F_Y \alpha L t_p \beta}{(1-\alpha-\beta)} \quad \text{.....(3.4-9)}$$

The moment in the panel ($M_{Y_{Panel}}$) can be derived by multiplying this shear force by the height (H), which yields:

$$M_{Y_{Panel}} = \frac{0.6F_Y \beta H \alpha L t_p}{(1-\alpha-\beta)} = \frac{0.6F_Y Vol_{Panel}}{(1-\alpha-\beta)} \quad \text{.....(3.4-10)}$$

Following the same procedure for determining the stiffness associated with plastic hinges forming in the column flanges as in the Krawinkler model, the scaling factor of $(1-\alpha-\beta)$ again arises. This is due to the relationship shown earlier in Equation 3.3-18 where the rotation θ_Y was set equal to the ratio of M_{Panel} to K_{Panel}. Accounting for this difference results in the following two relationships for the Scissors models' column flange hinge properties:

$$K_{Flange} = \frac{0.75Gb_{cf}t_{cf}^2}{(1-\alpha-\beta)^2} \quad \text{.....(3.4-11)}$$

$$M_{Y_{Flange}} = \frac{1.8F_Y b_{cf} t_{cf}^2}{(1-\alpha-\beta)} \quad \text{.....(3.4-12)}$$

3.5 Summary and Discussion

From the previous derivations, the following relationships were rederived for the 1978 Krawinkler model:

$$K_{Panel} = Gd_c d_b t_p \qquad M_{Y_{Panel}} = 0.6F_Y d_c d_b t_p \quad \text{.....(3.5-1)}$$

$$K_{Flange} = 0.75Gb_{cf} t_{cf}^2 \qquad M_{Y_{Flange}} = 1.8F_Y b_{cf} t_{cf}^2 \quad \text{.....(3.5-2)}$$

Looking at Equation 3.4-8 and Equation 3.4-10 through Equation 3.4-12, the Scissors model can be related to the Krawinkler model with the following relationships:

$$K_{Scissors} = \frac{K_{Krawinkler}}{(1-\alpha-\beta)^2} \qquad M_{Y_{Scissors}} = \frac{M_{Y_{Krawinkler}}}{(1-\alpha-\beta)} \quad \text{.....(3.5-3)}$$

where

$$\alpha = \frac{d_c - t_{cf}}{L} \qquad \beta = \frac{d_b - t_{bf}}{H} \quad \text{.....(3.5-4)}$$

L = Length of beam span H = Height of column span

There are some general observations that should also be noted. First, from the above derivations, it appears that $(1-\rho)$ calculated using Equation 3.2-1 is indeed intended to fulfill the same role as $(1-\alpha-\beta)$ although it is clear that they will not give the same results. According to its definition, ρ is approximately equal to β. Considering this, typical values for α, β and ρ are used and comparisons given in Table 3.5-1. Looking at these values, it is obvious that the use of $(1-\rho)$ instead of $(1-\alpha-\beta)$ will result in a strength and a stiffness that will be underestimated by a significant amount compared to the results that would be obtained by the Krawinkler model.

Table 3.5-1: Scissors Scaling Factor Comparisons

Typical Values	$(1-\alpha-\beta)$	$(1-\alpha-\beta)^2$	$(1-\rho)\cong(1-\beta)$	$\frac{1}{(1-\alpha-\beta)}$	$\frac{1}{(1-\alpha-\beta)^2}$	$\frac{1}{(1-\rho)}$
$\alpha \cong 0.1$ $\beta \cong 0.2$	0.7	0.49	0.8	1.43	2.00	1.25
$\alpha \cong 0.2$ $\beta \cong 0.2$	0.6	0.36	0.8	1.67	2.78	1.25

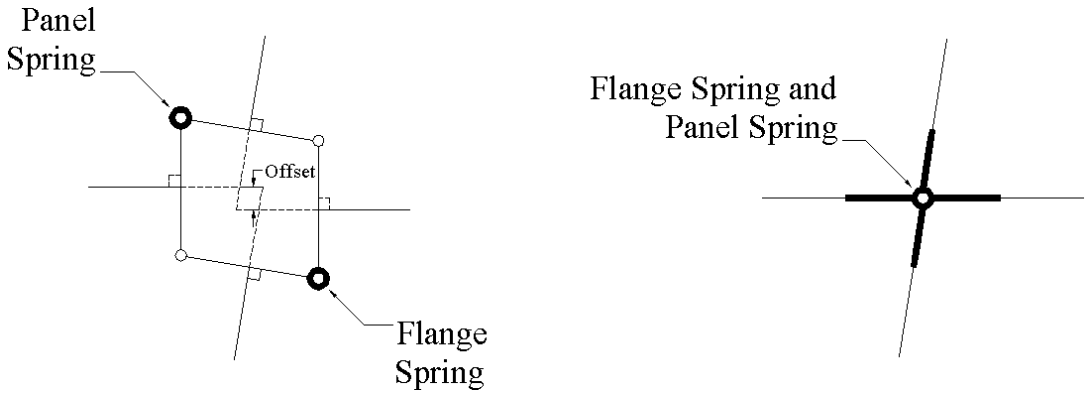

Figure 3.5-1: Deformed Krawinkler and Scissors Models

Also, the Krawinkler and Scissors models, shown in their deformed configuration in Figure 3.5-1, do have a definite kinematic difference between them. For the Krawinkler model, when it progresses through its "racking" motion, the ninety-degree angle between the columns, girders and the rigid links that make up the PZ boundary is maintained. This causes an offset to develop between the column centerlines and the girder centerlines shown in Figure 3.5-1. Due to the PZ hinges being placed at the intersection of the column and girder lines, this offset cannot be mimicked by the Scissors model. The ninety-degree angle cannot be maintained, so the "racking" motion is instead simulated by a scissor's type action. In addition, neither model currently has the ability

to account for the flexural deformation in the PZ region nor to account for the use of continuity plates. Finally, the use of α and β in the Scissors model requires that the column heights and girder spans remain constant throughout the entire frame. If this is not the case, the Krawinkler model has to be used.

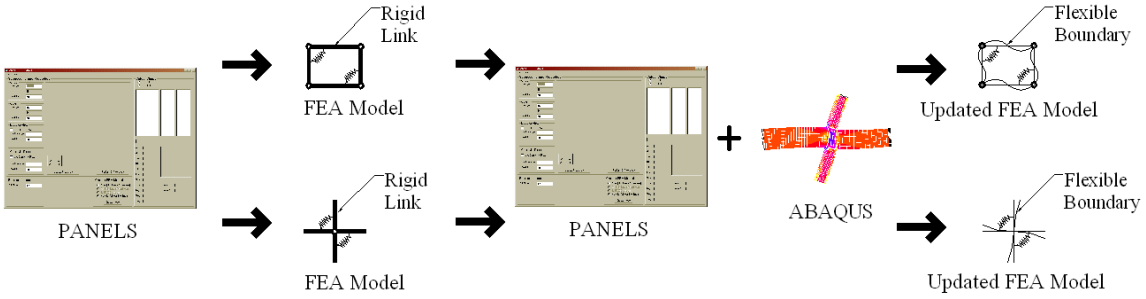

Figure 3.5-2: Research Flow Chart

In this chapter both FEA models (Krawinkler and Scissors) shown in Figure 3.5-2 have been presented. So at this point the only other component of the flow chart that has been introduced is the PANELS components. This still leaves including the contribution made by continuity plates to the beam/column joint (Chapter 4), quantifying the PZ flexure component of drift (Chapter 4), an in-depth comparison of the Krawinkler and Scissors (Chapter 5), comparing PANELS, the Krawinkler model and Scissors model to test data (Chapter 6) and update both the Krawinkler model and Scissors model to include the contribution of flexure in the PZ region (Chapter 7).

4 Elastic Model Modification to Account for Panel Zone Flexure

4.1 Introduction and Scope

The elastic deflections calculated by PANELS, using the elastic equations developed in Chapter 2, need to be evaluated to determine how the computed results correspond to those obtained using finite element analysis (FEA). This will be done in a three-step process. First, the drift of the subassemblages determined by PANELS is calculated without accounting for PZ flexure and compared to those obtained from a Krawinkler model, which does not include the column flange hinges. Performing this evaluation ensures that the major elastic strain energy sources have been adequately accounted for to justify attributing all additional deflection determined in a later PANELS versus FEA comparison to the PZ flexure component. Next, elastic FEA models created using ABAQUS (Hibbitt, Karlsson and Sorensen 2001) are used to quantify the total drift of the subassemblage. These results are used to determine the amount of drift to be associated to PZ flexure. Since the stress distribution in the PZ region is highly indeterminate, a means to account for it is established. Using statistics and results from ABAQUS, a scalar to multiply to the moment of inertia in the column and girder PZ flexure formulas in PANELS is developed to overcome this indeterminate stress condition. Finally, an elastic comparison between the Krawinkler model without column flange hinges and the PANELS formulas including PZ flexure will be conducted. This is done to show the significance of not including PZ flexure in the Krawinkler model.

4.2 PANELS vs. Krawinkler (Without Panel Zone Flexure)

To determine the ability of the PANELS equations to accurately predict the deflection of the cruciform subassemblage, a series of analyses was performed comparing their results with the deflection determined from linear elastic Drain-2DX (Prakash at al. 1993) models. The purpose of these analyses was to ensure that all the components of drift calculated by PANELS, except the flexural component in the PZ region, correlate exactly to the results using the Krawinkler model that did not include the inelastic column flange hinge. Since the PZ flexure component involves the highly indeterminate stress condition within the PZ discussed in Chapter 2, it was felt that this comparison was necessary to ensure that the elastic mathematical formulations and the elastic modeling techniques used were correct before addressing the PZ flexure component. The program RAM XLinea (Charney 2000), which acts as a pre-processor, processor and post-processor for Drain-2DX, was used to perform the analysis. Both Drain-2DX and XLinea are used interchangeably as a naming convention for the results determined from these FEA models.

The wide flange sections used were chosen based on the current design practice of strong column/weak beam and are the same used throughout this study. The linear elastic Drain-2DX models were based on the properties derived by Krawinkler in 1978 except that no yielding was allowed to occur in the subassembly. Also, the additional stiffness attributed to plastic hinges developing in the column flanges was not included. This was due to the fact that this phenomenon, which was determined experimentally, is an inelastic contribution and was not included in the PANELS formula derivations. Since the contributions of continuity plates cannot be included in Krawinkler models, these members were not included in the comparisons for this portion of the study. The height (H) was fixed at 150 in. and the length (L) was set equal to 120 in., 240 in. or 360 in.. For the Cruciform and End models, a horizontal 1000-kip force was applied to both the top and bottom of the column. A single 1000-kip horizontal load was placed on the column for the Corner and Tee models. The response was assumed to be elastic even though stresses due to this 1000-kip load may be well in excess of yield.

As seen in Table 4.2-1 and Table 4.2-2 below, there is an exact correlation between the PANELS formulas and the Drain-2DX models when all the elastic deformation components except for PZ flexure are considered. This same procedure was then repeated for the other three subassemblage configurations. Again, in Table 4.2-3 through Table 4.2-8, the PANELS and Krawinkler results are identical. Assuming that the Krawinkler model is complete, this verifies that all the major sources of elastic strain energy other than PZ flexure have been properly accounted for in PANELS.

Table 4.2-1: Cruciform -PANELS vs. Drain-2DX (No Doubler)

Girder	Column	Girder Span (in.)	Doubler Plate	Continuity Plate	Drain-2DX (in.)	PANELS (in.)	% diff.
W36x210	W24x335	120	no	no	1.92	1.92	0.00
		240			2.48	2.48	0.00
		360			3.06	3.06	0.00
W36x135	W24x207	120	no	no	3.17	3.17	0.00
		240			4.18	4.18	0.00
		360			5.17	5.17	0.00
W30x132	W21x201	120	no	no	4.41	4.41	0.00
		240			5.78	5.78	0.00
		360			7.13	7.13	0.00
W30x116	W21x166	120	no	no	5.32	5.32	0.00
		240			6.97	6.97	0.00
		360			8.56	8.56	0.00
W27x178	W30x173	120	no	no	3.69	3.69	0.00
		240			5.05	5.05	0.00
		360			6.24	6.24	0.00
W27x178	W14x426	120	no	no	3.91	3.91	0.00
		240			4.88	4.88	0.00
		360			5.94	5.94	0.00
W21x101	W30x173	120	no	no	5.93	5.93	0.00
		240			9.21	9.21	0.00
		360			12.43	12.43	0.00
W21x101	W14x426	120	no	no	6.65	6.65	0.00
		240			9.45	9.45	0.00
		360			12.51	12.51	0.00

Table 4.2-2: Cruciform - PANELS vs. Drain-2DX (Doubler)

Girder	Column	Girder Span (in.)	Doubler Plate	Continuity Plate	Drain-2DX (in.)	PANELS (in.)	% diff.
W36x210	W24x335	120	yes	no	1.70	1.70	0.00
		240			2.17	2.17	0.00
		360			2.71	2.71	0.00
W36x135	W24x207	120	yes	no	2.78	2.78	0.00
		240			3.63	3.63	0.00
		360			4.57	4.57	0.00
W30x132	W21x201	120	yes	no	3.81	3.81	0.00
		240			5.00	5.00	0.00
		360			6.28	6.28	0.00
W30x116	W21x166	120	yes	no	4.58	4.58	0.00
		240			6.01	6.01	0.00
		360			7.52	7.52	0.00
W27x178	W30x173	120	yes	no	3.12	3.12	0.00
		240			4.21	4.21	0.00
		360			5.30	5.30	0.00
W27x178	W14x426	120	yes	no	3.38	3.38	0.00
		240			4.24	4.24	0.00
		360			5.26	5.26	0.00
W21x101	W30x173	120	yes	no	5.08	5.08	0.00
		240			8.00	8.00	0.00
		360			11.08	11.08	0.00
W21x101	W14x426	120	yes	no	5.87	5.87	0.00
		240			8.54	8.54	0.00
		360			11.54	11.54	0.00

Table 4.2-3: Corner - PANELS vs. Drain-2DX (No Doubler)

Girder	Column	Girder Span (in.)	Doubler Plate	Continuity Plate	Drain-2DX (in.)	PANELS (in.)	% diff.
W36x210	W24x335	120	no	no	0.89	0.89	0.00
		240			1.13	1.13	0.00
		360			1.43	1.43	0.00
W36x135	W24x207	120	no	no	1.46	1.46	0.00
		240			1.88	1.89	0.00
		360			2.40	2.40	0.00
W30x132	W21x201	120	no	no	1.96	1.96	0.00
		240			2.55	2.55	0.00
		360			3.23	3.23	0.00
W30x116	W21x166	120	no	no	2.34	2.34	0.00
		240			3.05	3.05	0.00
		360			3.85	3.85	0.00
W27x178	W30x173	120	no	no	1.61	1.61	0.00
		240			2.12	2.12	0.00
		360			2.69	2.69	0.00
W27x178	W14x426	120	no	no	2.97	2.97	0.00
		240			4.34	4.34	0.00
		360			5.90	5.90	0.00
W21x101	W30x173	120	no	no	2.60	2.60	0.00
		240			4.04	4.04	0.00
		360			5.63	5.63	0.00
W21x101	W14x426	120	no	no	2.97	2.97	0.00
		240			4.33	4.34	0.00
		360			5.90	5.90	0.00

Table 4.2-4: Corner - PANELS vs. Drain-2DX (Doubler Plate)

Girder	Column	Girder Span (in.)	Doubler Plate	Continuity Plate	Drain-2DX (in.)	PANELS (in.)	% diff.
W36x210	W24x335	120	yes	no	0.83	0.83	0.00
		240			1.05	1.05	0.00
		360			1.34	1.34	0.00
W36x135	W24x207	120	yes	no	1.36	1.36	0.00
		240			1.75	1.75	0.00
		360			2.25	2.25	0.00
W30x132	W21x201	120	yes	no	1.81	1.81	0.00
		240			2.35	2.35	0.00
		360			3.02	3.02	0.00
W30x116	W21x166	120	yes	no	2.16	2.16	0.00
		240			2.81	2.81	0.00
		360			3.59	3.59	0.00
W27x178	W30x173	120	yes	no	1.47	1.47	0.00
		240			1.91	1.91	0.00
		360			2.46	2.46	0.00
W27x178	W14x426	120	yes	no	1.58	1.58	0.00
		240			1.99	1.99	0.00
		360			2.52	2.52	0.00
W21x101	W30x173	120	yes	no	2.38	2.38	0.00
		240			3.74	3.74	0.00
		360			5.30	5.30	0.00
W21x101	W14x426	120	yes	no	2.77	2.77	0.00
		240			4.11	4.11	0.00
		360			5.66	5.66	0.00

Table 4.2-5: End - PANELS vs. Drain-2DX (No Doubler)

Girder	Column	Girder Span (in.)	Doubler Plate	Continuity Plate	Drain-2DX (in.)	PANELS (in.)	% diff.
W36x210	W24x335	120	no	no	2.79	2.79	0.00
		240			3.62	3.62	0.00
		360			4.67	4.67	0.00
W36x135	W24x207	120	no	no	4.53	4.53	0.00
		240			6.04	6.04	0.00
		360			7.86	7.86	0.00
W30x132	W21x201	120	no	no	6.15	6.15	0.00
		240			8.29	8.29	0.00
		360			10.80	10.80	0.00
W30x116	W21x166	120	no	no	7.31	7.31	0.00
		240			9.89	9.89	0.00
		360			12.85	12.85	0.00
W27x178	W30x173	120	no	no	5.08	5.08	0.00
		240			6.99	6.99	0.00
		360			9.10	9.10	0.00
W27x178	W14x426	120	no	no	10.29	10.29	0.00
		240			15.48	15.48	0.00
		360			21.46	21.46	0.00
W21x101	W30x173	120	no	no	8.81	8.81	0.00
		240			14.33	14.33	0.00
		360			20.41	20.41	0.00
W21x101	W14x426	120	no	no	10.29	10.29	0.00
		240			15.48	15.48	0.00
		360			21.46	21.46	0.00

Table 4.2-6: End - PANELS vs. Drain-2DX (Doubler Plate)

Girder	Column	Girder Span (in.)	Doubler Plate	Continuity Plate	Drain-2DX (in.)	PANELS (in.)	% diff.
W36x210	W24x335	120	yes	no	2.57	2.57	0.00
		240			3.30	3.30	0.00
		360			4.33	4.33	0.00
W36x135	W24x207	120	yes	no	4.14	4.14	0.00
		240			5.49	5.49	0.00
		360			7.26	7.26	0.00
W30x132	W21x201	120	yes	no	5.55	5.55	0.00
		240			7.51	7.51	0.00
		360			9.95	9.95	0.00
W30x116	W21x166	120	yes	no	6.57	6.57	0.00
		240			8.93	8.93	0.00
		360			11.81	11.81	0.00
W27x178	W30x173	120	yes	no	4.51	4.51	0.00
		240			6.15	6.15	0.00
		360			8.16	8.16	0.00
W27x178	W14x426	120	yes	no	4.97	4.97	0.00
		240			6.48	6.48	0.00
		360			8.45	8.45	0.00
W21x101	W30x173	120	yes	no	7.97	7.97	0.00
		240			13.12	13.12	0.00
		360			19.06	19.06	0.00
W21x101	W14x426	120	yes	no	9.51	9.51	0.00
		240			14.56	14.56	0.00
		360			20.49	20.49	0.00

Table 4.2-7: Tee - PANELS vs. Drain-2DX (No Doubler)

Girder	Column	Girder Span (in.)	Doubler Plate	Continuity Plate	Drain-2DX (in.)	PANELS (in.)	% diff.
W36x210	W24x335	120	no	no	0.67	0.67	0.00
		240			0.85	0.85	0.00
		360			1.02	1.02	0.00
W36x135	W24x207	120	no	no	1.12	1.12	0.00
		240			1.42	1.42	0.00
		360			1.72	1.72	0.00
W30x132	W21x201	120	no	no	1.52	1.52	0.00
		240			1.92	1.92	0.00
		360			2.31	2.31	0.00
W30x116	W21x166	120	no	no	1.85	1.85	0.00
		240			2.32	2.32	0.00
		360			2.78	2.78	0.00
W27x178	W30x173	120	no	no	1.26	1.26	0.00
		240			1.64	1.64	0.00
		360			1.98	1.98	0.00
W27x178	W14x426	120	no	no	2.06	2.06	0.00
		240			2.83	2.83	0.00
		360			3.66	3.66	0.00
W21x101	W30x173	120	no	no	1.87	1.87	0.00
		240			2.76	2.76	0.00
		360			3.64	3.64	0.00
W21x101	W14x426	120	no	no	2.06	2.06	0.00
		240			2.83	2.83	0.00
		360			3.66	3.66	0.00

Table 4.2-8: Tee - PANELS vs. Drain-2DX (Doubler)

Girder	Column	Girder Span (in.)	Doubler Plate	Continuity Plate	Drain-2DX (in.)	PANELS (in.)	% diff.
W36x210	W24x335	120	yes	no	0.62	0.62	0.00
		240			0.77	0.77	0.00
		360			0.94	0.94	0.00
W36x135	W24x207	120	yes	no	1.02	1.02	0.00
		240			1.29	1.29	0.00
		360			1.57	1.57	0.00
W30x132	W21x201	120	yes	no	1.38	1.38	0.00
		240			1.72	1.72	0.00
		360			2.10	2.10	0.00
W30x116	W21x166	120	yes	no	1.66	1.66	0.00
		240			2.08	2.08	0.00
		360			2.52	2.52	0.00
W27x178	W30x173	120	yes	no	1.12	1.12	0.00
		240			1.43	1.43	0.00
		360			1.74	1.74	0.00
W27x178	W14x426	120	yes	no	1.18	1.18	0.00
		240			1.43	1.43	0.00
		360			1.72	1.73	0.00
W21x101	W30x173	120	yes	no	1.66	1.66	0.00
		240			2.46	2.46	0.00
		360			3.30	3.30	0.00
W21x101	W14x426	120	yes	no	1.86	1.86	0.00
		240			2.60	2.60	0.00
		360			3.42	3.42	0.00

4.3 ABAQUS Models

The next segment of this research was to develop a finite element model of the beam/column joint to determine how to account for the drift contribution due to PZ flexure in PANELS and to examine the effects of including continuity plates in the beam/column joint. The program ABAQUS was selected to perform this task. It was chosen based on its reputation as an excellent linear/nonlinear finite element analysis tool, which would allow the development of a model that could also be used later for inelastic comparisons.

To model the component of each subassembly, a 4-node shell element (S4) was chosen. According to the ABAQUS User's Manual (Hibbitt et al. 2001), this element is a general-purpose element that can be used to model both thick and thin shell sections. Transverse shear deformations and through-thickness strains become more important as the material becomes thicker. Unlike some other ABAQUS shell elements, the S4 element has no actual thickness.

One drawback with using shell elements to model wide flange sections is the overlap of material at the interface of the webs and flanges shown in Figure 4.3-1. This problem is exacerbated when continuity plates and doubler plates are also included. To account for this doubling of material, the thicknesses of the shells were reduced by scaling them based on the excess of moment of inertia created by the overlap. At the flange/web interface, the thickness of the flanges was reduced, leaving the web thickness constant. The continuity plate's and doubler plate's individual shell thicknesses were adjusted in the same manner. Again looking at Figure 4.3-1, another point that should be made is that the models created in ABAQUS did not include the fillets at the interface of rolled wide flange sections' webs and flanges.

Figure 4.3-1: Material Overlap of Shell Elements

To simulate the rigid interface that occurs at the boundary of the flanges and webs of rolled wide flange sections, all six degrees of freedom of the nodes that coincided at these interfaces were constrained using the ABAQUS "Tie" option. The area of these constraints was then set equal to the surface area of the flange/web interface. When they were included, the "Tie" option was also used to constrain the continuity plates to the column web and flanges to simulate the welds used to attach these members.

To eliminate the effects of local stress concentrations at the support nodes and at the nodes where the horizontal load was applied, plates made of rigid elements (R3D4) were attached to the structure. The loads were then applied as a body force throughout the volume of the rigid plate to distribute them evenly across the width of the top and the bottom of the column.

Before any subassemblages were created, a simple cantilever model, shown in its deformed configuration in Figure 4.3-2, was built and analyzed, comparing its deflections to the theoretical results considering displacement due to shear and flexure. This was done to ensure that the technique used to reduce the model's shell thickness and the constraint methods used gave results similar to those found in accordance to elastic beam theory. For this model, the nodes on the top of the model were given a fixed boundary condition. A horizontal load of 1000-kips was then applied at the free end as a body force throughout the volume of the rigid plate. While this 1000-kip load could cause significant yielding in an inelastic cantilever model, this large of a force has no bearing

on the elastic results presented. For use in the hand calculations, tip deflection was computed as:

$$\delta = \frac{VL^3}{3EI} + \frac{VL}{GA^*} \quad \text{.....(4.3-1)}$$

with the shear area (A^*) calculated using:

$$A^* = \left(d_{c,nom} - t_{cf}\right)t_{cw} \quad \text{.....(4.3-2)}$$

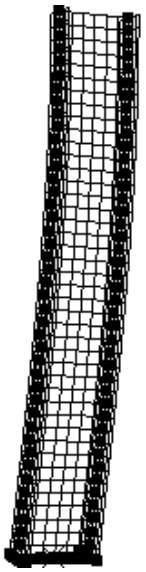

Figure 4.3-2: Deformed ABAQUS Cantilever Model

The results from this cantilever comparison are shown below in Table 4.3-1.

Table 4.3-1: ABAQUS Cantilever Model: Results

Section	Shear Area $(in.^2)$	I $(in.^4)$	Length (in.)	Flexure $\frac{VL^3}{3EI}$ (in.)	Shear $\frac{VL}{GA^*}$ (in.)	Total (in.)	ABAQUS (in.)	% diff.
W36x300	33.09	20300	120	2.41	0.56	2.97	3.08	3.59
			240	19.31	1.12	20.43	20.89	2.22
			360	65.16	1.68	66.84	68.04	1.76
W14x730	53.69	14300	120	0.98	0.33	1.30	1.35	3.30
			240	7.83	0.65	8.48	8.65	1.99
			360	26.42	0.98	27.39	27.80	1.46
W14x426	29.44	6600	120	1.39	0.20	1.59	1.60	0.61
			240	11.11	0.40	11.51	11.44	0.63
			360	37.50	0.60	38.10	37.69	1.10
W27x178	19.29	7020	120	3.01	0.37	3.37	3.42	1.32
			240	24.08	0.73	24.81	24.80	0.02
			360	81.25	1.10	82.35	81.85	0.61
W21x101	10.30	2420	120	2.83	0.56	3.39	3.51	3.39
			240	22.63	1.12	23.75	24.27	2.14
			360	76.39	1.67	78.07	79.41	1.69
W14x132	8.82	1530	120	8.21	1.04	9.25	9.47	2.27
			240	65.66	2.09	67.75	68.53	1.14
			360	221.60	3.13	224.74	226.40	0.74
W24x94	12.06	2700	120	12.98	1.22	14.20	14.55	2.39
			240	103.85	2.44	106.29	107.40	1.03
			360	350.51	3.66	354.17	356.20	0.57

Looking at the results above, it is observed that the methods used to model the test sections give results that are very close to what was predicted using basic mechanics. While they may be considered slightly on the flexible side, the exact amount of shear area that resists shear deformation in this model is indeterminate. The use of Equation 4.3-2 is just an estimation and will create some variability. Also, the moment of inertia values in Table 4.3-1 included the additional moment of inertia due to the fillets. The additional material associated with the fillets would cause the moment of inertia calculated using Equation 4.3-1 to be more than the ABAQUS values. The larger errors in Table 4.3-1 are for the shorter spans, indicating an error in the shear area. Considering that the results for all of the 360-in. span models are within 2 percent, the modeling techniques used should be considered adequate. The conclusions of this chapter would not have changed even if we obtained an exact correlation here.

With the adjustments to the ABAQUS model deemed accurate, a number of cruciform models were created using the same wide flange sections previously used in the PANELS versus Krawinkler elastic comparison. An example of a deformed model is shown in Figure 4.3-3. The nodes that are observed in this figure are ABAQUS's graphic representation of the node-based constraints that were applied to the model. When used, the doubler plates were sized using ¾ of the thickness of the column web rounded to the nearest $^{1}/_{16}$ of an in.. Instead of including additional shell elements to model the doubler plates, the thickness of the doubler plate was added to the thickness of the column web shells in the PZ region. Modeling the PZ in this manner assumes that plug welds are used to connect the doubler plate to the column web. The continuity plates' thicknesses were set equal to the thickness of the girder flange and were also rounded to the nearest $^{1}/_{16}$ of an in.. The column height (H) was fixed at 150 in. and the distance between supports (L) was set equal to 120, 240 or 360 in..

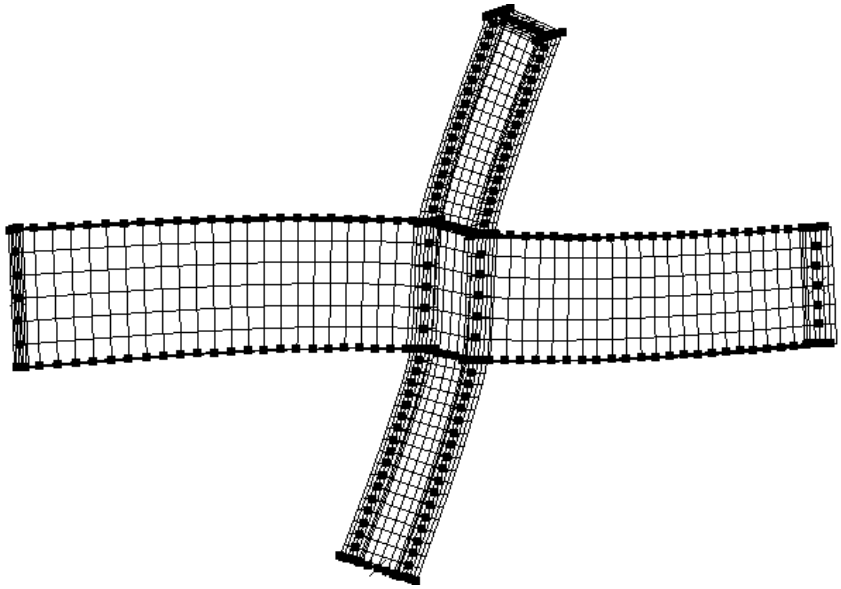

Figure 4.3-3: Deformed ABAQUS Cruciform Subassembly

One verification besides force equilibrium, which was also checked, for determining whether the FEA model was correct is that the stress distributions of the members in the Cruciform model had to display symmetry. As seen in Figure 4.3-4, the models in this study exhibited this behavior.

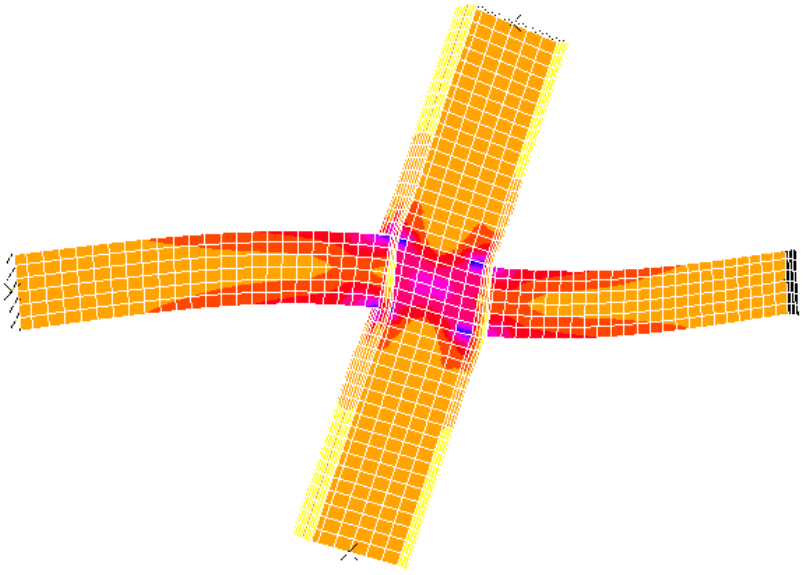

Figure 4.3-4: Stress Distribution of ABAQUS Cruciform Subassembly

4.4 Modeling Approach for Panel Zone Flexure and Continuity Plates

With the results from ABAQUS now available, the next step was to determine how to account for the flexural deformation component and the continuity plates in PANELS. Unfortunately, the Krawinkler model in its current form cannot include continuity plates. This not only eliminated any elastic strain energy comparisons but required an assumption to be made as to what influence continuity plates have on the shear and flexural components of drift in the PZ region. Since the continuity plates do not contribute to the calculated shear area, their contribution in the PANELS equations was considered to be in girder flexural deformation only.

Due to the highly indeterminate stress conditions inside the PZ region, the moment of inertia used for flexural deformation for the columns and girder is difficult to determine. In previous research (Charney and Johnson, 1986), the moment of inertia of the girder was chosen to be used for I_{PZ} in the girder PZ flexure formula, Equation 2.3-15, and the moment of inertia of the column I_{Col}, Equation 2.3-13, for the column's contribution. In the research described herein, this and three other options were investigated to determine the best way to handle the unknown. Originally for all four options investigated, the full moment of inertia of the column, I_{Col}, was used for the column PZ flexure contribution. This was done because of the difficulty associated with adjusting two unknown values at one time. Once an accurate method of computing I_{PZ} was determined, the validity of using I_{Col} was investigated. I_{PZ} was chosen to be adjusted first because it was felt that there would be more variability associated with it. Unlike the column, the girder does not actually pass through the beam/column joint. Being able to isolate I_{PZ} would make accounting for I_{Col} much simpler.

Initially, it was established that using the full moment of inertia of the girder, done previously, resulted in a PANELS model that was too stiff when compared to the ABAQUS results. To account for this overestimation of stiffness, a multiplier of 0.7 on the moment of inertia of the girder was included, which gave better results. Seeing that it

made sense that the calculated moment of inertial of the PZ region based on individual plates defining the components of the beam/column joint, I_{PL}, should be included in the development of its flexural contribution, it was used in all three of the remaining options. The other three values for I_{PZ} investigated are:

1. I_{PL} + 0.25 I of Column
2. I_{PL} + 0.3 I of Girder
3. $1.7I_{Col,PZT} + I_{Cont}$

where I_{PL} is equal to

$$I_{PL} = I_{Col,PZT} + I_{Cont}$$

$$= \frac{t_{PZ}\beta H^3}{12} + \frac{2(bf_c - tw_c)(t_{Cont})^3}{12} + 2(bf_c - tw_c)t_{Cont}\left(\frac{\beta H}{2}\right)^2 \quad \text{.....(4.4-1)}$$

Using this formulation again ignores the fillets associated with wide-flange sections.

In the subsequent tables, Table 4.4-1 through Table 4.4-4, are the comparisons of the four different ways of handling the variability in I_{PZ} that were investigated using the same combinations of cross-sections that were used in Section 4.2. The results presented in these tables are based on the percent difference values comparing the total drift calculated by PANELS using one of the previously defined methods to account for PZ flexure with the ABAQUS models. The minimum, maximum and average of the values, the sum of the squares of deviation (DEVSQ), the standard deviation (STD) and finally the variance (VAR) were determined on models that were analyzed with and without continuity and doubler plates and a combination of the two. The formulas for the statistical calculations are given below.

$$DEVSQ = \sum (x - Avg)^2 \quad \text{.....(4.4-2)}$$

$$STD = \sqrt{\frac{n\sum x^2 - \left(\sum x\right)^2}{n(n-1)}} \quad \text{.....(4.4-3)}$$

$$VAR = \frac{n\sum x^2 - \left(\sum x\right)^2}{n(n-1)} \quad \text{.....(4.4-4)}$$

Looking at Table 4.4-1 through Table 4.4-3, it is observed that the three equations that included the moment of inertia of members outside the PZ region create a lot of variation in their results. Not only is there a large disparity between the minimum and maximum values, it is also evident in the statistical evaluations that were performed. Using $1.7I_{Col,PZT} + I_{Cont}$ (Table 4.4-4) for determining the moment of inertia used to calculate the girder component of PZ flexure compared well with the PANELS results. There was little disparity between the minimum and maximum values, and the studies performed showed that the results correlated well with each other. Upon completion of this assessment, it was decided that using 1.7 times the calculated moment of inertia of the plate plus the unfactored moment of inertia of the continuity plate gave the best results. It is debatable that the scalar could be reduced a small amount to bring the average percent difference closer to unity. This was not done due to the desire to present as simple a scaling factor as possible, which still resulted in calculated deflections that correlated well with the ABAQUS model data.

Table 4.4-1: PANELS Formulas vs. ABAQUS with 0.7 I of Girder

	Doubler: no Continuity: no	Doubler: yes Continuity: no	Doubler: no Continuity: yes	Doubler: yes Continuity: yes
Max	10.81	9.74	1.45	1.87
Min	-5.60	-4.22	-3.99	-3.37
Avg	1.33	1.39	-0.77	-0.04
DEVSQ	673.39	429.49	56.14	38.27
STD	5.41	4.32	1.56	1.29
Var	29.28	18.67	2.44	1.66

Table 4.4-2: PANELS Formulas vs. ABAQUS with I_{PL} + 0.25 I of Column

	Doubler: no Continuity: no	Doubler: yes Continuity: no	Doubler: no Continuity: yes	Doubler: yes Continuity: yes
Max	13.03	11.96	3.11	3.62
Min	-2.22	-1.25	-2.40	0.38
Avg	3.92	4.07	0.03	1.43
DEVSQ	616.18	521.45	58.05	54.63
STD	5.18	4.76	1.59	1.54
Var	26.79	22.67	2.52	2.38

Table 4.4-3: PANELS Formulas vs. ABAQUS with I_{PL} + 0.3 I of Girder

	Doubler: no Continuity: no	Doubler: yes Continuity: no	Doubler: no Continuity: yes	Doubler: yes Continuity: yes
Max	7.45	5.75	1.65	1.94
Min	-4.12	-4.43	-3.13	-2.99
Avg	0.58	0.34	-0.52	0.24
DEVSQ	318.18	155.86	40.46	31.31
STD	3.72	2.60	1.33	1.17
Var	13.83	6.78	1.76	1.36

Table 4.4-4: PANELS Formulas vs. ABAQUS with $1.7I_{Col,PZT} + I_{Cont}$

	Doubler: no Continuity: no	Doubler: yes Continuity: no	Doubler: no Continuity: yes	Doubler: yes Continuity: yes
Max	0.42	0.07	1.01	1.21
Min	-3.50	-4.90	-2.74	-0.29
Avg	-1.76	-2.09	-0.63	0.69
DEVSQ	51.19	55.61	29.90	25.48
STD	1.49	1.55	1.14	1.05
Var	2.23	2.42	1.30	1.11

To verify the effectiveness of the proposed multiplier to emulate the stress relationship occurring in the PZ region, moment diagrams were generated using the ABAQUS results and compared to the proposed theoretical equation. For the example shown in Figure 4.4-1, a 240-in. W27x178 girder and a 150-in. W30x173 column with two ½-in. thick double plates and 1-$^{3}/_{16}$ in. continuity plates were used. As seen in Figure 4.4-1, the proposed equation matches very well to the ABAQUS results.

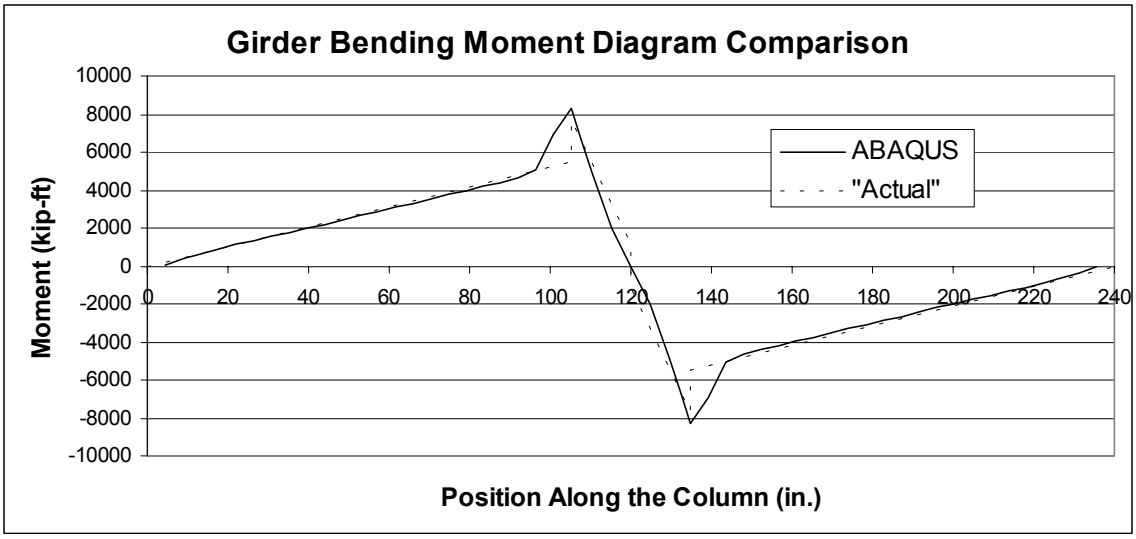

Figure 4.4-1: Girder Bending Moment Diagram Comparison

The same procedure was then performed on the column of the ABAQUS model to determine if this jump in bending moment occurred in the columns as well. As seen in Figure 4.4-2, it did occur. To account for this, the scaling factor of 1.7 used in the girder PZ flexure formula was reduced to 1.5 and this new multiplier was also included in the column PZ flexure formula, changing Equation 2.3-13 to:

$$Actual\ \delta_{PZ,CF} = \frac{VH^3\beta}{6EI_{Col}}\left[\alpha(1-\beta)+\frac{(1-\alpha-\beta)^2}{3}\right] \quad \text{.....(4.4-3)}$$

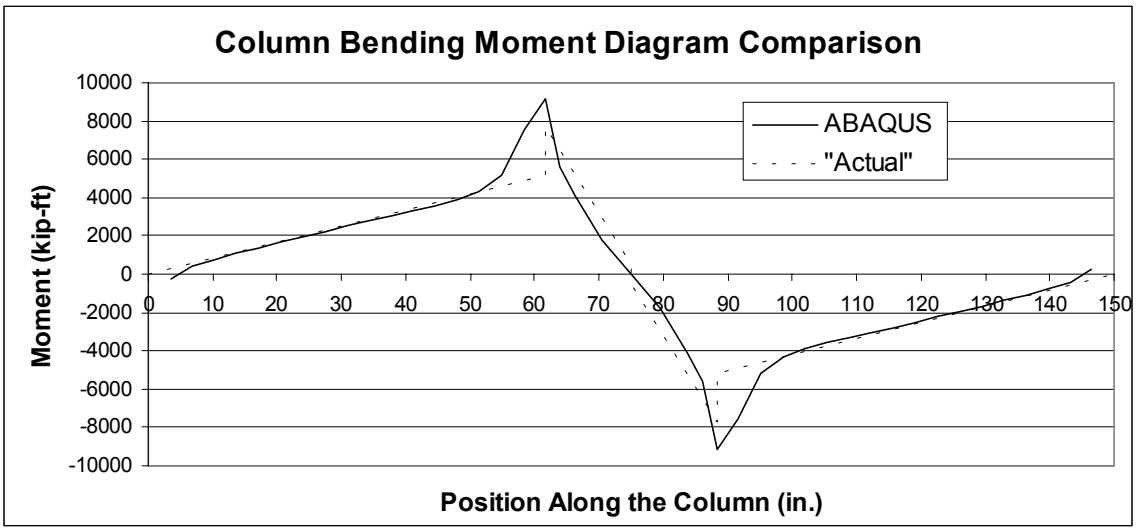

Figure 4.4-2: Column Bending Moment Diagram Comparison

The new statistical results due to this change are shown in Table 4.4-5. While the values did change some, the results are still statistically sound.

Table 4.4-5: PANELS Formulas vs. ABAQUS with 1.5 x I

	Doubler: no Continuity: no	Doubler: yes Continuity: no	Doubler: no Continuity: yes	Doubler: yes Continuity: yes
Max	1.20	5.12	1.65	2.85
Min	-3.61	0.89	-2.04	0.28
Avg	-1.28	3.17	0.43	1.98
DEVSQ	63.58	34.57	24.72	8.82
STD	1.66	1.23	1.04	0.62
Var	2.76	1.50	1.07	0.38

The effect of using the 1.5 multiplier for the column and PZ moment of inertia versus the deflections determined using ABAQUS for all the analytical comparisons performed are shown in Table 4.4-6 through Table 4.4-9. In these examples, the same eight different column/girder cruciform configurations used previously were compared. The girder spans were again varied and effects of continuity and doubler plate were examined.

Table 4.4-6: Cruciform - PANELS vs. ABAQUS (No Doubler, No Continuity)

Girder	Column	Span (in.)	Doubler Plate	Continuity Plate	PANELS (in.)	ABAQUS (in.)	% diff.
W36x210	W24x335	120	no	no	2.20	2.15	2.56
		240			2.80	2.75	1.67
		360			3.38	3.34	1.32
W36x135	W24x207	120	no	no	3.64	3.66	0.55
		240			4.69	4.74	1.16
		360			5.70	5.76	1.20
W30x132	W21x201	120	no	no	5.03	5.01	0.44
		240			6.46	6.47	0.20
		360			7.83	7.86	0.38
W30x116	W21x166	120	no	no	6.08	6.11	0.49
		240			7.80	7.87	0.98
		360			9.42	9.51	1.00
W27x178	W30x173	120	no	no	4.72	4.61	2.43
		240			6.33	6.26	1.23
		360			7.62	7.55	0.87
W27x178	W14x426	120	no	no	4.27	4.19	3.40
		240			5.26	5.18	1.55
		360			6.32	6.24	1.25
W21x101	W30x173	120	no	no	7.87	7.60	3.61
		240			11.71	11.42	2.57
		360			15.13	14.82	2.12
W21x101	W14x426	120	no	no	7.21	6.97	3.40
		240			10.06	9.77	3.02
		360			13.14	12.82	2.50

Table 4.4-7: Cruciform - PANELS vs. ABAQUS (Doubler, No Continuity)

Girder	Column	Span (in.)	Doubler Plate	Continuity Plate	PANELS (in.)	ABAQUS (in.)	% diff.
W36x210	W24x335	120	yes	no	1.90	1.92	0.89
		240			2.39	2.43	1.81
		360			2.93	2.99	1.81
W36x135	W24x207	120	yes	no	3.12	3.23	3.29
		240			3.98	4.15	3.91
		360			4.92	5.11	3.58
W30x132	W21x201	120	yes	no	4.25	4.38	2.95
		240			5.46	5.65	3.45
		360			6.75	6.97	3.24
W30x116	W21x166	120	yes	no	5.12	5.31	3.65
		240			6.57	6.85	3.99
		360			8.10	8.40	3.63
W27x178	W30x173	120	yes	no	3.76	3.92	4.06
		240			4.99	5.25	5.12
		360			6.13	6.43	4.80
W27x178	W14x426	120	yes	no	3.64	3.75	2.88
		240			4.51	4.64	2.93
		360			5.53	5.67	2.57
W21x101	W30x173	120	yes	no	6.23	6.55	4.80
		240			9.46	9.93	4.76
		360			12.65	13.17	3.94
W21x101	W14x426	120	yes	no	6.24	6.36	1.87
		240			8.93	9.05	1.30
		360			11.94	12.05	0.94

Table 4.4-8: Cruciform - PANELS vs. ABAQUS (No Doubler, Continuity)

Girder	Column	Span (in.)	Doubler Plate	Continuity Plate	PANELS (in.)	ABAQUS (in.)	% diff.
W36x210	W24x335	120	no	yes	2.10	2.08	1.01
		240			2.67	2.66	0.38
		360			3.24	3.24	0.00
W36x135	W24x207	120	no	yes	3.48	3.51	1.00
		240			4.48	4.54	1.23
		360			5.48	5.54	1.23
W30x132	W21x201	120	no	yes	4.76	4.79	0.69
		240			6.14	6.20	1.02
		360			7.49	7.57	1.07
W30x116	W21x166	120	no	yes	5.74	5.81	1.20
		240			7.40	7.50	1.40
		360			8.99	9.12	1.36
W27x178	W30x173	120	no	yes	4.00	4.04	1.01
		240			5.40	5.46	1.19
		360			6.60	6.68	1.15
W27x178	W14x426	120	no	yes	4.14	4.12	0.41
		240			5.11	5.10	0.27
		360			6.17	6.15	0.21
W21x101	W30x173	120	no	yes	6.45	6.56	1.65
		240			9.84	9.96	1.20
		360			13.10	13.22	0.89
W21x101	W14x426	120	no	yes	6.96	6.82	2.04
		240			9.79	9.66	1.27
		360			12.85	12.70	1.12

Table 4.4-9: Cruciform - PANELS vs. ABAQUS (Doubler, Continuity)

Girder	Column	Span (in.)	Doubler Plate	Continuity Plate	PANELS (in.)	ABAQUS (in.)	% diff.
W36x210	W24x335	120	yes	yes	1.86	1.86	0.00
		240			2.33	2.36	0.98
		360			2.88	2.91	1.07
W36x135	W24x207	120	yes	yes	3.05	3.11	1.83
		240			3.90	3.99	2.25
		360			4.84	4.94	2.11
W30x132	W21x201	120	yes	yes	4.13	4.21	1.85
		240			5.32	5.44	2.24
		360			6.60	6.74	2.15
W30x116	W21x166	120	yes	yes	4.97	5.08	2.24
		240			6.40	6.55	2.43
		360			7.91	8.09	2.26
W27x178	W30x173	120	yes	yes	3.41	3.48	2.04
		240			4.53	4.64	2.37
		360			5.63	5.75	2.04
W27x178	W14x426	120	yes	yes	3.59	3.69	2.74
		240			4.45	4.57	2.71
		360			5.47	5.60	2.37
W21x101	W30x173	120	yes	yes	5.55	5.72	2.85
		240			8.57	8.77	2.28
		360			11.68	11.89	1.75
W21x101	W14x426	120	yes	yes	6.14	6.28	2.17
		240			8.82	8.95	1.45
		360			11.83	11.95	1.05

The preceding analysis process was then repeated on the Corner, End and Tee subassemblages. Since the overall area of influence of the stress in the PZ is different for each subassembly, the scaling factor for I_{PZ} will be different for each. In addition, the force interactions in these subassemblies are no longer symmetric. Not only are axial forces not present in the columns and girders, but the PZ region's highly indeterminate stress distributions become even more convoluted, making an accurate assessment difficult at best. Both of these combine to increase the likelihood of errors in ascertaining a reliable factor to estimate the drift contribution of these three subassemblages. Therefore, instead of determining a new multiplier for each, 1.5 is still used. The results for the remaining three subassemblages are shown in Table 4.4-10 through Table 4.4-21. While this does create a debatable point, it should be noted that the total number of these three subassemblages only accounts for around twenty percent of all the subassemblages in the entire structure. Since this is just one component of the total assembly's drift, this increased probability of error will not significantly affect the structure's total estimated drift.

Table 4.4-10: Corner - PANELS vs. ABAQUS (No Doubler, No Continuity)

Girder	Column	Span (in.)	Doubler Plate	Continuity Plate	PANELS (in.)	ABAQUS (in.)	% diff.
W36x210	W24x335	120	no	no	1.15	1.17	1.20
		240			1.43	1.46	2.20
		360			1.73	1.77	2.26
W36x135	W24x207	120	no	no	1.90	1.97	3.31
		240			2.38	2.48	4.00
		360			2.91	3.02	3.68
W30x132	W21x201	120	no	no	2.54	2.62	3.13
		240			3.19	3.32	3.97
		360			3.89	4.04	3.78
W30x116	W21x166	120	no	no	3.06	3.18	3.68
		240			3.84	4.01	4.36
		360			4.67	4.86	4.09
W27x178	W30x173	120	no	no	2.60	2.57	1.40
		240			3.26	3.37	3.09
		360			3.89	4.04	3.86
W27x178	W14x426	120	no	no	3.51	3.61	2.96
		240			4.91	5.05	2.75
		360			6.49	6.64	2.26
W21x101	W30x173	120	no	no	4.60	4.35	5.89
		240			6.34	6.35	0.13
		360			8.04	8.14	1.18
W21x101	W14x426	120	no	no	3.51	3.61	2.96
		240			4.91	5.05	2.75
		360			6.49	6.64	2.26

Table 4.4-11: Corner - PANELS vs. ABAQUS (Doubler, No Continuity)

Girder	Column	Span (in.)	Doubler Plate	Continuity Plate	PANELS (in.)	ABAQUS (in.)	% diff.
W36x210	W24x335	120	yes	no	1.03	1.07	3.28
		240			1.27	1.32	3.71
		360			1.57	1.62	3.39
W36x135	W24x207	120	yes	no	1.69	1.78	4.68
		240			2.12	2.23	4.85
		360			2.63	2.74	4.34
W30x132	W21x201	120	yes	no	2.23	2.36	5.14
		240			2.82	2.98	5.40
		360			3.50	3.68	4.87
W30x116	W21x166	120	yes	no	2.69	2.84	5.52
		240			3.39	3.59	5.66
		360			4.18	4.41	5.08
W27x178	W30x173	120	yes	no	2.08	2.20	5.49
		240			2.62	2.86	8.49
		360			3.20	3.48	8.24
W27x178	W14x426	120	yes	no	1.85	1.96	5.52
		240			2.29	2.41	5.19
		360			2.82	2.96	4.60
W21x101	W30x173	120	yes	no	3.57	3.73	4.47
		240			5.09	5.50	7.43
		360			6.71	7.20	6.82
W21x101	W14x426	120	yes	no	3.14	3.34	5.94
		240			4.49	4.72	4.87
		360			6.05	6.29	3.81

Table 4.4-12: Corner - PANELS vs. ABAQUS (No Doubler, Continuity)

Girder	Column	Span (in.)	Doubler Plate	Continuity Plate	PANELS (in.)	ABAQUS (in.)	% diff.
W36x210	W24x335	120	no	yes	1.07	1.07	0.00
		240			1.32	1.32	0.00
		360			1.63	1.63	0.00
W36x135	W24x207	120	no	yes	1.76	1.78	1.18
		240			2.22	2.24	0.76
		360			2.74	2.76	0.62
W30x132	W21x201	120	no	yes	2.31	2.34	1.41
		240			2.93	2.97	1.21
		360			3.62	3.66	1.12
W30x116	W21x166	120	no	yes	2.77	2.81	1.60
		240			3.51	3.56	1.27
		360			4.33	4.38	1.14
W27x178	W30x173	120	no	yes	1.91	1.94	1.39
		240			2.46	2.50	1.60
		360			3.05	3.09	1.52
W27x178	W14x426	120	no	yes	1.95	1.99	1.76
		240			2.42	2.45	1.27
		360			2.96	2.99	1.14
W21x101	W30x173	120	no	yes	3.12	3.15	0.73
		240			4.65	4.71	1.32
		360			6.26	6.34	1.20
W21x101	W14x426	120	no	yes	3.28	3.35	2.09
		240			4.67	4.74	1.46
		360			6.24	6.31	1.09

Table 4.4-13: Corner - PANELS vs. ABAQUS (Doubler, Continuity)

Girder	Column	Span (in.)	Doubler Plate	Continuity Plate	PANELS (in.)	ABAQUS (in.)	% diff.
W36x210	W24x335	120	yes	yes	1.00	1.00	0.00
		240			1.23	1.23	0.00
		360			1.52	1.53	0.26
W36x135	W24x207	120	yes	yes	1.64	1.66	1.21
		240			2.05	2.07	0.82
		360			2.56	2.58	0.70
W30x132	W21x201	120	yes	yes	2.13	2.17	1.61
		240			2.71	2.75	1.46
		360			3.38	3.43	1.34
W30x116	W21x166	120	yes	yes	2.56	2.60	1.65
		240			3.24	3.29	1.37
		360			4.03	4.08	1.22
W27x178	W30x173	120	yes	yes	1.75	1.78	1.69
		240			2.23	2.28	1.93
		360			2.79	2.84	1.83
W27x178	W14x426	120	yes	yes	1.80	1.86	2.91
		240			2.24	2.29	2.40
		360			2.77	2.83	2.08
W21x101	W30x173	120	yes	yes	2.86	2.90	1.55
		240			4.28	4.37	1.95
		360			5.86	5.96	1.66
W21x101	W14x426	120	yes	yes	3.05	3.16	3.54
		240			4.40	4.51	2.57
		360			5.96	6.07	1.91

Table 4.4-14: End - PANELS vs. ABAQUS (No Doubler, No Continuity)

Girder	Column	Span (in.)	Doubler Plate	Continuity Plate	PANELS (in.)	ABAQUS (in.)	% diff.
W36x210	W24x335	120	no	no	3.32	3.38	1.63
		240			4.22	4.33	2.65
		360			5.30	5.44	2.57
W36x135	W24x207	120	no	no	5.40	5.67	4.85
		240			7.01	7.41	5.40
		360			8.88	9.34	4.87
W30x132	W21x201	120	no	no	7.34	7.63	3.79
		240			9.63	10.08	4.44
		360			12.19	12.71	4.12
W30x116	W21x166	120	no	no	8.77	9.22	4.87
		240			11.52	12.17	5.31
		360			14.55	15.28	4.81
W27x178	W30x173	120	no	no	7.44	7.56	1.59
		240			9.87	10.30	4.17
		360			12.17	12.72	4.31
W27x178	W14x426	120	no	no	11.47	11.42	0.39
		240			16.78	16.72	0.33
		360			22.80	22.72	0.33
W21x101	W30x173	120	no	no	13.58	13.29	2.18
		240			20.23	20.32	0.43
		360			26.72	26.94	0.81
W21x101	W14x426	120	no	no	11.47	11.42	0.39
		240			16.78	16.72	0.33
		360			22.80	22.72	0.33

Table 4.4-15: End - PANELS vs. ABAQUS (Doubler, No Continuity)

Girder	Column	Span (in.)	Doubler Plate	Continuity Plate	PANELS (in.)	ABAQUS (in.)	% diff.
W36x210	W24x335	120	yes	no	2.91	3.07	5.15
		240			3.68	3.92	6.00
		360			4.72	4.98	5.30
W36x135	W24x207	120	yes	no	4.70	5.09	7.70
		240			6.10	6.63	7.98
		360			7.89	8.48	6.89
W30x132	W21x201	120	yes	no	6.31	6.81	7.38
		240			8.35	9.03	7.55
		360			10.81	11.58	6.62
W30x116	W21x166	120	yes	no	7.51	8.18	8.24
		240			9.96	10.84	8.20
		360			12.87	13.85	7.10
W27x178	W30x173	120	yes	no	5.91	6.55	9.79
		240			7.83	8.85	11.55
		360			9.95	11.12	10.48
W27x178	W14x426	120	yes	no	5.39	5.74	5.98
		240			6.93	7.35	5.73
		360			8.91	9.36	4.88
W21x101	W30x173	120	yes	no	10.72	11.72	8.53
		240			16.51	18.12	8.89
		360			22.68	24.50	7.43
W21x101	W14x426	120	yes	no	10.23	10.69	4.26
		240			15.35	15.85	3.21
		360			21.29	21.82	2.42

Table 4.4-16: End - PANELS vs. ABAQUS (No Doubler, Continuity)

Girder	Column	Span (in.)	Doubler Plate	Continuity Plate	PANELS (in.)	ABAQUS (in.)	% diff.
W36x210	W24x335	120	no	yes	3.07	3.13	1.95
		240			3.92	4.01	2.24
		360			4.98	5.09	2.04
W36x135	W24x207	120	no	yes	5.00	5.20	3.71
		240			6.55	6.78	3.45
		360			8.39	8.65	3.05
W30x132	W21x201	120	no	yes	6.70	6.92	3.18
		240			8.89	9.19	3.24
		360			11.41	11.76	2.98
W30x116	W21x166	120	no	yes	7.97	8.27	3.59
		240			10.60	10.98	3.49
		360			13.57	14.01	3.12
W27x178	W30x173	120	no	yes	5.67	5.90	3.97
		240			7.66	7.99	4.12
		360			9.81	10.19	3.70
W27x178	W14x426	120	no	yes	5.85	5.96	1.86
		240			7.49	7.62	1.73
		360			9.50	9.65	1.56
W21x101	W30x173	120	no	yes	9.97	10.40	4.10
		240			15.73	16.31	3.56
		360			21.90	22.54	2.85
W21x101	W14x426	120	no	yes	10.88	10.99	1.04
		240			16.12	16.21	0.54
		360			22.11	22.18	0.31

Table 4.4-17: End - PANELS vs. ABAQUS (Doubler, Continuity)

Girder	Column	Span (in.)	Doubler Plate	Continuity Plate	PANELS (in.)	ABAQUS (in.)	% diff.
W36x210	W24x335	120	yes	yes	2.81	2.90	2.97
		240			3.56	3.68	3.37
		360			4.59	4.73	2.96
W36x135	W24x207	120	yes	yes	4.54	4.74	4.32
		240			5.92	6.18	4.24
		360			7.70	7.99	3.69
W30x132	W21x201	120	yes	yes	6.04	6.29	4.12
		240			8.03	8.37	4.17
		360			10.48	10.88	3.71
W30x116	W21x166	120	yes	yes	7.15	7.49	4.43
		240			9.54	9.97	4.26
		360			12.44	12.92	3.74
W27x178	W30x173	120	yes	yes	5.04	5.30	4.87
		240			6.76	7.12	5.11
		360			8.80	9.22	4.50
W27x178	W14x426	120	yes	yes	5.27	5.50	4.22
		240			6.80	7.07	3.85
		360			8.77	9.06	3.26
W21x101	W30x173	120	yes	yes	9.00	9.49	5.17
		240			14.36	15.01	4.39
		360			20.37	21.10	3.45
W21x101	W14x426	120	yes	yes	10.00	10.35	3.35
		240			15.08	15.44	2.31
		360			21.02	21.38	1.68

Table 4.4-18: Tee - PANELS vs. ABAQUS (No Doubler, No Continuity)

Girder	Column	Span (in.)	Doubler Plate	Continuity Plate	PANELS (in.)	ABAQUS (in.)	% diff.
W36x210	W24x335	120	no	no	0.83	0.82	0.46
		240			1.02	1.01	0.89
		360			1.21	1.20	0.92
W36x135	W24x207	120	no	no	1.39	1.40	1.21
		240			1.72	1.73	0.75
		360			2.03	2.04	0.39
W30x132	W21x201	120	no	no	1.85	1.88	1.49
		240			2.28	2.31	1.17
		360			2.68	2.71	1.00
W30x116	W21x166	120	no	no	2.25	2.29	2.01
		240			2.76	2.81	1.50
		360			3.24	3.28	1.22
W27x178	W30x173	120	no	no	1.61	1.67	3.59
		240			2.07	2.15	3.68
		360			2.44	2.52	3.37
W27x178	W14x426	120	no	no	2.30	2.36	2.54
		240			3.10	3.15	1.78
		360			3.94	3.99	1.38
W21x101	W30x173	120	no	no	2.43	2.58	5.55
		240			3.48	3.67	5.16
		360			4.40	4.61	4.41
W21x101	W14x426	120	no	no	2.30	2.36	2.54
		240			3.10	3.15	1.78
		360			3.94	3.99	1.38

Table 4.4-19: Tee - PANELS vs. ABAQUS (Doubler, No Continuity)

Girder	Column	Span (in.)	Doubler Plate	Continuity Plate	PANELS (in.)	ABAQUS (in.)	% diff.
W36x210	W24x335	120	yes	no	0.75	0.75	0.00
		240			0.92	0.92	0.00
		360			1.09	1.09	0.00
W36x135	W24x207	120	yes	no	1.26	1.27	1.26
		240			1.54	1.56	0.83
		360			1.84	1.85	0.54
W30x132	W21x201	120	yes	no	1.65	1.69	2.07
		240			2.03	2.07	1.79
		360			2.41	2.45	1.55
W30x116	W21x166	120	yes	no	2.01	2.06	2.38
		240			2.46	2.51	1.96
		360			2.91	2.96	1.62
W27x178	W30x173	120	yes	no	1.37	1.45	5.78
		240			1.73	1.84	5.87
		360			2.06	2.18	5.37
W27x178	W14x426	120	yes	no	1.38	1.42	2.76
		240			1.65	1.68	2.32
		360			1.94	1.98	2.07
W21x101	W30x173	120	yes	no	2.02	2.23	9.12
		240			2.91	3.18	8.34
		360			3.78	4.07	6.98
W21x101	W14x426	120	yes	no	2.06	2.17	4.85
		240			2.81	2.92	3.63
		360			3.64	3.74	2.86

Table 4.4-20: Tee - PANELS vs. ABAQUS (No Doubler, Continuity)

Girder	Column	Span (in.)	Doubler Plate	Continuity Plate	PANELS (in.)	ABAQUS (in.)	% diff.
W36x210	W24x335	120	no	yes	0.80	0.79	1.30
		240			0.99	0.97	2.03
		360			1.17	1.15	2.09
W36x135	W24x207	120	no	yes	1.34	1.34	0.00
		240			1.67	1.65	1.03
		360			1.98	1.96	1.23
W30x132	W21x201	120	no	yes	1.78	1.78	0.00
		240			2.20	2.19	0.37
		360			2.60	2.59	0.43
W30x116	W21x166	120	no	yes	2.16	2.17	0.41
		240			2.66	2.66	0.00
		360			3.13	3.12	0.42
W27x178	W30x173	120	no	yes	1.43	1.46	1.65
		240			1.84	1.85	0.81
		360			2.18	2.19	0.59
W27x178	W14x426	120	no	yes	1.50	1.51	0.53
		240			1.80	1.79	0.11
		360			2.10	2.10	0.00
W21x101	W30x173	120	no	yes	2.08	2.15	3.35
		240			3.01	3.08	2.18
		360			3.90	3.96	1.64
W21x101	W14x426	120	no	yes	2.24	2.29	2.05
		240			3.03	3.06	1.21
		360			3.86	3.90	0.85

Table 4.4-21: Tee - PANELS vs. ABAQUS (Doubler, Continuity)

Girder	Column	Span (in.)	Doubler Plate	Continuity Plate	PANELS (in.)	ABAQUS (in.)	% diff.
W36x210	W24x335	120	yes	yes	0.74	0.73	1.37
		240			0.91	0.89	2.08
		360			1.08	1.06	1.98
W36x135	W24x207	120	yes	yes	1.24	1.23	0.73
		240			1.52	1.50	1.40
		360			1.82	1.79	1.51
W30x132	W21x201	120	yes	yes	1.62	1.63	0.06
		240			2.00	1.99	0.40
		360			2.38	2.37	0.42
W30x116	W21x166	120	yes	yes	1.97	1.97	0.00
		240			2.41	2.40	0.46
		360			2.86	2.85	0.53
W27x178	W30x173	120	yes	yes	1.23	1.30	5.75
		240			1.62	1.64	1.04
		360			1.94	1.95	0.77
W27x178	W14x426	120	yes	yes	1.36	1.39	1.73
		240			1.63	1.65	1.15
		360			1.93	1.95	0.98
W21x101	W30x173	120	yes	yes	1.85	1.93	3.84
		240			2.69	2.76	2.71
		360			3.54	3.62	2.05
W21x101	W14x426	120	yes	yes	2.04	2.11	3.69
		240			2.78	2.86	2.52
		360			3.61	3.68	1.93

4.5 Comparison between Krawinkler and PANELS Approach (Elastic)

The final elastic comparison in this study was performed to investigate the deflection differences between the PANELS formulations and elastic Krawinkler models that did not include the column flange stiffness component. This was done to address any questions that could arise concerning the differences between the two models. Looking at Table 4.5-1 through Table 4.5-8, there is constantly a significant difference between the results from PANELS and those obtained using the Krawinkler model. This difference is solely due to the Krawinkler model's inability to account for the flexural component of drift within the PZ region, making the Krawinkler model stiffer than the ABAQUS models. Accounting for this difference in stiffness is addressed in Chapter 7.

Table 4.5-1: Corner - PANELS vs. Krawinkler (No Doubler)

Girder	Column	Span (in.)	Doubler Plate	Continuity Plate	PANELS (in.)	Krawinkler (in.)	% diff.
W36x210	W24x335	120	no	no	1.15	0.89	29.81
		240			1.43	1.13	26.11
		360			1.73	1.43	21.19
W36x135	W24x207	120	no	no	1.90	1.46	30.14
		240			2.38	1.88	26.44
		360			2.91	2.40	21.04
W30x132	W21x201	120	no	no	2.54	1.96	29.69
		240			3.19	2.55	25.06
		360			3.89	3.23	20.46
W30x116	W21x166	120	no	no	3.06	2.34	30.85
		240			3.84	3.05	25.84
		360			4.67	3.85	21.17
W27x178	W30x173	120	no	no	2.60	1.61	61.55
		240			3.26	2.12	53.96
		360			3.89	2.69	44.46
W27x178	W14x426	120	no	no	3.51	2.97	18.05
		240			4.91	4.33	13.44
		360			6.49	5.90	9.97
W21x101	W30x173	120	no	no	4.60	2.59	77.64
		240			6.34	4.04	57.03
		360			8.04	5.63	42.84
W21x101	W14x426	120	no	no	3.51	2.97	18.05
		240			4.91	4.33	13.44
		360			6.49	5.90	9.97

Table 4.5-2: Corner- PANELS vs. Krawinkler (Doubler)

Girder	Column	Span (in.)	Doubler Plate	Continuity Plate	PANELS (in.)	Krawinkler (in.)	% diff.
W36x210	W24x335	120	yes	no	1.03	0.83	23.77
		240			1.27	1.05	21.05
		360			1.57	1.34	16.94
W36x135	W24x207	120	yes	no	1.69	1.36	24.41
		240			2.12	1.75	20.97
		360			2.63	2.25	16.67
W30x132	W21x201	120	yes	no	2.23	1.81	23.43
		240			2.82	2.35	19.91
		360			3.50	3.01	16.18
W30x116	W21x166	120	yes	no	2.69	2.16	24.35
		240			3.39	2.81	20.46
		360			4.18	3.59	16.55
W27x178	W30x173	120	yes	no	2.08	1.46	42.67
		240			2.62	1.91	37.12
		360			3.20	2.46	29.88
W27x178	W14x426	120	yes	no	1.85	1.57	17.71
		240			2.29	1.99	14.82
		360			2.82	2.52	11.94
W21x101	W30x173	120	yes	no	3.57	2.38	49.79
		240			5.09	3.74	36.18
		360			6.71	5.30	26.62
W21x101	W14x426	120	yes	no	3.14	2.77	13.25
		240			4.49	4.10	9.61
		360			6.05	5.65	7.13

Table 4.5-3: Cruciform – PANELS vs. Krawinkler (No Doubler)

Girder	Column	Span (in.)	Doubler Plate	Continuity Plate	PANELS (in.)	Krawinkler (in.)	% diff.
W36x210	W24x335	120	no	no	2.20	1.92	12.85
		240			2.80	2.48	11.37
		360			3.38	3.06	9.57
W36x135	W24x207	120	no	no	3.64	3.17	13.01
		240			4.69	4.18	10.86
		360			5.70	5.16	9.39
W30x132	W21x201	120	no	no	5.03	4.41	12.33
		240			6.46	5.78	10.48
		360			7.83	7.12	9.02
W30x116	W21x166	120	no	no	6.08	5.32	12.44
		240			7.80	6.97	10.61
		360			9.42	8.56	9.10
W27x178	W30x173	120	no	no	4.72	3.69	21.86
		240			6.33	5.04	20.42
		360			7.62	6.24	18.07
W27x178	W14x426	120	no	no	4.27	3.91	8.37
		240			5.26	4.88	7.15
		360			6.32	5.94	5.95
W21x101	W30x173	120	no	no	7.87	5.92	24.80
		240			11.71	9.21	21.37
		360			15.13	12.43	17.87
W21x101	W14x426	120	no	no	7.21	6.65	7.70
		240			10.06	9.45	6.09
		360			13.14	12.51	4.77

Table 4.5-4: Cruciform – PANELS vs. Krawinkler (Doubler)

Girder	Column	Span (in.)	Doubler Plate	Continuity Plate	PANELS (in.)	Krawinkler (in.)	% diff.
W36x210	W24x335	120	yes	no	1.90	1.70	10.57
		240			2.39	2.17	9.05
		360			2.93	2.71	7.57
W36x135	W24x207	120	yes	no	3.12	2.78	10.90
		240			3.98	3.63	8.89
		360			4.92	4.56	7.37
W30x132	W21x201	120	yes	no	4.25	3.81	10.33
		240			5.46	5.00	8.37
		360			6.75	6.28	6.91
W30x116	W21x166	120	yes	no	5.12	4.58	10.48
		240			6.57	6.01	8.57
		360			8.10	7.52	7.13
W27x178	W30x173	120	yes	no	3.76	3.12	17.00
		240			4.99	4.21	15.55
		360			6.13	5.30	13.47
W27x178	W14x426	120	yes	no	3.64	3.38	7.09
		240			4.51	4.24	5.94
		360			5.53	5.26	4.85
W21x101	W30x173	120	yes	no	6.23	5.08	18.51
		240			9.46	8.00	15.42
		360			12.65	11.08	12.43
W21x101	W14x426	120	yes	no	6.24	5.87	5.94
		240			8.93	8.54	4.35
		360			11.94	11.54	3.36

Table 4.5-5: End – PANELS vs. Krawinkler (No Doubler)

Girder	Column	Span (in.)	Doubler Plate	Continuity Plate	PANELS (in.)	Krawinkler (in.)	% diff.
W36x210	W24x335	120	no	no	3.32	2.79	19.03
		240			4.22	3.62	16.55
		360			5.30	4.67	13.49
W36x135	W24x207	120	no	no	5.40	4.53	19.14
		240			7.01	6.04	16.13
		360			8.88	7.86	12.99
W30x132	W21x201	120	no	no	7.34	6.14	19.56
		240			9.63	8.29	16.18
		360			12.19	10.80	12.87
W30x116	W21x166	120	no	no	8.77	7.31	19.99
		240			11.52	9.89	16.52
		360			14.55	12.85	13.21
W27x178	W30x173	120	no	no	7.44	5.08	46.46
		240			9.87	6.99	41.19
		360			12.17	9.10	33.78
W27x178	W14x426	120	no	no	11.47	10.29	11.44
		240			16.78	15.48	8.39
		360			22.80	21.46	6.22
W21x101	W30x173	120	no	no	13.58	8.81	54.19
		240			20.23	14.33	41.19
		360			26.72	20.41	30.93
W21x101	W14x426	120	no	no	11.47	10.29	11.44
		240			16.78	15.48	8.39
		360			22.80	21.46	6.22

Table 4.5-6: End – PANELS vs. Krawinkler (Doubler)

Girder	Column	Span (in.)	Doubler Plate	Continuity Plate	PANELS (in.)	Krawinkler (in.)	% diff.
W36x210	W24x335	120	yes	no	2.91	2.57	13.31
		240			3.68	3.30	11.55
		360			4.72	4.32	9.17
W36x135	W24x207	120	yes	no	4.70	4.14	13.43
		240			6.10	5.49	11.17
		360			7.89	7.26	8.73
W30x132	W21x201	120	yes	no	6.31	5.55	13.71
		240			8.35	7.50	11.28
		360			10.81	9.95	8.67
W30x116	W21x166	120	yes	no	7.51	6.57	14.28
		240			9.96	8.93	11.48
		360			12.87	11.81	8.96
W27x178	W30x173	120	yes	no	5.91	4.51	30.93
		240			7.83	6.15	27.33
		360			9.95	8.16	21.95
W27x178	W14x426	120	yes	no	5.39	4.97	8.51
		240			6.93	6.48	6.96
		360			8.91	8.45	5.41
W21x101	W30x173	120	yes	no	10.72	7.97	34.55
		240			16.51	13.12	25.82
		360			22.68	19.06	18.99
W21x101	W14x426	120	yes	no	10.23	9.51	7.60
		240			15.35	14.56	5.39
		360			21.29	20.49	3.91

Table 4.5-7: Tee – PANELS vs. Krawinkler (No Doubler)

Girder	Column	Span (in.)	Doubler Plate	Continuity Plate	PANELS (in.)	Krawinkler (in.)	% diff.
W36x210	W24x335	120	no	no	0.83	0.67	23.21
		240			1.02	0.85	20.78
		360			1.21	1.02	18.43
W36x135	W24x207	120	no	no	1.39	1.12	23.75
		240			1.72	1.42	21.13
		360			2.03	1.72	18.26
W30x132	W21x201	120	no	no	1.85	1.52	21.58
		240			2.28	1.92	18.70
		360			2.68	2.31	16.15
W30x116	W21x166	120	no	no	2.25	1.85	21.35
		240			2.76	2.32	19.09
		360			3.24	2.78	16.51
W27x178	W30x173	120	no	no	1.61	1.26	27.86
		240			2.07	1.64	26.16
		360			2.44	1.98	22.98
W27x178	W14x426	120	no	no	2.30	2.06	11.75
		240			3.10	2.83	9.40
		360			3.94	3.66	7.54
W21x101	W30x173	120	no	no	2.43	1.87	30.11
		240			3.48	2.76	25.94
		360			4.40	3.64	20.99
W21x101	W14x426	120	no	no	2.30	2.06	11.75
		240			3.10	2.83	9.40
		360			3.94	3.66	7.54

Table 4.5-8: Tee – PANELS vs. Krawinkler (Doubler)

Girder	Column	Span (in.)	Doubler Plate	Continuity Plate	PANELS (in.)	Krawinkler (in.)	% diff.
W36x210	W24x335	120	yes	no	0.75	0.62	22.08
		240			0.92	0.77	19.64
		360			1.09	0.94	16.76
W36x135	W24x207	120	yes	no	1.26	1.02	23.04
		240			1.54	1.28	20.63
		360			1.84	1.57	17.26
W30x132	W21x201	120	yes	no	1.65	1.37	20.66
		240			2.03	1.72	17.97
		360			2.41	2.10	14.90
W30x116	W21x166	120	yes	no	2.01	1.66	20.84
		240			2.46	2.08	18.13
		360			2.91	2.52	15.44
W27x178	W30x173	120	yes	no	1.37	1.12	22.32
		240			1.73	1.43	21.12
		360			2.06	1.74	18.51
W27x178	W14x426	120	yes	no	1.38	1.18	16.61
		240			1.65	1.43	15.03
		360			1.94	1.72	12.91
W21x101	W30x173	120	yes	no	2.02	1.66	21.87
		240			2.91	2.46	18.37
		360			3.78	3.30	14.67
W21x101	W14x426	120	yes	no	2.06	1.86	10.75
		240			2.81	2.60	8.15
		360			3.64	3.42	6.35

4.6 Discussions and Conclusions

Assuming that the Drain-2DX Krawinkler models and the ABAQUS models give an accurate representation of the PZ region, the following conclusions from the above analyses can be made. First, Table 4.2-1 through Table 4.2-8 show when that the contribution due to PZ flexure is ignored, the derived PANELS equations account for all the remaining significant sources of elastic strain energy. This correlation between the Drain-2DX models and PANELS was essential, considering that all the remaining elastic deformation determined using the ABAQUS models was attributed to PZ flexure in the PANELS equations. Next, Table 4.4-6 through Table 4.4-9 show the comparisons between PANELS and ABAQUS cruciform models. Using the 1.5 multiplier developed in Section 4.4 for both the column and girder PZ flexural components, the PANELS formulas calculated an overall drift which corresponded well to the drift of an equivalent ABAQUS model. The ABAQUS models that included the effects of continuity plates displayed less stiffness than what was determined using PANELS, but even the largest variation of results is still within five percent. As discussed in Section 4.4, the current Krawinkler model does not have a way to account for the use of continuity plates in the beam/column subassembly. The inability to perform an elastic strain energy comparison and/or the constraints used to model the welds at the interfaces of the beam/column joint components could account for this difference. Whether or not the techniques used to develop the ABAQUS models are correct are addressed in Chapter 6 when models are compared to actual subassemblage test data. Finally, the Krawinkler model is often cited for overestimating the stiffness of a beam/column joint (Kim and Engelhardt 1995 and 2002). The results in Table 4.5-1 through Table 4.5-8 also agree with this point. The difference is that this thesis attributes the overestimation of stiffness to the elastic PZ flexure component, while Kim and Engelhardt (1995 and 2002) attribute it to the overestimation of stiffness of the inelastic column flanges hinges. Again, this will be addressed in Chapter 6 when the ABAQUS models are compared to subassemblage test data and in Chapter 7 when elastic modifications to the Krawinkler and Scissors models are presented.

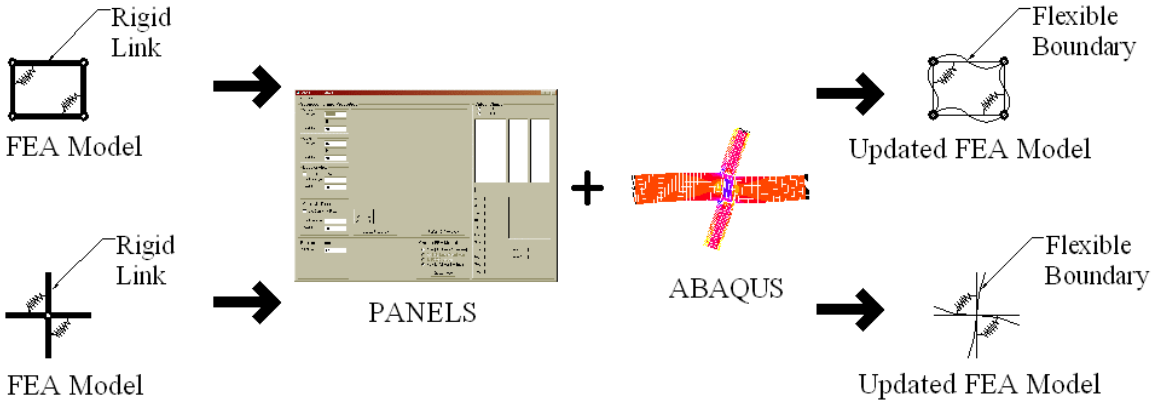

Figure 4.6-1: Thesis Flow Chart

At this point in this thesis, the PANELS components have been presented, the two FEA models (Krawinkler and Scissors) have been developed, the additional subassemblage displacement attributed to PZ flexure has been quantified using ABAQUS and a method of including this additional drift and the contribution of continuity plates in PANELS has been determined. The remaining issues that need to be dealt with before the FEA model modifications (Chapter 7) can be undertaken are which FEA model (Krawinkler or Scissors) to use in the proposed modifications (Chapter 5) and, when compared to test data whether the PANELS and ABAQUS results presented so far are even valid (Chapter 6).

5 Inelastic Model Comparisons

5.1 Introduction and Scope

The ability to accurately model the inelastic deformations of the beam/column joint region is crucial when performing inelastic static pushover and dynamic analysis. Without accounting for all the elastic and inelastic sources of deformation, the model will not display proper hinge sequencing nor give an appropriate estimation of drift or strength. In this portion of the study, the two inelastic models that were developed in Chapter 3 are compared in a variety of structural configurations to determine how differences in their behavior might affect structural response. It was initially believed that the kinematic differences between the Krawinkler and Scissors models, discussed in Chapter 3, would have a definite impact on the ability of the Scissors model to accurately predict the total drift of a structure when used in an inelastic static pushover analysis. It was felt that although their responses should be identical when a zero-moment condition was maintained at the mid-spans of the girders and columns, when placed in a more realistic structural configuration with full continuity, the inability of the Scissors model to maintain the 90 degree angle at the interface of the beam/column joint would cause a significant difference in the responses of the two models. To investigate whether or not this hypothesis was true, a series of comparisons were developed with the focus being:

1. Using the derivations from Chapter 3, compare the force/displacement responses of individual Krawinkler and Scissors subassemblages to ensure that the models have equivalent force-displacement responses when subjected to an equivalent shear force.

2. Show that both PZ models give the same force/displacement response for a complete structure that has internal hinges at mid-span of the structure's columns and girders. This maintains the boundary conditions consistent with the subassemblage models and allows examination of response in the context of a full frame.

3. Due to kinematic differences in the models and the fact that the α and β constants of the Scissors model rely on the location of the moment inflection points in the girders and columns, show that the Krawinkler and Scissors PZ models give different results when the mid-span hinges are not included in the full structure.

4. Determine any differences in the two models when subjected to multiple design scenarios – models with and without P-delta, with and without gravity forces, different bay widths, etc. – to determine if/when the Scissors model can be a viable replacement for the Krawinkler model when performing an inelastic static pushover analysis on a complete structure.

The design of the following models adheres to the current design practice of strong column/weak beam to ensure that plastic hinging outside the PZ region is limited mainly to the girders. For both the columns and girders, a Type 2 beam/column element was used. Due to possible problems associated with Drain-2DX's (Prakash at al. 1993) P-M interaction for this element type, modifications were made to the girders of the structure by Charney (2002). The geometric properties of the Type 2 elements used were identical to those found in the current version of the AISC-LRFD (2001) manual, but their +/- yield moments were set extremely high to ensure that they would not yield. Type 4 hinge elements were then added to model the plastic hinges that develop in the girders. Two of these elements are placed at each girder hinge location. The first hinge is elastic/perfectly plastic and represents the initial stiffness and yield strength of the girder. The second hinge represents the girders' post-yielding stiffness. The PZ and column flange hinge properties were developed using the equations in Chapter 3.

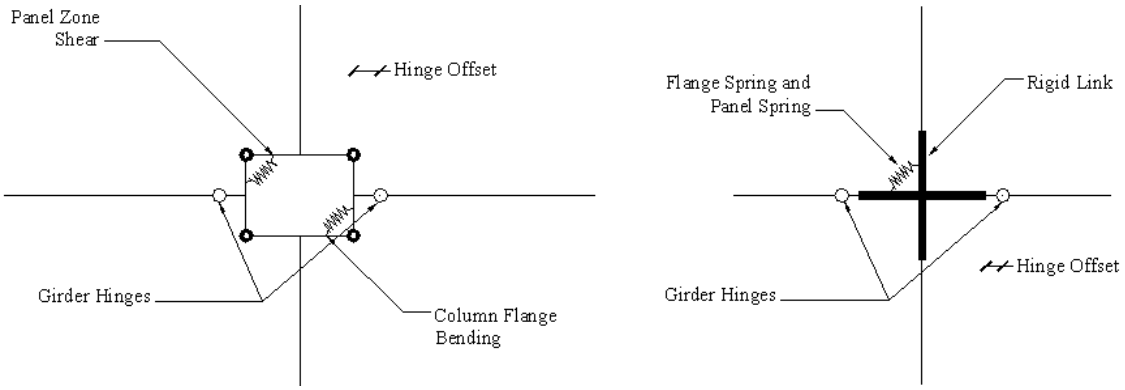

Figure 5.1-1: Model Hinge Location for the Structural Subassemblages

5.2 Comparison between Krawinkler and Scissors

5.2.1 Subassemblages

To begin this segment of the study, a large number of subassemblage models were analyzed using Drain-2DX. These models were made up of different component combinations including Cruciform, Corner, End and Tee subassemblages. With the height of the columns fixed at 150 in. for all analyses herein, different subassemblies were created that were an arrangement of wide flange sections with a combination of the following:

1. With/without column yielding
2. With/without girder yielding
3. With/without doubler plates
4. Variation in number of bays and bay widths

For all four types of subassemblage models, the definitions of α and β are based on the definitions detailed in Chapter 1. Figure 5.2-1 through

Figure 5.2-4 show the force/displacement results from one series of tests that included PZ hinges, girder hinges and the column flange hinges using the properties of a W24x84 girder, with no doubler plate, and a W21x122 column. The Drain-2DX input

files for all the subassemblages shown in Figure 5.2-2 through Figure 5.2-4 are given in Appendix B. For these tests, gravity loads and P-delta effects were not included. As seen in these figures, the responses of the two models are identical, not only in yielding patterns but also in the sequence of hinging of the individual models. All the remaining subassemblages shown in Table 5.2-1 were modeled and displayed identical behavior.

Table 5.2-1: 6-Story 28-Ft Bay Krawinkler Model and Scissors Model Properties

L (in.)	336
H (in.)	150
Von Mises Yield Constant	0.6
Fy (ksi)	50
Poisson's ratio	0.3
G (ksi)	11154
E (ksi)	29000

Krawinkler Models

Beam	tf	d	βH
	in	in	in
W24x84	0.77	24.1	23.33
W24x84	0.77	24.1	23.33
W24x84	0.77	24.1	23.33
W27x94	0.745	26.92	26.175
W27x94	0.745	26.92	26.175
W27x94	0.745	26.92	26.175
W27x94	0.745	26.92	26.175
W27x94	0.745	26.92	26.175
W27x94	0.745	26.92	26.175

Scissors Models

Beam	α
W24x84	0.0617
W24x84	0.0617
W24x84	0.0617
W27x94	0.0622
W27x94	0.0622
W27x94	0.0622
W27x94	0.0637
W27x94	0.0637
W27x94	0.0637

Column	tf	d	αL	bf	tw	Doubler
	in	in	in	in	in	in
W21x122	0.96	21.68	20.74	12.4	0.6	0.000
W21x122	0.96	21.68	20.74	12.4	0.6	0.750
W21x122	0.96	21.68	20.74	12.4	0.6	1.000
W21x147	1.15	22.06	20.91	12.51	0.72	0.000
W21x147	1.15	22.06	20.91	12.51	0.72	0.750
W21x147	1.15	22.06	20.91	12.51	0.72	1.000
W21x201	1.63	23.03	21.4	12.575	0.91	0.000
W21x201	1.63	23.03	21.4	12.575	0.91	0.600
W21x201	1.63	23.03	21.4	12.575	0.91	0.875

Column	β	1-α-β
W21x122	0.1555	0.7827
W21x122	0.1555	0.7827
W21x122	0.1555	0.7827
W21x147	0.1745	0.7633
W21x147	0.1745	0.7633
W21x147	0.1745	0.7633
W21x201	0.1745	0.7618
W21x201	0.1745	0.7618
W21x201	0.1745	0.7618

Krawinkler Models

Column	Beam	Panel		Flange	
		My	K	My	K
		in-k	in-k/rad	in-k	in-k/rad
W21x122	W24x84	8710	3238168	1029	95598
W21x122	W24x84	19597	7285878	1029	95598
W21x122	W24x84	23225	8635115	1029	95598
W21x147	W27x94	11822	4395395	1489	138401
W21x147	W27x94	24137	8973931	1489	138401
W21x147	W27x94	28242	10500109	1489	138401
W21x201	W27x94	15292	5685472	3007	279492
W21x201	W27x94	25375	9434134	3007	279492
W21x201	W27x94	29996	11152272	3007	279492

Scissors Models

Panel		Flange	
My	K	My	K
in-k	in-k/rad	in-k	in-k/rad
11127	5285229	1314	156032
25036	11891765	1314	156032
29672	14093944	1314	156032
15489	7544734	1951	237566
31623	15403832	1951	237566
37001	18023531	1951	237566
20073	9796562	3947	481589
33308	16255834	3947	481589
39374	19216334	3947	481589

Note: depths defined center to center of flange

Girder Hinges

	First Component			Second Component		
Girder	My	K	Strain	My	K	Strain
	in-k	in-k/rad	Hardening	in-k	in-k/rad	Hardening
W24x84	11025	Huge	0.000	1196	326000	0.284
W27x94	13538	Huge	0.000	1494	450129	0.285

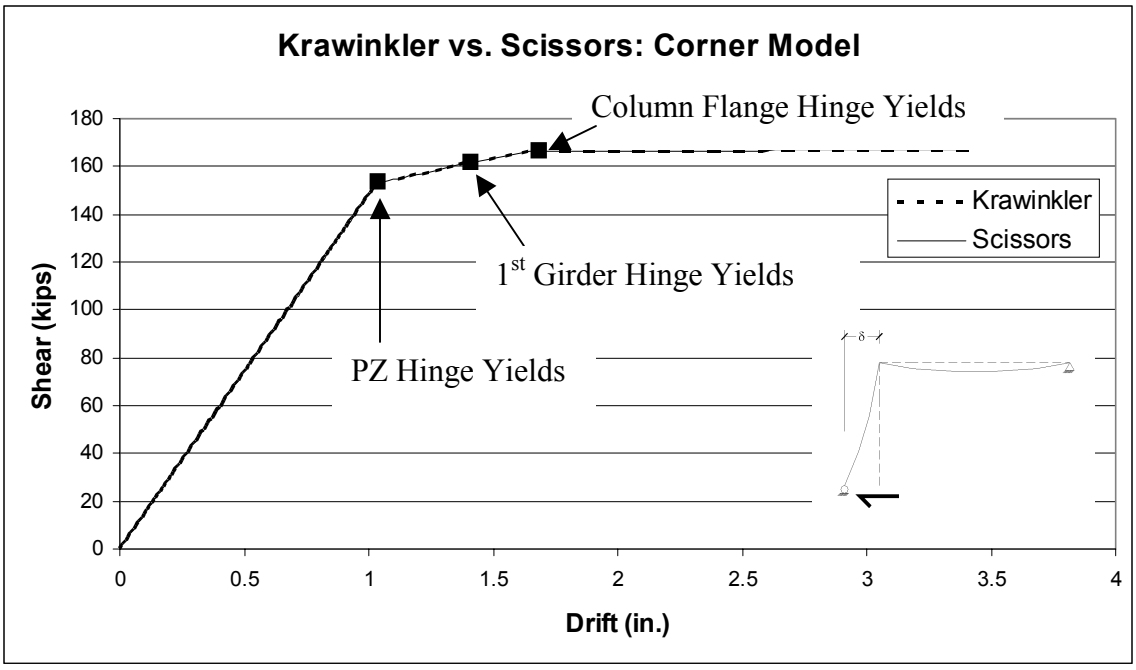

Figure 5.2-1: Krawinkler vs. Scissors Corner Subassembly Comparison

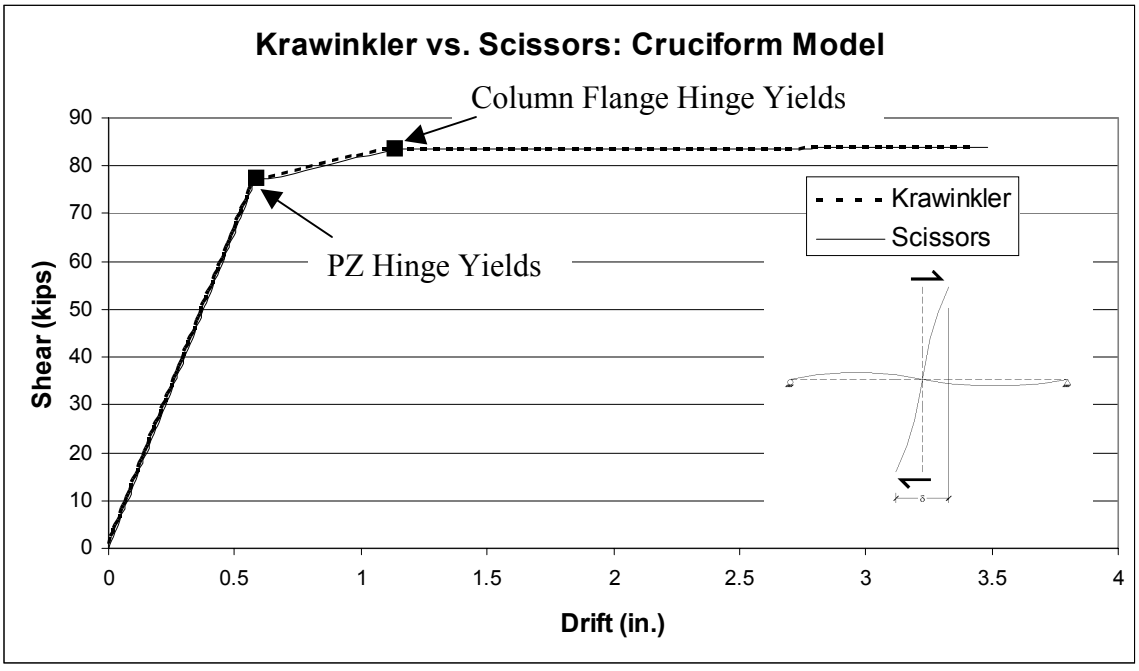

Figure 5.2-2: Krawinkler vs. Scissors Cruciform Subassembly Comparison

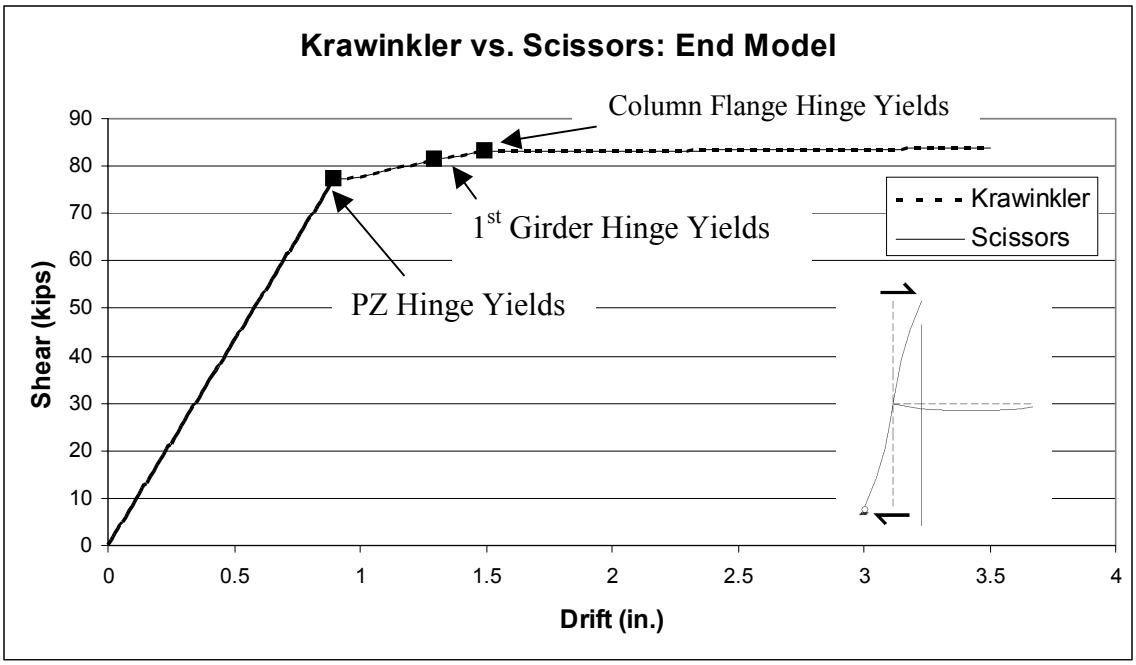

Figure 5.2-3: Krawinkler vs. Scissors End Subassembly Comparison

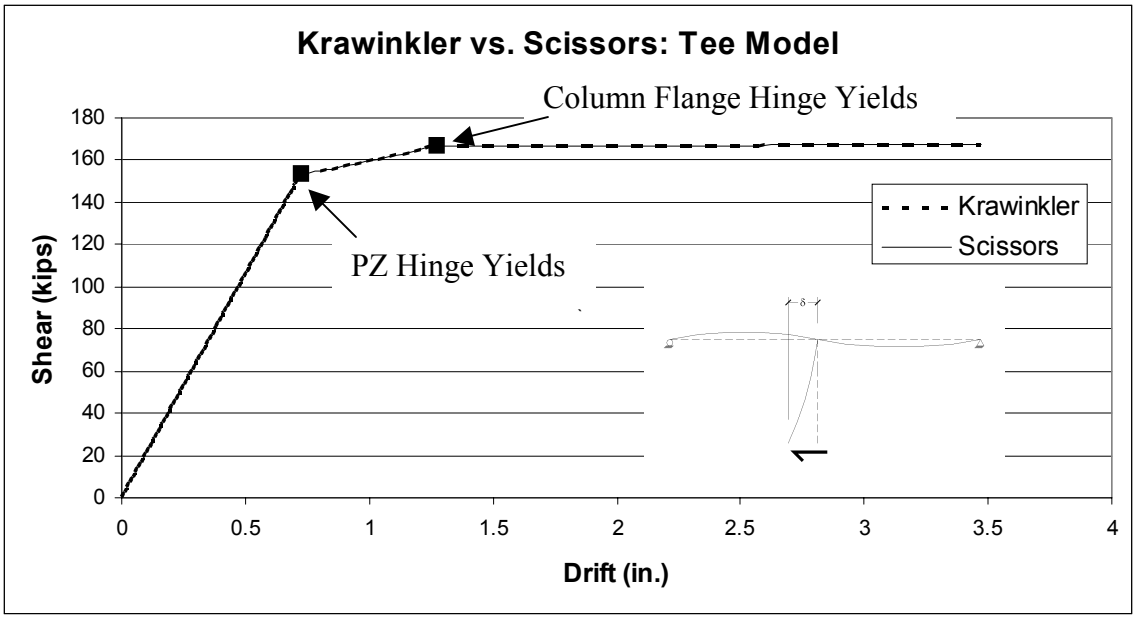

Figure 5.2-4: Krawinkler vs. Scissors Tee Subassembly Comparison

The observed halving of strength capacity of the Cruciform and End subassemblages, seen in Figure 5.2-2 and Figure 5.2-3, is due to loads being applied to both the top and bottom column. The additional plastic hinge, Figure 5.2-3 and Figure 5.2-4, which develops in the girder is due to there only being one girder to resist the applied force in the End and Tee subassemblages.

An illustration of the kinematic differences between the Krawinkler and Scissors models is given in Figure 5.2-5. This figure was created by including both Krawinkler and Scissors Cruciform subassemblages used to create Figure 5.2-2 into the same Drain-2DX input file. As observed in this figure, the offset discussed in Chapter 3 is clearly visible. To compensate for this offset, the Scissors model obviously experiences less overall rotation of its columns and girders to transverse through the same overall displacement. The numerical difference in rotation is given in Table 5.2-2.

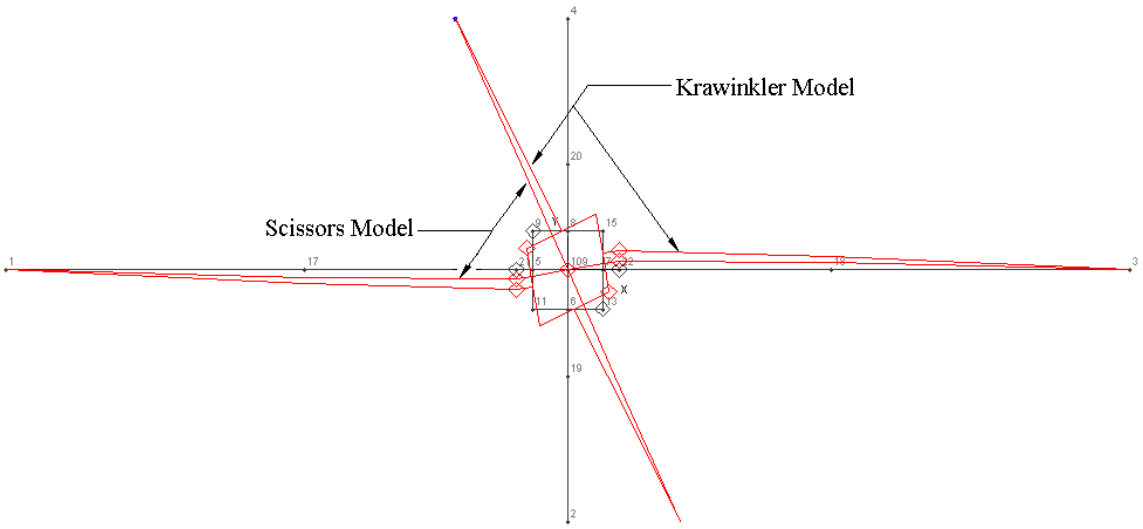

Figure 5.2-5: Relative Rotations of Krawinkler and Scissors Models

Table 5.2-2: Rotation at the End Bottom Column Node

Model	Rotation (rad)
Krawinkler	0.0950
Scissors	0.0803

Note that the rotations at the ends of the columns do not correlate well. The consequences of the rotational compatibility differences between the two models not being maintained is addressed in the comparison between the Krawinkler and Scissors models in Section 5.2.3.

5.2.2 Frames with Mid-Span and Mid-Height Hinges

With the exact correlation of the force/displacement response between the Krawinkler and Scissors models confirmed, two six-story five-bay models were developed and analyzed, again using Drain-2DX. A nonlinear static pushover analysis was performed on each frame in order to show that with identical properties other than the Krawinkler and Scissors PZ hinge models (Figure 5.2-6 shows a Scissors model representation), the load/deflection plots would be identical if mid-span and mid-height hinges were included in the columns and girders. This is consistent with the boundary condition analysis assumptions that were used when developing the equations for both models.

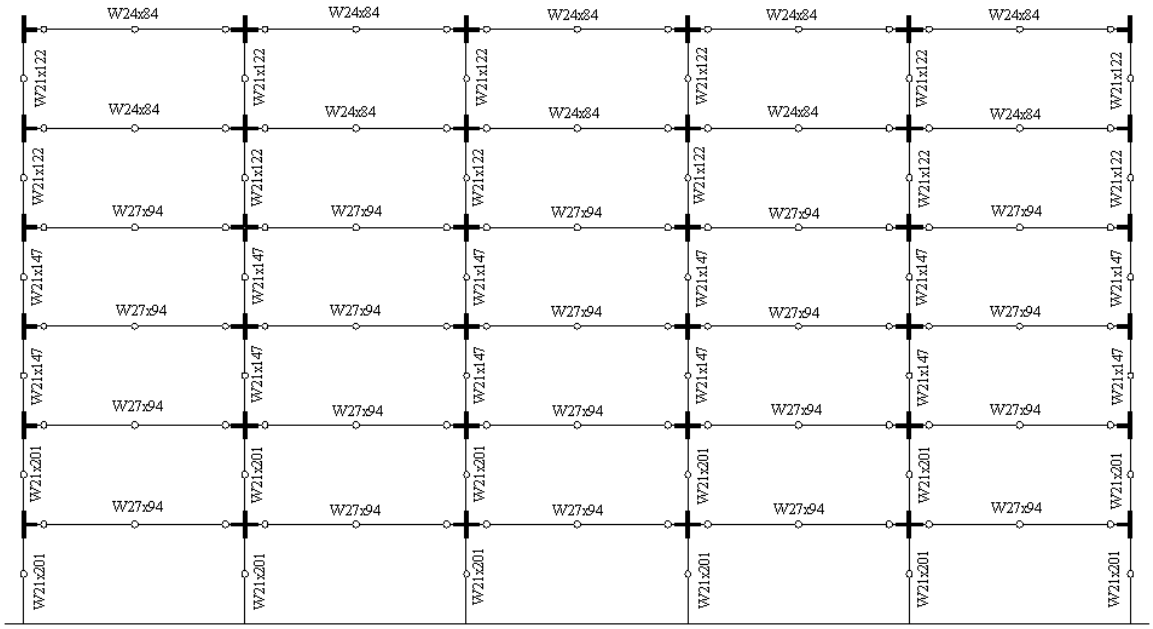

Figure 5.2-6: Scissors Models with Mid-Span Hinges

Then, if the mid-span and mid-height hinges were removed (Figure 5.2-7 shows a Krawinkler model representation) there would no longer be the structural conditions present to necessarily allow the moment at the midspans of the columns and the girders to be zero. This change in modeling parameters modifies not only the resultant moments but the comparative kinematic behavior between the models as well. Since the Krawinkler model spring properties have nothing to do with the dimensions outside the joint, the locations of the points of inflection of the moments in the girders and columns have no effect on the model. However, this is not the case with the Scissors model. With its reliance on $(1-\alpha-\beta)$, the locations of the inflection points will have impact because the developed model's properties assume that they occur at the mid-span of the columns and girder.

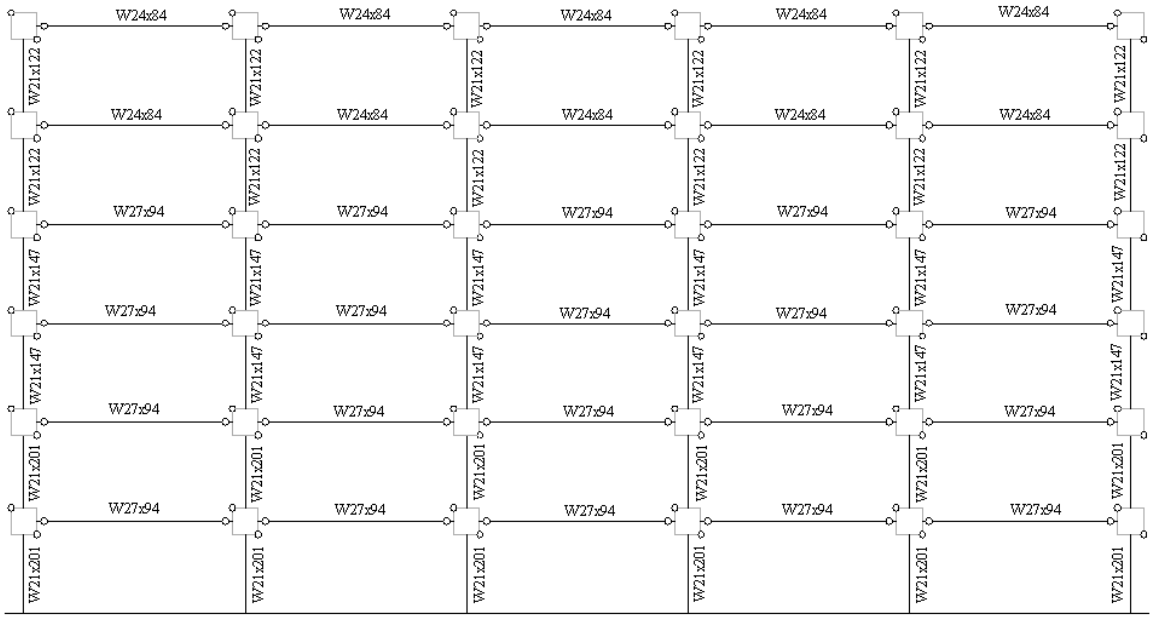

Figure 5.2-7: Krawinkler without Mid-Span Hinges

Following the outline presented above, a total of four models was analyzed:

- Mid-span and mid-height hinge Krawinkler
- Mid-span and mid-height hinge Scissors
- Full continuity Krawinkler
- Full continuity Scissors

Inelastic static pushover analyses were performed on all four models using the same lateral load pattern determined via the equivalent lateral force method following the guideline established in the 2000 International Building Code (2000). For comparison purposes, each model was forced to displace 42 in.. This was done to ensure that a large number of the PZ and column flange hinges yielded to allow for a contrast study of the Krawinkler and Scissor models. P-delta forces, as well as gravity forces, were also included in these analyses. The Krawinkler and Scissor hinge properties for these models

are found in Table 5.2-1. For this series of analyses, no doubler plates were used in any of the beam/column joints. The girder hinge properties, developed by Charney (2001) and shown at the bottom of Table 5.2-1, represent the yielding and strain hardening associated with this plastic hinging in the girders. Since they should yield before the column, this procedure was not repeated for the columns. Even if some of the Type 2 elements used to model the columns did yield, not explicitly modeling their plastic hinges, as was done in the girders, should not cause a significant error. For the changes in column sizes on Level 2 and Level 4 of the structure, column splices were used. They are located 50 in. above the top of the beam/column connections. The wide flange section sizes, locations and the tabulated properties used in the models are in their representative figures and in Table 5.2-1.

The results from all four investigations are shown in Figure 5.2-8 through Figure 5.2-11. The plots shown are the force/displacement responses and their associated tangent stiffness/displacement for each model. To determine the value for the tangent stiffness, the change in shear from one load step to the next was divided by the change in displacement during the step. This plot gives a visual representation of when yielding occurs during the force/displacement response. As seen in the first set of figures, even though they are not great, differences between the Krawinkler and Scissors models do exist when the midspan hinges are removed. In the second set of figures, models with mid-span hinges, both the Krawinkler and Scissors models' responses were identical.

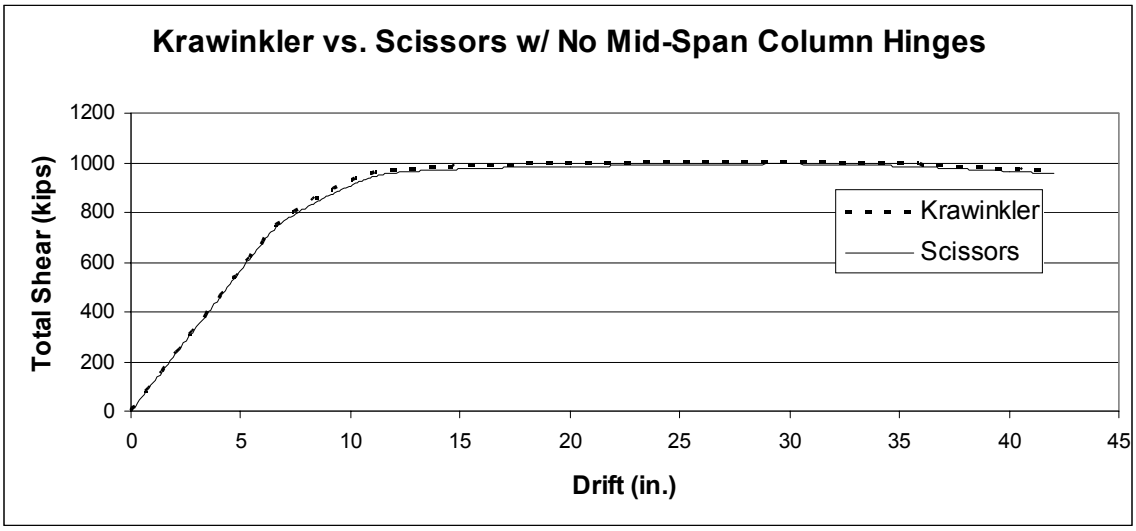

Figure 5.2-8: 6S-5B-28Ft Krawinkler vs. Scissors: No Mid-Span Hinges, Force/Displacement

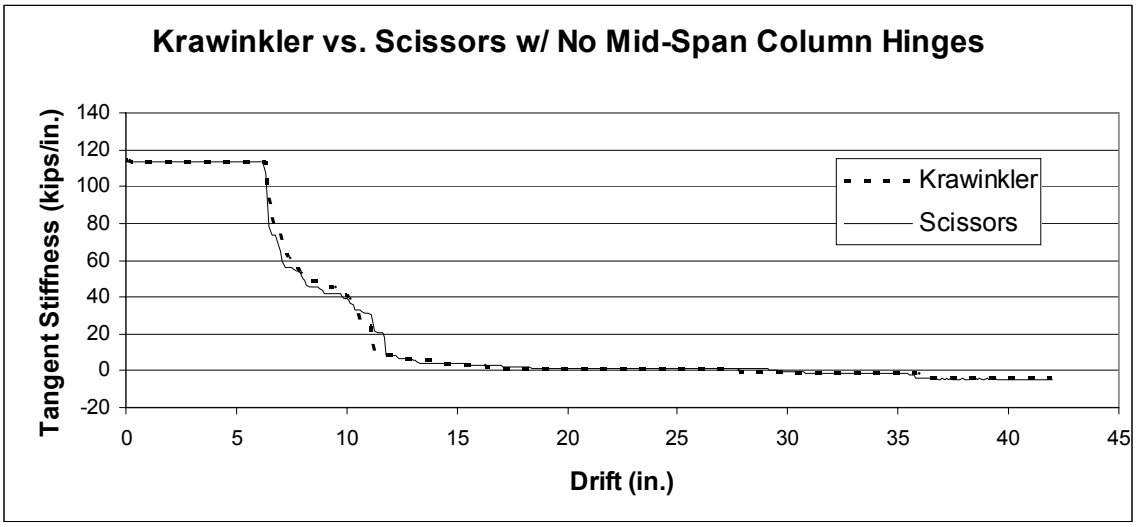

Figure 5.2-9: 6S-5B-28Ft Krawinkler vs. Scissors: No Mid-Span Hinges, Tangent Stiffness

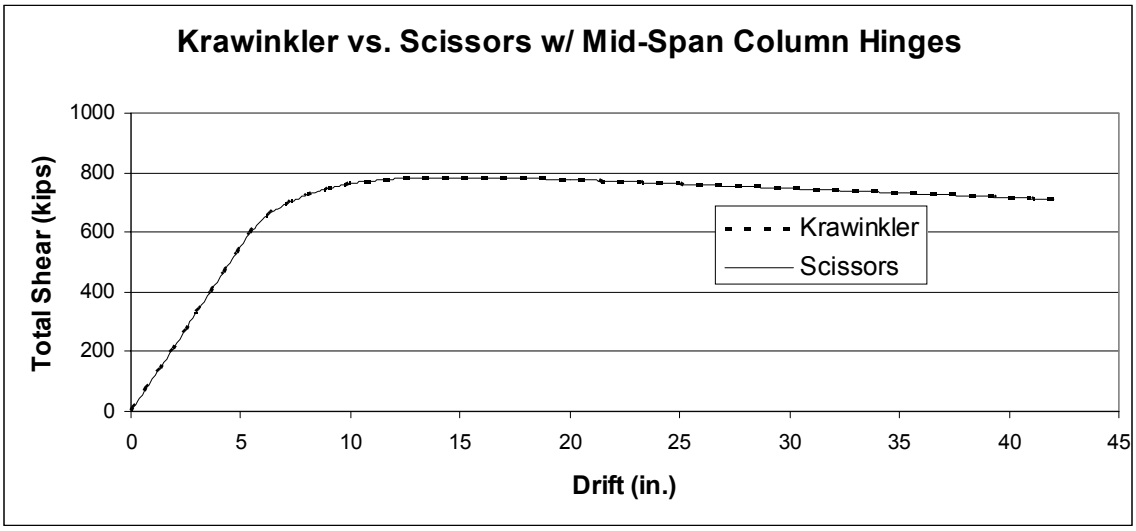

Figure 5.2-10: 6S-5B-28Ft Krawinkler vs. Scissors: Mid-Span Hinges, Force/Displacement

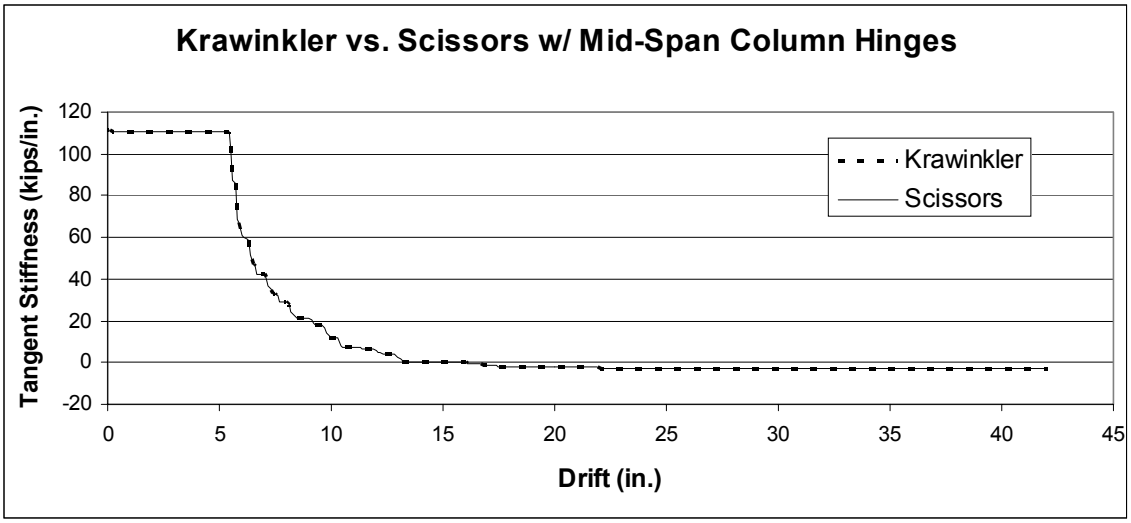

Figure 5.2-11: 6S-5B-28Ft Krawinkler vs. Scissors: Mid-Span Hinges, Tangent Stiffness

5.2.3 Continuous Frames

To determine the potential consequences of this difference between the two PZ models, structures were built using both the Krawinkler and Scissors PZ models, varying the following design loads and geometric properties:

1. Bay widths of 18, 24, 30 and 36 ft.
2. Frames with/without gravity load
3. Frames with/without P-delta forces
4. Panel zones with thick, thin and no doubler plates
5. Different numbers of bays and stories

The models in this series of tests used the six-story, five-bay model previously developed as a template. All the geometric properties were left the same except the change in stiffness of the PZ hinges due to the adjustment in bay-widths for the Scissors models. This series was very comprehensive, checking the effect of doubler plates, gravity loading, P-delta effects and differences in girder span lengths. The stiffness values listed in the following tables are the calculated tangent stiffness determined by dividing the per step change in shear by the change in displacement. First yield was the shear force observed at the first reduction in tangent stiffness. The shear value is the force present in the frame at a displacement of 3% of the total building height. The doubler plate sizes are the same as those shown in the twenty-eight ft span model shown in Table 5.2-1. To differentiate between the panel zones with thick, thin and no doubler plate, the naming convention of Strong, Weak and None is used. The choice in size was not based on AISC Seismic Provisions (1997) shear strength requirement but included to determine what a variation in size may cause. The results are shown below in Table 5.2-3 through Table 5.2-8.

Table 5.2-3: 6-Story 5-Bay Krawinkler vs. Scissors: Initial Stiffness Comparison

Bay Width (ft)	Gravity Load	P-Delta	Panel Zone Strengthening	Krawinkler Initial Stiffness (Kips/in.)	Scissors Initial Stiffness (Kips/in.)	% diff.
18	yes	yes	Strong	177.5	176.9	0.34
			Weak	174.5	173.8	0.40
			None	158.9	157.9	0.63
24	yes	yes	Strong	149.5	148.9	0.40
			Weak	147.2	146.6	0.41
			None	135.3	134.5	0.59
30	yes	yes	Strong	128.2	127.7	0.39
			Weak	126.5	125.9	0.47
			None	117.3	116.6	0.60
36	yes	yes	Strong	112	111.5	0.45
			Weak	110.6	110.2	0.36
			None	103.4	102.8	0.58

Table 5.2-4: 6-Story 5-Bay Krawinkler vs. Scissors: Initial Stiffness Comparison

Bay Width (ft)	Gravity Load	P-Delta	Panel Zone Strengthening	Krawinkler Initial Stiffness (Kips/in.)	Scissors Initial Stiffness (Kips/in.)	% diff.
18	yes	no	Strong	185.9	185.3	0.32
			Weak	182.8	182.2	0.33
			None	167.1	166.2	0.54
24	yes	no	Strong	157.8	157.3	0.32
			Weak	155.5	155	0.32
			None	143.6	142.8	0.56
30	yes	no	Strong	136.6	136.1	0.37
			Weak	134.8	134.3	0.37
			None	125.6	124.9	0.56
36	yes	no	Strong	120.3	119.9	0.33
			Weak	119	118.5	0.42
			None	111.7	111.1	0.54
18	no	no	Strong	185.9	185.3	0.32
			Weak	182.8	182.2	0.33
			None	167.1	166.2	0.54
24	no	no	Strong	157.8	157.3	0.32
			Weak	155.5	155	0.32
			None	143.6	142.8	0.56
30	no	no	Strong	136.6	136.1	0.37
			Weak	134.8	134.3	0.37
			None	125.6	124.9	0.56
36	no	no	Strong	120.3	119.9	0.33
			Weak	119	118.5	0.42
			None	111.7	111.1	0.54

Table 5.2-5: 6-Story 5-Bay Krawinkler vs. Scissors: 1st Yield Comparison

Bay Width (ft)	Gravity Load	P-Delta	Panel Zone Strengthening	Krawinkler 1st Yield (Kips)	Scissors 1st Yield (Kips)	% diff.
18	yes	yes	Strong	834	831	0.36
			Weak	820	817	0.37
			None	763	758	0.66
24	yes	yes	Strong	807	804	0.37
			Weak	795	791	0.50
			None	757	738	2.51
30	yes	yes	Strong	795	792	0.38
			Weak	784	781	0.38
			None	750	722	3.73
36	yes	yes	Strong	784	781	0.38
			Weak	774	771	0.39
			None	744	719	3.36

Table 5.2-6: 6-Story 5-Bay Krawinkler vs. Scissors: 1st Yield Comparison

Bay Width (ft)	Gravity Load	P-Delta	Panel Zone Strengthening	Krawinkler 1st Yield (Kips)	Scissors 1st Yield (Kips)	% diff.
18	yes	no	Strong	892	871	2.35
			Weak	877	889	1.37
			None	819	797	2.69
24	yes	no	Strong	868	865	0.35
			Weak	855	852	0.35
			None	804	785	2.36
30	yes	no	Strong	847	844	0.35
			Weak	836	833	0.36
			None	804	774	3.73
36	yes	no	Strong	842	839	0.36
			Weak	845	841	0.47
			None	804	777	3.36
18	no	no	Strong	911	908	0.33
			Weak	913	893	2.19
			None	834	812	2.64
24	no	no	Strong	899	896	0.33
			Weak	886	883	0.34
			None	817	785	3.92
30	no	no	Strong	888	884	0.45
			Weak	889	886	0.34
			None	804	786	2.24
36	no	no	Strong	902	887	1.66
			Weak	892	899	0.78
			None	804	777	3.36

Table 5.2-7: 6-Story 5-Bay Krawinkler vs. Scissors: Shear @ 3% Drift Comparison

Bay Width (ft)	Gravity Load	P-Delta	Panel Zone Strengthening	Krawinkler Shear @ 3% Drift (kips)	Scissors Shear @ 3% Drift (kips)	% diff.
18	yes	yes	Strong	1298	1296	0.15
			Weak	1286	1281	0.39
			None	1173	1158	1.28
24	yes	yes	Strong	1234	1234	0.00
			Weak	1232	1231	0.08
			None	1123	1110	1.16
30	yes	yes	Strong	1199	1198	0.08
			Weak	1197	1197	0.00
			None	1090	1070	1.83
36	yes	yes	Strong	1173	1172	0.09
			Weak	1171	1171	0.00
			None	1064	1051	1.22

Table 5.2-8: 6-Story 5-Bay Krawinkler vs. Scissors: Shear @ 3% Drift Comparison

Bay Width (ft)	Gravity Load	P-Delta	Panel Zone Strengthening	Krawinkler Shear @ 3% Drift (kips)	Scissors Shear @ 3% Drift (kips)	% diff.
18	yes	no	Strong	1794	1791	0.17
			Weak	1774	1769	0.28
			None	1588	1576	0.76
24	yes	no	Strong	1717	1716	0.06
			Weak	1703	1698	0.29
			None	1527	1517	0.65
30	yes	no	Strong	1667	1666	0.06
			Weak	1657	1652	0.30
			None	1490	1478	0.81
36	yes	no	Strong	1630	1629	0.06
			Weak	1622	1617	0.31
			None	1459	1449	0.69
18	no	no	Strong	1794	1791	0.17
			Weak	1774	1769	0.28
			None	1588	1576	0.76
24	no	no	Strong	1717	1716	0.06
			Weak	1703	1698	0.29
			None	1528	1517	0.72
30	no	no	Strong	1667	1666	0.06
			Weak	1657	1651	0.36
			None	1491	1479	0.80
36	no	no	Strong	1630	1629	0.06
			Weak	1622	1617	0.31
			None	1459	1449	0.69

Initially it was thought that there would be a large disparity between the responses of the Krawinkler and Scissors PZ models. As seen from the percent differences in the above tables, there was very little variation between the two. The difference in shear at 3% drift was never more than 2% and was typically less than1%. The load/deflection and tangent stiffness/deflection plots of all the models were virtually identical to the 28-ft bay-width model's results shown in Figure 5.2-8 and Figure 5.2-9 above. As seen in these plots, the difference in the total responses throughout the 42 in. of deflection is virtually nonexistent. Considering the extensive number of indeterminacies involved in structural modeling, this suggested that there was no real advantage using the Krawinkler model over the Scissors model for these structures. These results were unexpected, so more models were analyzed to verify these results.

The next set of tests used three-story four-bay models using the sections shown in Figure 5.2-12 and the properties in Table 5.2-9. The member sizes shown were used in all eight models. Considering the results from the previous tests, these models were modified to localize the majority of the yielding to the PZ region to accentuate the kinematic differences. To accomplish this, the secondary stiffness hinge property associated with the strain-hardening component in the girder hinges was set at an arbitrarily higher value. All tests conducted were static pushover analyses with a total deflection of 13.5 in.. P-delta effects and gravity were ignored.

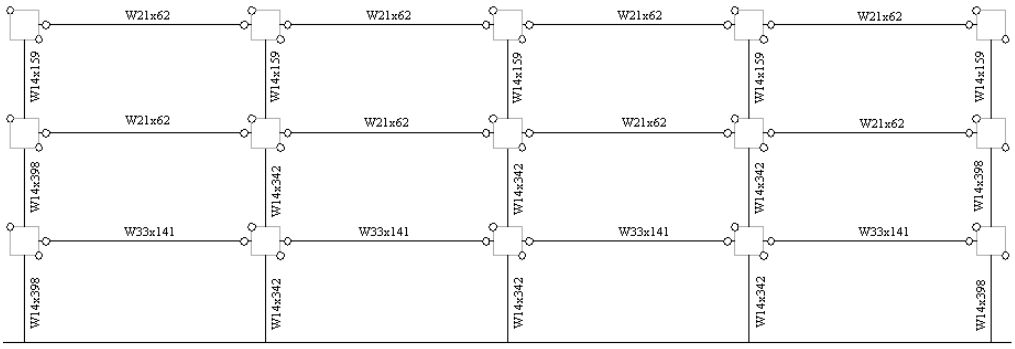

Figure 5.2-12: 3-Story 4-Bay Model

Table 5.2-9: Example 3-Story 4-Bay Krawinkler and Scissors Models Properties

L (in.)	360
H (in.)	150
Von Mises Yield Constant	0.6
Fy (ksi)	50
Poisson's ratio	0.3
G (ksi)	11154
E (ksi)	29000

Krawinkler Models

Beam	tf	d	βH
	in	in	in
W33x141	0.96	33.30	32.34
W33x141	0.96	33.30	32.34
W21x62	0.62	20.99	20.38

Column	tf	d	αL	bf	tw	Doubler
	in	in	in	in	in	in
W14x398	16.59	2.85	18.29	15.45	1.77	0.00
W14x342	16.36	2.47	17.54	15.07	1.54	0.00
W14x159	15.57	1.19	14.98	13.79	0.75	0.00

Scissors Model

Beam	α
W33x141	0.0429
W33x141	0.0419
W21x62	0.0383

Column	β	1-α-β
W14x398	0.2156	0.7415
W14x342	0.2156	0.7425
W14x159	0.1358	0.8259

Krawinkler Models

Column	Beam	Panel		Flange	
		My	K	My	K
		in-k	in-k/rad	in-k	in-k/rad
W14x398	W33x141	26523	9861111	12085	1123303
W14x342	W33x141	22516	8371411	8983	834955
W14x159	W21x62	6280	2334763	1984	184386

Scissors Model

Panel		Flange	
My	K	My	K
in-k	in-k/rad	in-k	in-k/rad
35770	17935223.28	16298	2043044
30323	15183092.26	12098	1514345
7604	3423172.416	2402	270343

Note: depths defined center to center of flange

Girder Hinges

Girder	First Component			Second Component		
	My	K	Strain	My	K	Strain
	in-k	in-k/rad	Hardening	in-k	in-k/rad	Hardening
W33x141	22400	Huge	0.000	2240	500000	0.3
W21x62	6350	Huge	0.000	635	500000	0.3

Table 5.2-10: 3-Story 4-Bay Krawinkler vs. Scissors: Test Results

Bay Width (ft)	Krawinkler			Scissors		
	Initial K (Kips/in.)	1st Yield (Kips)	Shear @ 3% Drift (Kips)	Initial K (Kips/in.)	1st Yield (Kips)	Shear @ 3% Drift (Kips)
18	247.1	548	1525	244.9	504	1486
24	217.1	558	1292	215.2	512	1256
30	193.8	574	1255	192.1	525	1226
36	175.3	592	1224	173.8	537	1190

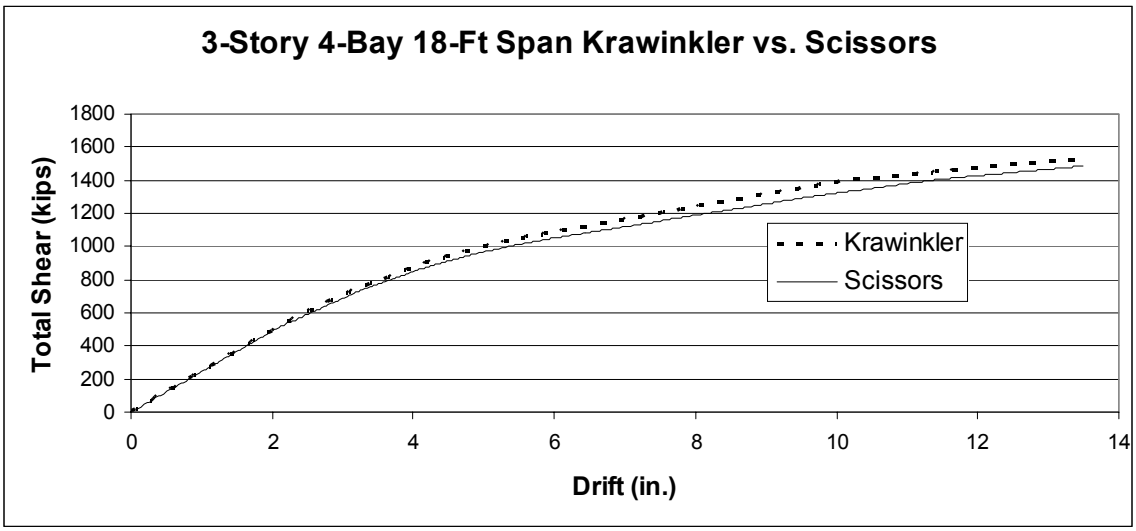

Figure 5.2-13: 3S-4B-18Ft Krawinkler vs. Scissors: Force/Displacement

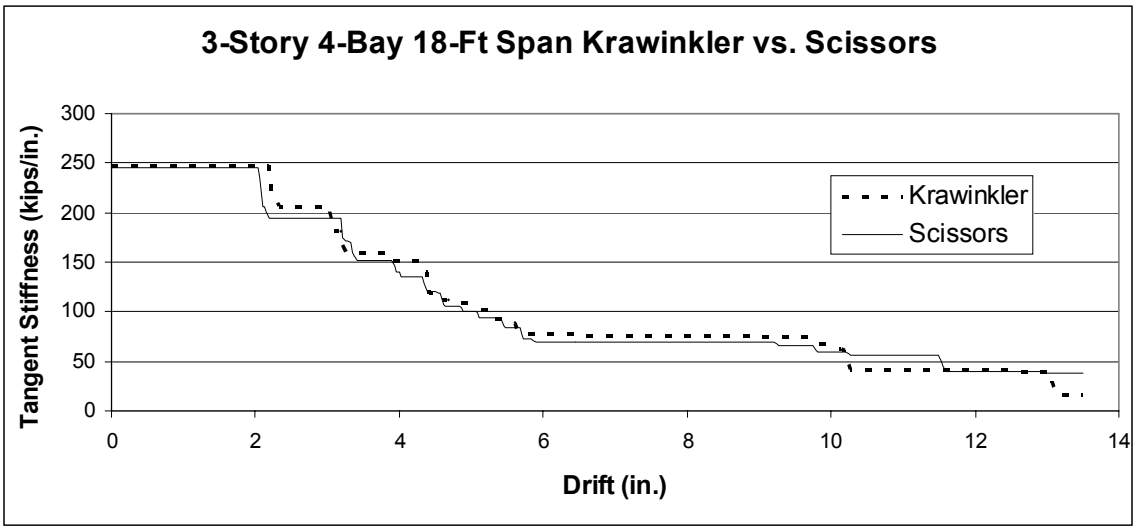

Figure 5.2-14: 3S-4B-18Ft Krawinkler vs. Scissors: Tangent Stiffness

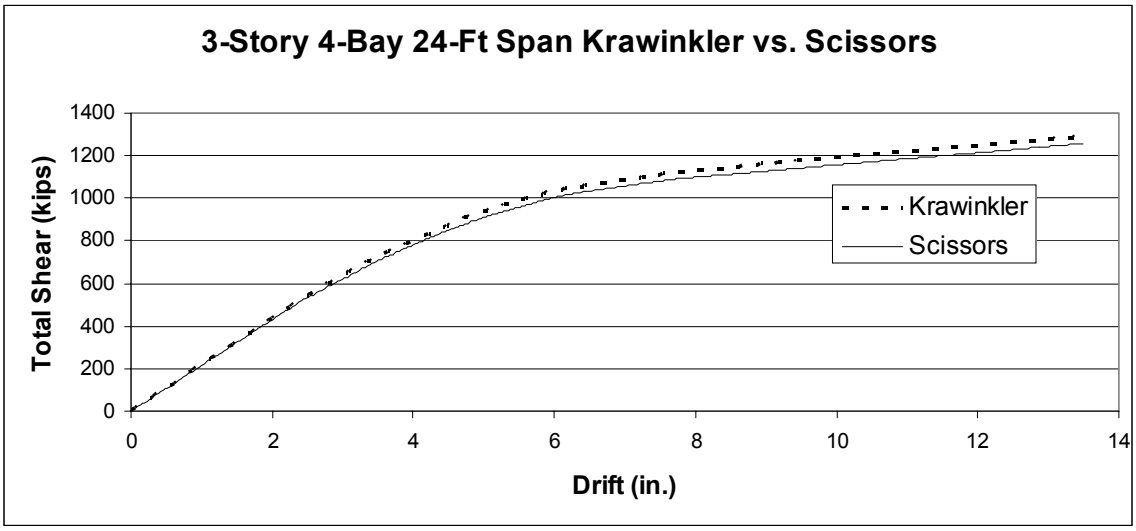

Figure 5.2-15: 3S-4B-24Ft Krawinkler vs. Scissors: Force/Displacement

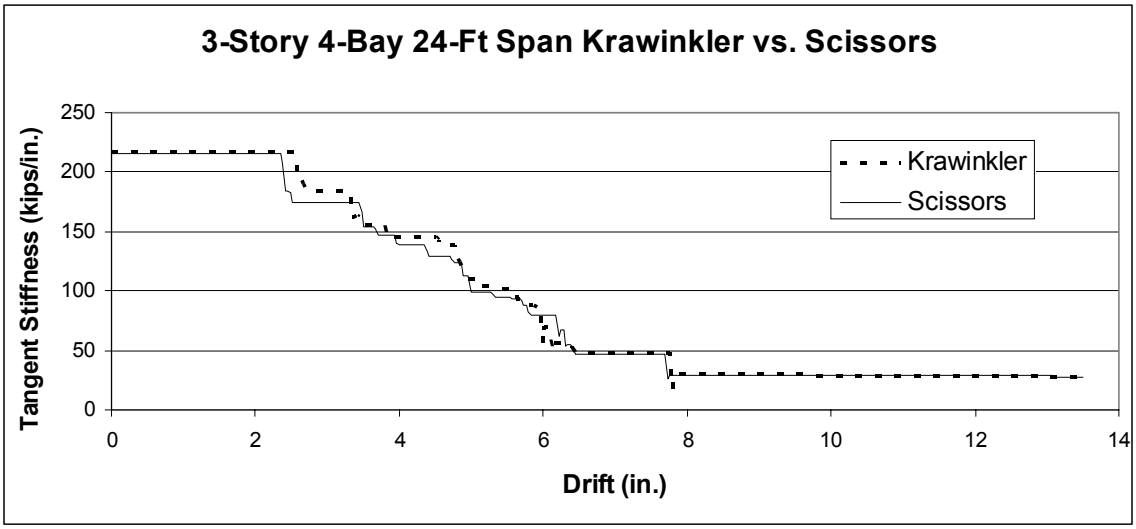

Figure 5.2-16: 3S-4B-24Ft Krawinkler vs. Scissors: Tangent Stiffness

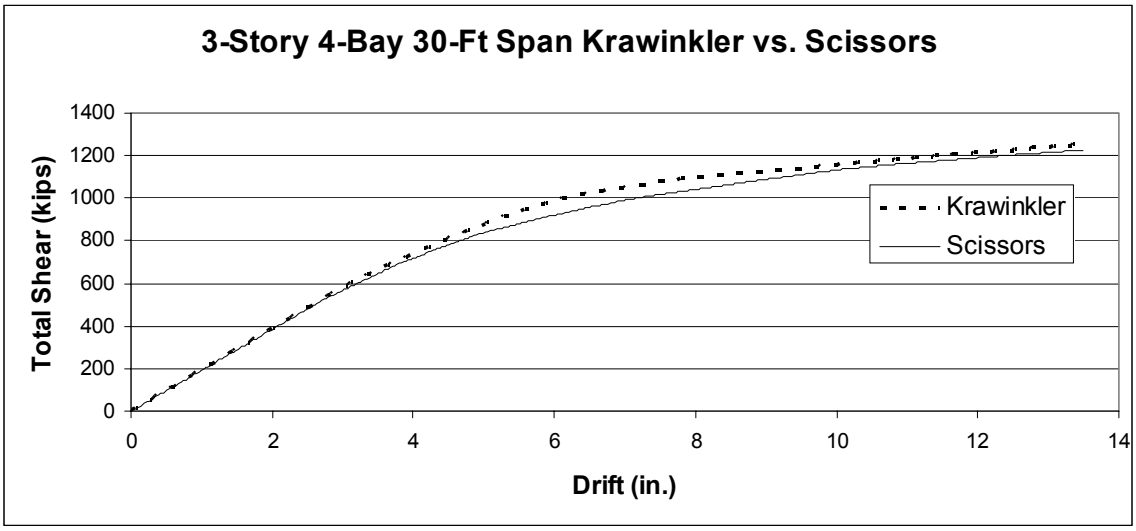

Figure 5.2-17: 3S-4B-30Ft Krawinkler vs. Scissors: Force/Displacement

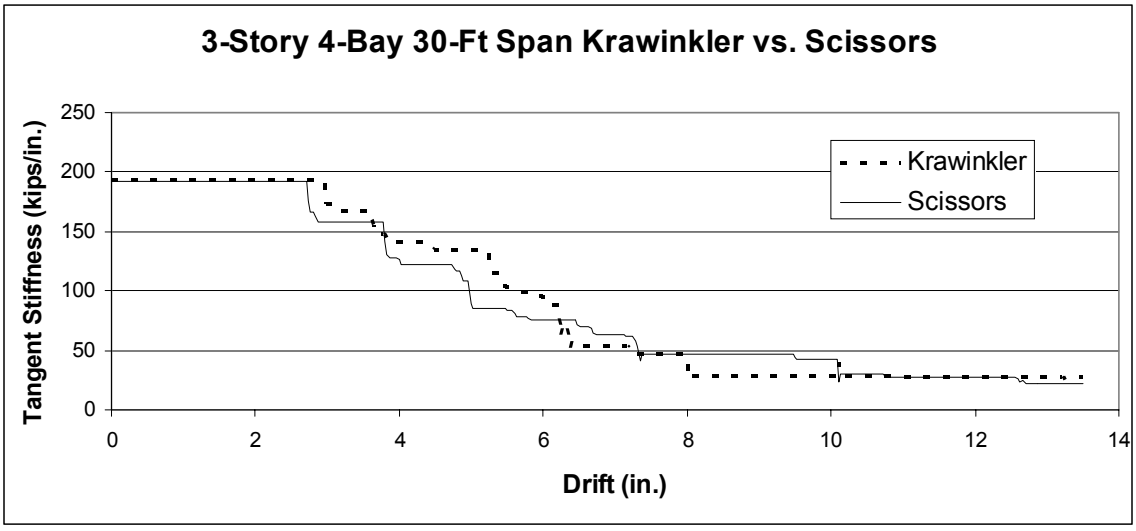

Figure 5.2-18: 3S-4B-30Ft Krawinkler vs. Scissors: Tangent Stiffness

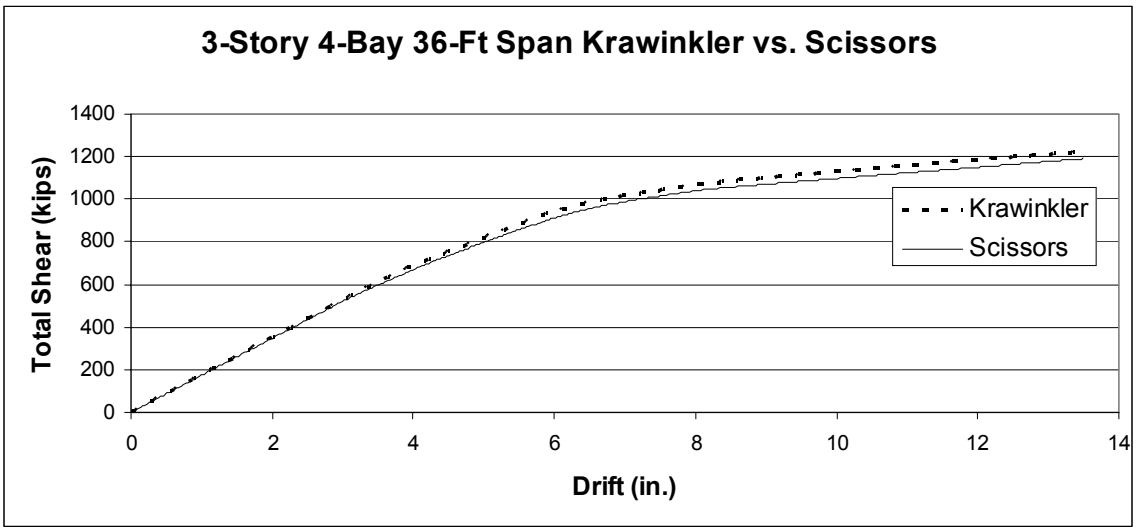

Figure 5.2-19: 3S-4B-36Ft Krawinkler vs. Scissors: Force/Displacement

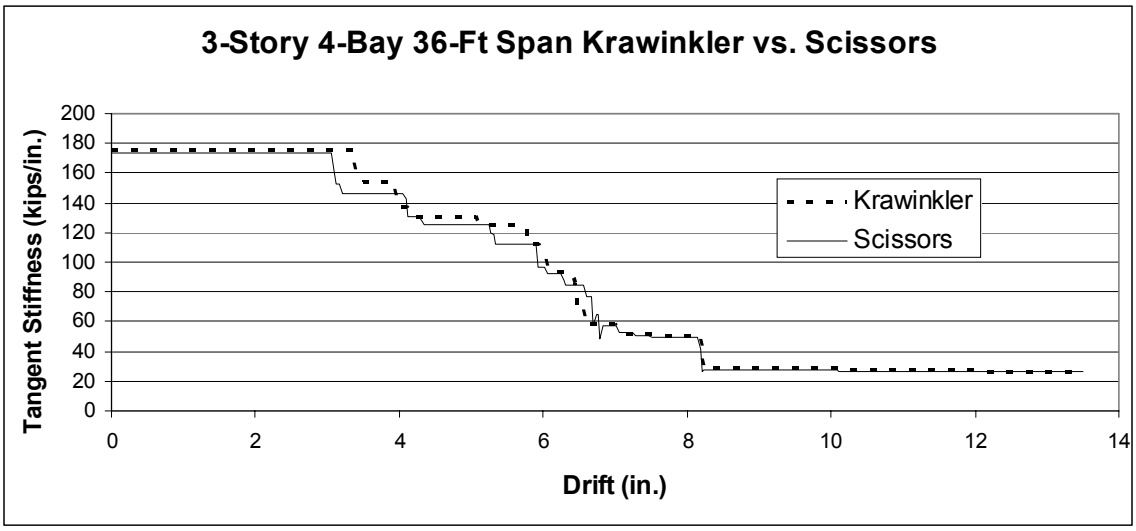

Figure 5.2-20: 3S-4B-36Ft Krawinkler vs. Scissors: Tangent Stiffness

Table 5.2-11: 3-Story 4-Bay Krawinkler vs. Scissors: Comparison

Bay Width (ft)	% Differences		
	Initial K (Kips/in.)	1st Yield (Kips)	Shear @ 3% Drift (Kips)
18	0.89	8.03	2.56
24	0.88	8.24	2.79
30	0.88	8.54	2.31
36	0.86	9.29	2.78

While the overall differences (Table 5.2-10 and Table 5.2-11) did increase, these results still indicated that there was little variation between the Krawinkler and Scissors models. The plots above (Figure 5.2-13 through Figure 5.2-20) also visually confirm this.

A third series of tests was developed to determine if the kinematic distinctions between the Krawinkler and Scissors models could ever cause a significant difference between the two model types. For this investigation, three-story two-bay models were used (the Krawinkler representation is shown in Figure 5.2-21). Since there was a noticeable increase in the percent differences between the two models in the previous example, these models were developed to allow yielding to occur only in the PZ region. To ensure that all yielding was localized in the panel zone, no hinge elements were used outside of this region and the girder and column Type 2 elements' yield moments were then set to an exceedingly high value. The hinge and geometric properties used in this series of models can be found in Table 5.2-12. The Scissors hinge properties will once again change depending on the bay-width of the model. Static pushover analyses were then performed to determine each model's force/displacement and tangent stiffness/displacement relationships. Two other structural models were also compared in this series of tests. They were identical to the first two in every respect except that hinging was allowed to occur outside the PZ region. This was done to show the significance of yielding in the girders outside the PZ region on the overall response of the

Krawinkler and Scissors models. The results from all four models are included in the plots below.

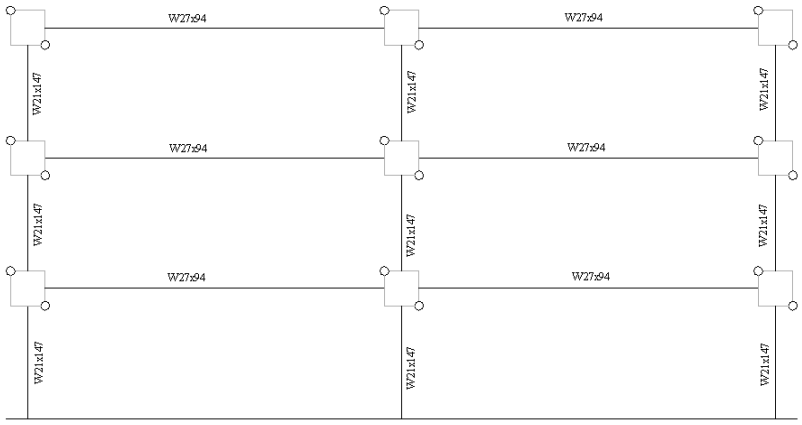

Figure 5.2-21: 3-Story 2-Bay Model

Table 5.2-12: Example 3-Story 2-Bay Krawinkler and Scissors Models Properties

L (in.)	432
H (in.)	150
Von Mises Yield Constant	0.6
Fy (ksi)	50
Poisson's ratio	0.3
G (ksi)	11154
E (ksi)	29000

Krawinkler Models

Beam	tf	d	βH
	in	in	in
W27x94	0.745	26.92	26.175
W27x94	0.745	26.92	26.175

Column	tf	d	αL	bf	tw	Doubler
	in	in	in	in	in	in
W21x147	12.51	1.15	22.06	20.91	0.72	0.500

Scissors Models

Beam	α
W27x94	0.0484

Column	β	1-α-β
W21x147	0.1745	0.7771

Krawinkler Models

Column	Beam	Panel		Flange	
		My	K	My	K
		in-k	in-k/rad	in-k	in-k/rad
		20032	7447752	1489	138401

Scissors Models

Panel		Flange	
My	K	My	K
in-k	in-k/rad	in-k	in-k/rad
25778	12333164	1916	229186

Note: depths defined center to center of flange

Girder Hinges

	First Component			Second Component		
Girder	My	K	Strain	My	K	Strain
	in-k	in-k/rad	Hardening	in-k	in-k/rad	Hardening
W27x94	13538	Huge	0.000	1494	450129	0.285

Table 5.2-13: 3-Story 2-Bay Krawinkler vs. Scissors: No Girder or Column Yielding

Bay Width (ft)	Krawinkler			Scissors		
	Initial K (Kips/in.)	1st Yield (Kips)	Shear @ 3% Drift (Kips)	Initial K (Kips/in..)	1st Yield (Kips)	Shear @ 3% Drift (Kips)
18	155.4	351	860	153.7	328	805
24	136.9	350	817	136.9	337	788
30	122.4	357	782	123	347	764
36	111	367	753	110.4	347	718

Table 5.2-14: 3-Story 2-Bay Krawinkler vs. Scissors: Girder and Column Yielding

Bay Width (ft)	Krawinkler			Scissors		
	Initial K (Kips/in.)	1st Yield (Kips)	Shear @ 3% Drift (Kips)	Initial K (Kips/in.)	1st Yield (Kips)	Shear @ 3% Drift (Kips)
18	155.4	351	609	153.7	328	601
24	136.9	350	588	136.9	337	587
30	122.4	357	573	123	347	576
36	111	367	559	110.4	347	561

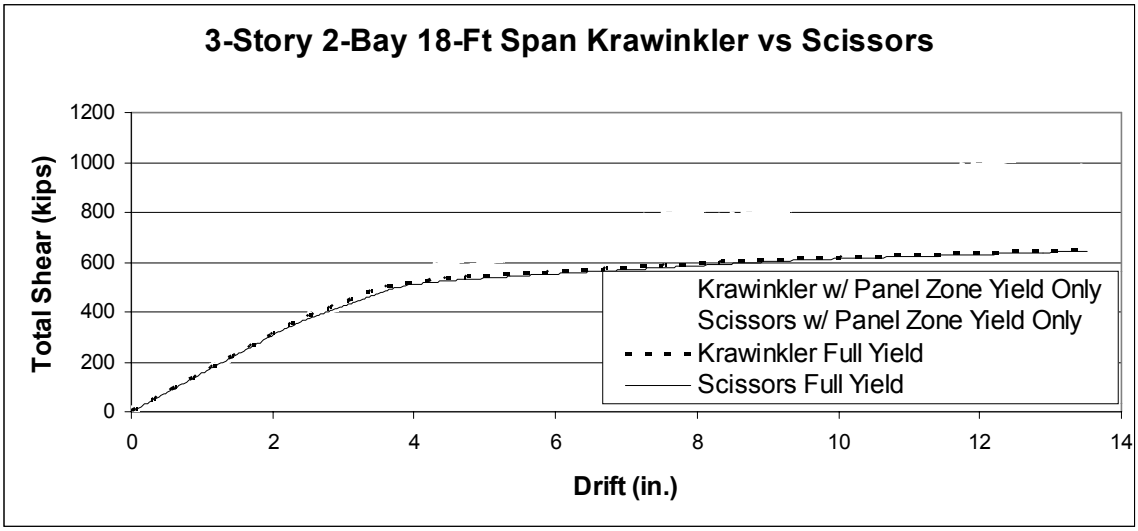

Figure 5.2-22: 3S-2B-18Ft Krawinkler vs. Scissors: Force/Displacement

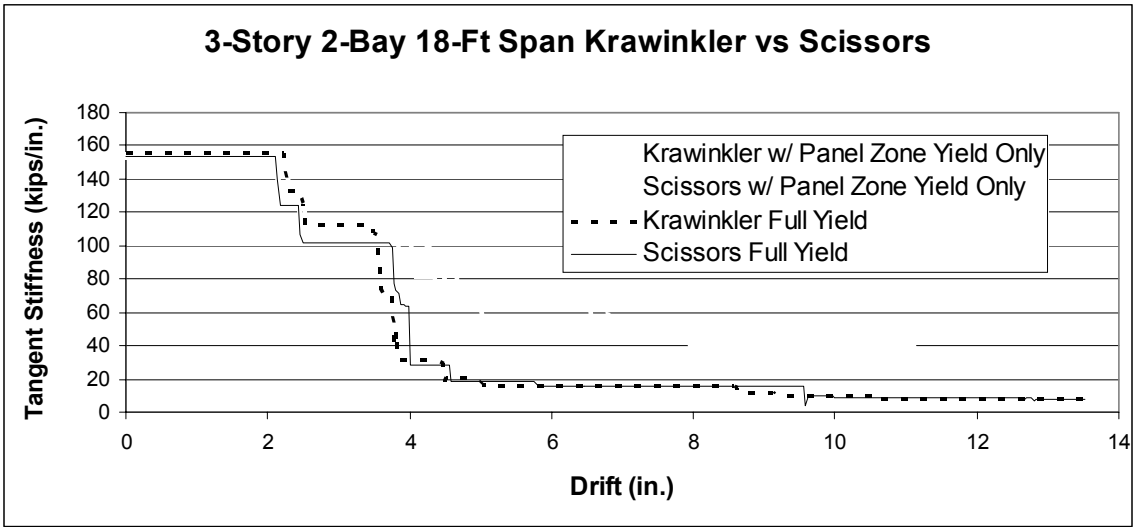

Figure 5.2-23: 3S-2B-18Ft Krawinkler vs. Scissors: Tangent Stiffness

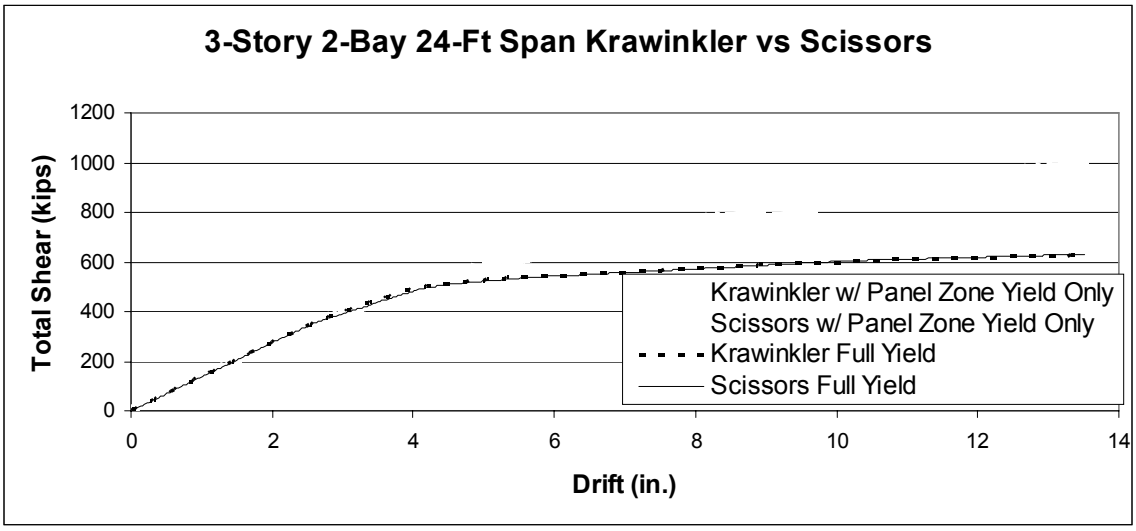

Figure 5.2-24: 3S-2B-24Ft Krawinkler vs. Scissors: Force/Displacement

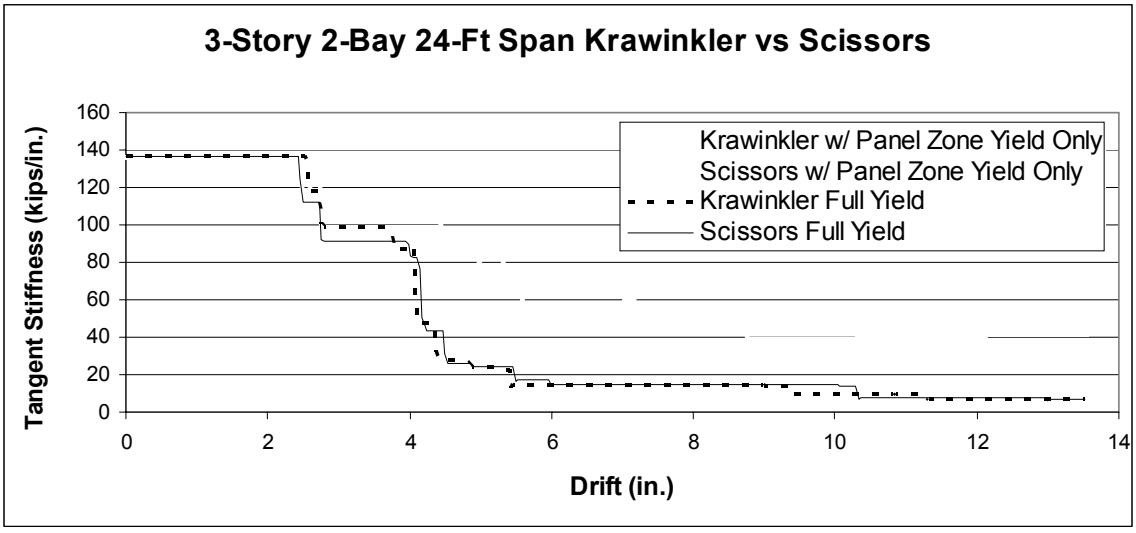

Figure 5.2-25: 3S-2B-24Ft Krawinkler vs. Scissors: Tangent Stiffness

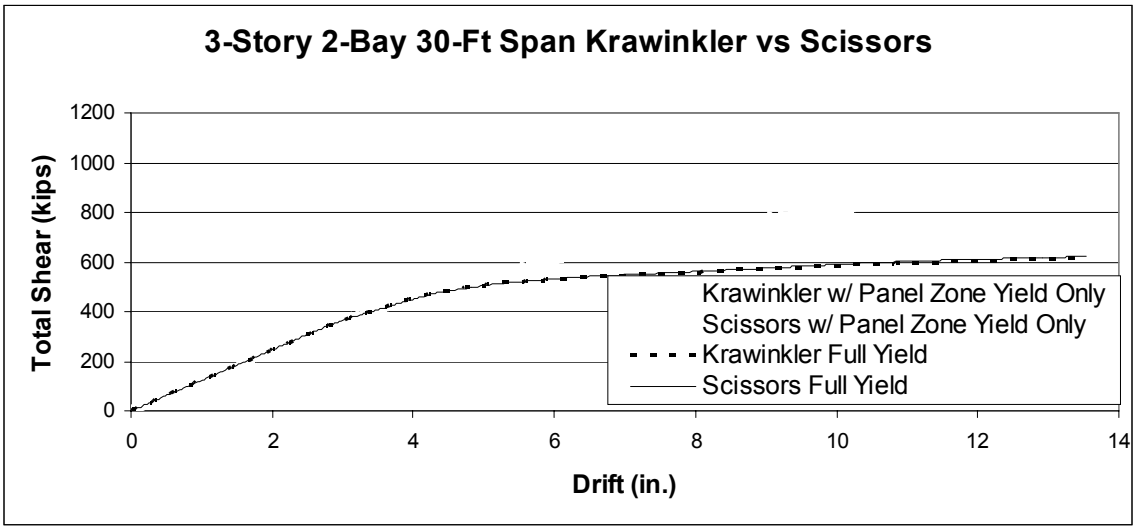

Figure 5.2-26: 3S-2B-30Ft Krawinkler vs. Scissors: Force/Displacement

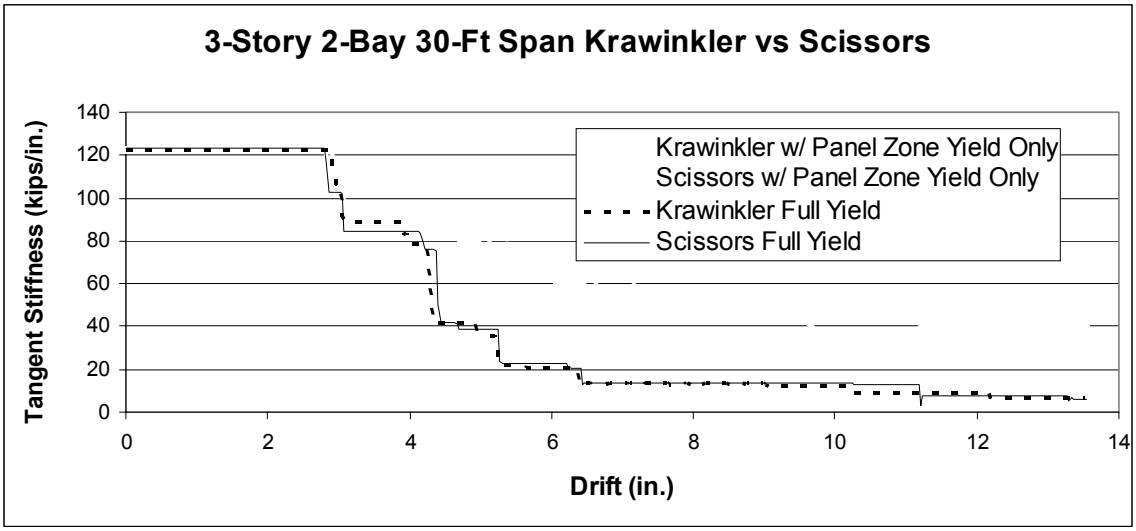

Figure 5.2-27: 3S-2B-30Ft Krawinkler vs. Scissors: Tangent Stiffness

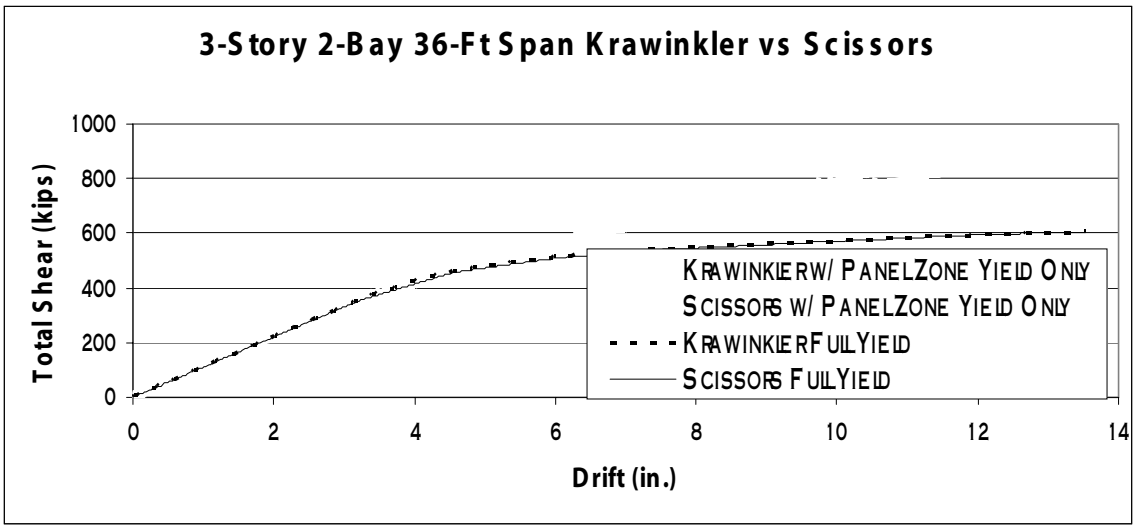

Figure 5.2-28: 3S-2B-36Ft Krawinkler vs. Scissors: Force/Displacement

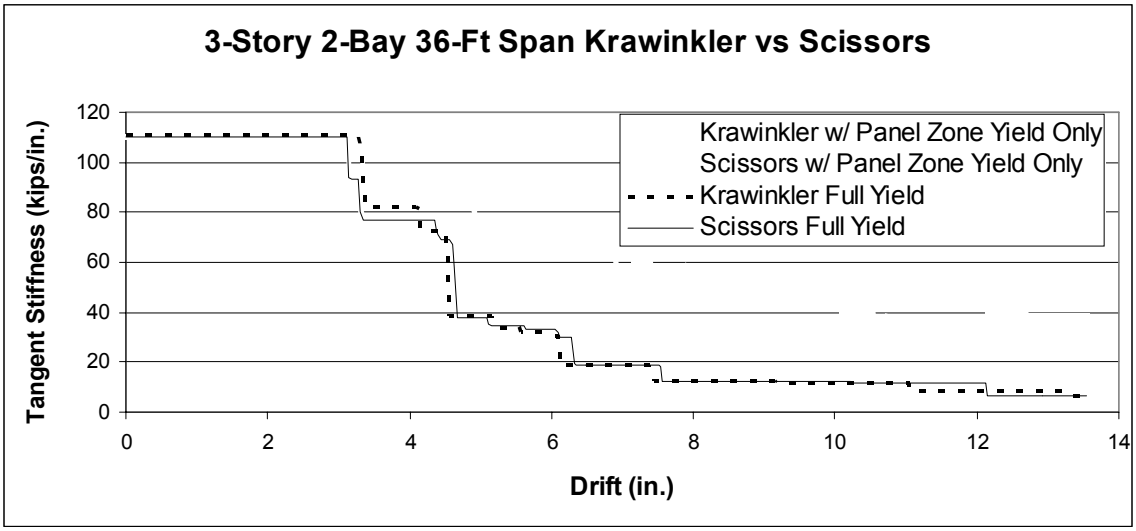

Figure 5.2-29: 3S-2B-36Ft Krawinkler vs. Scissors: Tangent Stiffness

Table 5.2-15: 3-Story 2-Bay No Girder or Column Yielding: Comparison

Bay Width (ft)	% Differences		
	Initial K (Kips/in.)	1st Yield (Kips)	Shear @ 3% Drift (Kips)
18	1.09	6.55	6.40
24	0.00	3.71	3.55
30	0.49	2.80	2.30
36	0.54	5.45	4.65

Table 5.2-16: 3-Story 2-Bay Girder and Column Yielding: Comparison

Bay Width (ft)	% Differences		
	Initial K (Kips/in.)	1st Yield (Kips)	Shear @ 3% Drift (Kips)
18	1.09	6.55	1.31
24	0.00	3.71	0.17
30	0.49	2.80	0.52
36	0.54	5.45	0.36

The above plots (Figure 5.2-22 through Figure 5.2-29) seem to indicate that there actually is a large difference between the two model types but it is negated by the additional plastic deformation/rotation located in the girders and columns. This rotation not only decreases the overall force that the structure can withstand but also allows the Scissors model components to remain closer to the ninety degree angle difference discussed previously. This is also confirmed by the percent differences shown in Table 5.2-15 and Table 5.2-16. To verify this observation, an additional test was performed on the original six-story five-bay model. The response of the original 28-ft bay-width model was compared to one in which the yield moments in the columns and the girder hinges were set very high to ensure that only the PZ hinges yielded. The results of this test can be found in Table 5.2-17 through Table 5.2-20 and Figure 5.2-30 and Figure 5.2-31 below.

Table 5.2-17: 6-Story 5-Bay Krawinkler vs. Scissors: No Girder or Column Yielding

Bay Width (ft)	Krawinkler			Scissors		
	Initial K (Kips/in.)	1st Yield (Kips)	Shear @ 3% Drift (Kips)	Initial K (Kips/in.)	1st Yield (Kips)	Shear @ 3% Drift (Kips)
28	113.9	728	1409	113.4	714	1336

Table 5.2-18: 6-Story 5-Bay Krawinkler vs. Scissors: Girder and Column Yielding

Bay Width (ft)	Krawinkler			Scissors		
	Initial K (Kips/in.)	1st Yield (Kips)	Shear @ 3% Drift (Kips)	Initial K (Kips/in.)	1st Yield (Kips)	Shear @ 3% Drift (Kips)
28	113.9	728	1001	113.4	714	990

Table 5.2-19: 3-Story 2-Bay No Girder or Column Yielding: Comparison

Bay Width (ft)	% Differences		
	Initial K (Kips/in.)	1st Yield (Kips)	Shear @ 3% Drift (Kips)
28	0.44	1.92	5.18

Table 5.2-20: 3-Story 2-Bay No Girder or Column Yielding: Comparison

Bay Width (ft)	% Differences		
	Initial K (Kips/in.)	1st Yield (Kips)	Shear @ 3% Drift (Kips)
28	0.44	1.92	1.10

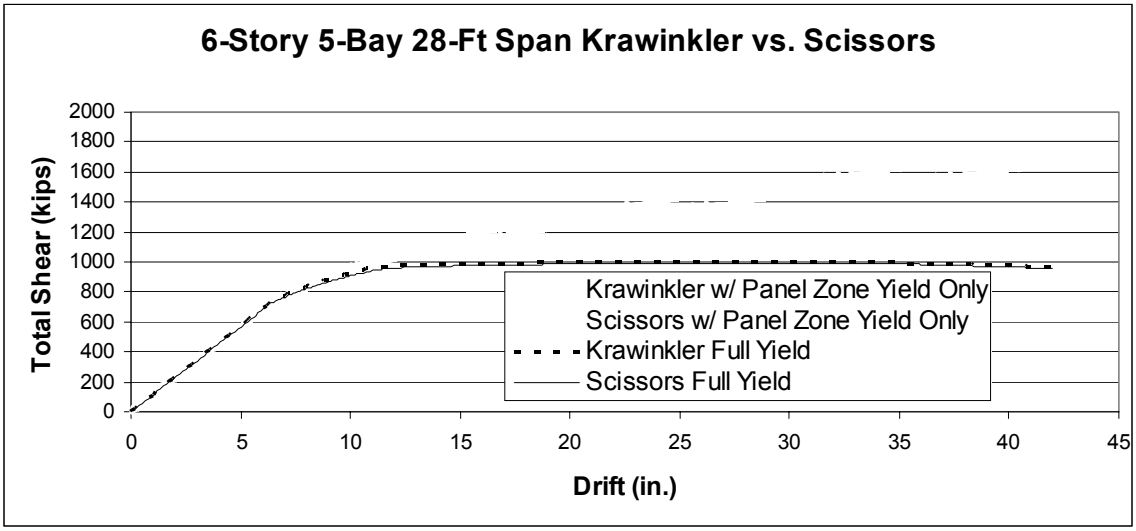

Figure 5.2-30: 6S-5B-28Ft Krawinkler vs. Scissors: Force/Displacement

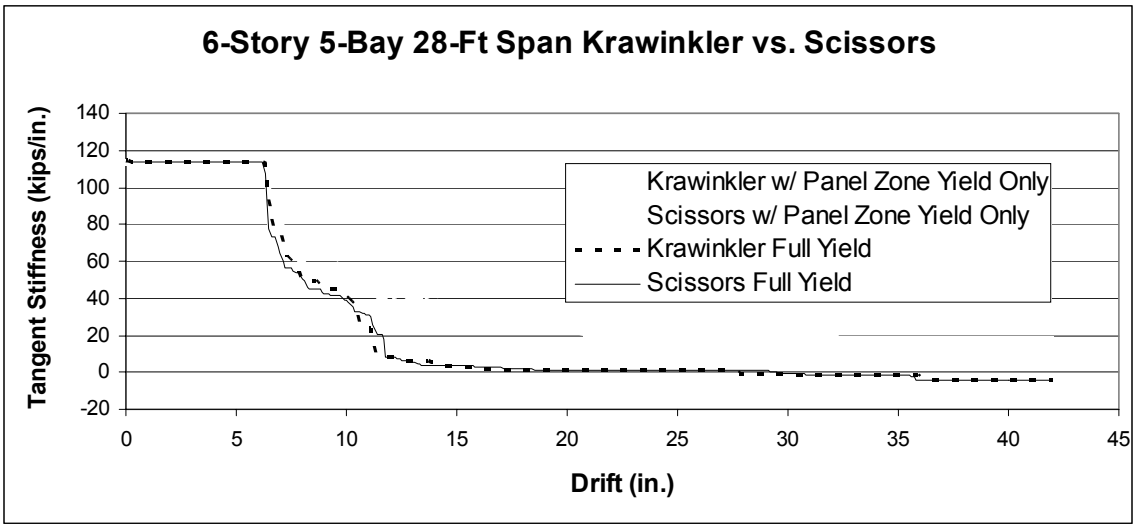

Figure 5.2-31: 6S-5B-28Ft Krawinkler vs. Scissors: Tangent Stiffness

Again, the models, which only allowed plastic deformation to occur in the PZ region, had significant differences between them. This confirmed that the plastic rotation that occurs in the girders is large enough to override the kinematic differences of the Krawinkler and Scissors model.

5.2.4 Use of Scissors Model with Krawinkler Properties

In the literature, it appears that it is common practice for a Scissors model to be used but with the Krawinkler properties (Krawinkler and Mohasseb 1987, Kim and Engelhardt 1995 and 2002, Schneider and Amidi 1998, Foutch and Yun 2002). A final frame test, also on the original 28-ft bay width model, was performed to quantify the differences in response of two models which are identical other than the change in the Scissor model's spring properties. The values for the PZ hinge properties used are located in Table 5.2-1 above. These models were also evaluated using a static pushover analysis including both gravity and P-delta effects.

Table 5.2-21: 6-Story 5-Bay Scissors Model w/ Krawinkler Properties: Results

Bay Width (ft)	Scissors w/ Krawinkler Properties			Scissors w/ Scissors Properties		
	Initial K (Kips/in.)	1st Yield (Kips)	Shear @ 3% Drift (Kips)	Initial K (Kips/in.)	1st Yield (Kips)	Shear @ 3% Drift (Kips)
28	100.3	551	884	113.4	714	994

Table 5.2-22: 6-Story 5-Bay Scissors Model w/ Krawinkler Properties: Comparison

Bay Width (ft)	% Differences		
	Initial K (Kips/in.)	1st Yield (Kips)	Shear @ 3% Drift (Kips)
28	13.06	29.58	12.44

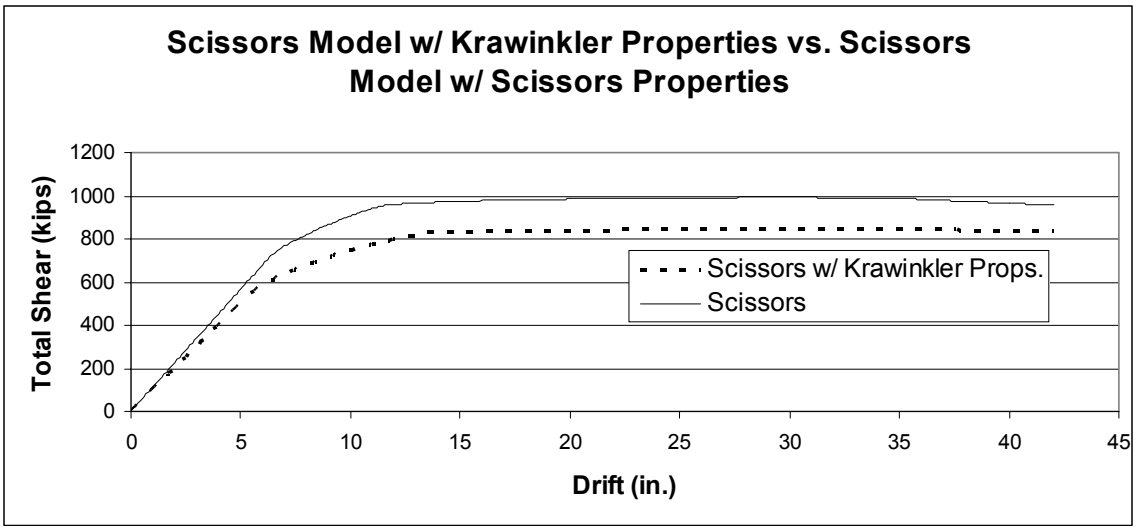

Figure 5.2-32: Scissors Model w/ Krawinkler Properties vs. Scissors Model w/ Scissors Properties: Force/Displacement

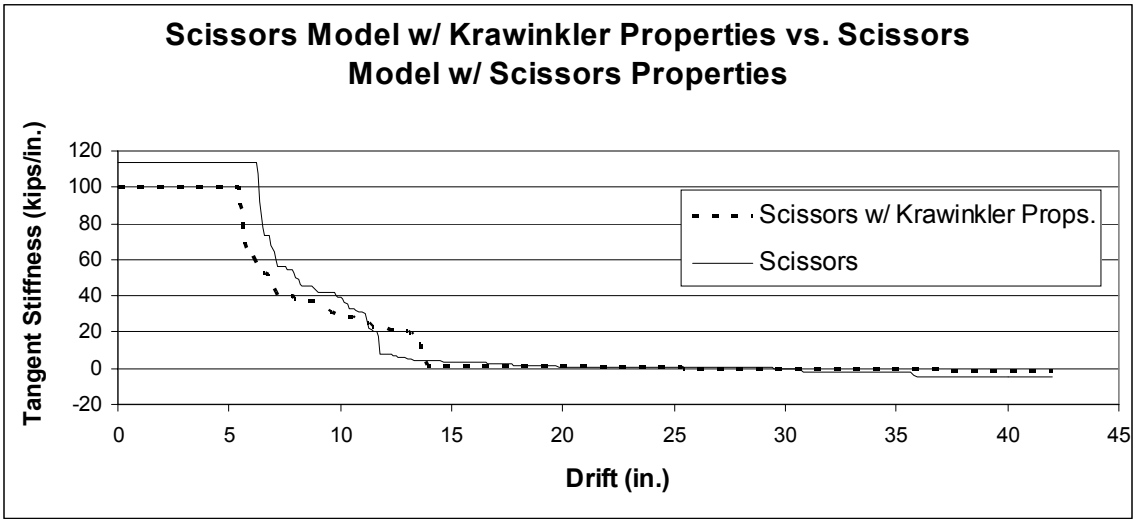

Figure 5.2-33: Scissors Model w/ Krawinkler Properties vs. Scissors Model w/ Scissors Properties: Tangent Stiffness

As would be expected from comparing the large differences in the yield and stiffness values between the two models in Table 5.2-21 and Table 5.2-22, these results do not correlate well. Using Krawinkler properties for a Scissors model makes the structure much less stiff and strong than it would be if the properties developed for use with the Scissors model were used. This difference in stiffness obviously has a direct effect on the pushover but may even be more significant when determining modal response and frequencies for dynamic analysis and may affect the sequencing of yielding.

5.3 Summary and Discussion

With the similarities in the results between the Krawinkler and Scissors models, using the Scissors model for nonlinear static pushover analysis would make the most sense. With its reduced number of modeling components, the number of degrees of freedom is drastically reduced. This reduction will shorten both the time required to build the model and to complete the analysis. This being said, there are still many instances in which the Scissors model should not be used. If the bay widths or story heights are not constant throughout the structure, there is no way to accurately determine the α and β coefficients used in the Scissors model's strength and stiffness property equations. As shown in the comparison of a Scissors model versus a Scissors model with Krawinkler properties, a haphazard treatment of these properties can have a significant impact on the response of the structural model to the applied loads. None of the above analyses addresses the inability of the Krawinkler or Scissors model to include continuity plates or the additional deflection due to PZ flexure. These limitations will be addressed in the new model development in Chapter 7.

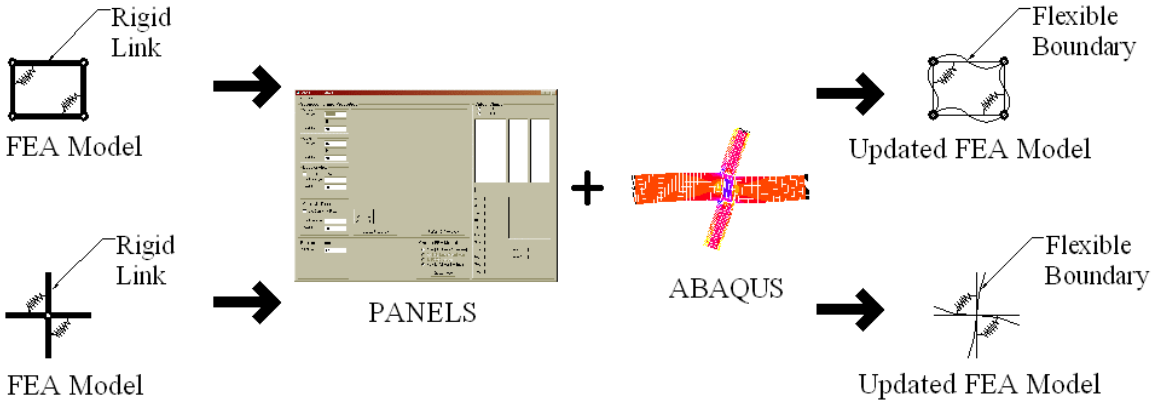

Figure 5.3-1: Thesis Flow Chart

Looking at Figure 5.3-1, all the elements necessary to modify the FEA models to account for continuity plates and PZ flexure have been presented. With the similarity in the response between the Krawinkler and Scissors models, these modifications will be made to both of them (Chapter 7). The only remaining issue before this task is undertaken is whether the results from PANELS, ABAQUS, and Drain-2DX(using both the Krawinkler model and Scissors model) compares favorably with actual test data (Chapter 6).

6 Correlation with SAC Test Results

6.1 Introduction and Scope

During the 1994 Northridge Earthquake, a number of unexpected failures were attributed to brittle weld failures at the beam/column joint interface. Since the design of steel moment resisting frames (SMRF) is based on the belief that the beam/column joint would remain ductile and withstand repeated cycles of large inelastic deformations, the cause of these failures had to be addressed. In response to this demand, the SAC Joint Venture, an acronym for the partnership made up of the Structural Engineers Association of California (SEAOC), the Applied Technology Council (ATC) and California Universities for Research in Earthquake Engineering (CUREe), combined with the Federal Emergency Management Agency (FEMA) to carry out an in-depth study of SMRFs (FEMA 1995, 1996 and 2000). The focus of this study was to determine why the failures occurred, what methods could be employed in the field to repair the defective connections and what improvements needed to be made to the current design and construction practices to ensure that this type of brittle failure would not occur again.

In this portion of the research results presented, the PANELS formulas (developed in Chapter 2 and Chapter 4) and the ABAQUS models (developed in Chapter 4) are compared to four bare frame cruciform assemblies tested at Lehigh University (Ricles et al. 2002) during Phase II of the SAC Steel Project. The intent of these comparisons is to determine the effectiveness of the PANELS equations and the ABAQUS models to imitate the response from experimental tests. This was done to validate the ABAQUS modeling techniques used, since they are the basis of all the previous assertions made in this thesis. Good correlation with experimental results will provide additional support to the author's assertions that neglecting the effects of PZ flexure and the addition of continuity plates causes errors in estimating a subassemblage's elastic drift when the Krawinkler or Scissors model is used.

6.2 Literature Review

From the lack of published material in the early 1990's on the subject, it appears that leaders in the experimental arena felt that the questions involved in PZ phenomena had been answered. There was one group of experiments (Schneider, Roeder and Carpenter 1993), which analyzed the interaction between yielding of the PZ using strong column/weak beam (SCWB) and weak column/strong beam (WCSB) techniques to determine the overall ductility demand of the sub-assemblage of each. These experiments validated using the PZ to dissipate earthquake energy, although the results from the code equations were disputed. However, the last line of the conclusions in that paper foreshadowed the direction of the experimental research for the last few years of the twentieth century: "…care must be made in the design and detailing of these frames to provided satisfactory performance."

The 1994 Northridge earthquake completely altered the design community's outlook on the efficacy of the beam/column moment connections to dissipate earthquake energy. Even though there were no major collapses of SMRF buildings, more than 200 structures experienced brittle weld fractures at the beam/column interface. From the beginning, these failures were attributed to allowing the PZ to deform inelastically, which placed a high demand on weld ductility, especially in the tension flange (Liew and Chen 1995). Due to this poor performance, the entire design philosophy of the beam/column joint was reevaluated. At the forefront in this endeavor were the SAC Joint Venture and FEMA who coordinated and funded the two phases of research to determine how to repair the structures damaged in the Northridge earthquake and what design changes need to be made to ensure that this type of failure did not occur in the future.

The research for that project was broken down into six different categories: materials and fracture, joints and inspection, connection performance, system performance, performance prediction and evaluation and past performance of steel buildings in earthquakes. Phase I of this project was devoted to developing welding guidelines, quality insurance, post earthquake action and quality insurance. The focus of

Phase II was to foster innovation in design while still developing reliable and cost effective seismic design criteria and standards of practice for SMRFs (Kunnath and Malley 2002). The final results from this study have all been published and are available through the Federal Emergency Management Agency (1995, 1996 and 2000).

One segment of Phase I was a critical review of pre-Northridge beam/column joints (Whittaker et al. 1998) to determine why so many beam/column joints fractured. From a review of the literature on previous full-scale tests of beam/column joints, doubt was cast on the ability of a beam to experience a mean plastic rotation of 0.03 radians (established by SAC as a target plastic hinge rotation) even under controlled lab conditions because of the variability in groove weld performance. The quality of workmanship in these welds was recognized to be the critical factor in the overall connection performance. Also at fault was the design practice of detailing SMRF's with only two vertical bays of seismic framing in each direction. The original moment resisting frames of the 1960s and 1970s were designed as multiple bays of seismic resisting framing, allowing the designers to use smaller columns. As the importance of proper weld detailing became apparent, inspections of all SMRF joints in a structural system were required. With the increase in the cost of labor, it became more cost effective to eliminate the number of joints to be inspected by reducing the number of seismic resisting elements and increasing the column and beam sizes of the remaining moment resisting frames than to continue using multiple seismic resisting bays. The effects of this change were unknown since virtually all of the beam/column experiments that had been previously performed were on smaller column and beam sections (Whittaker et al. 1998). Nevertheless, it is obvious that this decision significantly reduced the overall redundancy of the structure.

Full-scale tests of these pre-Northridge connections were performed (Whittaker et al. 1998) and the results were then compared to models developed using Drain-2DX. Using welding practices that more closely simulated the outcome experienced in the field, the results from these experiments were plastic deformation responses that were highly variable and poor. The PZ distortions caused kinks in the column flanges, which

resulted in highly localized strains that caused weld fractures. Another significant find was how much the variability in steel strength changes the connection's performance characteristics. First using nominal material properties, then followed by the values from the coupon, the data clearly showed the uncertainties associated with designing a beam/column joint including PZ deformation. After failure, the subassemblies were re-welded to determine the effectiveness of this currently used mitigation procedure. These repaired assemblies also performed poorly, casting doubt on their effectiveness. The conclusion reached by the authors of that paper was that the PZ region should be designed to remain elastic and requiring all plastic hinges to be developed in the beams.

Phase I also included some very detailed finite element analysis (FEA) and statistical analysis based upon the initial SAC tests and earlier tests performed. One example (El-Tawil et al. 1999) was FEA models of SMRF tests (Popov et al. 1996) to examine the effects of panel zone yielding on the behavior of SMRFs. These models were extremely detailed, including weld access holes, shear tabs, etc., with the intent of determining the stress distributions at the weld contact surfaces of the beam/column joint to develop a better understanding of the stress distributions which could cause a brittle weld failure. From this study, it was concluded that designing a PZ which allows for large deformations (weak PZ) in the PZ region can lead to a greater potential for brittle failure. Although the plastic rotations of the beams were much smaller, the large rotations within the PZ region created a critical stress condition. Detailed statistical analysis by Roeder and Foutch (1996) of numerous cyclic tests performed on SMRF subassemblages also showed that when a weak PZ was used, the potential for brittle failure at the welds of the beam/column interface was much higher.

With the vast amount of detailed information available from Phase I, researchers began Phase II of the SAC Steel Project. For the test data used in the comparisons contained within this thesis, the data from experiments on the performance of an improved beam/column moment connection (Ricles et al. 2002) was used. In these experiments, updated connection details were employed to develop a subassemblage which would allow for a mean plastic rotation of 0.03 radians. By modifying the shape

of the weld access hole to minimize the plastic strain at the toe of the access hole region, the target goal of 0.03 radians was achieved. The shape of this modified access hole was based on a nonlinear FEA parametric study by Ricles et al. (2000) and Mao et al. (2001). A total of eleven tests was performed, six on End subassemblages and five on Cruciform subassemblages. These test sections both included and excluded continuity plates, which was an added bonus since their contribution is a focus of this study. The reader is encouraged to examine all three of the above articles for the full details of the updates presented.

Other experimental research conducted during Phase II was the use of reduced beam sections for moment connections (Jones et al. 2002, Chi and Uang 2002, Gilton and Uang 2002), cover plate, flange plate and end-plate moment connections (Kim et al. 2002, Schneider and Teeraparbwong 2002, Sumner and Murray 2002). The focus of all these experiments was again to develop connection details which would allow for a 0.03 radian plastic rotation to be achieved that were still constructible and cost effective. None of these aforementioned tests were used in the data comparisons and again, the reader is encouraged to read the above documents for the details of the individual results.

6.3 Linear Elastic Response (PANELS)

To evaluate the effectiveness of the elastic modeling techniques developed and implemented in PANELS, a series of comparisons was performed between PANELS and test results (Ricles 2002) from Phase II of the Sac Steel project. A summary of the geometric and material properties for each test is located in Table 6.3-1 through Table 6.3-4 below. These properties will be used for both the elastic and inelastic comparisons. For a complete description of the subassemblages used, the reader can refer to either Ricles (2002) or www.Sacsteel.org.

Table 6.3-1: Lehigh Test C1 (Ricles 2002): Geometric and Material Properties

Member	Size	Length (in.)	Grade	Yield Stress (ksi)	
				Mill Certs.	Coupon Test
Girder	W36x150	354	A572 Grade 50	57	56.7 flange 62.9 web
Column	W14x398	156	A572 Grade 50	54	53.2 flange 52.2 web
Continuity Plate	N/A		N/A	N/A	N/A
Doubler Plate	(2) @ ¾”		A572 Grade 50	57	57.1

Table 6.3-2: Lehigh Test C2 (Ricles 2002): Geometric and Material Properties

Member	Size	Length (in.)	Grade	Yield Stress (ksi)	
				Mill Certs.	Coupon Test
Girder	W36x150	354	A572 Grade 50	57	56.7 flange 62.9 web
Column	W14x398	156	A572 Grade 50	54	53.2 flange 52.2 web
Continuity Plate	(4) @ 1”		A572 Grade 50	57	57.1
Doubler Plate	(2) @ ¾”		A572 Grade 50	56	53.0

Table 6.3-3: Lehigh Test C3 (Ricles 2002): Geometric and Material Properties

Member	Size	Length (in.)	Grade	Yield Stress (ksi)	
				Mill Certs	Coupon Test
Girder	W36x150	354	A572 Grade 50	56	55.1 flange 61.8 web
Column	W27x258	156	A572 Grade 50	53	50.2 flange 55.7 web
Continuity Plate	N/A		N/A	N/A	N/A
Doubler Plate	(2) @ $^{5}/_{8}$"		A572 Grade 50	63.8	64.5

Table 6.3-4: Lehigh Test C4 (Ricles 2002): Geometric and Material Properties

Member	Size	Length (in.)	Grade	Yield Stress (ksi)	
				Mill Certs	Coupon Test
Girder	W36x150	354	A572 Grade 50	56	55.1 flange 61.8 web
Column	W27x258	156	A572 Grade 50	53	50.2 flange 55.7 web
Continuity Plate	(4) @ 1"		A572 Grade 50	63.8	64.5
Doubler Plate	(2) @ $^{5}/_{8}$"		A572 Grade 50	56	64.5

Using the test data from these four experiments, plots comparing the elastic response of the cruciform tests to the results determined by PANELS were developed and are shown in the four figures below.

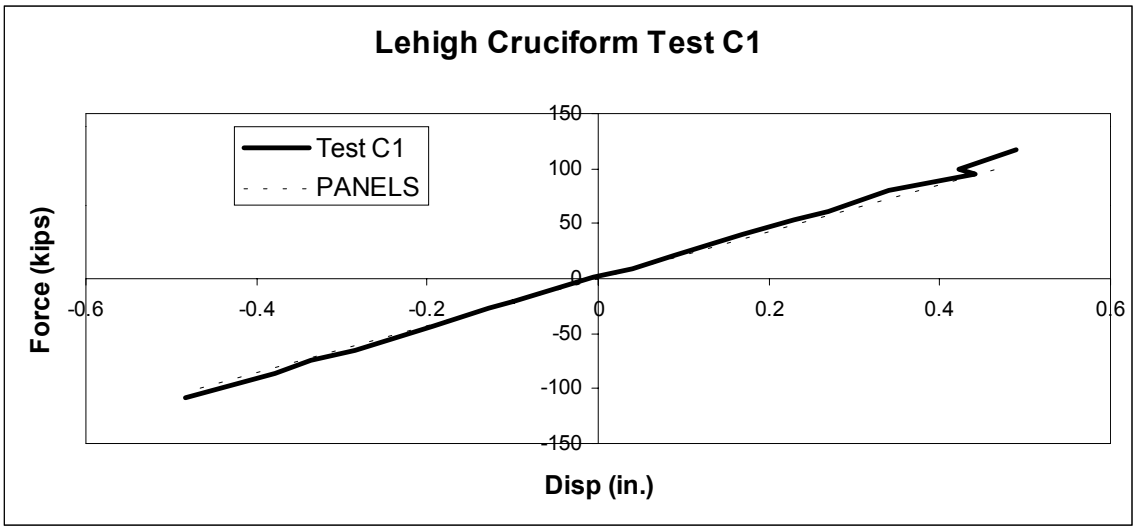

Figure 6.3-1: Lehigh Test C1 (Ricles 2002): Elastic Comparison

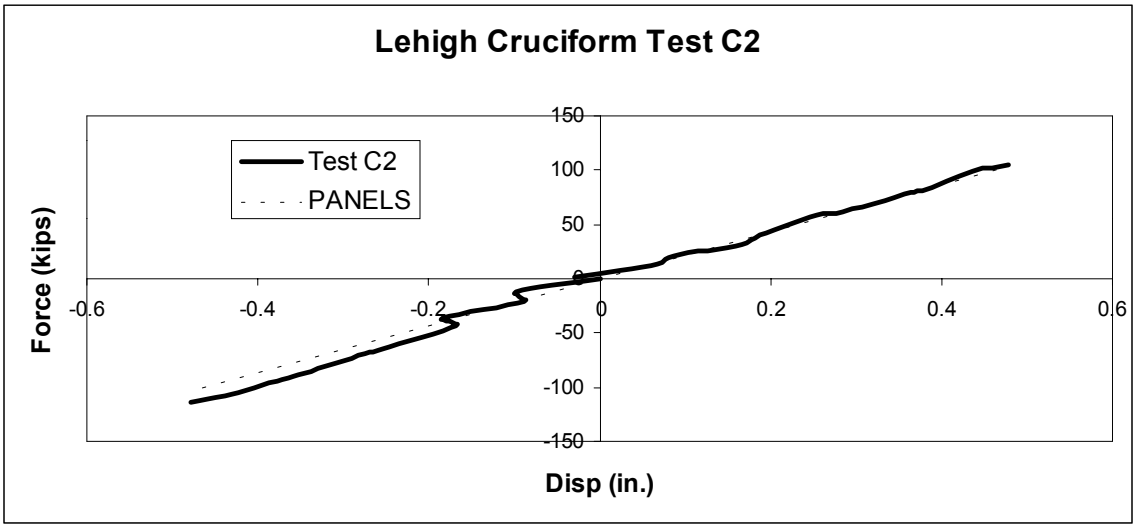

Figure 6.3-2: Lehigh Test C2 (Ricles 2002): Elastic Comparison

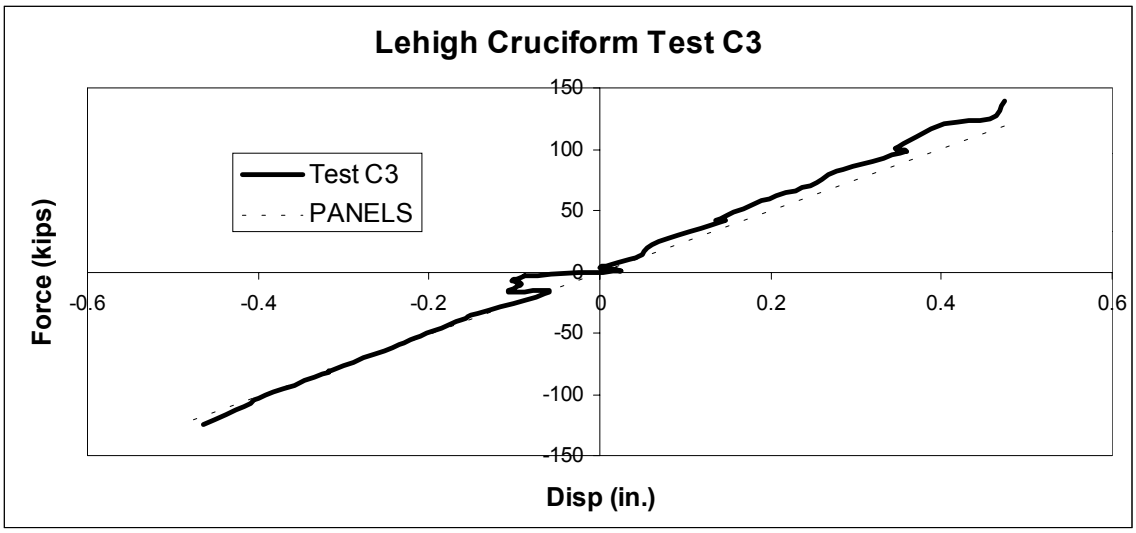

Figure 6.3-3: Lehigh Test C3 (Ricles 2002): Elastic Comparison

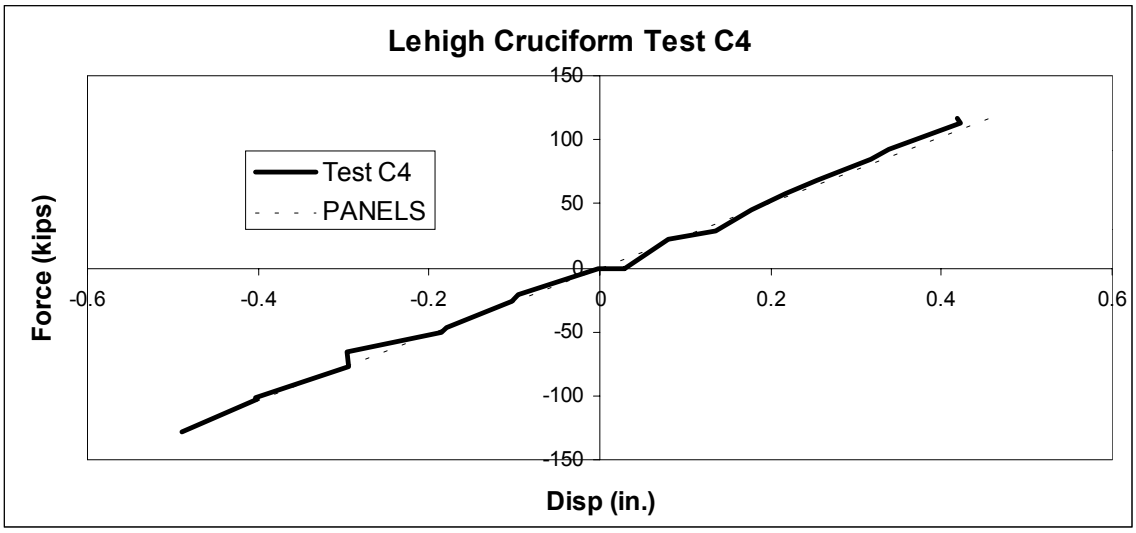

Figure 6.3-4: Lehigh Test C4 (Ricles 2002): Elastic Comparison

As seen in the four preceding figures, the results from PANELS correlate very well with all four cruciform tests. The stiffness from the Lehigh tests C1 and C4 compared to the PANELS data is virtually indistinguishable. Correspondingly, for tests C2 and C3, if the jumps in the data are ignored and only the slopes of the test data versus the PANELS plots compared, the plots match up very well.

6.4 Inelastic Response (ABAQUS)

With a confirmation of the ability of PANELS to accurately model the elastic deflections of a cruciform subassemblage, inelastic comparisons between the four Lehigh tests performed by Dr. Ricles (2002) and four representative models developed using ABAQUS and the properties in Table 6.3-1 through 6.3-4 were performed. The results from these comparisons are shown in Figure 6.4-1 through 6.4-4. In these figures, both the raw test data and adjusted test data are plotted versus the ABAQUS results.

The tests performed by Dr. Ricles were cyclic in nature. To make a comparison with the ABAQUS models, the data was restructured to represent a monotonic test. This was accomplished by first tabulating the load and corresponding deflection for each cycle. A separate table of data was then created starting from the initial cycle, and was then based on the maximum load of each preceding cycle. When the load exceeded the maximum value from the preceding cycle, the remaining test data was added to the new table. The process was continued until the maximum load was reached. At this point, the data was considered displacement controlled. The remaining data corresponding to the maximum displacement from each concurrent cycle was then added to this new table until the maximum displacement was achieved. Since large deformations are not the focus of this study, the data at the larger displacements was then removed. The data was then plotted and named according to its representative test designation.

Looking at these test data plots in the figures below, it is observed that there appears to be some "play" in the test configuration and/or data acquisition system. In an attempt to account for this, the test data was revised. This was achieved by shifting the data points where an observable jump in the data occurred, then adjusting the remaining data associated with the particular jump to have the same slope as observed in the original test data. These are the adjusted plots shown below.

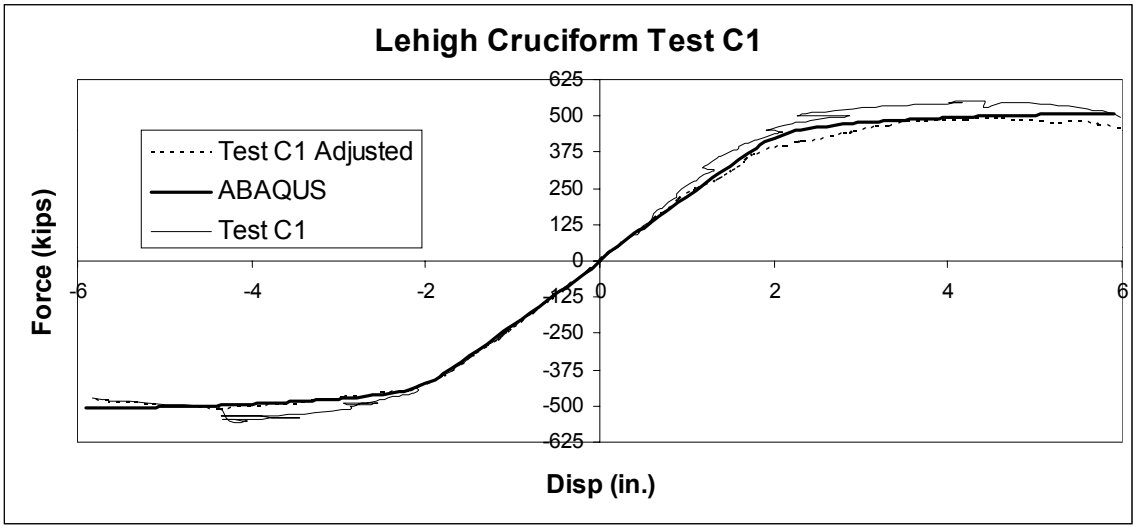

Figure 6.4-1: Lehigh Test C1 (Ricles 2002): Inelastic Comparison

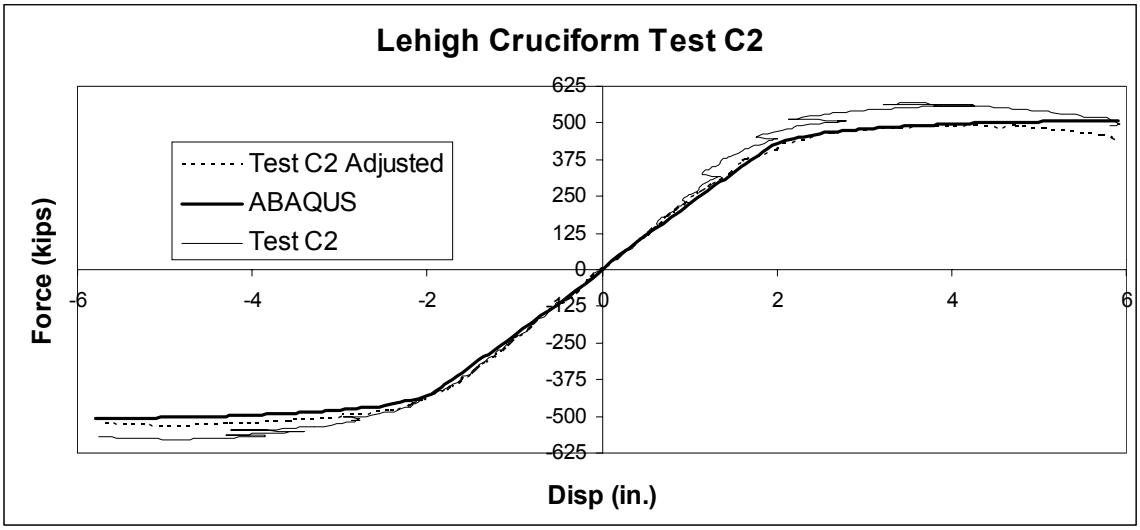

Figure 6.4-2: Lehigh Test C2 (Ricles 2002): Inelastic Comparison

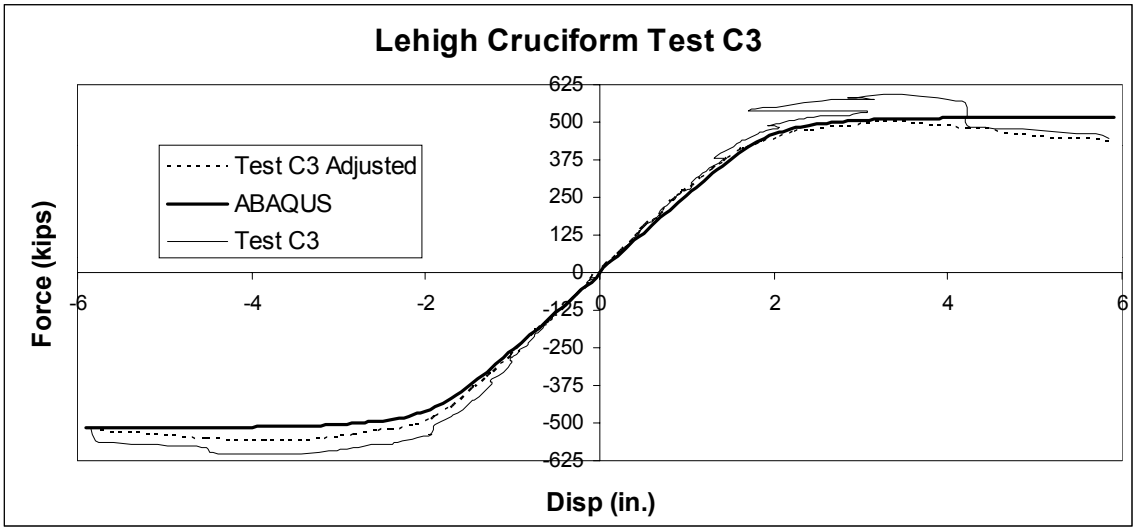

Figure 6.4-3: Lehigh Test C3 (Ricles 2002): Inelastic Comparison

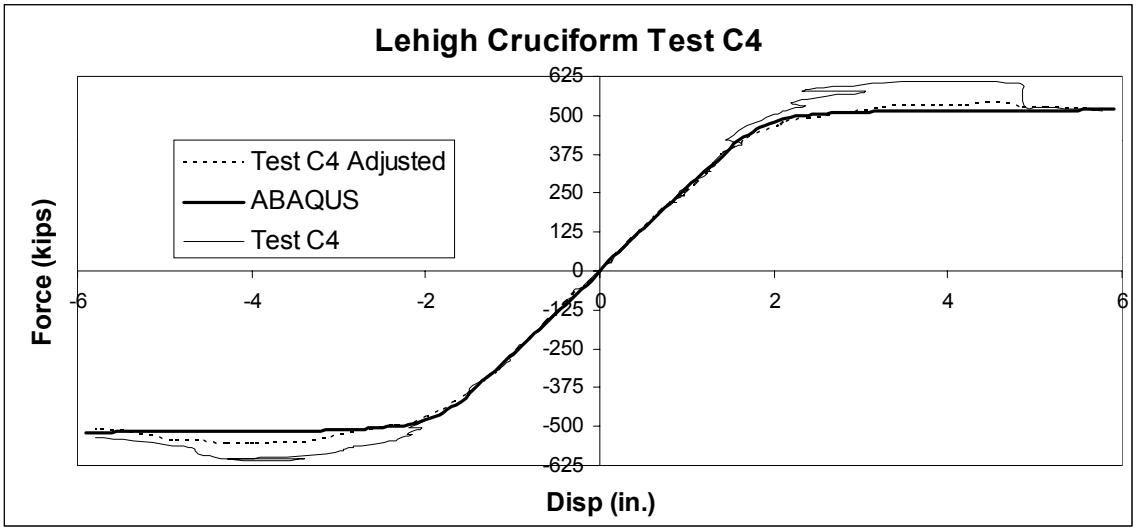

Figure 6.4-4: Lehigh Test C4 (Ricles 2002): Inelastic Comparison

As observed in the above plots, there is a close correlation between the ABAQUS models and the Lehigh test data (Ricles 2002) not only in the elastic portions of the curves but in the inelastic region as well. Considering that the ABAQUS models did not include any of the connection details - weld access holes, shear tabs, etc. - they do a good job predicting the actual behavior of the tested subassemblage. If more detail were put into modeling the actual connections at the beam/column interface and accounting for the change in strain hardening that occurs as the subassemblage experiences more yielding, etc., the ABAQUS models could be made even more accurate. Since the purpose of this inelastic comparison was only to show that the ABAQUS models used to develop the elastic PANELS equations in Chapter 2 and Chapter 4 are accurate and that they could also represent inelastic behavior for small deformations, the modifications were not performed.

6.5 Summary and Discussion

Table 6.5-1 gives a final summary of the elastic drift comparison between the four Lehigh Cruciform subassemblages (Ricles 2002) and the values determined using the PANELS equations.

Table 6.5-1: Lehigh Tests (Ricles 2002) vs. PANELS: Elastic Drift Comparison

Test	Applied Load (kips)	Estimated Experimental Drift (in.)	PANELS Drift (in.)
C1	100	0.475	0.482
C2	100	0.475	0.480
C3	100	0.398	0.407
C4	100	0.396	0.401

The estimated experimental drift was determined by calculating the slope of a "best fit" linear equation that started at (0, 0) and back-calculating for the displacement at a force of 100 kips. Again, the PANELS formulas do an excellent job estimating the overall drift of the subassemblage. One interesting observation from this data is that the continuity plates appear to have less of an effect in the elastic portion of drift for these subassemblages than what is determined by PANELS. In fact, looking at the total inelastic response in Figure 6.1-1 through Figure 6.1-4, continuity plates seem to have little effect at all in the response of the tested subassemblies. Nevertheless, including these components causes both the ABAQUS models and the PANELS formulas to more closely emulate the Lehigh test data (Ricles 2002). It is possible that this increased stiffness in the PANELS equations and the ABAQUS models, when continuity plates are included, makes up for a small difference in stiffness that is present in models that do not include continuity plates. However, considering that the ABAQUS models do not include the weld access holes, shear tabs and other connection details which would change the model's response, the above test comparisons give results that are more than adequate. Due to the correlation between the PANELS formulas and the ABAQUS

models with Dr. Ricles' Cruciform subassemblage test data, it can be concluded that accounting for the PZ flexure component of drift, which was done in the PANELS formulations, is necessary to accurately estimate the subassemblage's total elastic drift.

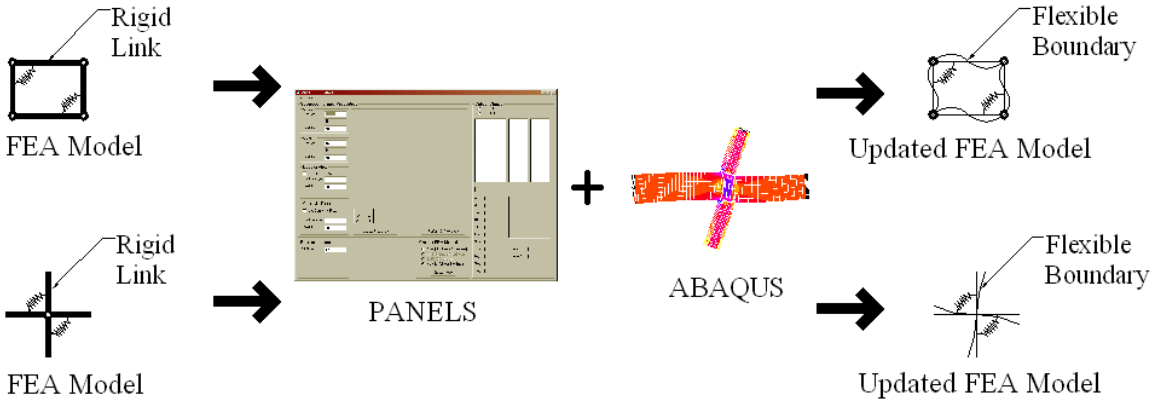

Figure 6.5-1: Thesis Flow Chart

Looking at the pictorial representation of research conducted in Figure 6.5-1, the reader can see that all the tools necessary to modify the Krawinkler and Scissors models have been presented and their reliability has been demonstrated in the tests data comparisons. A proposed method for including this component in both the Krawinkler and Scissors models will now be given in Chapter 7. Chapter 7 also includes inelastic comparisons of the Krawinkler and Scissors models with the Lehigh test data (Ricles 2002) before and after the adjustments to the models are made.

7 New Model Recommendations

7.1 Introduction

With the results from the SAC test comparisons verifying the PANELS equations, and the ABAQUS models correlating well with test data, two methods of accounting for flexural deformation and including the contribution of continuity plates in the PZ region of the beam/column joint models were investigated for both the Krawinkler and Scissors models. The first technique was to adjust the area of the rigid links to allow them to include axial deformation. Since the Scissors model does not physically represent the shape of the PZ boundary, it was not included in this portion of the investigation. The second method was to adjust the flexural properties of the rigid links making up the PZ region, allowing them to represent the additional drift through bending. Since this bending behavior is not dependent on the shape of the PZ region, both the Krawinkler and Scissors models were investigated.

For the results presented in Section 7.2, only the cruciform subassemblages were examined using the same cross-sections and component sizes which were used previously in this study. The models developed did not allow yielding to occur within the subassemblage, since the PZ flexure component now being included has been considered elastic throughout this study. In addition, the column flange hinges associated with plastic hinges forming at $4\theta_Y$ were not included, since this is an inelastic component. Finally, Type 4 Drain-2DX (Prakash at al. 1993) elements used to model the plastic hinges that develop in the girders were not included. It was felt that Type 2 Drain-2DX elements would provide the necessary accuracy.

In Section 7.3, comparisons are made between the original Krawinkler and Scissors models, the Updated Krawinkler and Updated Scissors model, the ABAQUS models and the Ricles' subassemblage test data. As in Chapter 6, this is an inelastic comparison. Unfortunately, the test from Lehigh (Ricles 2002) did not include PZ yielding so a final comparison is made between the four PZ models and ABAQUS.

7.2 Proposed Changes to the Krawinkler and Scissors Models to Represent Flexural Deformation

With the Krawinkler model, the boundaries of the PZ are treated as rigid links. In this proposed update to the Krawinkler model, these rigid links are given geometric properties based on the components that make up the PZ region. For the first trial, the area of each link is back-calculated based on the moment of inertia being equal to the area of the link multiplied by the distance from the neutral axis squared. For the two links representing the column, the moment of inertia value used in the back-calculation is set equal to the moment of inertia of the column. The moment of inertia used for the links associated with the girders is set equal to I_{PZ} determined using Equation 4.4-1. To ensure that these links did not bend in flexure or yield, their respective moments of inertia and yield moments were set at an exceedingly high value.

A graphical representation of the results from adjusting the area properties of the Krawinkler model is shown below in Figure 7.2-1. In this example, it is seen that allowing for axial deformation in the members making up the PZ region caused the model to display some very peculiar behavior. The right side of the model appears to deform axially much more than the left, causing the model to undergo uplift. While this instance is the most extreme example of this behavior which was observed, in an additional investigation of other beam/column size combinations, this deformation pattern was repeated. There was a complete loss of symmetry in the response of the model, which led to the decision to abandon this method of adjustment. This loss of symmetry is most likely due to the PZ spring introducing axial forces into the flexible boundaries. Although these forces are always present, making the area of the link exceedingly high eliminates their effect in the models. By reducing the area of the rigid links, the axial force from the spring is able to contribute to the subassemblage's drift, causing the nonsymmetric deformation pattern shown.

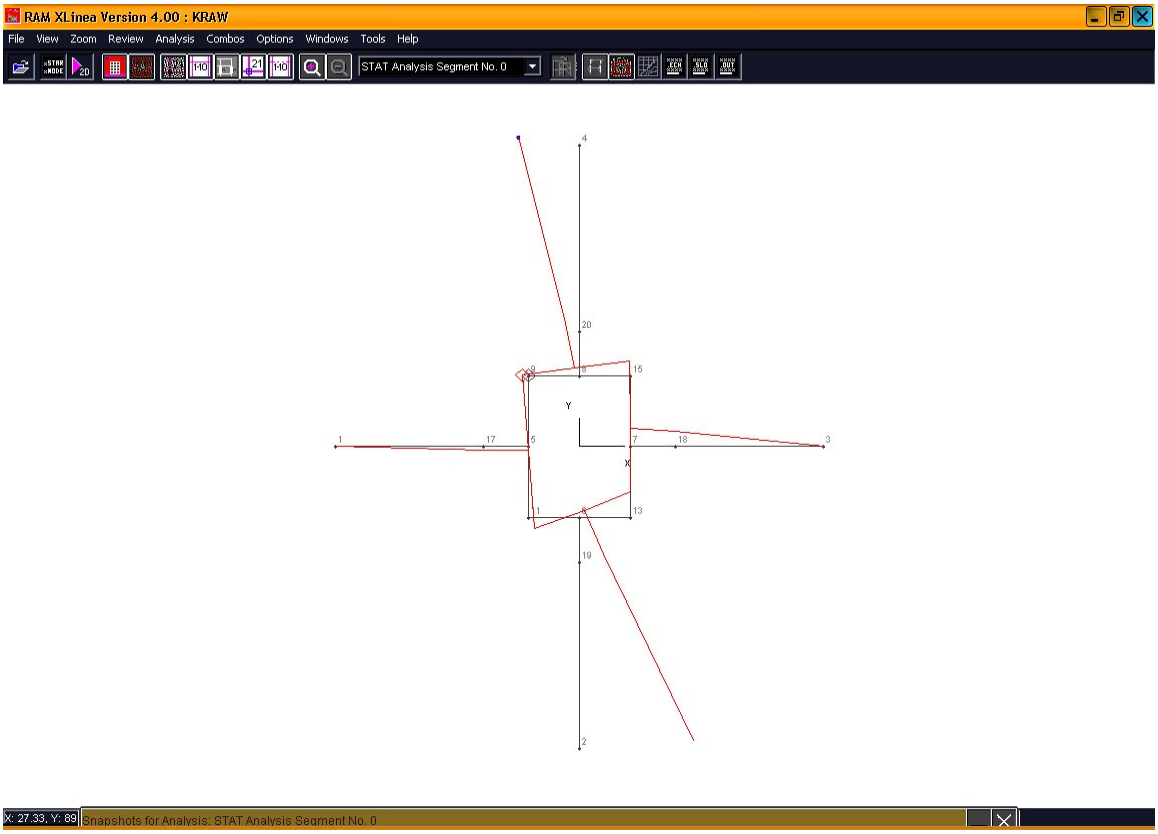

Figure 7.2-1: Drain-2DX Representation of Altered Krawinkler Model

The second method of adjustment, which was applied to both PZ models, is to allow the rigid links that define the PZ boundaries to deform in flexure by replacing both the Krawinkler and Scissors models' infinite moment of inertia values with ones which would result in an overall deflection that compared favorably to the deflection determined using an equivalent model in PANELS.

To accomplish this, the relationship between the drift attributed to PZ flexure from PANELS and from the Drain-2DX models is determined. This was done using the principle of virtual work. For the Krawinkler model and Scissors models, the moments at the beam/column interface due to the applied shear force V_C, determined using Figure 2.3-3, are shown in Figure 7.2-2.

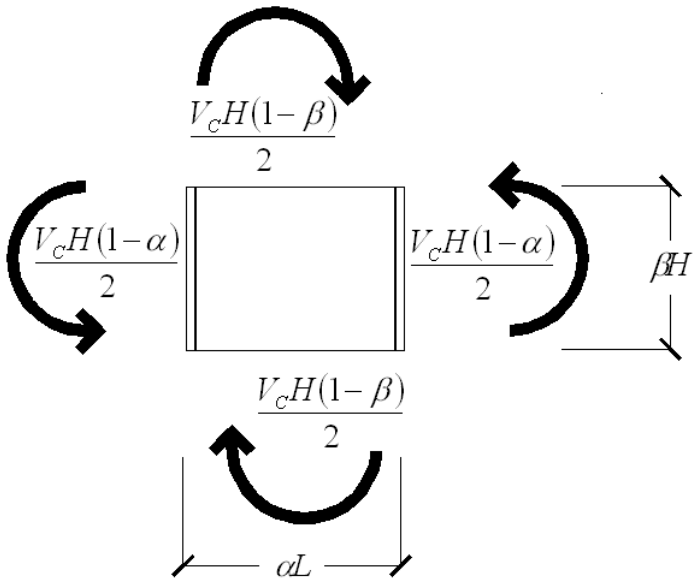

Figure 7.2-2: Model Moments at the Beam/Column Joint Interface

With the links forming the PZ no longer being rigid, the applied moments will give the beam/column joint of the Krawinkler model a deflected shape shown in Figure 7.2-3.

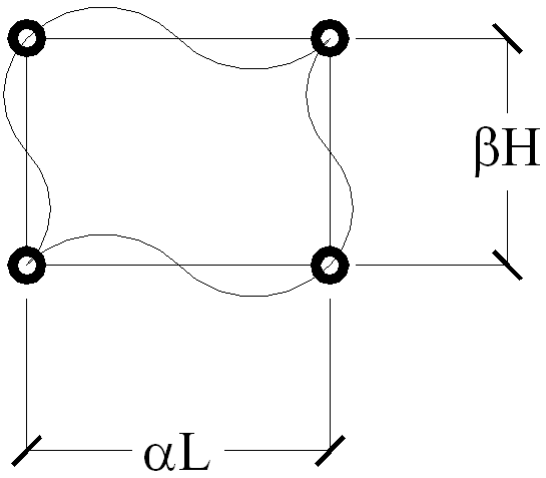

Figure 7.2-3: Krawinkler Model Beam/Column Joint Deflected Shape

This deflected shape will result in the moment diagrams shown in Figure 7.2-4.

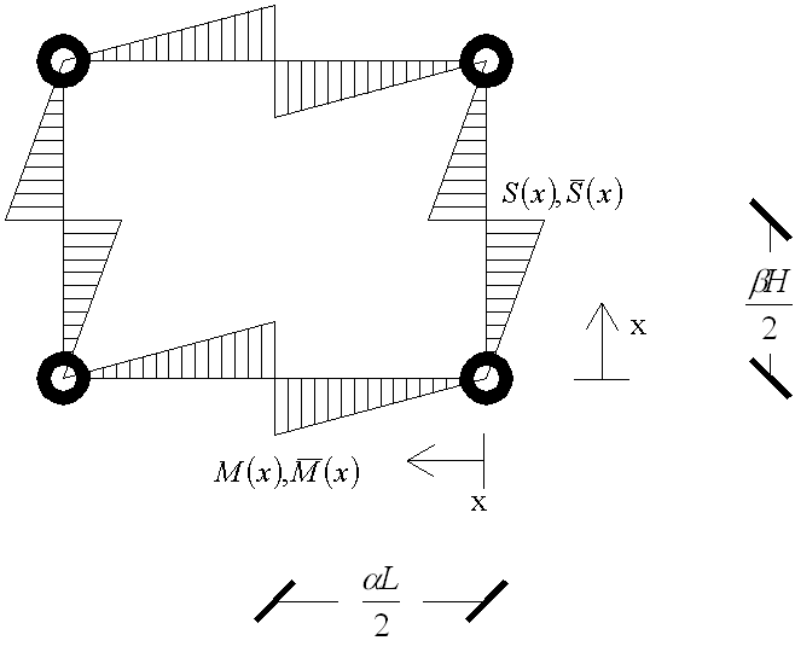

Figure 7.2-4: Krawinkler Model Boundary Moment Diagram

Using virtual work, Equation 2.1-3, the mathematical relations for the Drain-2DX Krawinkler models can be developed and are given in Equation 7.2-1 and Equation 7.2-2.

$$\delta_{ColFlex,Kraw} = 4\int_0^{\frac{\beta H}{2}} \frac{S(x)\bar{S}(x)}{K_{1K} EI_{Col}} dx \quad \text{.....(7.2-1)}$$

$$\delta_{GirFlex,Kraw} = 4\int_0^{\frac{\alpha L}{2}} \frac{M(x)\bar{M}(x)}{K_{2K} EI_{PL}} dx \quad \text{.....(7.2-2)}$$

where

$S(x)$and $M(x)$ are the moments due to the real force V_C. $\bar{S}(x)$ and $\bar{M}(x)$ are the moments due to an applied virtual force. K_{1K} and K_{2K} are constants which are included to adjust the bending properties of the Krawinkler Drain-2DX models to equal the PANELS results. The formula for I_{PL} was developed in Chapter 4 and is repeated below for convenience.

$$I_{PL} = I_{Col,PZT} + I_{Cont} \quad \text{.....(7.2-3)}$$

Using Figure 7.2-4 and the moments at the boundaries shown in Figure 7.2-2, the moment equations for use in Equation 7.2-1 and Equation 7.2-2 are equal to

$$S(x) = \frac{V_C(1-\alpha)}{2\beta}(x) \quad \text{.....(7.2-4)}$$

$$M(x) = \frac{V_C H(1-\beta)}{2\alpha L}(x) \quad \text{.....(7.2-5)}$$

Substituting these equations into Equation 7.2-1 and Equation 7.2-2 respectively , setting Equation 7.2-1 equal to Equation 2.3-13,

$$Actual\ \delta_{PZ,CF} = \frac{VH^3\beta}{6EI_{Col}}\left[\alpha(1-\beta) + \frac{(1-\alpha-\beta)^2}{3}\right]$$

Equation 7.2-2 equal to Equation 2.3-15,

$$Actual\ \delta_{PZ,GF} = \frac{VH^2\alpha L}{4EI_{PZ}}\left[\beta(1-\alpha) + \frac{(1-\alpha-\beta)^2}{3}\right]$$

and solving in terms K_{1K} and K_{2K} gives:

$$K_{1K} = \frac{3(1-\alpha)^2}{4\left(3\alpha(1-\beta) + (1-\alpha-\beta)^2\right)} \quad \text{.....(7.2-6)}$$

$$K_{2K} = \frac{I_{PZ}(1-\beta)^2}{2I_{PL}\left[3\beta(1-\alpha) + (1-\alpha-\beta)^2\right]} \quad \text{.....(7.2-7)}$$

where

$$I_{PZ} = 1.5I_{Col,PZT} + I_{Cont} \quad \text{.....(7.2-8)}$$

To enable this model to work, the PZ springs in the corners of the Krawinkler model must be removed. This is due to the spring not allowing for a zero moment condition at the intersection of the flexible boundaries as shown in Figure 7.2-4. A

simple way to eliminate this spring is to replace it with a cross-braced system that models the spring stiffness with axial deformation as shown in Figure 7.2-5. This was modeled in Drain-2DX by using truss elements (Type 1) for the crossed braced system and beam elements (type 2) for the flexible boundary.

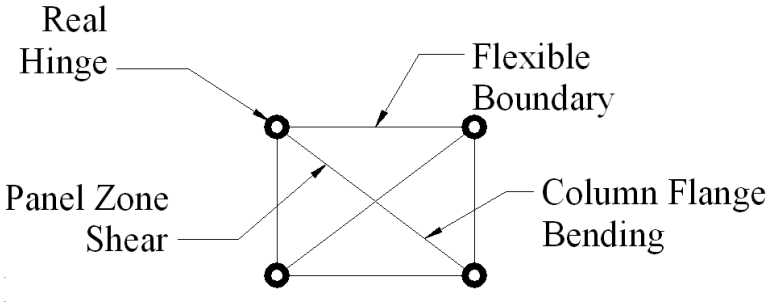

Figure 7.2-5: Updated Krawinkler Model

The properties for the PZ hinge can be developed in the same manner as in Chapter 3.

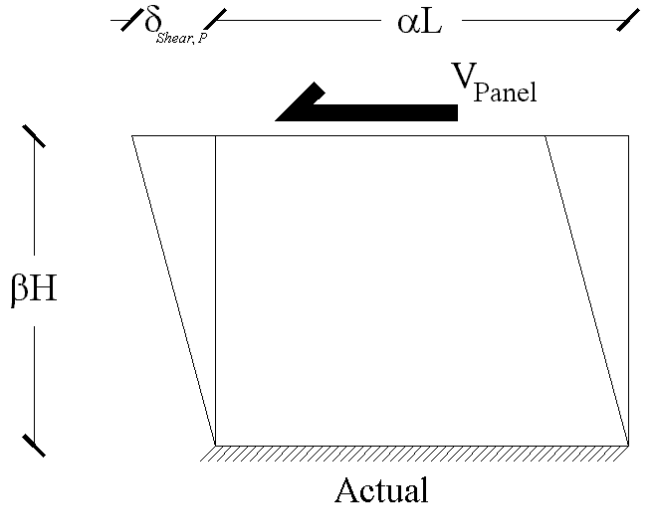

Figure 7.2-6: Krawinkler Panel Zone Stiffness

Applying the virtual work equation (7.2-6)

$$U_{Shear} = \int_0^{\beta H} \frac{V_{R,Panel} V_{V,Panel}}{G A} dx \quad \text{.....(7.2-9)}$$

to the actual $V-\delta$ relationship shown in Figure 7.2-6, the displacement ($\delta_{Shear,P}$) of the panel due to the shear force (V_{Panel}) is equal to

$$\delta_{Shear,P} = \frac{V_{Panel}\,\beta H}{G\,t_p\,\alpha L} \quad \text{.....(7.2-10)}$$

Organizing this relationship in terms of horizontal stiffness gives:

$$\frac{V_{Panel}}{\delta_{Shear,P}} = \frac{G\,t_p\,\alpha L}{\beta H} \quad \text{.....(7.2-11)}$$

For axial deformation, the stiffness K_{Panel} is equal to

$$K_{Panel} = \frac{E\overline{A}}{\hat{L}}cos^2\theta \quad \text{.....(7.2-12)}$$

where

$$\hat{L} = \sqrt{(\beta H)^2 + (\alpha L)^2} \quad \text{.....(7.2-13)}$$

$$cos\theta = \frac{\alpha L}{\sqrt{(\beta H)^2 + (\alpha L)^2}} \quad \text{.....(7.2-14)}$$

Substituting and setting Equation 7.2-11 equal to Equation 7.2-12 and solving in terms of the area ($\overline{A}$)gives:

$$\overline{A} = \frac{G\,t_p\,\alpha L\sqrt{(\beta H)^2 + (\alpha L)^2}}{E\beta H cos^2\theta} \quad \text{.....(7.2-15)}$$

This area ($\overline{A}$) represents the necessary area to develop the stiffness for a single axial member to model the PZ shear stiffness only.

Using Von Mises yield Criterion, it was shown earlier that the shear force in the panel zone is equal to

$$V_{Y,Panel} = 0.6F_Y d_c t_p = 0.6F_Y \alpha L t_p \quad \text{.....(7.2-16)}$$

Using this shear force, the yield stress for the axial member, $Stress_{Y,Panel}$, representing PZ shear is equal to

$$Stress_{Y,Panel} = \frac{V_{Y,Panel}}{\overline{A}} = \left(\frac{0.6F_Y \alpha L t_p}{\cos\theta} \right) \Bigg/ \left(\frac{G\, t_p\, \alpha L \sqrt{(\beta H)^2 + (\alpha L)^2}}{E\beta H \cos^2\theta} \right) \quad ...(7.2\text{-}16)$$

Simplifying this equation makes $Stress_{Y,Panel}$ equal to

$$Stress_{Y,Panel} = \frac{0.6F_Y E\beta H \cos\theta}{G\sqrt{(\beta H)^2 + (\alpha L)^2}} \quad .....(7.2\text{-}17)$$

Since the purpose of this exercise is to develop a model that would include PZ flexure, the additional modifications to include the column flange stiffness were not included in the comparisons presented since PANELS does not include the column flange stiffness component. But for completeness, the derivation of the column flange stiffness properties for use with the axial members is as follows.

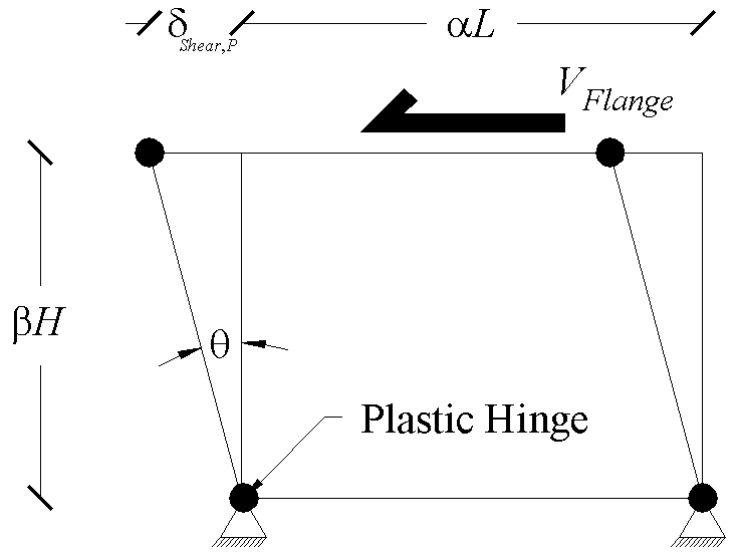

Figure 7.2-7: Krawinkler Plastic Hinges in the Column Flanges

The same procedure that was used to derive the column hinge spring stiffness will be used again to develop the axial stiffness for the diagonal bars. As was shown earlier, the rotation θ_Y is equal to

$$\theta_Y = \frac{M_{Panel}}{K_{Panel,\theta}} = \frac{0.6F_Y}{G} \quad \text{.....(7.2-18)}$$

Using Figure 7.2-7 and small angle theory, the deflection $\delta_{Shear,Y}$ is equated to θ_Y

$$\delta_{Shear,Y} = \theta_Y \beta H \quad \text{.....(7.2-19)}$$

Solving Equation 7.2-18 in terms of $\delta_{Shear,Y}$ gives

$$\delta_{Shear,Y} = \frac{0.6F_Y \beta H}{G} \quad \text{.....(7.2-20)}$$

Accounting for Krawinkler's $4\theta_Y$ assumption, the flange stiffness ($K_{Flanges}$) was shown to be equal to

$$K_{Flanges} = \frac{M_{Y_{Flange}}}{4\theta_Y} = 0.75\, G b_{cf} t_{cf}^{\ 2} \quad \text{.....(7.2-21)}$$

where

$$M_{Y_{Flange}} = 1.8\, V_{Flange}\, \beta H = 1.8 F_Y b_{cf}\, t_{cf}^{\ 2} \quad \text{.....(7.2-22)}$$

Rewriting Equation 7.2-21 in terms of V_{Flange} and $\delta_{Shear,Y}$ makes $K_{Flanges}$ equal to

$$K_{Flanges} = \frac{0.75\, G b_{cf} t_{cf}^{\ 2}}{(\beta H)^2} \quad \text{.....(7.2-23)}$$

The axial stiffness of the diagonal members is equal to

$$K_{Flanges} = \frac{E\hat{A}}{\hat{L}} cos^2\theta \quad \text{.....(7.2-24)}$$

where

$cos^2\theta$ and $\hat{L}$ use the same mathematical relationship defined previously.

Setting Equation 7.2-23 equal to Equation 7.2-24 and solving in terms of $\hat{A}$ gives:

$$\hat{A} = \frac{0.75\, G b_{cf} t_{cf}^{\,2} \hat{L}}{E(\beta H)^2 \cos^2\theta} \quad \text{.....(7.2-25)}$$

From Equation 7.2-22, the shear forces that creates plastic hinges to form in the column flanges is equal to

$$V_{Flange} = \frac{F_Y b_{cf}\, t_{cf}^{\,2}}{\beta H} \quad \text{.....(7.2-26)}$$

Accounting for the 1.8 factor developed by Krawinkler (1978), the stress in the axial member representing the column flange component, $Stress_{Col\ Flange}$, is equal to

$$Stress_{Col\ Flange} = \frac{1.8 V_{Flange}}{\hat{A}} = \left(\frac{1.8 F_Y b_{cf}\, t_{cf}^{\,2} \Big/ \beta H}{\cos\theta} \right) \Bigg/ \left(\frac{0.75\, G b_{cf} t_{cf}^{\,2} \hat{L}}{E(\beta H)^2 \cos^2\theta} \right) \quad \text{(7.2-26)}$$

This equation can be simplified to make $Stress_{Col\ Flange}$ equal to

$$Stress_{Col\ Flange} = \frac{2.4 F_Y E \beta H \cos\theta}{G\hat{L}} \quad \text{.....(7.2-27)}$$

Using this Updated Krawinkler model, a series of models was developed to allow for a comparison with the output from PANELS. It is shown in Table 7.2-1.

Table 7.2-1: PANELS vs. Updated Krawinkler (Elastic)

Girder	Column	Span (in.)	Doubler Plate	Continuity Plate	PANELS (in.)	Krawinkler (in.)	% diff.
W36x210	W24x335	120	no	no	2.20	2.20	0.00
		240			2.80	2.80	0.00
		360			3.38	3.38	0.00
W36x210	W24x335	120	yes	no	1.90	1.90	0.00
		240			2.39	2.39	0.00
		360			2.93	2.93	0.00
W36x210	W24x335	120	no	yes	2.10	2.10	0.00
		240			2.67	2.67	0.00
		360			3.24	3.24	0.00
W36x210	W24x335	120	yes	yes	1.86	1.86	0.00
		240			2.33	2.33	0.00
		360			2.88	2.88	0.00

As seen in the above table, there is an exact correlation between the Updated Krawinkler models and the drift calculated by PANELS.

The process was then repeated again for the Scissors model. With the links forming the PZ no longer being rigid, the applied moments will give the beam/column joint of the Scissors model a deflected shape shown in Figure 7.2-8.

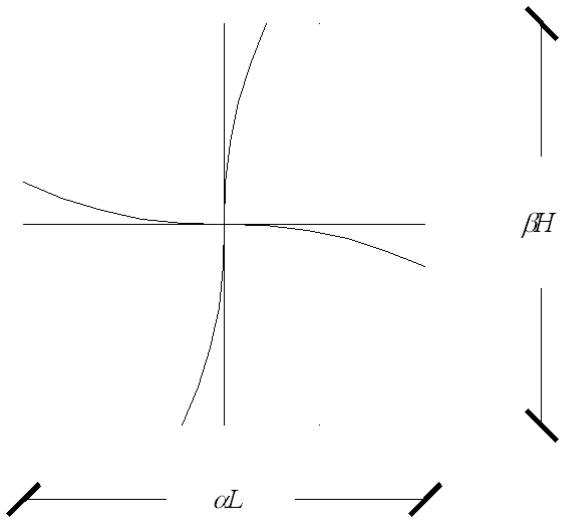

Figure 7.2-8: Scissor Model Beam/Column Joint Deflected Shape Model

This deflected shape will result in the moment diagrams shown in Figure 7.2-9.

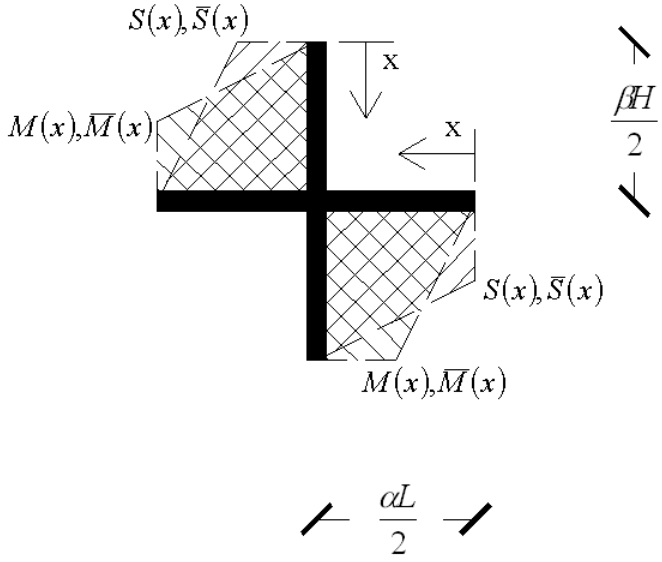

Figure 7.2-9: Scissors Model Boundary Moment Diagram

Again using virtual work, Equation 2.1-3, the Drain-2DX Scissors models' mathematical relationships are shown in Equation 7.2-25 and Equation. 7.2-26:

$$\delta_{ColFlex,Sciss} = 2\int_0^{\frac{\beta H}{2}} \frac{S(x)\overline{S}(x)}{K_{S1}EI_{Col}}dx \quad \text{.....(7.2-25)}$$

$$\delta_{GirFlex,Sciss} = 2\int_0^{\frac{\alpha L}{2}} \frac{M(x)\overline{M}(x)}{K_{S2}EI_{PL}}dx \quad \text{.....(7.2-26)}$$

$$I_{PL} = I_{Col,PZT} + I_{Cont} \quad \text{.....(7.2-27)}$$

Using Figure 7.2-9 and the moments at the boundaries shown in Figure 7.2-2, the moment equations for use in Equation 7.2-25 and Equation 7.2-26 are equal to

$$S(x) = -V_C\left(x - \frac{H}{2}\right) \quad \text{.....(7.2-28)}$$

$$M(x) = \frac{-V_C H}{L}\left(x - \frac{L}{2}\right) \quad \text{.....(7.2-29)}$$

Substituting these equations into Equation 7.2-25 and Equation 7.2-26, respectively, setting the results from Equation 7.2-25 equal to the PZ column flexure formula, Equation 2.3-13, and the results from Equation 7.2-26 equal to the PZ girder flexure formula, Equation 2.3-15, and solving in terms K_{1S} and K_{2S} gives

$$K_{1S} = \frac{9\left[\frac{\beta^2}{3} - \beta + 1\right]}{2\left(3\alpha(1-\beta) + (1-\alpha-\beta)^2\right)} \quad \text{.....(7.2-30)}$$

$$K_{2S} = \frac{I_{PZ}\left(\alpha^2 - 3\alpha + 3\right)}{I_{PL}\left(3\beta(1-\alpha) + (1-\alpha-\beta)^2\right)} \quad \text{.....(7.2-31)}$$

where

$$I_{PZ} = 1.5I_{Col,PZT} + I_{Cont} \quad \text{.....(7.2-32)}$$

Unlike the Krawinkler model, no modifications are necessary on the Scissors model. This is due to the moments in the PZ spring and the column flange spring being

identical to the moment at the center of the model. A comparison of the Updated Scissors model to the output from PANELS is shown in Table 7.2-2.

Table 7.2-2: PANELS vs. Updated Scissors (Elastic)

Girder	Column	Span (in.)	Doubler Plate	Continuity Plate	PANELS (in.)	Scissors (in.)	% diff.
W36x210	W24x335	120	no	no	2.20	2.20	0.00
		240			2.80	2.80	0.00
		360			3.38	3.38	0.00
W36x210	W24x335	120	yes	no	1.90	1.90	0.00
		240			2.39	2.39	0.00
		360			2.93	2.93	0.00
W36x210	W24x335	120	no	yes	2.10	2.10	0.00
		240			2.67	2.67	0.00
		360			3.24	3.24	0.00
W36x210	W24x335	120	yes	yes	1.86	1.86	0.00
		240			2.33	2.33	0.00
		360			2.88	2.88	0.00

As seen in the above table, there is an exact correlation between the Updated Scissors models and the drift calculated by PANELS.

The values for K_{1K}, K_{2K}, K_{1S} and K_{2S} for the beam/column joint sections used throughout this study are given in Table 7.2-3 and Table 7.2-6 below.

Table 7.2-3: Calculated Drain 2-DX K Constants (No Doubler, No Continuity)

Girder	Column	Span (in.)	Doubler Plate	Continuity Plate	K_{1K}	K_{2K}	K_{1S}	K_{2S}
W36x210	W24x335	120	no	no	0.60	0.50	4.48	4.18
		240			0.89	0.41	5.22	3.79
		360			1.01	0.38	5.49	3.68
W36x135	W24x207	120	no	no	0.61	0.50	4.51	4.17
		240			0.90	0.41	5.22	3.79
		360			1.01	0.39	5.48	3.69
W30x132	W21x201	120	no	no	0.62	0.56	4.47	4.29
		240			0.62	0.56	4.47	4.29
		360			0.95	0.44	5.26	3.83
W30x116	W21x166	120	no	no	0.62	0.56	4.48	4.28
		240			0.86	0.47	5.06	3.93
		360			0.95	0.44	5.26	3.83
W27x178	W30x173	120	no	no	0.46	0.69	4.00	4.74
		240			0.73	0.53	4.73	4.15
		360			0.84	0.49	5.00	3.99
W27x178	W14x426	120	no	no	0.71	0.54	4.68	4.18
		240			0.96	0.45	5.25	3.86
		360			0.89	0.47	5.10	3.93
W21x101	W30x173	120	no	no	0.42	0.80	3.85	5.03
		240			0.67	0.61	4.52	4.37
		360			0.77	0.56	4.76	4.19
W21x101	W14x426	120	no	no	0.65	0.62	4.48	4.40
		240			0.81	0.55	4.86	4.13
		360			0.88	0.52	4.99	4.04

Table 7.2-4: Calculated Drain 2-DX K Constants (No Doubler, Continuity)

Girder	Column	Span (in.)	Doubler Plate	Continuity Plate	K_{1K}	K_{2K}	K_{1S}	K_{2S}
W36x210	W24x335	120	no	yes	0.60	0.39	4.48	3.24
		240			0.89	0.41	5.22	2.94
		360			1.01	0.38	5.49	2.85
W36x135	W24x207	120	no	yes	0.61	0.50	4.51	3.25
		240			0.90	0.41	5.22	2.96
		360			1.01	0.39	5.48	2.87
W30x132	W21x201	120	no	yes	0.62	0.56	4.47	3.25
		240			0.62	0.56	4.47	3.25
		360			0.95	0.44	5.26	2.90
W30x116	W21x166	120	no	yes	0.62	0.56	4.48	3.23
		240			0.86	0.47	5.06	2.96
		360			0.95	0.44	5.26	2.89
W27x178	W30x173	120	no	yes	0.46	0.69	4.00	3.39
		240			0.73	0.53	4.73	2.97
		360			0.84	0.49	5.00	2.85
W27x178	W14x426	120	no	yes	0.71	0.54	4.68	3.24
		240			0.96	0.45	5.25	2.99
		360			0.89	0.47	5.10	3.04
W21x101	W30x173	120	no	yes	0.42	0.80	3.85	3.63
		240			0.67	0.61	4.52	3.15
		360			0.77	0.56	4.76	3.02
W21x101	W14x426	120	no	yes	0.65	0.62	4.48	3.45
		240			0.81	0.55	4.86	3.23
		360			0.88	0.52	4.99	3.17

Table 7.2-5: Calculated Drain 2-DX K Constants (Doubler, No Continuity)

Girder	Column	Span (in.)	Doubler Plate	Continuity Plate	K_{1K}	K_{2K}	K_{1S}	K_{2S}
W36x210	W24x335	120	yes	no	0.60	0.50	4.48	4.18
		240			0.89	0.41	5.22	3.79
		360			1.01	0.38	5.49	3.68
W36x135	W24x207	120	yes	no	0.61	0.50	4.51	4.17
		240			0.90	0.41	5.22	3.79
		360			1.01	0.39	5.48	3.69
W30x132	W21x201	120	yes	no	0.62	0.56	4.47	4.29
		240			0.62	0.56	4.47	4.29
		360			0.95	0.44	5.26	3.83
W30x116	W21x166	120	yes	no	0.62	0.56	4.48	4.28
		240			0.86	0.47	5.06	3.93
		360			0.95	0.44	5.26	3.83
W27x178	W30x173	120	yes	no	0.46	0.69	4.00	4.74
		240			0.73	0.53	4.73	4.15
		360			0.84	0.49	5.00	3.99
W27x178	W14x426	120	yes	no	0.71	0.54	4.68	4.18
		240			0.96	0.45	5.25	3.86
		360			0.89	0.47	5.10	3.93
W21x101	W30x173	120	yes	no	0.42	0.80	3.85	5.03
		240			0.67	0.61	4.52	4.37
		360			0.77	0.56	4.76	4.19
W21x101	W14x426	120	yes	no	0.65	0.62	4.48	4.40
		240			0.81	0.55	4.86	4.13
		360			0.88	0.52	4.99	4.04

Table 7.2-6: Calculated Drain 2-DX K Constants (Doubler, Continuity)

Girder	Column	Span (in.)	Doubler Plate	Continuity Plate	K_{1K}	K_{2K}	K_{1S}	K_{2S}
W36x210	W24x335	120	yes	yes	0.60	0.42	4.48	3.46
		240			0.89	0.34	5.22	3.14
		360			1.01	0.32	5.49	3.05
W36x135	W24x207	120	yes	yes	0.61	0.42	4.51	3.46
		240			0.90	0.34	5.22	3.15
		360			1.01	0.32	5.48	3.06
W30x132	W21x201	120	yes	yes	0.62	0.45	4.47	3.45
		240			0.86	0.37	5.06	3.16
		360			0.95	0.35	5.26	3.08
W30x116	W21x166	120	yes	yes	0.62	0.44	4.48	3.42
		240			0.86	0.37	5.06	3.14
		360			0.95	0.35	5.26	3.06
W27x178	W30x173	120	yes	yes	0.46	0.51	4.00	3.53
		240			0.73	0.40	4.73	3.09
		360			0.84	0.36	5.00	2.98
W27x178	W14x426	120	yes	yes	0.71	0.45	4.68	3.46
		240			0.96	0.38	5.25	3.19
		360			0.89	0.39	5.10	3.25
W21x101	W30x173	120	yes	yes	0.42	0.61	3.85	3.79
		240			0.67	0.46	4.52	3.29
		360			0.77	0.43	4.76	3.16
W21x101	W14x426	120	yes	yes	0.65	0.52	4.48	3.69
		240			0.81	0.46	4.86	3.46
		360			0.88	0.44	4.99	3.39

Using these tables, an average value for K_{1K}, K_{2K}, K_{1S} and K_{2S} can be developed for use with the either the Updated Krawinkler model or Scissors model if the actual *K* values are not going to be used. This portion of the study is being performed for comparison purposes to see if an average value for K_{1K}, K_{2K}, K_{1S} and K_{2S} will give reliable results.

Table 7.2-7: Average K constant Values

K_{1K}	K_{2K}	K_{1S}	K_{2S}
0.8	0.5	4.8	3.7

An example of the results obtained using these average values for K_{1K}, K_{2K}, K_{1S} and K_{2S} for one beam/column joint subassemblage is given in the two tables below.

Table 7.2-8: Updated Krawinkler Model with Average K Constants: Results

Girder	Column	Span (in.)	Doubler Plate	Continuity Plate	PANELS (in.)	Updated Krawinkler (in.)	% diff.
W36x210	W24x335	120	no	no	2.20	2.18	1.04
			yes	no	1.90	1.88	1.32
			no	yes	2.10	2.06	1.76
			yes	yes	1.86	1.82	1.94
		240	no	no	2.80	2.76	1.36
			yes	no	2.39	2.38	0.25
			no	yes	2.67	2.64	0.98
			yes	yes	2.33	2.32	0.56
		360	no	no	3.38	3.34	1.30
			yes	no	2.93	2.92	0.41
			no	yes	3.24	3.22	0.71
			yes	yes	2.88	2.86	0.52

Table 7.2-9: Updated Scissors Model with Average K Constants: Results

Girder	Column	Span (in.)	Doubler Plate	Continuity Plate	PANELS (in.)	Updated Scissors (in.)	% diff.
W36x210	W24x335	120	no	no	2.20	2.22	0.77
			yes	no	1.90	1.91	0.37
			no	yes	2.10	2.08	0.81
			yes	yes	1.86	1.85	0.54
		240	no	no	2.80	2.82	0.79
			yes	no	2.39	2.40	0.59
			no	yes	2.67	2.64	0.98
			yes	yes	2.33	2.32	0.56
		360	no	no	3.38	3.40	0.47
			yes	no	2.93	2.94	0.27
			no	yes	3.24	3.20	1.33
			yes	yes	2.88	2.88	0.00

The results from these comparisons show that the average value works better for K_{1S} and K_{2S} than it does for K_{1K} and K_{2K}. This can be attributed to the fact that as *K* becomes larger the percent difference between it and the actual value for *K* becomes less. But there is some definite variability inherent in using the average *K* values. From the results obtained, it is recommended that the true calculated values for K_{1K}, K_{2K}, K_{1S} and K_{2S} be used if PZ flexure is to be included in the beam/column joint model. These values can be easily determined using a spreadsheet and were easily implemented in PANELS.

Another option instead of using the average value from the entire table is to use the average value over a specified length. These values are based on a column height of 150 in.. Although a comparison is not performed, they are given below for reference.

Table 7.2-10: Girder Length Specific Average K Constant Values

Span (in.)	K_{1K}	K_{2K}	K_{1S}	K_{2S}
120	0.57	0.55	4.24	3.80
240	0.81	0.47	4.94	3.58
360	0.91	0.44	5.17	3.47

7.3 Inelastic Model Comparisons

The final evaluation of this study was to compare the Krawinkler model, Scissors model and their updated counterparts with the four SAC tests, performed by Dr. James Ricles of Lehigh University (2002), used previously. The properties used to develop the Drain-2DX models are shown in Table 7.3-1 (tests C1 and C2) and Table 7.3-2 (tests C3 and C4). The girder hinge properties were again developed using the same method as outlined in Chapter 4 (Charney 2002). The updated model properties, which are used to include the elastic PZ flexure component, were determined using the methods in Section 7.2. Applying the identical boundary conditions which were used in the four SAC tests (Ricles 2002), each model was forced to displace a total of 6 in. (measured from the tip of the bottom of the column to the top of the column) using displacement controlled analysis, and the resulting shear forces in the column were determined. The results for all sixteen force/displacement comparisons are shown below. For every Drain-2DX model developed using the SAC cruciform test setup, the hinges that represented yielding of the PZ and the plastic hinges that formed in the column flanges did not yield. This is the reason for only two observable yield points in all of the comparative figures below.

Table 7.3-1: Lehigh Models C1 and C2: Krawinkler and Scissors Properties

L (in.)	354
H (in.)	156
Von Mises Yield Constant	0.6
Fy (ksi)	56
Poisson's ratio	0.3
G (ksi)	11154
E (ksi)	29000

Krawinkler Models

Beam	tf	d	βH
	in	in	in
W36x150	0.94	35.9	34.96

Column	tf	d	αL	bf	tw	Doubler
	in	in	in	in	in	in
W14x398	2.85	18.3	15.45	16.6	1.77	1.500

Scissors Models

Beam	α
W36x150	0.0436

Column	β	1-α-β
W14x398	0.2241	0.7323

Krawinkler Models

Column	Beam	Panel		Flange	
		My	K	My	K
		in-k	in-k/rad	in-k	in-k/rad
W14x398	W36x150	59345	19700276	13591	1127934

Scissors Models

Panel		Flange	
My	K	My	K
in-k	in-k/rad	in-k	in-k/rad
81045	36740880	18561	2103589

Note: depths defined center to center of flange

Girder Hinges

	First Component			Second Component		
Girder	My	K	Strain	My	K	Strain
	in-k	in-k/rad	Hardening	in-k	in-k/rad	Hardening
W36x150	30583	Huge	0.000	2617	405741	0.3

Table 7.3-2: Lehigh Models C3 and C4: Krawinkler and Scissors Properties

L (in.)	354
H (in.)	156
Von Mises Yield Constant	0.6
Fy (ksi)	56
Poisson's ratio	0.3
G (ksi)	11154
E (ksi)	29000

Krawinkler Models

Beam	tf	d	βH
	in	in	in
W36x150	0.94	35.9	34.96

Column	tf	d	αL	bf	tw	Doubler
	in	in	in	in	in	in
W27x258	1.77	29	27.23	14.3	0.98	1.250

Scissors Models

Beam	α
W36x150	0.0769

Column	β	1-α-β
W27x258	0.2241	0.6990

Krawinkler Models

Column	Beam	Panel		Flange	
		My	K	My	K
		in-k	in-k/rad	in-k	in-k/rad
W27x258	W36x150	71329	23678194	4516	374773

Scissors Models

Panel		Flange	
My	K	My	K
in-k	in-k/rad	in-k	in-k/rad
102047	48464461	6461	767085

Note: depths defined center to center of flange

Girder Hinges

	First Component			Second Component		
Girder	My	K	Strain	My	K	Strain
	in-k	in-k/rad	Hardening	in-k	in-k/rad	Hardening
W36x150	30583	Huge	0.000	2617	405741	0.3

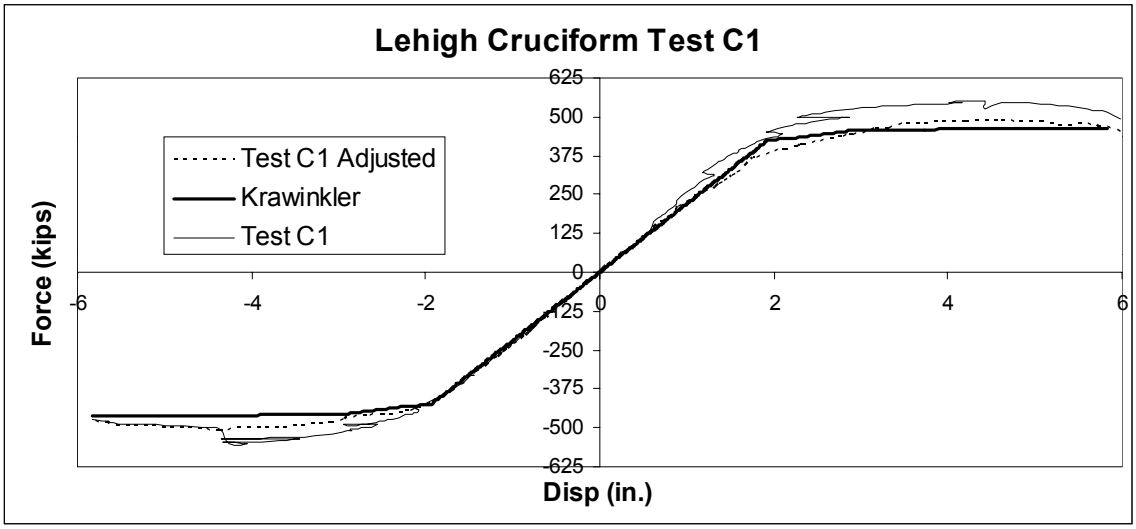

Figure 7.3-1: Krawinkler Model vs. Lehigh Test C1 (Ricles 2002)

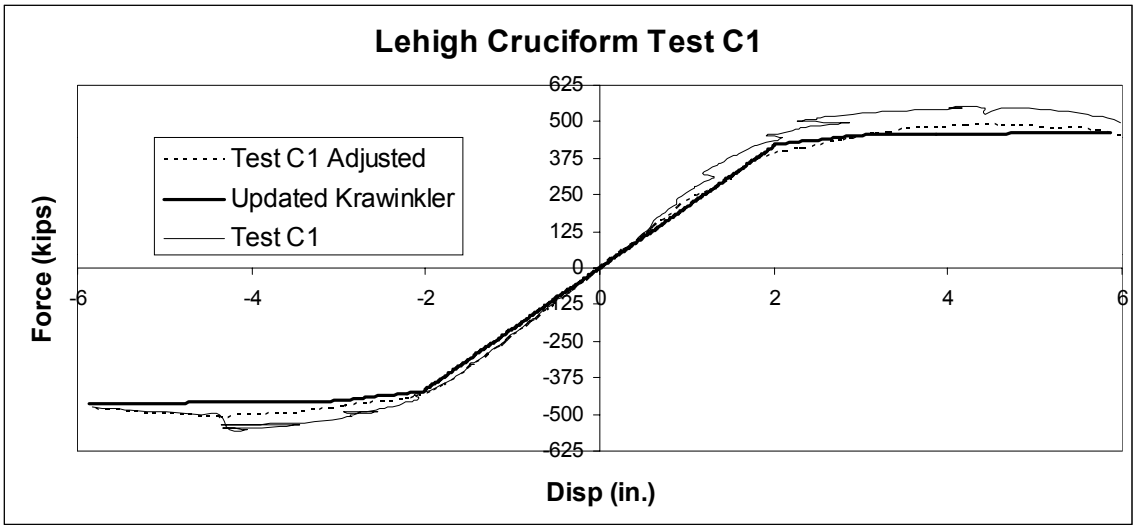

Figure 7.3-2: Updated Krawinkler Model vs. Lehigh Test C1 (Ricles 2002)

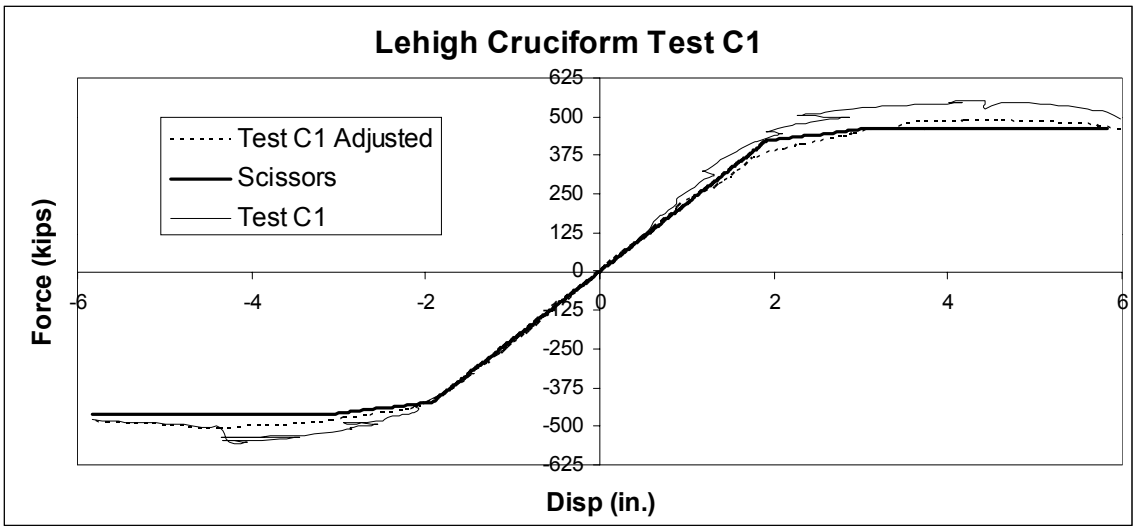

Figure 7.3-3: Scissors Model vs. Lehigh Test C1 (Ricles 2002)

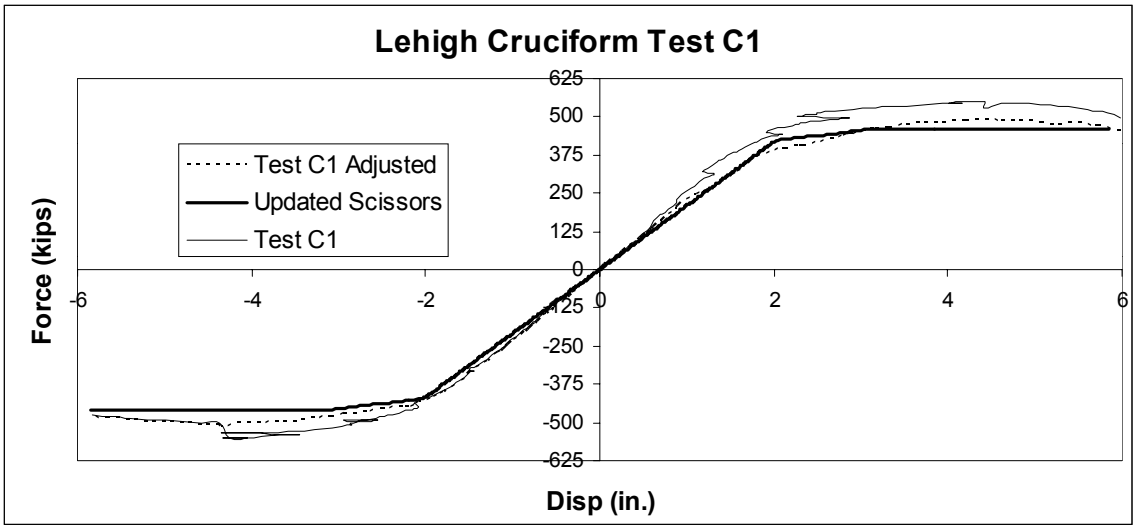

Figure 7.3-4: Updated Scissors Model vs. Lehigh Test C1 (Ricles 2002)

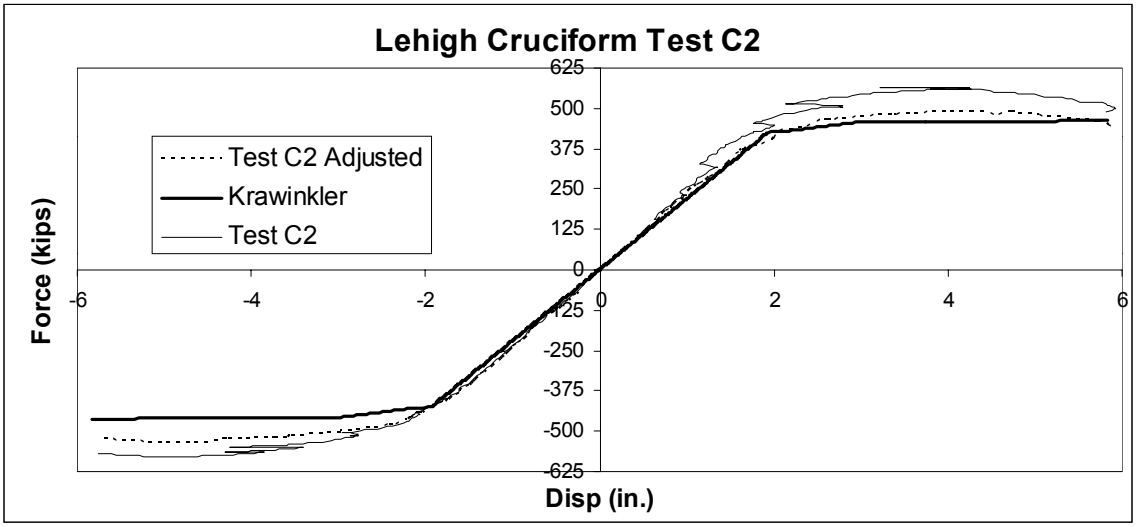

Figure 7.3-5: Krawinkler Model vs. Lehigh Test C2 (Ricles 2002)

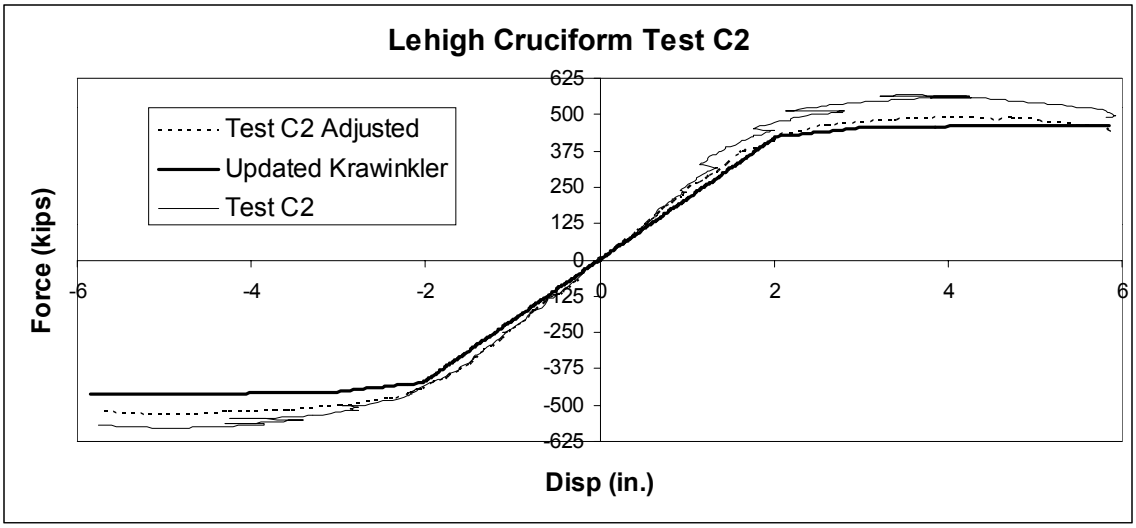

Figure 7.3-6: Updated Krawinkler Model vs. Lehigh Test C2 (Ricles 2002)

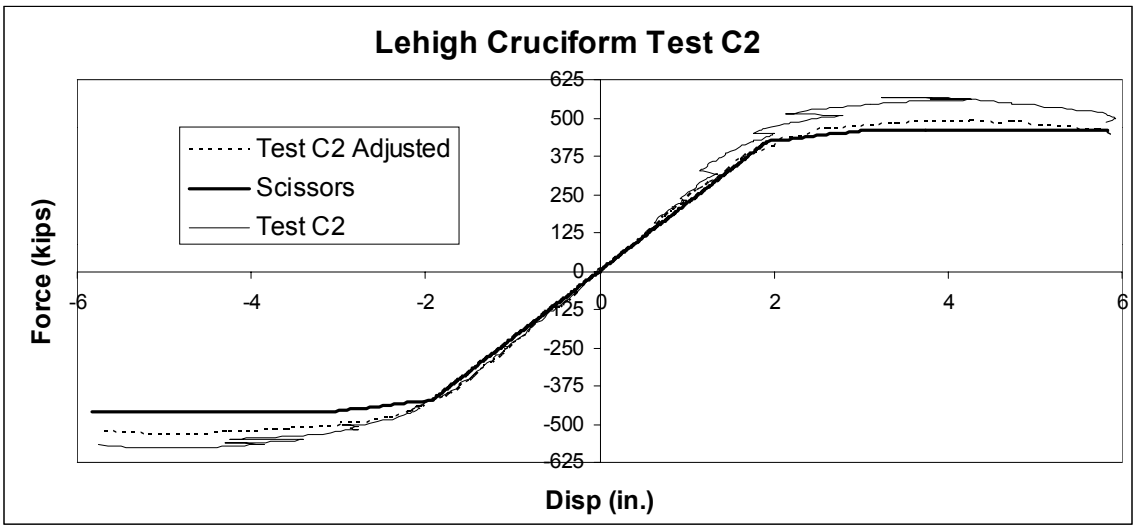

Figure 7.3-7: Scissors Model vs. Lehigh Test C2 (Ricles 2002)

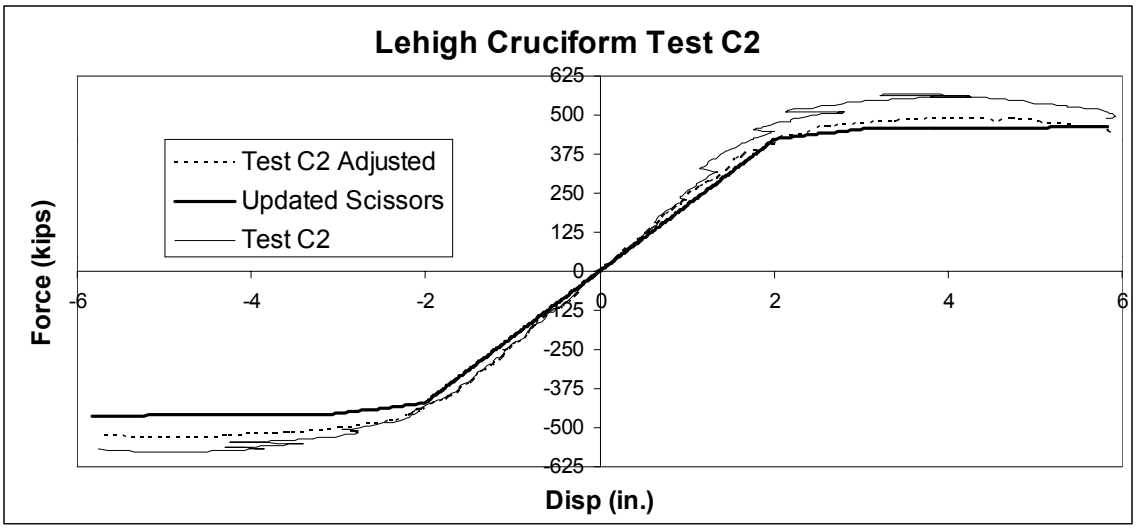

Figure 7.3-8: Updated Scissors Model vs. Lehigh Test C2 (Ricles 2002)

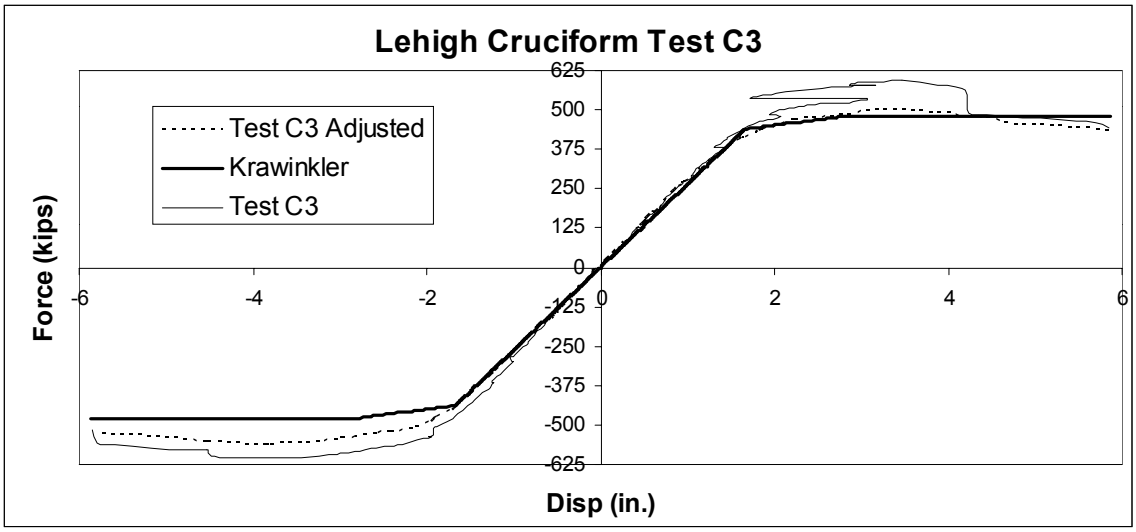

Figure 7.3-9: Krawinkler Model vs. Lehigh Test C3 (Ricles 2002)

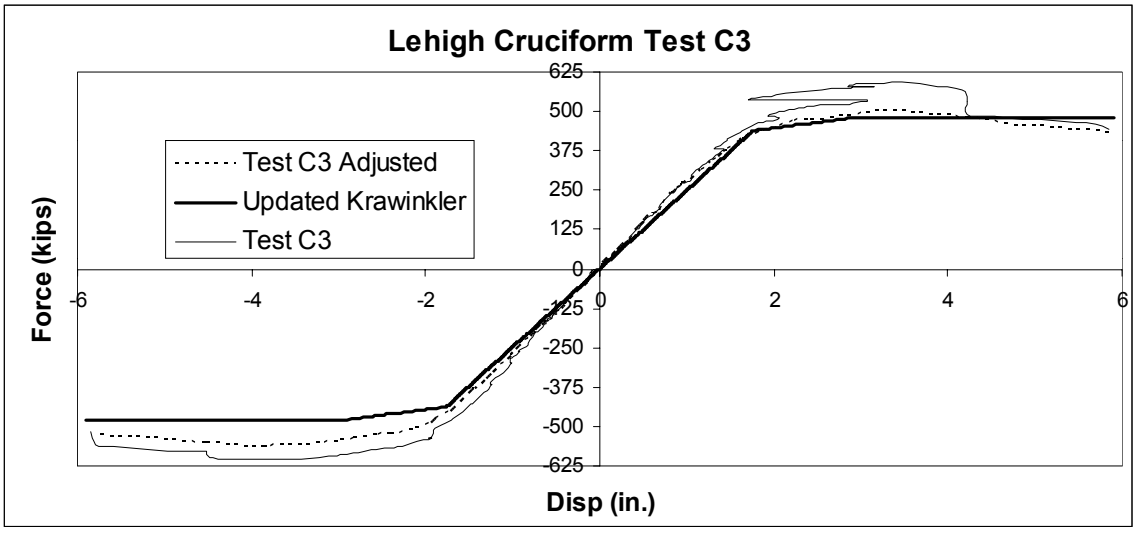

Figure 7.3-10: Updated Krawinkler Model vs. Lehigh Test C3 (Ricles 2002)

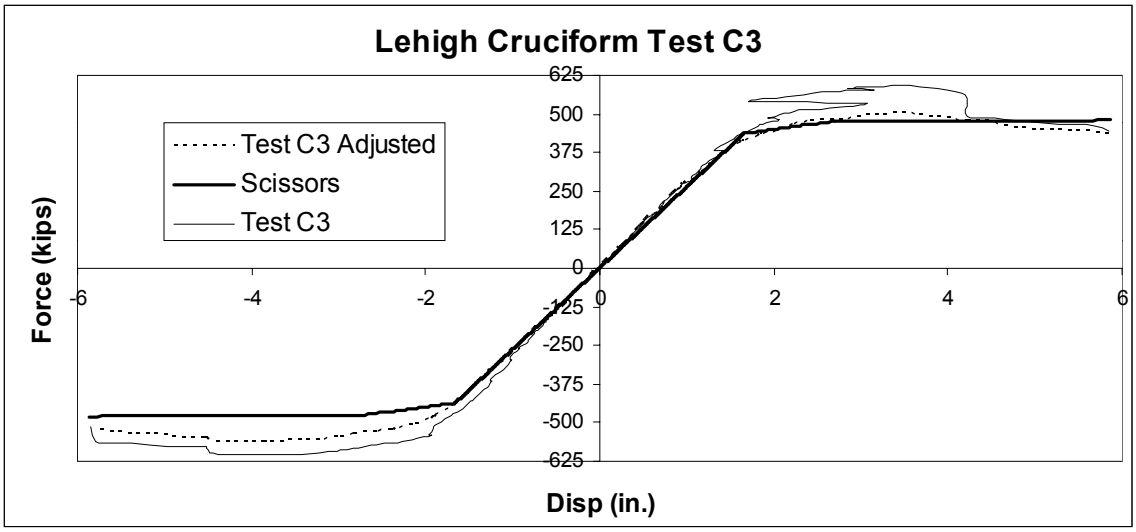

Figure 7.3-11: Scissors Model vs. Lehigh Test C3 (Ricles 2002)

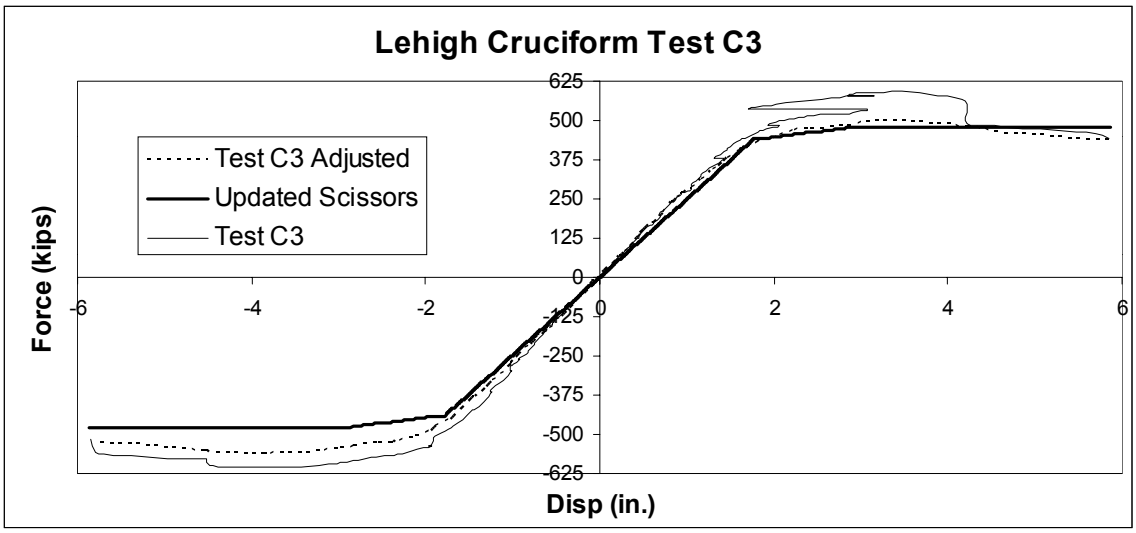

Figure 7.3-12: Updated Scissors Model vs. Lehigh Test C3 (Ricles 2002)

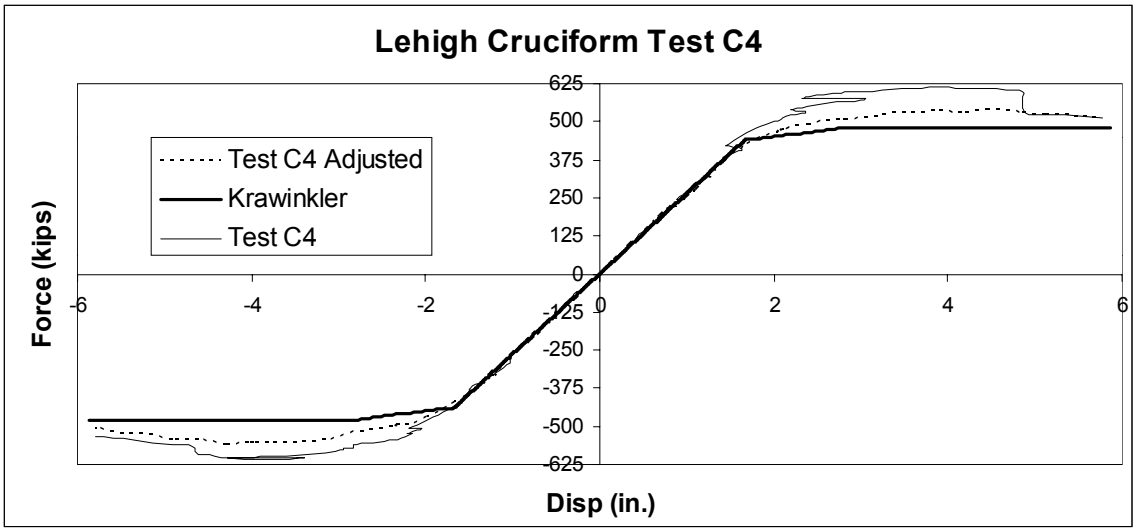

Figure 7.3-13: Krawinkler Model vs. Lehigh Test C4 (Ricles 2002)

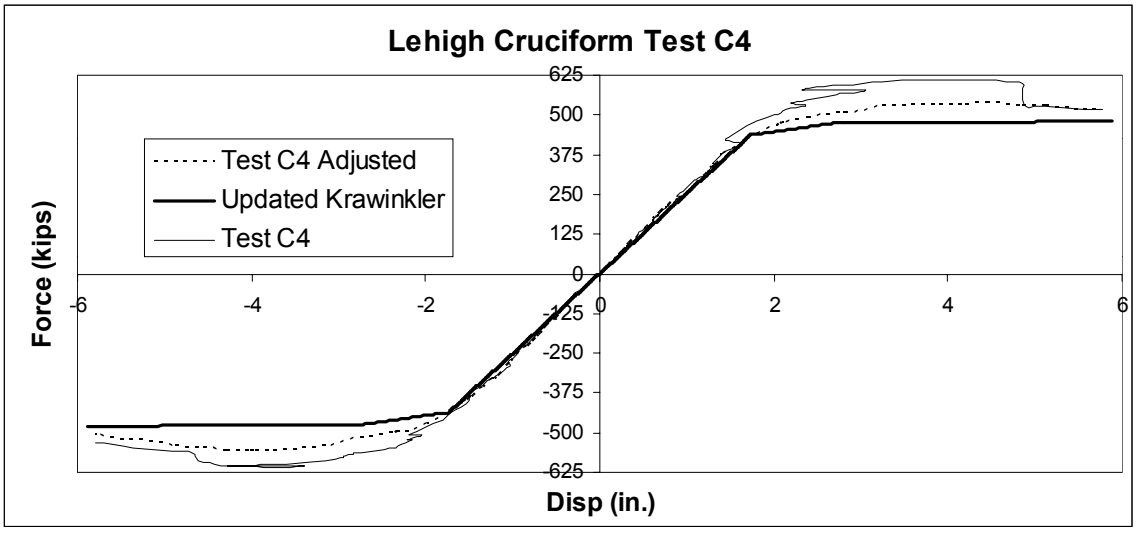

Figure 7.3-14: Updated Krawinkler Model vs. Lehigh Test C4 (Ricles 2002)

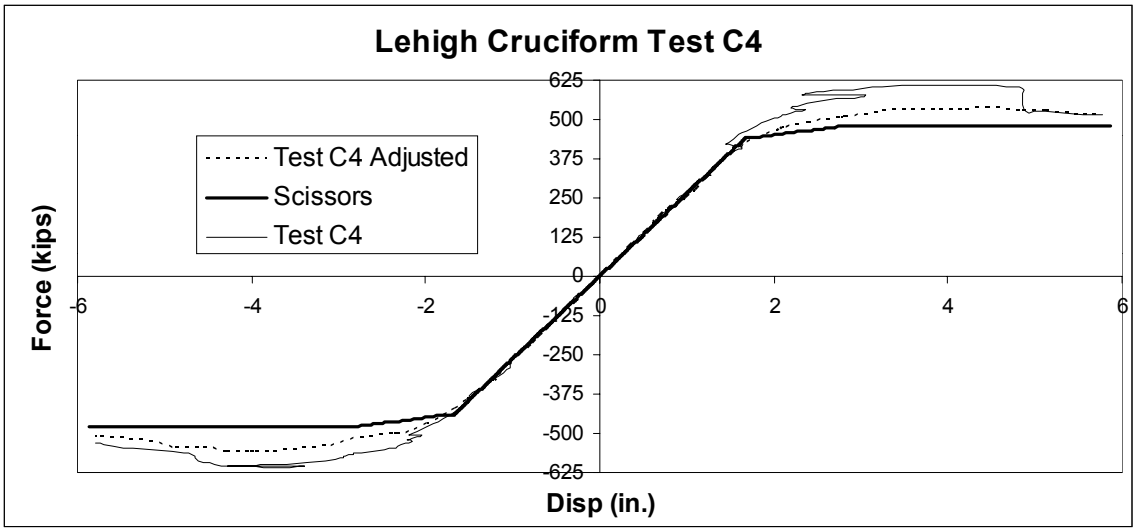

Figure 7.3-15: Scissors Model vs. Lehigh Test C4 (Ricles 2002)

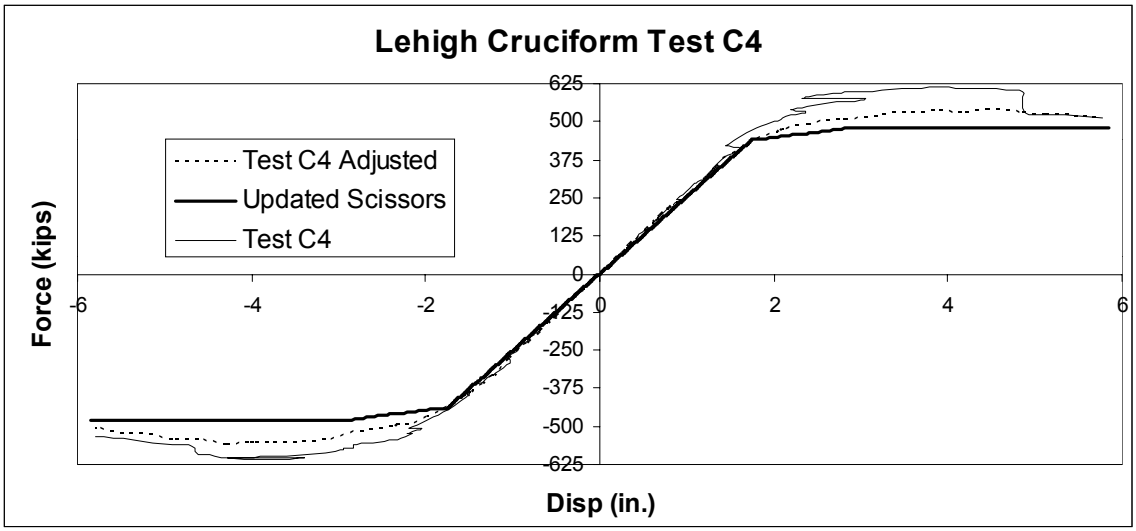

Figure 7.3-16: Updated Scissors Model vs. Lehigh Test C4 (Ricles 2002)

As seen in the above figures, all four models appear to give a good approximation of the responses from all four Lehigh SAC tests. To get a better understanding of the responses determined from the four Drain-2DX models, the results from each test using all four Drain-2DX models were plotted in the same graph along with the Adjusted SAC test data and the results from the ABAQUS nonlinear models for the corresponding cruciform subassemblage. To increase the resolution of the graphs, only the positive response cycle over a smaller displacement was plotted. These results are shown in Figure 7.3-17 through Figure 7.3-20 below.

Looking at these four figures, it is obvious that the adjustments to the model did reduce the initial stiffness of each test, causing the updated models to more closely resemble the results from the ABAQUS models, on which the changes to the Krawinkler and Scissors models were based. The updated models also appear to do a better job of mimicking the initial stiffness and response of the actual test data. This comparison is hampered by the fact that there is still some "play" in the data as a result of the manner in which the subassemblages were tested. Another interesting observation is that not only do the Krawinkler and Scissors models have identical responses (which was also shown in Chapter 4), but their updated counterparts do as well. Finally, as observed in all four figures once both hinges in the girders yield, the responses of all four Drain-2DX models are identical.

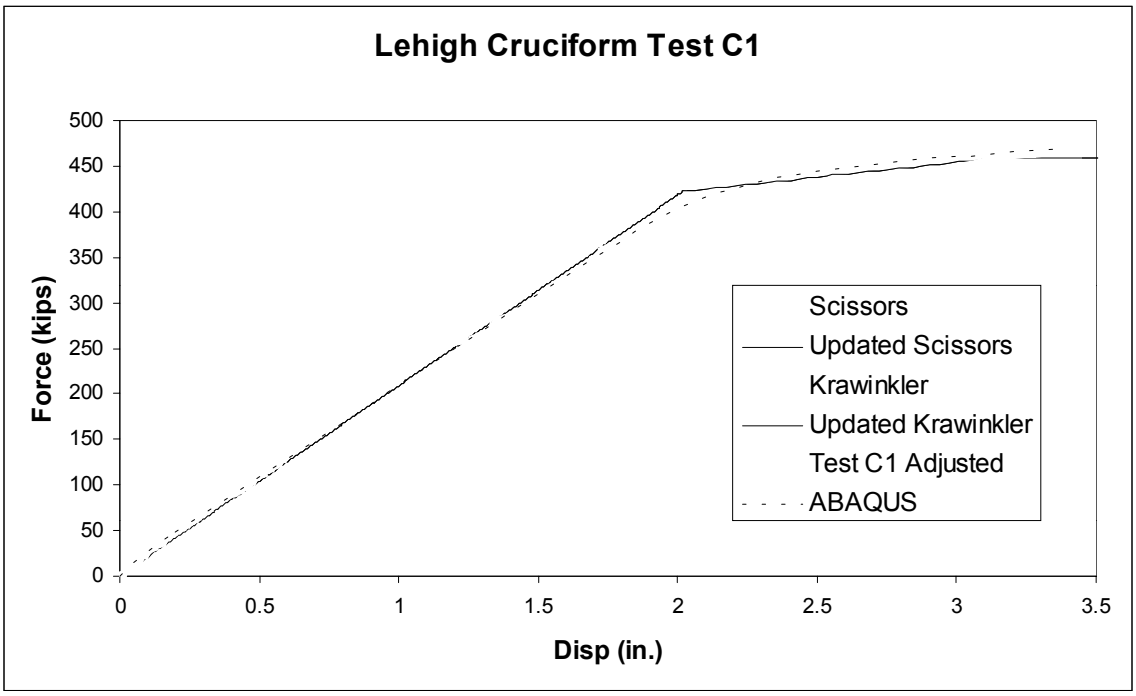

Figure 7.3-17: Complete FEA Comparison for Lehigh Test C1 (Ricles 2002)

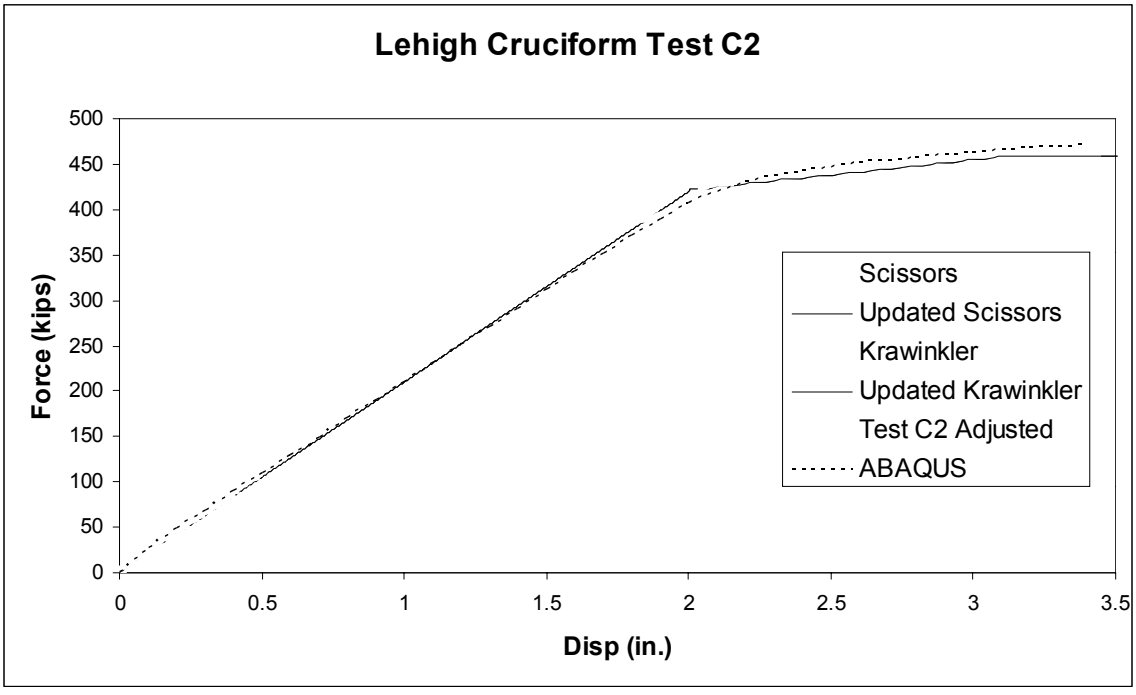

Figure 7.3-18: Complete FEA Comparison for Lehigh Test C2 (Ricles 2002)

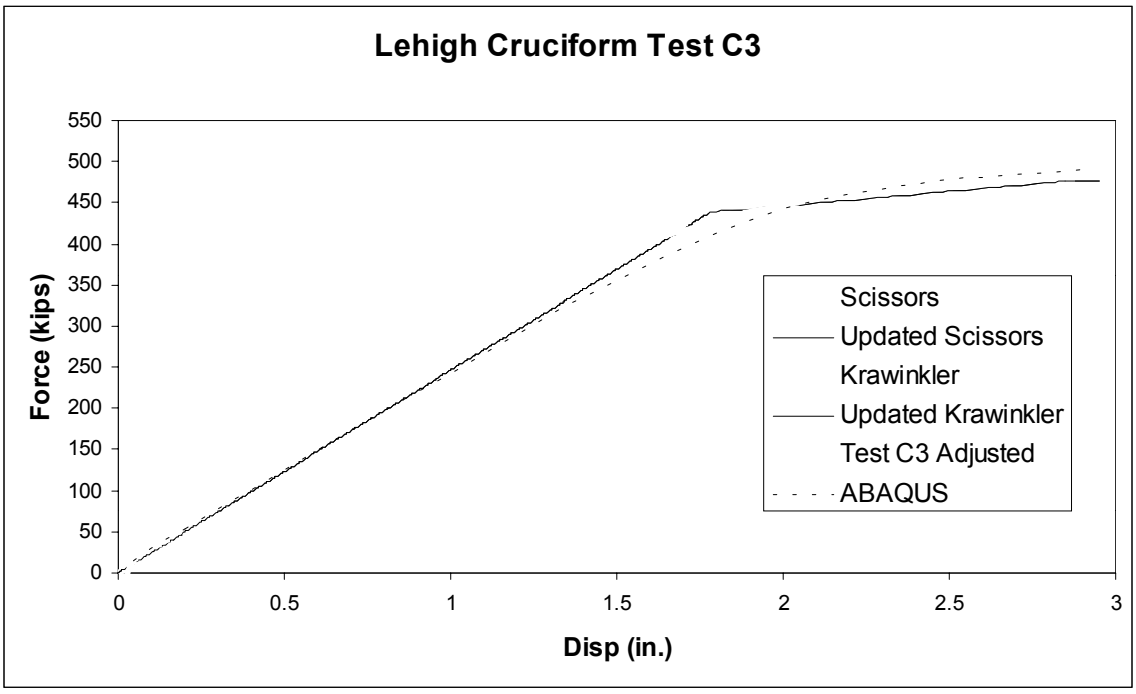

Figure 7.3-19: Complete FEA Comparison for Lehigh Test C3 (Ricles 2002)

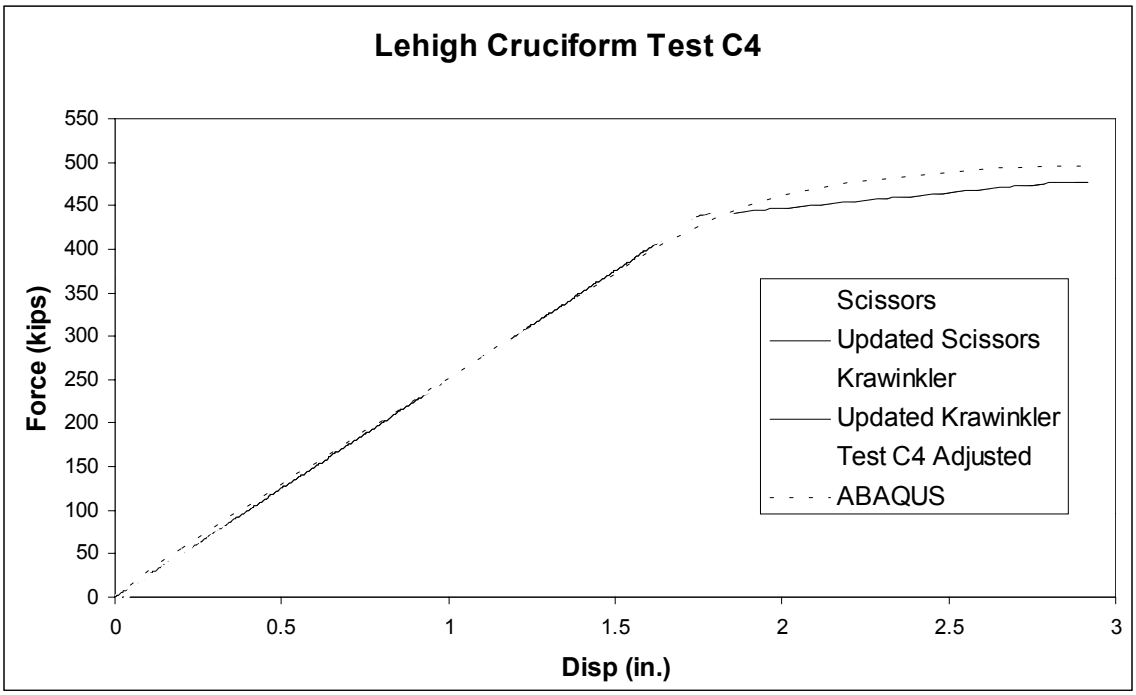

Figure 7.3-20: Complete FEA Comparison for Lehigh Test C4 (Ricles 2002)

Unfortunately, the test assemblages from the Ricles' Lehigh tests did not include beam/column joints without doubler plates. None of the panel zone hinges yielded in any of the tests, making a complete determination of the effectiveness the inelastic components of the models impossible. In an attempt to examine this shortcoming, the four models, Krawinkler, Scissors, Updated Krawinkler and Updated Scissors, were compared to an inelastic ABAQUS model using the same Cruciform subassemblage examined in Chapter 5 where the girder hinges and the column flange hinges developed use a W24x84 girder, with no doubler plate, and a W21x122 column. The results from this study are shown in Figure 7.3-21 below.

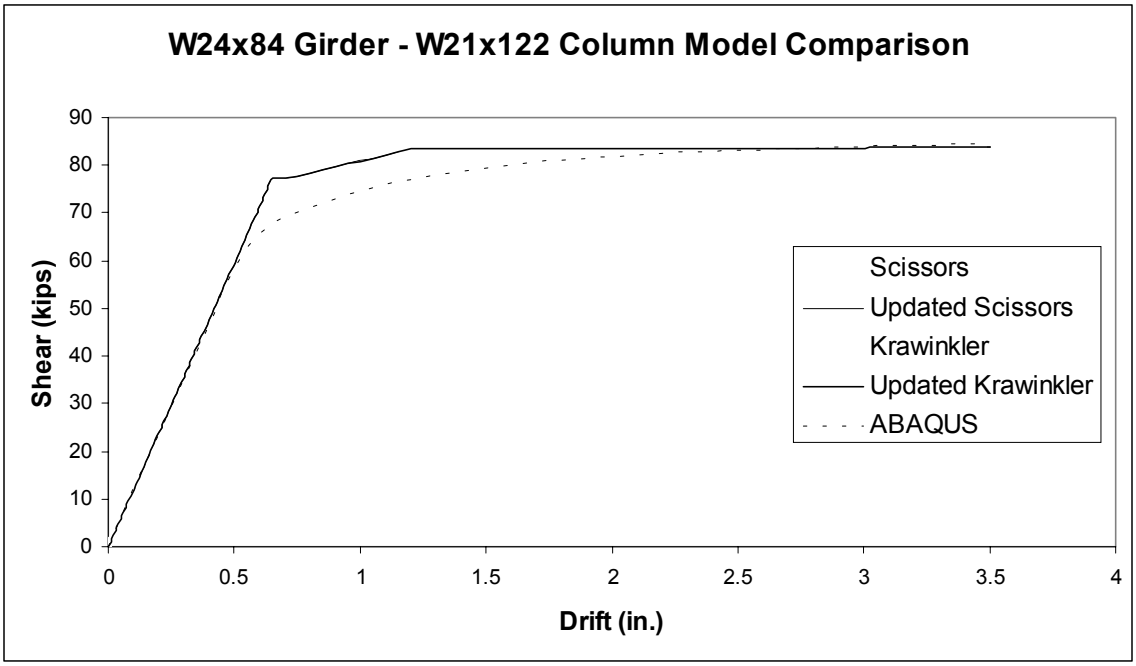

Figure 7.3-21: W24x84 Girder- W21x122 Column Model Comparison

Again it is seen that the updated model compares more favorably to the ABAQUS results.

7.4 Conclusions and Recommendations

As shown in the above tables in Section 7.2, by including flexural properties in the Krawinkler and Scissors models, the overall elastic drift results compare much more favorably to the PANELS results than the original models did in Chapter 4 (Table 4.5-1 through Table 4.5-8). This was to be expected since neither the original Krawinkler model nor original Scissors model included the flexural component of drift in the PZ region. As has been shown throughout this document, neglecting this source of elastic strain energy will cause the overall elastic drift of a subassemblage to be underestimated.

At the outset of this research, one of the major goals was to determine if the differences between the Krawinkler model and Scissors model discussed in Chapter 4 would cause the Scissors model to behave differently than the Krawinkler model. This has not been the case. Due to the evidence contained within this thesis, it is the author's recommendation to use the Updated Scissors model for elastic and inelastic static pushover analysis.

The modifications to the Krawinkler and Scissors models both appear to give better results when compared to the Ricles' Lehigh test data and the inelastic ABAQUS models. Since this research was more concerned with elastic responses and small displacements for the inelastic region, modifications were not made to the inelastic properties of the Krawinkler or Scissors models. Modifications to the inelastic properties were performed by Foutch and Yun (2002) and Kim and Engelhardt (1995 and 2002). In both references, it was observed that the inelastic column flange spring causes the model to underestimate the drift of subassemblages with thick column flanges. Combining this underestimation in drift from the inelastic response with the underestimation of drift in the elastic region (due to not including the PZ flexural component) will definitely cause the subassemblage's results to be unconservative. The reader is encouraged to examine these documents for the details of these updates.

The K_{1K}, K_{2K}, K_{1S} and K_{2S} formulas presented will certainly result in beam/column joint models that are more conservative compared to the Krawinkler

models and Scissors model that do not include PZ flexure. The use of the average *K* was shown to give results that displayed a significant amount of variability. Considering that the use of the average *K* values would assume that the values presented will work for all beam/column joint configurations, it is the author's recommendation to use the calculated values of *K* to ensure that the PZ flexural component of drift is properly accounted for.

8 Critical Review of the Results Presented and Recommendations for Further Research

8.1 Elastic Models

The elastic models described in Chapter 2 were derived using the principle of virtual work, and were then compared to elastic Krawinkler (Chapter 3) finite element models created for use in Drain-2DX. For all the elastic components of drift except PZ flexure, these formulas were shown to correlate exactly with these models. Assuming that all remaining significant elastic strain energy sources were accounted for and the applied forces were modeled properly, this suggests that the remaining elastic components in the PANELS formulas, the Krawinkler model and the Scissors model presented are accurate.

The development of the elastic PZ flexural properties presented in Chapter 4 is definitely debatable. The method used to model the wide-flange sections in ABAQUS resembled plate girders more than wide-flange section. Not including the fillets at the intersection of the flanges and webs will cause the ABAQUS subassemblages to experience more drift that they would have if this additional material were included. In retrospect, more effort should have been spent to develop models where the percent differences of the cantilever models (Table 4.3-1) were closer to zero. By accounting for all the additional drift determined from the ABAQUS models to PZ flexure in the PANELS formulas, the importance of this drift component may be somewhat overstated by these results. However, the ABAQUS models presented correlated very well with the test results from Lehigh. However, this could be due to modeling the connections at the beam/column interface as infinitely rigid. Using the "Tie" option in ABAQUS assumes that there is no flexibility at the beam/column interface. This constraint condition is virtually impossible to obtain in a real test setup. A slight amount of flexibility in the beam/column joint will increase the overall drift. Since the differences being accounted for are in tenths of an in., this underestimating of the amount of cross-section material and overestimating the constraints would provide logical reasoning for this serendipitous

occurrence. Also debatable is the 1.5 multiplier used for adjusting the moment of inertia values in both PZ flexure formulas. Again this was based on the ABAQUS finite element models. The model constraints at the intersection of the girder and column flanges could make these stresses arbitrarily higher than what would occur in a real experimental setup. Without test data to determine the stress conditions at this interface, there is no way to ensure that this adjustment is correct. But, a high stress condition causing brittle weld ruptures at this interface was the most cited reason for failure of the beam/column joint in the Northridge earthquake and is a common mode of failure in subassemblage tests. With this in consideration, the 1.5 factor is more than plausible and was justified in the results presented.

8.2 Inelastic Models

From the literature review performed, it is obvious there is a tremendous amount of confusion associated with the use of the Krawinkler and Scissors models and their associated properties. This can be directly attributed to the multiple mathematical definitions used by Krawinkler for the stiffness terms he has developed. This is perpetuated by the fact that Dr. Krawinkler and his associates no longer include the stiffness values they are using in their models with the strength terms from Equation 3.3-22 (AISC 1997). By not refuting the ρ term he presented (1975) in his final version of his formulas (1978), the door was left open for multiple interpretations. To convolute the problem even more, Dr. Krawinkler now promotes the use of the Scissors model for inelastic static pushover analysis (FEMA 355C 2001). Although this thesis also makes the same recommendation, the FEMA document does so based the results of the Krawinkler model. As was shown in Table 3.5-1, not including $(1-\alpha-\beta)$ will cause the strength term to be underestimated by approximately 1.5 times and the stiffness by 2 to 3 times the appropriate value. The comparisons presented in Chapter 5 show that when properly modeled, there is an exact correlation in the drift between the Krawinkler and Scissors. If the Krawinkler properties are used with a Scissors model, this would not be the case. This was shown in Chapter 5 (Figure 5.2-32 and Figure 5.2-33).

The papers presented by Kim and Engelhardt (1995 and 2002) give the best example of the confusion that has been created. The $(1-\rho)$ factor is included in their derivation for both the strength and stiffness of the model. The strange thing is that the $(1-\rho)$ factor is presented in a manner that attributes it to the 1978 Krawinkler derivations. The authors then use the representation shown in Figure 8.2-1 for hinging within the PZ. According to their description, the elastic panel zone hinge is only effective until a rotation of θ_Y is achieved, after which it no longer contributes to the stiffness of the model until a rotation of $4\theta_Y$ is achieved. At that time only the column flanges contribute to the stiffness of the PZ region until the rotation is $4\theta_Y$. The stiffness associated with strain hardening still remains but is only attributed to the elastic panel zone spring.

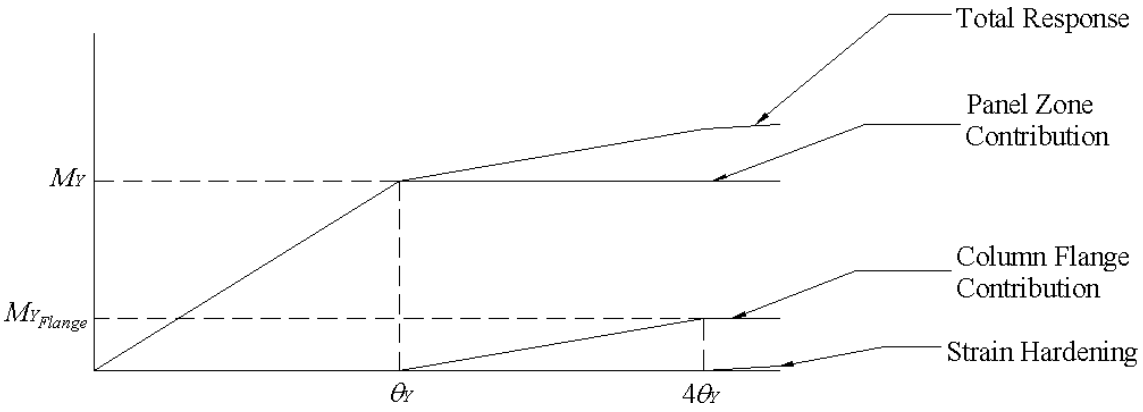

Figure 8.2-1: Kim and Engelhardt Moment-Curvature Relationship

This is not only difficult to justify behaviorally, but how this was actually modeled in the computer was never addressed. Although it is easy to modify the spring stiffness to create this representation, the papers ignore this issue. Considering all these differences, their correlation with the test data presented is remarkable. Again, as was shown in Table 3.5-1, using a Scissors model with $(1-\rho)$ instead of $(1-\alpha-\beta)^2$ still does not account for the large differences in stiffness associated with the two models. Considering that the most recent paper is not referenced (Krawinkler 1978), the modeling

techniques are not defined and the inelastic stiffness term is also arbitrarily adjusted, the results from these papers are questionable at best.

The derivations presented herein show that there is a significant mathematical difference between the Krawinkler and Scissors models, $(1-\alpha-\beta)$ or $(1-\alpha-\beta)^2$, that must be included if the Scissors model is used. The derivations also show that use of $(1-\alpha-\beta)$ and $(1-\alpha-\beta)^2$ presented for application with the Scissors model in this paper is due to the physical differences between the Krawinkler and Scissors models and has nothing to do with the beneficial effects of column shear above and below the joint, which was the basis of $(1-\rho)$. Ignoring the PZ flexure component that was developed in Chapter 7, the only term that was not derived mathematically for both the Krawinkler and Scissors models in this paper is the 1.8 factor for the column flange strength term determined through experiments and included in the current AISC seismic provisions (1997). When used for inelastic static pushover analysis, the representative mathematical strength and stiffness terms for each model presented in Chapter 3 should not be used.

The differences between the Krawinkler and Scissors models ended up being much less significant than was originally expected. It was initially believed that the kinematic differences in the models, and the fact that the Scissors model is dependent on the location of the moment inflection points in the columns and girders outside the PZ region, would cause the two models to have large disparities between them. This ended up not being the case. It is the author's belief that the difference in response between the two models was not significant because the rotation of the girders' plastic hinges were so large relatively the differences between the Krawinkler and Scissors model discussed in Chapter 5 that the differences between the Krawinkler and Scissors models did not have a significant impact on the total structure response.

8.3 Updated Models

It is the author's opinion that PZ flexure, developed in Chapter 7, should also be included. However, the modifications made to the Krawinkler and Scissors models to

account for PZ flexure are debatable. Any time a fictitious property is used, the possibility for error is present. It is plausible that the *K* multipliers developed will not accurately account for PZ flexure, just as the 1.8 multiplier for column flange strength has been shown to overestimate strength in beam/column joints with thick flange columns. Compounding this is that this fictitious property is based on the results of finite element analysis models. Even though the models showed good correlation with the test data, more error was introduced when the test data itself was modified to account for disparities in it. All the modifications made to the test data and the exclusion of the fillets of the beam/column sections increased the total drift of the subassemblages, which would cause the total drift of a complete structure to be overestimated. This overestimation is conservative in the design of the full structure.

8.4 Research Recommendations

It is obvious from the confusion associated with the elastic quantities of drift in the Krawinkler and Scissors models that monotonic subassemblage tests need to be performed with a concentration on the elastic drift and small displacements. It is fully understandable that the SAC tests did not include these criteria since their objective was to ensure that the ultimate strength, based on 0.03 radian rotation, of a beam/column subassemblage subjected to large deformations was adequate. But, how can these ultimate strength criteria be implemented if the models used to represent them are not complete? It is the author's belief that the derivations of the Krawinkler and Scissors models from Chapter 3 are correct but not complete. The PZ flexural component needs to be included within the model to accurately represent the total response of a subassemblage as well as a complete structure. Small displacement test data would ensure that the method to include the PZ flexure component presented in Chapter 7 give an accurate representation of the subassemblage's response. The test data from Lehigh, while helpful, included a large amount of "play" in the data, making a determination of the accuracy of the ABAQUS models used to establish the PZ flexural component difficult. Data that had a higher resolution and better quality would provide verification that the ABAQUS models, generated by PANELS, are accurate.

A glaring issue discovered during the literature review is the need to determine the proper moment-curvature relationship to be used for the beam/column model. At least two different models seem to be used. The first which was used in this study, is shown in Figure 8.4-1.

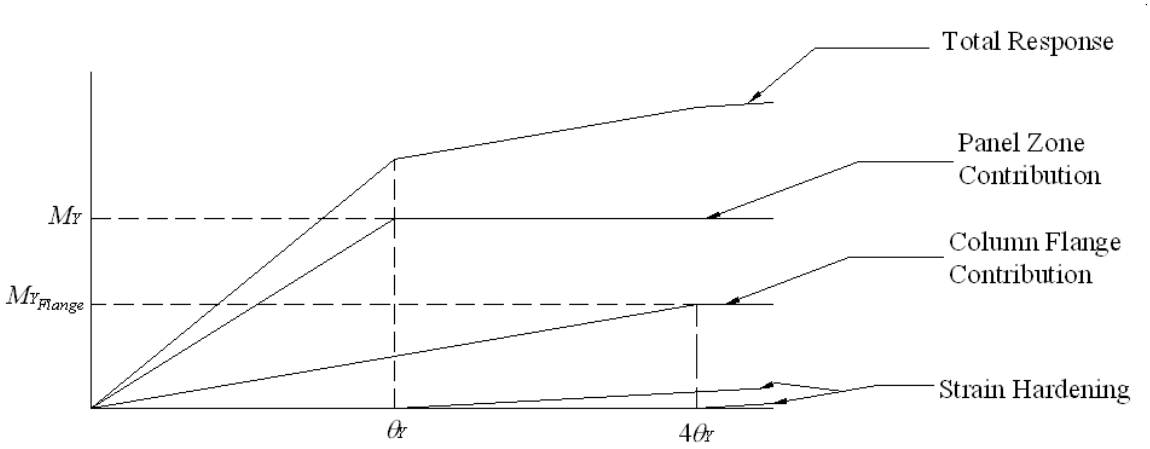

Figure 8.4-1: Moment-Curvature Relationship

The second is the Kim and Engelhardt representation shown above in Figure 8.2-1. While it is the author's belief that the relationship shown in Figure 8.4-1 is behaviorally more sound, verification of this will require experimental testing.

While it is felt that the Updated Scissors model is adequate for a majority of inelastic static pushover analyses, the question still lingers as to when the Scissors model should not be used. It is obvious that the Scissors model should not be used when unequal bay lengths and story heights are used since there is no way to determine the appropriate α and β values. Although the results presented herein showed that gravity loading, P-delta effects and span lengths had little effect on the comparative responses of the two models, more time should be spent on this issue to ensure that the Scissors model is a reliable replacement for the Krawinkler model.

Appendix A: PANELS Program User's Manual

A.1 Introduction

PANELS is a stand alone program used to determine the elastic deflections due to lateral loads of four different subassembly types as well as a pre-processor for elastic/inelastic ABAQUS and Drain-2DX subassembly models. Initially developed by Dr. Finley Charney, PANELS was updated and modified to be used for the analysis contained within this thesis.

A.2 Updated Capabilities of PANELS

- Determine elastic deflections of Cruciform, Corner, End and Tee models using the formulas developed in this thesis.
- Generate ABAQUS and Drain-2DX inelastic input files using the current AISC-LRFD (2001) steel section properties.

A.3 The PANELS Interfaces

A.3.1 Main User Interface

When PANELS.exe is first executed, the main user's interface, Figure A.3-1, will be displayed. This interface will allow the user to select the wide flange sections for the beam/column subassembly, input the column and girder length and yield stress, add doubler and continuity plates' sizes and yield stresses, update the applied loads, and access the FEA Model and Drift Analysis modules.

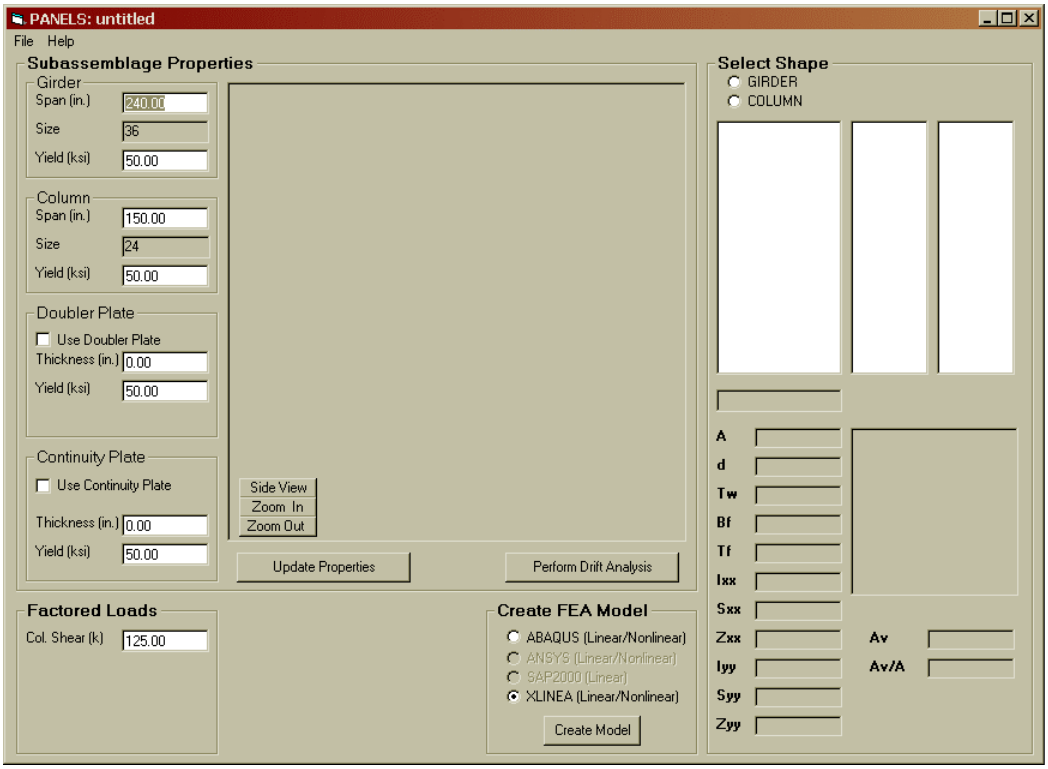

Figure A.3-1: Main Use Interface

A.3.2 Selecting a Shape

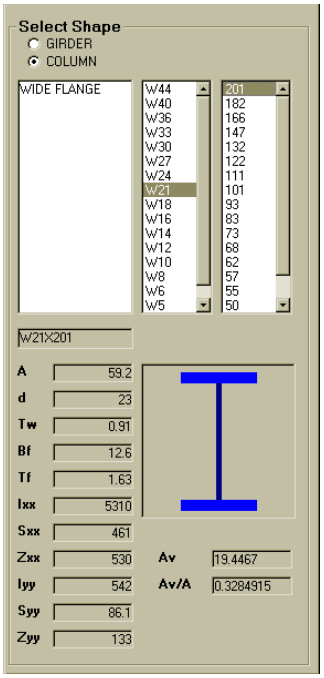

Figure A.3-2: Select Shape Frame

The Select Shape frame, Figure A.3-2, is used to pick the girder and column shapes to be used in the beam/column subassembly. To select a shape, first choose whether the section will be a girder or column by picking the appropriate option button in the upper left corner of the frame. Next, place the pointer over "WIDE FLANGE" in the left list box and left-click the mouse. A list of wide flange section nominal depths from the 2001 AISC-LRFD manual will then appear in the middle list box. Position the pointer over the desired wide flange section and left-click the

mouse. This will load all of the available weights for the wide flange section that was selected. Place the pointer over the appropriate section weight and again left-click the mouse. This loads the section properties into the text boxes and draws the representation of the section. None of the section properties displayed have been modified to account for the use of $d_c = d_{c,\,nom} - t_{cf}$ and $d_b = d_{b,\,nom} - t_{bf}$ except the shear area Av. The option to do so is available within the modules in which this factor applies.

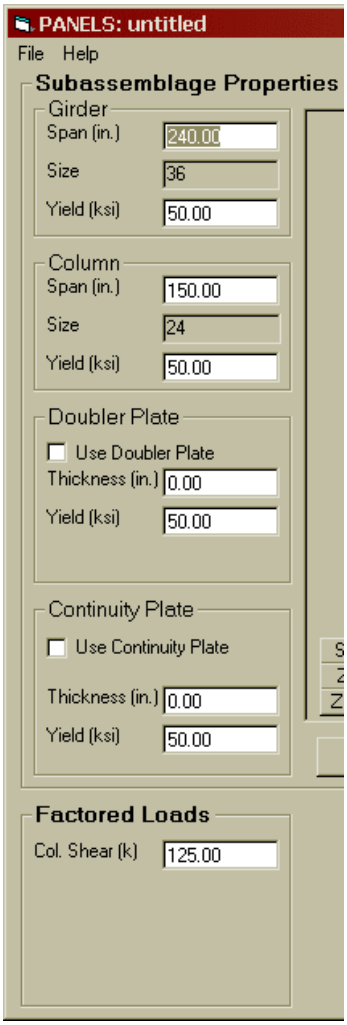

Figure A.3-3: Subassembly Property Frame

A.3.3 Subassemblage Properties

The Subassembly Properties frame, Figure A.3-3 is where the height of the column and width of the girder, as well as the material properties, are entered. This is also where the size and material properties of the doubler and continuity are input.

A.3.3.1 Girder and Column

The girder and column span lengths are based on a cruciform subassembly. In the design modules, if a Corner, End or Tee model is selected, PANELS internally adjusts the section's length based on its centerline dimensions of a cruciform shape. To account for this difference in dimensions, double the length from the end of the wide flange section to the center of the PZ for the member to which this applies. This is illustrated in Figure A.3-4. To model the Corner subassembly shown, instead of entering the column height of $\frac{H}{2}$, the height H based on the Cruciform shape must be entered. The girder length $\frac{L}{2}$ must also be entered based upon the Cruciform section length L.

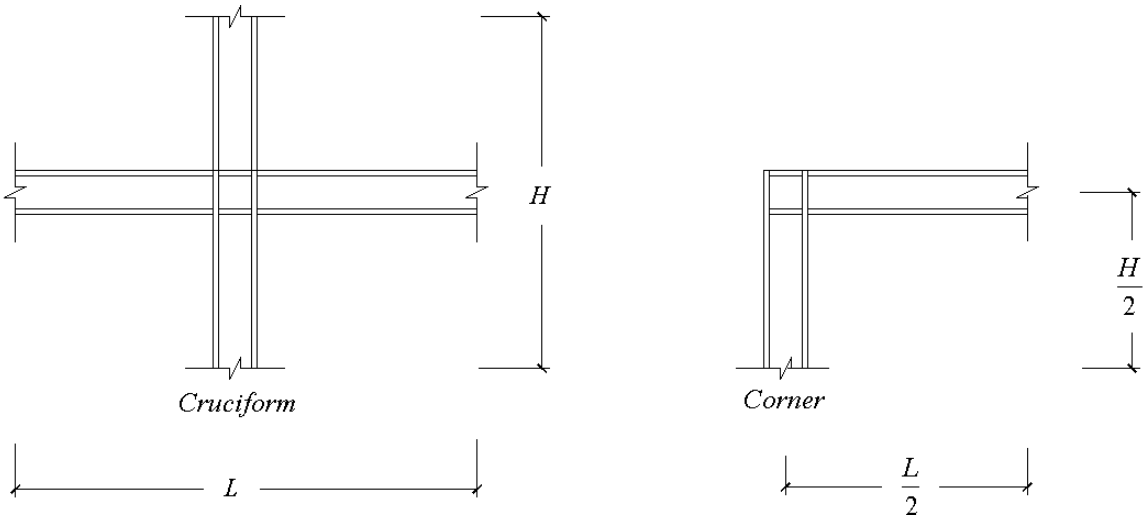

Figure A.3-4: PANELS Column and Girder Dimension Determination

A.3.3.2 Doubler Plate and Continuity Plate

If doubler plates and/or continuity plates are to be used, this is where their respective properties are entered. The doubler plate thickness is the total thickness of the plate added to the PZ region. If the model calls for a plate being placed on both sides of the beam/column joint region, add the two plate thicknesses together and enter the total thickness in the appropriate text box. For shell models, PANELS adjusts the thickness of the column web to account for the increase in thickness instead of adding additional elements to the model. This method of modeling the doubler plates does not allow for a separate yield stress to be used for the column webs and the doubler plates. For the solid element model, the doubler plates are an independent part of the model. This allows a different yield stress to be used for the column web and doubler plates in inelastic analysis.

The continuity plate thickness is the thickness of an individual plate, not the sum of the thicknesses of all the stiffeners used. PANELS assumes that there are a total of four plates of this size and yield stress, two being located at the top of the PZ region and two at the bottom, for all of it calculations. The width of the plate is assumed to be ½ of the width of the column flange minus ½ the column web thickness.

There are check boxes in both of these frames to allow the user to determine whether or not the doubler plates and continuity plates are included. This choice is also given in the Drift Analysis and Create ABAQUS design modules but, they must be checked here to allow for their use within the program. If they are not checked or their respective thicknesses are set to zero, the option to include them in the two previously mentioned modules will not be given.

A.3.3.3 Factored Load

The factored load is the load that will be applied at both the top and the bottom of the Cruciform and End subassemblies. For the Corner and Tee subassemblages, only one applied load will be added to the top of the column at the value specified in the text box.

A.3.4 Create a FEA

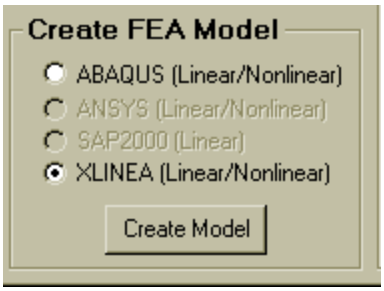

Figure A.3-5: Create FEA Model Frame

There are currently two different finite element model types that PANELS will create. They are shown in Figure A.3-5. To pick a model type, select the appropriate option button, place the cursor over the Create Model button and click the left mouse button. This will open the selected models module, which enables the user to create a finite element model.

A.3.5 Visual Display

The main display, shown in Figure A.3-6, allows the user to have visual representation of the subassembly that will be analyzed. Only a Cruciform subassembly will be displayed.

A.3.5.1 Views

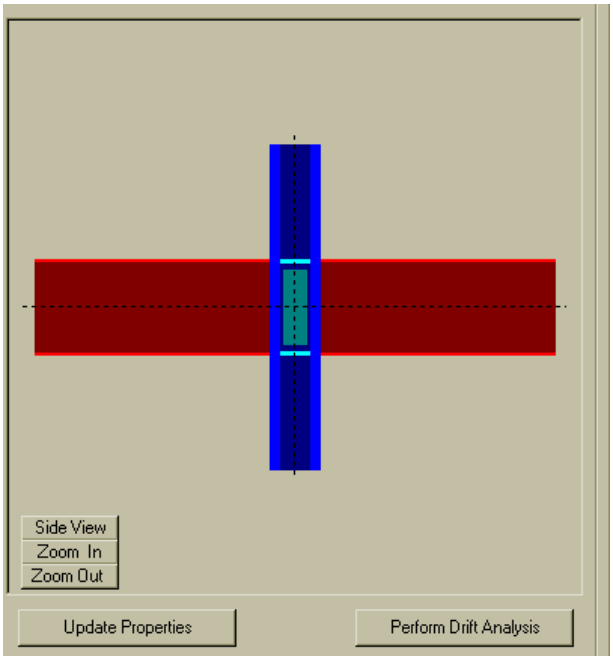

Figure A.3-6: Subassembly View Frame

Left clicking the mouse on the Side View button will rotate the figure ninety degrees into the frame, displaying the top of the subassembly. The button will then change to Top View. Clicking the button again will rotate the figure ninety degrees up and display the end view of the model and will switch the button name to End View. Selecting the button once more will return the figure back to its original display and change the button back to "Side View." The Zoom In and Zoom Out buttons are self-explanatory. These two buttons are included to enable the user to examine the subassembly more closely.

A.3.5.2 Update Properties and Perform Drift Analysis

The Update Properties button initiates the changes made in the Subassemblage Properties frame. It updates the values in PANELS and redraws the subassembly figure. The Perform Drift Analysis button opens the Subassembly Analysis module.

A.3.6 Subassembly Analysis

When the Perform Drift Analysis button in the main user interface is selected, the form shown in Figure A.3-7 is displayed. The purpose of this module is to determine the subassembly's drift using the elastic subassemblage model equations derived in Chapter 2. See that chapter for an explanation of the formulas used to derive the values in this figure.

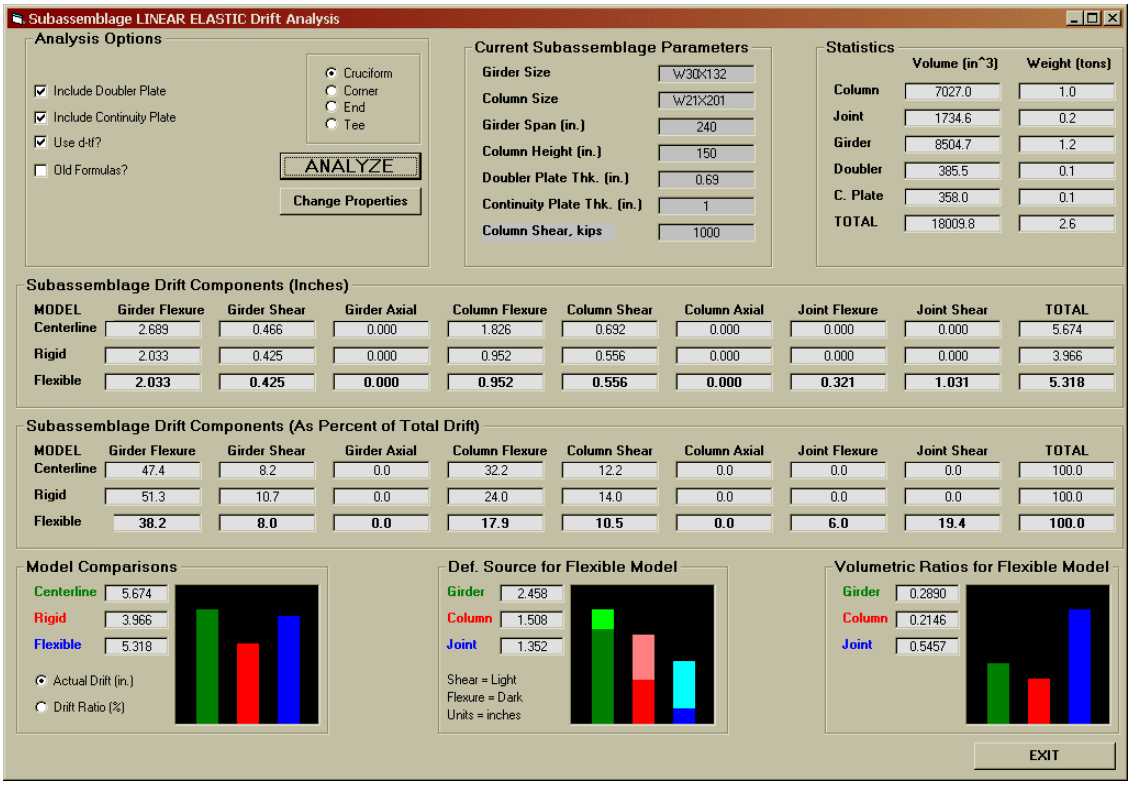

Figure A.3-7: Subassembly Analysis Module Frame

A.3.7 Analysis Options

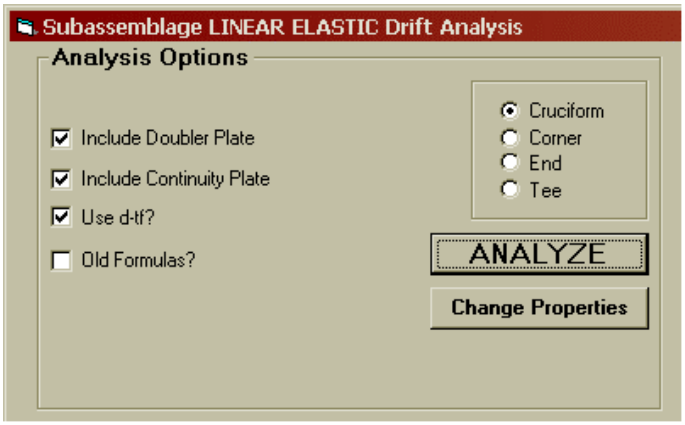

Figure A.3-8: Analysis Options Frame

The Old Formulas check box allows the user to decide which simplified moment diagram to use when calculating the deflections due to PZ flexure. If the old formulas option button is selected, the 1.5 multiplier developed in Chapter 4 is still used when calculating the displacement due to PZ flexure. A new multiplier based on the results from the ABAQUS study was not performed using the Simplified formulas, so the results using this check box will result in a model that is stiffer than those determined using the updated formulas. The rest of the check boxes seen in Figure A.3-8 are self-explanatory. They were included to rapidly analyze the four different subassemblies with different configurations and analysis assumptions.

The ANALYZE button tell PANELS to calculate the subassembly drift based on the selected section properties and analysis options, and then display the results in the Subassembly Drift Component frame. The "Change Properties" button displays the main user interface of PANELS to allow the user to change section sizes and properties.

A.3.8 Current Subassemblage Parameters Frame

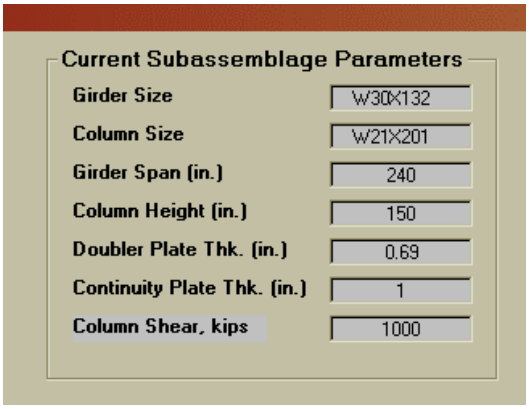

The Current Subassemblage Parameter Frame, Figure A.3-9, shows the column and girder sizes selected, the doubler plate and continuity plate thickness and the column shear force applied.

Figure A.3-9: Current Subassemblage Parameters

A.3.9 Subassembly Drift Components

After left clicking the ANALYZE button, the text fields in Figure A.3-10 will be updated to show the analysis results.

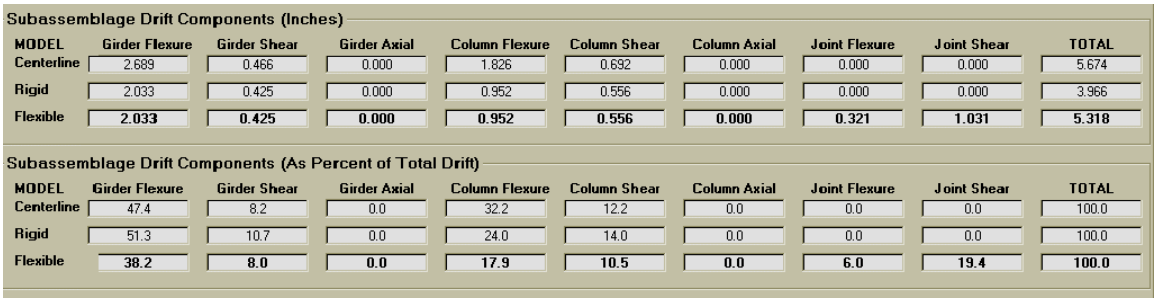

Figure A.3-10: Cruciform Subassembly Drift Components Frame

Using the properties shown in Figure 6.3-8 for reference, example calculations will be performed to show how the values for the "Flexible" cruciform subassembly in Figure A.3-10.

$$d_b = d_{b,nom} - t_{bf} = 30.3 \text{ in} - 1 \text{ in} = 29.3 \text{ in}$$

$$d_c = d_{c,nom} - t_{cf} = 23.0 \text{ in} - 1.6 \text{ in} = 21.4 \text{ in}$$

$$\frac{d_b}{2} = \frac{\beta H}{2} = \frac{29.3 \text{ in}}{3}$$

$$\frac{d_c}{2} = \frac{\alpha L}{2} = \frac{21.4\ \text{in}}{2}$$

$$\beta = \frac{\beta H/2}{H/2} = \frac{29.3\ \text{in}/2}{150\ \text{in}/2} = .195$$

$$\alpha = \frac{\alpha L/2}{L/2} = \frac{21.4\ \text{in}/2}{240\ \text{in}/2} = .089$$

$$\delta_{C,F} = \frac{VH^3}{12EI_C} * (1-\beta)^3 = \frac{1000\,\text{kips} * (150\,\text{in})^3}{12 * 29000\,\text{ksi} * 5310\,\text{in}^4} * (1-.195)^3 = 0.95\,\text{in}$$

$$\delta_{G,F} = \frac{VH^2 L}{12EI_G} * (1-\alpha)^3 = \frac{1000\,\text{kips} * (150\,\text{in})^2 * (240\,\text{in})}{12 * 29000\,\text{ksi} * 5770\,\text{in}^4} * (1-.089)^3 = 2.03\,\text{in}$$

$$\delta_{C,V} = \frac{VH}{A_C^* G} * (1-\beta) = \frac{1000\,\text{kips} * 150\,\text{in}}{19.45\,\text{in}^2 * 11154\,\text{ksi}} * (1-.195) = 0.56\,\text{in}$$

$$\delta_{G,V} = \frac{VH^2}{A_G^* GL} * (1-\alpha) = \frac{1000\,\text{kips} * (150\,\text{in})^2}{18.02\,\text{in}^2 * 11154\,\text{ksi} * 240\,\text{in}} * (1-.089) = 0.42\,\text{in}$$

$$New\ \delta_{PZ,CF} = \frac{VH^3\beta}{6EI_{Col}}\left[(1-\beta)^2 - (1-\beta)(1-\alpha-\beta) + \frac{(1-\alpha-\beta)^2}{3}\right] =$$

$$\frac{1000\,\text{kips} * (150\,\text{in})^3 * .195}{6 * 29000\,\text{ksi} * 5310\,\text{in}^4} * \left[(1-.195)^2 - (1-.195) * (1-.089-.195) + \frac{(1-.089-.195)^2}{3}\right] = 0.17\,\text{in}$$

$$I_{PZ} = 1.5 * I_{Pl} + I_{Cont} = 1.5 * \frac{tw_{PZ} * \beta H^3}{12} + \frac{2 * bf_c * (t_{Cont})^3}{12} + 2 * (bf_c - tw_{PZ}) * t_{Cont} * \left(\frac{\beta H}{2}\right)^2 =$$

$$1.5 * \frac{1.6\ \text{in} * (29.3\,\text{in})^3}{12} + \frac{2 * 12.6\,\text{in} * (1\,\text{in})^3}{12} + 2 * (12.6\,\text{in} - 1.6\,\text{in}) * 1\,\text{in} * \left(\frac{29.3\,\text{in}}{2}\right)^2 = 9755\,\text{in}^4$$

$$New\ \delta_{PZ,GF} = \frac{VH^2\alpha L}{4EI_{PZ}}\left[(1-\alpha)^2 - (1-\alpha)(1-\alpha-\beta) + \frac{(1-\alpha-\beta)^2}{3}\right] =$$

$$\frac{1000\,\text{kips} * (150\,\text{in})^2 * 21.4\,\text{in}}{4 * 29000\,\text{ksi} * 9755\,\text{in}^4} * \left[(1-.089)^2 - (1-.089) * (1-.089-.195) + \frac{(1-.089-.195)^2}{3}\right] = 0.15\,\text{in}$$

$$A_{PZ}^* = \alpha L(t_{DPl} + tw_C) = 21.4\,\text{in} * (.69\,\text{in} + .91\,\text{in}) = 34.24\,\text{in}^2$$

$$\delta_{PZ,V} = \frac{VH(1-\alpha-\beta)^2}{\beta A_{PZ}^* G} = \frac{1000\,\text{kips} * (150\,\text{in}) * (1-.089-.195)^2}{.195 * 34.24\,\text{in}^2 * 11154\,\text{ksi}} = 1.03\,\text{in}$$

Summing the above deflection values gives a total overall deflection of 5.32 in., which is the same value as in the Figure A.3-10 and in Table 4.4-9. Not including the PZ deflection contributions will give 3.97 in., which is the total deflection of the "Rigid" model. The "Centerline" model results can be determined by neglecting the PZ deflection contributions and dividing the remaining deflection terms by their respective $(1-\alpha)$, $(1-\alpha)^3$, $(1-\beta)$ or $(1-\beta)^3$ factor. This gives a total deflection of 5.67 in. that is also seen in Figure A.3-10.

A second example for a Corner model using the same section properties is given.

Subassemblage Drift Components (Inches)

MODEL	Girder Flexure	Girder Shear	Girder Axial	Column Flexure	Column Shear	Column Axial	Joint Flexure	Joint Shear	TOTAL
Centerline	1.345	0.233	0.097	0.913	0.346	0.014	0.000	0.000	2.947
Rigid	1.016	0.212	0.097	0.476	0.278	0.014	0.000	0.000	2.094
Flexible	1.016	0.212	0.097	0.476	0.278	0.014	0.345	0.258	2.705

Subassemblage Drift Components (As Percent of Total Drift)

MODEL	Girder Flexure	Girder Shear	Girder Axial	Column Flexure	Column Shear	Column Axial	Joint Flexure	Joint Shear	TOTAL
Centerline	45.6	7.9	3.3	31.0	11.7	0.5	0.0	0.0	100.0
Rigid	48.6	10.1	4.6	22.7	13.3	0.7	0.0	0.0	100.0
Flexible	40.4	8.4	3.9	18.9	11.1	0.5	6.5	10.2	100.0

Figure A.3-11: Corner Subassembly Drift Components Frame

$$\delta_{C,F} = \frac{1}{2} * \frac{VH^3}{12EI_C} * (1-\beta)^3 = \frac{1}{2} * .95\,\text{in} = 0.48\,\text{in}$$

$$\delta_{G,F} = \frac{1}{2} * \frac{VH^2 L}{12EI_G} * (1-\alpha)^3 = \frac{1}{2} * 2.03\,\text{in} = 1.02\,\text{in}$$

$$\delta_{C,V} = \frac{1}{2} * \frac{VH}{A_C^* G} * (1-\beta) = \frac{1}{2} * .56\,\text{in} = 0.28\,\text{in}$$

$$\delta_{G,V} = \frac{1}{2} * \frac{VH^2}{A_G^* GL} * (1-\alpha) = \frac{1}{2} * .42\,\text{in} = 0.21\,\text{in}$$

$$\delta_{G,A} = \frac{VL(1-\alpha)}{2EA_G} = \frac{1000\,\text{kips} * 240\,\text{in} * (1-.089)}{2 * 29000\,\text{ksi} * 38.9\,\text{in}} = 0.10\,\text{in}$$

$$\delta_{C,A} = \frac{VH^3(1-\beta)}{2EL^2 A_C} = \frac{1000\,\text{kips} * (150\,\text{in})^3 * (1-.195)}{2 * 29000\,\text{ksi} * (240\,\text{in})^2 * 59.2\,\text{in}} = 0.01\,\text{in}$$

$$\left[(1-\beta)^2 - (1-\beta)(1-\alpha-\beta) + \frac{(1-\alpha-\beta)^2}{3}\right] + \frac{V(1-\alpha)^2 \beta H^3}{24EI_C} =$$

$$\frac{1}{2} * .17_{\text{in}} + \frac{1000_{\text{kips}} * (1 - .089)^2 * .195 * (150_{\text{in}})^3}{24 * 29000_{\text{ksi}} * 5310_{\text{in}^4}} = 0.23_{\text{in}}$$

$$New\ \delta_{PZ,GF} = \frac{1}{2} * \frac{VH^2 \alpha L}{4EI_{PZ}} \left[(1-\alpha)^2 - (1-\alpha)(1-\alpha-\beta) + \frac{(1-\alpha-\beta)^2}{3} \right] + \frac{V(1-\beta)^2 H^2 \alpha L}{24EI_{PZ}} =$$

$$\frac{1}{2} * .15_{\text{in}} + \frac{1000_{\text{kips}} * (1 - .195)^2 (150_{\text{in}})^2 * 21.4_{\text{in}}}{24 * 29000_{\text{ksi}} * 9755_{\text{in}^4}} = 0.12_{\text{in}}$$

$$\delta_{PZ,V} = \frac{1}{4} * \frac{VH(1-\alpha-\beta)^2}{\beta A_{PZ}^{*} G} = \frac{1}{4} * 1.03_{\text{in}} = 0.26_{\text{in}}$$

Summing the above deflection values gives a total overall deflection of 2.71 in., which is the same value seen in Figure A.3-11 above as well as in Table 4.4-13.

A.3.10 Model Comparison

The Model Comparison Frame gives a visual comparison between the three model types and their individual drift components.

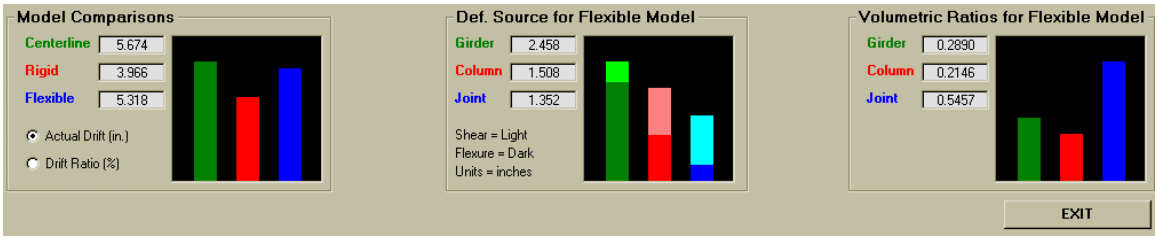

Figure A.3-12: Model Comparison Frame

A.3.11 ABAQUS Models

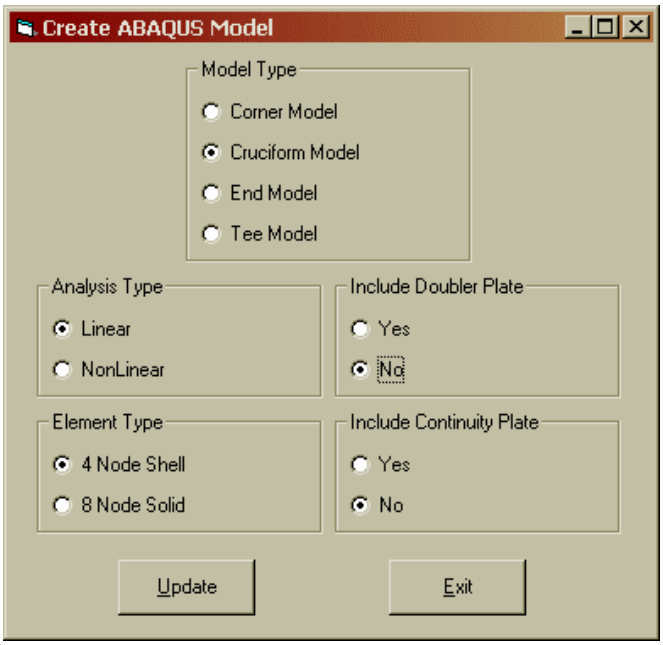

Figure A.3-13: Create ABAQUS Model Module

A.3.11.1 Model Configurations

Figure A.3-13 shows the Create ABAQUS Model module. The Model Type, Include Doubler Plate and Include Continuity Plate option buttons are self-explanatory. They were included to allow the user to quickly create multiple model types.

A.3.11.2 Analysis Type

The Analysis Type option button allows the user to select what type of analysis will be performed. The linear model assumes a Young's modulus value of 29000 ksi, a Poisson's ratio of 0.3 and that the steel exhibits isotropic behavior. The displacements are determined using the applied load, Figure A.3-3. For the NonLinear option, the first yield of the model is set at the yield stress chosen for the individual component, Figure A.3-3, with a strain-hardening ratio of 3 percent. The ABAQUS input files were arranged so that each region of the model was separate and could be given its own yield stress and strain hardening ratio. Please refer to the ABAQUS Users Manual (Hibbitt, Karlsson and Sorensen 2001) for directions on updating .inp files if these values need to be changed manually.

Since the nonlinear models take a large amount of time to run, the output is displacement controlled to help ensure that the solution will converge. This was also done because most test data is displacement controlled, making comparisons with the ABAQUS output easier. To match the boundary conditions of the Lehigh SAC test data,

the restraint conditions at the two girders were both changed; rollers and a pin support were applied to the bottom column. These restraint changes will reduce the total deflections by ½ compared to the support conditions used for the ABAQUS models used to derive the elastic PANELS equations. If inelastic comparisons are going to be made with the XLinea models created by PANELS, the .inp file will need to be updated manually. Please refer to the ABAQUS Users Manual for directions on updating the displacement controls and restraint conditions in the .inp files.

A.3.11.3 Element Type

The 4-Node Shell element button creates a shell element model using type S4 elements. For a complete description of the shell model and the restraint and constraint conditions associated with it, see Chapter 4 above and the ABAQUS User's Manual.

The 8-Node Solid button uses type C3D8 elements. The solid element models were not used in the analysis contained within this document. Therefore no description of them is contained in Chapter 4. The model's dimensions are based on the nominal depths of the wide flange sections used. This being the case, no modifications to the elements' depths were necessary due to overlap which was required with the shell elements. Each member of the subassemblage was modeled with four elements through the thickness. The doubler plates are modeled as separate components instead of adjusting the thickness of the PZ elements. For the member of the subassemblage, surfaced base constraints were used to simulate the welds in the model. When modeling the boundary conditions for all four subassemblages, the same manner of restraining the models was used for the solid elements as was done with the shell element in Chapter 4.

A.3.11.4 ABAQUS Model Update

When the Update button is selected, an ABAQUS input file called abaqusout.inp is created in the same directory where PANELS.exe is located.

A.3.12 XLinea Models

A.3.12.1 Model and Subassembly Type

The Model and Subassembly modules, Figure A.3-14, allow the user to select which model type will be built. See Chapter 3 for an explanation of the Krawinkler and Scissors model properties and Chapter 1 for a definition of the model shapes and assumptions used.

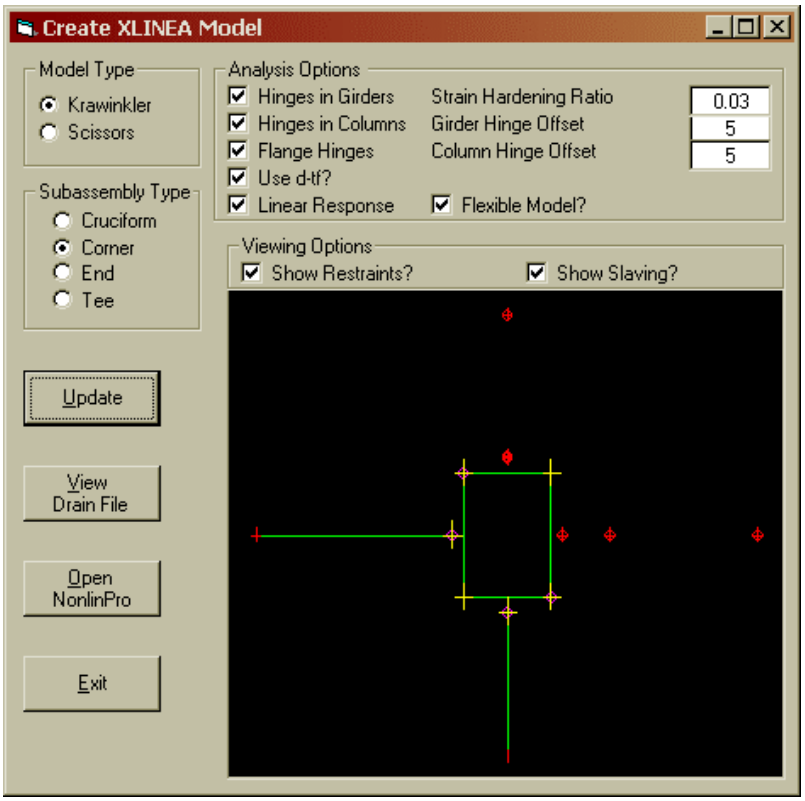

Figure A.3-14: Create XLinea Model Module

A.3.12.2 Analysis Options

Selecting the Hinge in the Girder and Hinge in the Column selection buttons will cause the module in Figure A.3-15 to appear when the update button is selected.

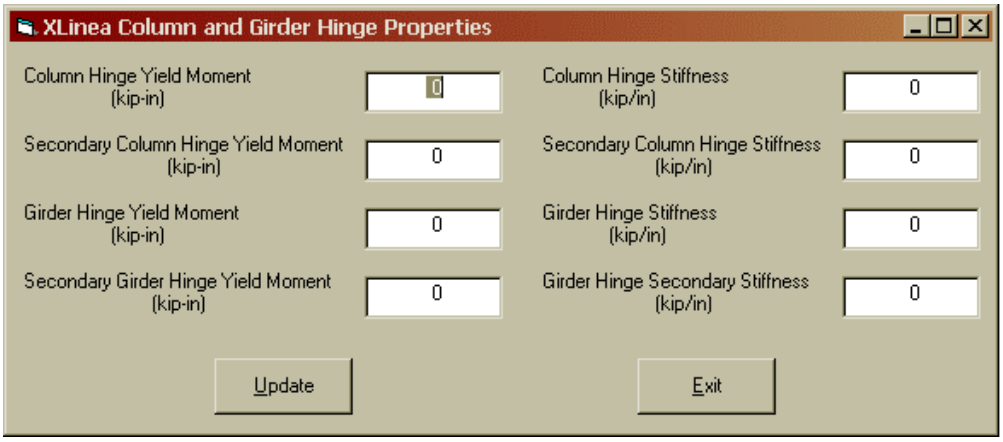

Figure A.3-15: Create XLinea Model Module

This is where the hinge properties used to overcome the shortcoming of the Drain-2DX Type-2 element, discussed in Chapter 5, are entered. See the reference paper (Charney 2002) for a description on how to develop these properties.

These two selection boxes will also allow the user to edit the girder and column offset values seen in Figure A.3-14. These values represent the distances from the PZ at which the plastic hinges in the girders and column will form. Again, see the reference paper (Charney 2002) for a description on how to determine these values.

The Flange Hinges and Linear Response selection boxes, Figure A.3-14, are included to rapidly develop models. The Linear Response selection box is included to create models to be compared with the linear elastic equation results. If the Flange Hinge box is selected, the stiffnesses of the inelastic hinges that develop in the column flanges are included in the model. If it is not selected, this component is ignored. See Chapter 3 for a description of this component's properties. The Linear Response selection box tells PANELS to create a model with the stiffness properties based on the selected girder and column properties, but will not allow any yielding to occur in the model.

Finally, the Flexible Model selection box allows the user to create a Drain-2DX input file which includes the effects of PZ flexure in the beam/column joint. The methods used to do this are outlined in Chapter 7. The current version of PANELS uses

K_{1K}, K_{2K}, K_{1S} and K_{2S} for the Updated Krawinkler and Updated Scissors models when calculating the flexural properties instead of the average values presented in Chapter 7.

A.3.12.3 Viewing Options

For the development of the XLinea input file, it was decided to include all the nodes necessary to model the Cruciform subassemblage and constrain all the unused nodes when the Corner, End and Tee model are generated. To give a graphic representation of the restraints and constraints in the model, these selection boxes were included. The shapes and color schemes of the restraints and constraints in Figure A.3-14 are identical to those seen in the XLinea post-processor.

A.3.12.4 Update

When the Update button is selected, an XLinea input file is created based on the model type and section properties selected and material and hinge properties entered. See Chapter 3 for the development of the model's individual properties. The file is named based on which type of model is created. If a Krawinkler model is selected, a file named Krawout.2dx is created. For a Scissors model, the output file is named SizzOut.2dx. Once created, both files are located in the same directory as PANELS.exe.

A.3.12.5 View Drain File

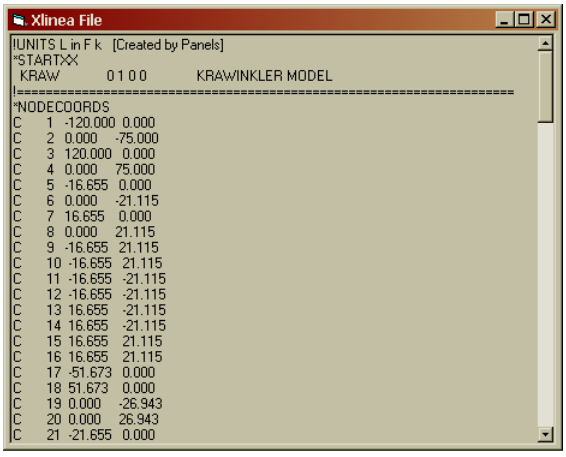

Figure A.3-16: XLinea File Viewer

When the View Drain File button is selected, it will cause the frame in Figure A.3-16 to come into view. This frame shows all the data in the input file but does not allow for any editing of the file. Any direct editing of the input file can be done either in a word processing program or directly in

the XLinea environment.

A.3.12.6 Open Nonlin Pro

Selecting this button runs RAM XLinea. In order for this button to operate properly, the XLinea executable file nlmain.exe must be in the following location: C:\Ram\Prog\nlmain.exe. The underlying code also contains the password that bypasses the software lock.

For any questions related to the operation of RAM XLinea or Drain-2DX, please refer to the program's user's manual.

Appendix B Sample Drain-2DX Input Files

B.1 Cruciform Krawinkler Model

```
!UNITS L in F k   [Created by PANELS]
*STARTXX
  KCru            0 1 0 0            KRAWINKLER MODEL
!====================================================================
*NODECOORDS
C       1   -168.000  0.000
C       2   0.000     -75.000
C       3   168.000   0.000
C       4   0.000     75.000
C       5   -10.370   0.000
C       6   0.000     -11.665
C       7   10.370    0.000
C       8   0.000     11.665
C       9   -10.370   11.665
C       10  -10.370   11.665
C       11  -10.370   -11.665
C       12  -10.370   -11.665
C       13  10.370    -11.665
C       14  10.370    -11.665
C       15  10.370    11.665
C       16  10.370    11.665
C       17  -78.815   0.000
C       18  78.815    0.000
C       19  0.000     -31.668
C       20  0.000     31.668
C       21  -15.370   0.000
C       22  15.370    0.000
C       23  -15.370   0.000
C       24  15.370    0.000
C       25  0.000     -11.665
C       26  0.000     11.665
C       27  0.000     -11.665
C       28  0.000     11.665
!================================================================
*RESTRAINTS
S 110         1
S 010         3
S 111        25
S 111        27
S 111        26
S 111        28
!================================================================
*SLAVING
S 110         9        10
S 110        11        12
S 110        13        14
S 110        15        16
```

```
S 110       21       23
S 110       22       24
!====================================================================
*ELEMENTGROUP
   2    0    0                    Columns of the model
   1    0    1
   1  29000      0.030  35.9      2960      4.0  4.0  2.0    12.4    0.3
   1    1   1000000   1000000
   1        2       19             1        1    1
   2       19        6             1        1    1
   3        4       20             1        1    1
   4       20        8             1        1    1
!====================================================================
*ELEMENTGROUP
   2    0    0                    Girder of the model
   1    0    1
   1  29000      0.030  24.7      2370      4.0  4.0  2.0    11.0    0.3
   1    1   1000000   1000000
   1        1       17             1        1    1
   2       17       21             1        1    1
   3       23        5             1        1    1
   4        3       18             1        1    1
   5       18       22             1        1    1
   6       24        7             1        1    1
!====================================================================
*ELEMENTGROUP
   2    0    0                    Rigid Links of the model
   2    0    1
   1  29000      0.030 1000000    1000000    4.0  4.0  2.0
   2  29000      0.030 1000000    1000000    4.0  4.0  2.0
   1    1   1000000   1000000
   1        5        9             1        1    1
   2       10        8             2        1    1
   3        8       16             2        1    1
   4       15        7             1        1    1
   5        7       13             1        1    1
   6       14        6             2        1    1
   7        6       12             2        1    1
   8       11        5             1        1    1
!====================================================================
*ELEMENTGROUP
   4    0    0                    Plastic hinges in the girders
   2
   1  1.E+14      1E-14  1.102E+4 1.102E+4  1.000E+00    3    0
   2  3.26E+5      0.030  1.196E+3 1.196E+3  1.000E+00    3    0
   1       21       23             1
   2       21       23             2
   3       22       24             1
   4       22       24             2
!====================================================================
*ELEMENTGROUP
   4    0    0                    Hinges in the Panel
   1
```

```
   1  3238169      0.000  8710     8710      1.000E+00    3    0
   1         9        10              1
!=================================================================='
*ELEMENTGROUP
   4    0    0                    Hinges in the Flanges
   1
   1  95598        0.030  1029     1029      1.000E+00    3    0
   1        13        14              1
!=================================================================='
*RESULTS
NSD    011
NSV    011
NSA    011
E      011
!=================================================================================
*NODALOAD
 test
S     500                        4
S    -500                        2
!=================================================================================
*PARAMETERS
OS       0    1    1
!=================================================================================
*STAT
N     test      -1.0
L 0.002381
D   2        4          .1         12
!=================================================================================
*STOP
```

B.2 Cruciform Scissors Model

```
!UNITS L in F k   [Created by Panels]
*STARTXX
  SCru            0 1 0 0            SCISSORS MODEL
!====================================================================
*NODECOORDS
C       1   -168.000  0.000
C       2   0.000     -75.000
C       3   168.000   0.000
C       4   0.000     75.000
C       5   -10.370   0.000
C       6   0.000     -11.665
C       7   10.370    0.000
C       8   0.000     11.665
C       9   0.000     0.000
C       10  0.000     0.000
C       11  -78.815   0.000
C       12  78.815    0.000
C       13  0.000     -31.668
C       14  0.000     31.668
C       15  -15.370   0.000
C       16  15.370    0.000
C       17  -15.370   0.000
C       18  15.370    0.000
C       19  0.000     -11.665
C       20  0.000     11.665
C       21  0.000     -11.665
C       22  0.000     11.665
!====================================================================
*RESTRAINTS
S 110         1
S 010         3
S 111        19
S 111        21
S 111        20
S 111        22
!====================================================================
*SLAVING
S 110         9        10
S 110        15        17
S 110        16        18
!====================================================================
*ELEMENTGROUP
   2    0    0                    Columns of the model
   1    0    1
   1  29000       0.030  35.9       2960      4.0  4.0  2.0    12.4    0.3
   1    1   1000000   1000000
   1         2        13             1         1    1
   2        13         6             1         1    1
   3         4        14             1         1    1
   4        14         8             1         1    1
```

```
!=============================================================
*ELEMENTGROUP
   2    0    0                    Girder of the model
   1    0    1
   1  29000       0.030  24.7       2370      4.0  4.0  2.0    11.0    0.3
   1    1   1000000   1000000
   1         1        11             1        1    1
   2        11        15             1        1    1
   3        17         5             1        1    1
   4         3        12             1        1    1
   5        12        16             1        1    1
   6        18         7             1        1    1
!=============================================================
*ELEMENTGROUP
   2    0    0                    Rigid Links of the model
   2    0    1
   1  29000       0.030 1000000    1000000    4.0  4.0  2.0
   2  29000       0.030 1000000    1000000    4.0  4.0  2.0
   1    1   1000000   1000000
   1         8        10             1        1    1
   2        10         6             1        1    1
   3         5         9            2        1    1
   4         9         7            2        1    1
!=============================================================
*ELEMENTGROUP
   4    0    0                    Hinges in the Panel
   2
   1  5285230      0.000  11127    11127     1.000E+00    3    0
   2  156032       0.030  1314     1314      1.000E+00    3    0
   1         9        10             1
   2         9        10             2
!=============================================================='
*ELEMENTGROUP
   4    0    0                    Plastic hinges in the girders
   2
   1  1.E+14       1E-14  1.102E+4 1.102E+4  1.000E+00    3    0
   2  3.26E+5      0.030  1.196E+3 1.196E+3  1.000E+00    3    0
   1        15        17             1
   2        15        17             2
   3        16        18             1
   4        16        18             2
!=============================================================
*RESULTS
NSD    011
NSV    011
NSA    011
E      011
!=============================================================================
*NODALOAD
 test
S     500                        4
S    -500                        2
!=============================================================================
```

```
*PARAMETERS
OS       0    1    1
!=========================================================================
*STAT
N     test      -1.0
L 0.002381
D   2        4          .1         12
!=========================================================================
*STOP
```

B.3 Corner Krawinkler Model

```
!UNITS L in F k   [Created by PANELS]
*STARTXX
  KCor            0 1 0 0            KRAWINKLER MODEL
!=================================================================
*NODECOORDS
C       1   -168.000  0.000
C       2   0.000     -75.000
C       3   168.000   0.000
C       4   0.000     75.000
C       5   -10.370   0.000
C       6   0.000     -11.665
C       7   10.370    0.000
C       8   0.000     11.665
C       9   -10.370   11.665
C       10  -10.370   11.665
C       11  -10.370   -11.665
C       12  -10.370   -11.665
C       13  10.370    -11.665
C       14  10.370    -11.665
C       15  10.370    11.665
C       16  10.370    11.665
C       17  -78.815   0.000
C       18  78.815    0.000
C       19  0.000     -31.668
C       20  0.000     31.668
C       21  -15.370   0.000
C       22  15.370    0.000
C       23  -15.370   0.000
C       24  15.370    0.000
C       25  0.000     -11.665
C       26  0.000     11.665
C       27  0.000     -11.665
C       28  0.000     11.665
!=============================================================
*RESTRAINTS
S 110         1
S 010         2
S 111         3
S 111        18
S 111        22
S 111        24
S 111         4
S 111        20
S 111        26
S 111        28
S 111        25
S 111        27
!=============================================================
*SLAVING
S 110         9        10
```

```
S 110       11       12
S 110       13       14
S 110       15       16
S 110       21       23
!=============================================================
*ELEMENTGROUP
   2    0    0                    Columns of the model
   1    0    1
   1  29000      0.030  35.9      2960      4.0  4.0  2.0    12.4    0.3
   1    1   1000000   1000000
   1        2       19             1        1    1
   2       19        6             1        1    1
!=============================================================
*ELEMENTGROUP
   2    0    0                    Girder of the model
   1    0    1
   1  29000      0.030  24.7      2370      4.0  4.0  2.0    11.0    0.3
   1    1   1000000   1000000
   1        1       17             1        1    1
   2       17       21             1        1    1
   3       23        5             1        1    1
!=============================================================
*ELEMENTGROUP
   2    0    0                    Rigid Links of the model
   2    0    1
   1  29000      0.030 1000000    1000000    4.0  4.0  2.0
   2  29000      0.030 1000000    1000000    4.0  4.0  2.0
   1    1   1000000   1000000
   1        5        9             1        1    1
   2       10        8             2        1    1
   3        8       16             2        1    1
   4       15        7             1        1    1
   5        7       13             1        1    1
   6       14        6             2        1    1
   7        6       12             2        1    1
   8       11        5             1        1    1
!=============================================================================
*ELEMENTGROUP
   4    0    0                    Plastic hinges in the girders
   2
   1  1.E+14      1E-14  1.102E+4 1.102E+4  1.000E+00    3    0
   2  3.26E+5      0.030  1.196E+3 1.196E+3  1.000E+00    3    0
   1       21       23             1
   2       21       23             2
   3       22       24             1
   4       22       24             2
!=============================================================
*ELEMENTGROUP
   4    0    0                    Hinges in the Panel
   1
   1  3238169      0.000  8710     8710      1.000E+00    3    0
   1        9       10             1
!=============================================================='
```

```
*ELEMENTGROUP
   4    0    0                    Hinges in the Flanges
   1
   1  95598       0.030  1029     1029      1.000E+00    3    0
   1        13        14              1
!=================================================================='
*RESULTS
NSD    011
NSV    011
NSA    011
E      011
!=================================================================
*NODALOAD
 test
S     500                        4
S    -500                        2
!=================================================================
*PARAMETERS
OS       0    1    1
!=================================================================
*STAT
N     test      -1.0
L 0.002381
D   2        4          .1         7
!=================================================================
*STOP
```

B.4 Corner Scissors Model

```
!UNITS L in F k   [Created by Panels]
*STARTXX
 SCor            0 1 0 0            SCISSORS MODEL
!====================================================================
*NODECOORDS
C      1  -168.000  0.000
C      2  0.000     -75.000
C      3  168.000   0.000
C      4  0.000     75.000
C      5  -10.370   0.000
C      6  0.000     -11.665
C      7  10.370    0.000
C      8  0.000     11.665
C      9  0.000     0.000
C      10 0.000     0.000
C      11 -78.815   0.000
C      12 78.815    0.000
C      13 0.000     -31.668
C      14 0.000     31.668
C      15 -15.370   0.000
C      16 15.370    0.000
C      17 -15.370   0.000
C      18 15.370    0.000
C      19 0.000     -11.665
C      20 0.000     11.665
C      21 0.000     -11.665
C      22 0.000     11.665
!====================================================================
*RESTRAINTS
S 110        1
S 010        2
S 111        3
S 111       12
S 111       16
S 111       18
S 211        4
S 111       14
S 111       20
S 111       22
S 111       19
S 111       21
!====================================================================
*SLAVING
S 110        9       10
S 110       15       17
!====================================================================
*ELEMENTGROUP
   2   0   0                    Columns of the model
   1   0   1
   1  29000      0.030  35.9      2960      4.0  4.0  2.0    12.4    0.3
```

```
   1    1   1000000   1000000
   1        2        13              1        1    1
   2       13         6              1        1    1
!=================================================================
*ELEMENTGROUP
   2    0    0                      Girder of the model
   1    0    1
   1  29000       0.030  24.7       2370      4.0  4.0  2.0    11.0    0.3
   1    1   1000000   1000000
   1        1        11              1        1    1
   2       11        15              1        1    1
   3       17         5              1        1    1
!=================================================================
*ELEMENTGROUP
   2    0    0                      Rigid Links of the model
   2    0    1
   1  29000       0.030 1000000    1000000    4.0  4.0  2.0
   2  29000       0.030 1000000    1000000    4.0  4.0  2.0
   1    1   1000000   1000000
   1        8        10              1        1    1
   2       10         6              1        1    1
   3        5         9             2        1    1
   4        9         7             2        1    1
!=================================================================
*ELEMENTGROUP
   4    0    0                      Hinges in the Panel
   2
   1  5285230      0.000  11127    11127     1.000E+00    3    0
   2  156032       0.030  1314     1314      1.000E+00    3    0
   1        9        10              1
   2        9        10              2
!=================================================================='
*ELEMENTGROUP
   4    0    0                      Plastic hinges in the girders
   2
   1  1.E+14       1E-14  1.102E+4 1.102E+4  1.000E+00    3    0
   2  3.26E+5      0.030  1.196E+3 1.196E+3  1.000E+00    3    0
   1        15       17              1
   2        15       17              2
   3        16       18              1
   4        16       18              2
!=================================================================
*RESULTS
NSD    011
NSV    011
NSA    011
E      011
!=================================================================================
*NODALOAD
 test
S     500                        4
S    -500                        2
!=================================================================
```

```
*PARAMETERS
OS       0    1    1
!=============================================================================
*STAT
N     test      -1.0
L 0.002381
D   2        4          .1         7
!=============================================================================
*STOP
```

B.5 End Krawinkler Model

```
!UNITS L in F k   [Created by PANELS]
*STARTXX
  KEnd            0 1 0 0            KRAWINKLER MODEL
!=================================================================
*NODECOORDS
C       1   -168.000  0.000
C       2   0.000     -75.000
C       3   168.000   0.000
C       4   0.000     75.000
C       5   -10.370   0.000
C       6   0.000     -11.665
C       7   10.370    0.000
C       8   0.000     11.665
C       9   -10.370   11.665
C       10  -10.370   11.665
C       11  -10.370   -11.665
C       12  -10.370   -11.665
C       13  10.370    -11.665
C       14  10.370    -11.665
C       15  10.370    11.665
C       16  10.370    11.665
C       17  -78.815   0.000
C       18  78.815    0.000
C       19  0.000     -31.668
C       20  0.000     31.668
C       21  -15.370   0.000
C       22  15.370    0.000
C       23  -15.370   0.000
C       24  15.370    0.000
C       25  0.000     -11.665
C       26  0.000     11.665
C       27  0.000     -11.665
C       28  0.000     11.665
!=============================================================
*RESTRAINTS
S 110         1
S 010         2
S 111         3
S 111        18
S 111        22
S 111        24
S 111        25
S 111        27
S 111        26
S 111        28
!=============================================================
*SLAVING
S 110         9        10
S 110        11        12
S 110        13        14
```

```
S 110       15       16
S 110       21       23
!=============================================================
*ELEMENTGROUP
   2    0    0                    Columns of the model
   1    0    1
   1  29000      0.030  35.9      2960      4.0  4.0  2.0    12.4    0.3
   1    1   1000000   1000000
   1        2       19             1        1    1
   2       19        6             1        1    1
   3        4       20             1        1    1
   4       20        8             1        1    1
!=============================================================
*ELEMENTGROUP
   2    0    0                    Girder of the model
   1    0    1
   1  29000      0.030  24.7      2370      4.0  4.0  2.0    11.0    0.3
   1    1   1000000   1000000
   1        1       17             1        1    1
   2       17       21             1        1    1
   3       23        5             1        1    1
!=============================================================
*ELEMENTGROUP
   2    0    0                    Rigid Links of the model
   2    0    1
   1  29000      0.030 1000000    1000000    4.0  4.0  2.0
   2  29000      0.030 1000000    1000000    4.0  4.0  2.0
   1    1   1000000   1000000
   1        5        9             1        1    1
   2       10        8             2        1    1
   3        8       16             2        1    1
   4       15        7             1        1    1
   5        7       13             1        1    1
   6       14        6             2        1    1
   7        6       12             2        1    1
   8       11        5             1        1    1
!=====================================================================
*ELEMENTGROUP
   4    0    0                    Plastic hinges in the girders
   2
   1  1.E+14      1E-14  1.102E+4 1.102E+4  1.000E+00    3    0
   2  3.26E+5      0.030  1.196E+3 1.196E+3  1.000E+00    3    0
   1       21       23             1
   2       21       23             2
   3       22       24             1
   4       22       24             2
!=============================================================
*ELEMENTGROUP
   4    0    0                    Hinges in the Panel
   1
   1  3238169      0.000  8710     8710      1.000E+00    3    0
   1        9       10             1
!=============================================================='
```

```
*ELEMENTGROUP
   4    0    0                    Hinges in the Flanges
   1
   1  95598       0.030  1029     1029      1.000E+00    3    0
   1        13       14             1
!=================================================================='
*RESULTS
NSD    011
NSV    011
NSA    011
E      011
!=================================================================
*NODALOAD
 test
S     500                      4
S    -500                      2
!=================================================================
*PARAMETERS
OS       0    1    1
!=================================================================
*STAT
N     test      -1.0
L 0.002381
D   2        4          .1         7
!=================================================================
*STOP
```

B.6 End Scissors Model

```
!UNITS L in F k   [Created by Panels]
*STARTXX
 SEnd            0 1 0 0            SCISSORS MODEL
!=====================================================================
*NODECOORDS
C      1   -168.000  0.000
C      2   0.000     -75.000
C      3   168.000   0.000
C      4   0.000     75.000
C      5   -10.370   0.000
C      6   0.000     -11.665
C      7   10.370    0.000
C      8   0.000     11.665
C      9   0.000     0.000
C      10  0.000     0.000
C      11  -78.815   0.000
C      12  78.815    0.000
C      13  0.000     -31.668
C      14  0.000     31.668
C      15  -15.370   0.000
C      16  15.370    0.000
C      17  -15.370   0.000
C      18  15.370    0.000
C      19  0.000     -11.665
C      20  0.000     11.665
C      21  0.000     -11.665
C      22  0.000     11.665
!=====================================================================
*RESTRAINTS
S 110        1
S 010        2
S 111        3
S 111       12
S 111       16
S 111       18
S 111       19
S 111       21
S 111       20
S 111       22
!=====================================================================
*SLAVING
S 110        9       10
S 110       15       17
!=====================================================================
*ELEMENTGROUP
   2   0   0                    Columns of the model
   1   0   1
   1  29000      0.030  35.9      2960      4.0  4.0  2.0    12.4    0.3
   1   1   1000000   1000000
   1       2       13            1        1    1
```

```
   2       13       6            1       1    1
   3       4       14            1       1    1
   4       14       8            1       1    1
!====================================================================
*ELEMENTGROUP
   2    0    0                   Girder of the model
   1    0    1
   1  29000      0.030  24.7      2370      4.0  4.0  2.0    11.0    0.3
   1    1   1000000   1000000
   1       1       11            1       1    1
   2       11      15            1       1    1
   3       17       5            1       1    1
!====================================================================
*ELEMENTGROUP
   2    0    0                   Rigid Links of the model
   2    0    1
   1  29000      0.030 1000000    1000000    4.0  4.0  2.0
   2  29000      0.030 1000000    1000000    4.0  4.0  2.0
   1    1   1000000   1000000
   1       8       10            1       1    1
   2       10       6            1       1    1
   3       5       9            2       1    1
   4       9       7            2       1    1
!====================================================================
*ELEMENTGROUP
   4    0    0                   Hinges in the Panel
   2
   1  5285230     0.000  11127    11127     1.000E+00    3    0
   2  156032      0.030  1314     1314      1.000E+00    3    0
   1       9       10            1
   2       9       10            2
!====================================================================='
*ELEMENTGROUP
   4    0    0                   Plastic hinges in the girders
   2
   1  1.E+14      1E-14  1.102E+4 1.102E+4  1.000E+00    3    0
   2  3.26E+5     0.030  1.196E+3 1.196E+3  1.000E+00    3    0
   1       15       17            1
   2       15       17            2
   3       16       18            1
   4       16       18            2
!====================================================================
*RESULTS
NSD    011
NSV    011
NSA    011
E      011
!=====================================================================================
*NODALOAD
 test
S     500                        4
S    -500                        2
!=====================================================================================
```

```
*PARAMETERS
OS       0    1    1
!=========================================================================
*STAT
N     test      -1.0
L 0.002381
D   2        4          .1         7
!=========================================================================
*STOP
```

B.7 Tee Krawinkler Model

```
!UNITS L in F k   [Created by PANELS]
*STARTXX
  KTee            0 1 0 0            KRAWINKLER MODEL
!=====================================================================
*NODECOORDS
C       1   -168.000  0.000
C       2   0.000     -75.000
C       3   168.000   0.000
C       4   0.000     75.000
C       5   -10.370   0.000
C       6   0.000     -11.665
C       7   10.370    0.000
C       8   0.000     11.665
C       9   -10.370   11.665
C       10  -10.370   11.665
C       11  -10.370   -11.665
C       12  -10.370   -11.665
C       13  10.370    -11.665
C       14  10.370    -11.665
C       15  10.370    11.665
C       16  10.370    11.665
C       17  -78.815   0.000
C       18  78.815    0.000
C       19  0.000     -31.668
C       20  0.000     31.668
C       21  -15.370   0.000
C       22  15.370    0.000
C       23  -15.370   0.000
C       24  15.370    0.000
C       25  0.000     -11.665
C       26  0.000     11.665
C       27  0.000     -11.665
C       28  0.000     11.665
!=============================================================
*RESTRAINTS
S 110         1
S 010         3
S 111         4
S 111        20
S 111        26
S 111        28
S 111        25
S 111        27
!=============================================================
*SLAVING
S 110         9        10
S 110        11        12
S 110        13        14
S 110        15        16
S 110        21        23
```

```
S 110       22       24
!=============================================================
*ELEMENTGROUP
   2    0    0                    Columns of the model
   1    0    1
   1  29000      0.030  35.9      2960     4.0  4.0  2.0    12.4    0.3
   1    1   1000000   1000000
   1        2       19             1        1    1
   2       19        6             1        1    1
!=============================================================
*ELEMENTGROUP
   2    0    0                    Girder of the model
   1    0    1
   1  29000      0.030  24.7      2370     4.0  4.0  2.0    11.0    0.3
   1    1   1000000   1000000
   1        1       17             1        1    1
   2       17       21             1        1    1
   3       23        5             1        1    1
   4        3       18             1        1    1
   5       18       22             1        1    1
   6       24        7             1        1    1
!=============================================================
*ELEMENTGROUP
   2    0    0                    Rigid Links of the model
   2    0    1
   1  29000      0.030 1000000    1000000    4.0  4.0  2.0
   2  29000      0.030 1000000    1000000    4.0  4.0  2.0
   1    1   1000000   1000000
   1        5        9             1        1    1
   2       10        8             2        1    1
   3        8       16             2        1    1
   4       15        7             1        1    1
   5        7       13             1        1    1
   6       14        6             2        1    1
   7        6       12             2        1    1
   8       11        5             1        1    1
!=============================================================================
*ELEMENTGROUP
   4    0    0                    Plastic hinges in the girders
   2
   1  1.E+14       1E-14  1.102E+4 1.102E+4  1.000E+00    3    0
   2  3.26E+5       0.030  1.196E+3 1.196E+3  1.000E+00    3    0
   1       21       23             1
   2       21       23             2
   3       22       24             1
   4       22       24             2
!=============================================================
*ELEMENTGROUP
   4    0    0                    Hinges in the Panel
   1
   1  3238169      0.000  8710     8710      1.000E+00    3    0
   1        9       10             1
!=============================================================='
```

```
*ELEMENTGROUP
   4    0    0                    Hinges in the Flanges
   1
   1  95598       0.030  1029     1029      1.000E+00    3    0
   1        13       14             1
!=================================================================='
*RESULTS
NSD    011
NSV    011
NSA    011
E      011
!=================================================================
*NODALOAD
 test
S     500                      4
S    -500                      2
!=================================================================
*PARAMETERS
OS       0    1    1
!=================================================================
*STAT
N     test      -1.0
L 0.002381
D   2        4          .1         7
!=================================================================
*STOP
```

B.8 Tee Scissors Model

```
!UNITS L in F k   [Created by Panels]
*STARTXX
  STee            0 1 0 0            SCISSORS MODEL
!====================================================================
*NODECOORDS
C       1   -168.000  0.000
C       2   0.000     -75.000
C       3   168.000   0.000
C       4   0.000     75.000
C       5   -10.370   0.000
C       6   0.000     -11.665
C       7   10.370    0.000
C       8   0.000     11.665
C       9   0.000     0.000
C       10  0.000     0.000
C       11  -78.815   0.000
C       12  78.815    0.000
C       13  0.000     -31.668
C       14  0.000     31.668
C       15  -15.370   0.000
C       16  15.370    0.000
C       17  -15.370   0.000
C       18  15.370    0.000
C       19  0.000     -11.665
C       20  0.000     11.665
C       21  0.000     -11.665
C       22  0.000     11.665
!====================================================================
*RESTRAINTS
S 110         1
S 010         3
S 211         4
S 111        14
S 111        20
S 111        22
S 111        19
S 111        21
!====================================================================
*SLAVING
S 110         9        10
S 110        15        17
S 110        16        18
!====================================================================
*ELEMENTGROUP
   2    0    0                    Columns of the model
   1    0    1
   1  29000       0.030  35.9       2960      4.0  4.0  2.0    12.4    0.3
   1    1   1000000   1000000
   1        2        13             1         1    1
   2       13         6             1         1    1
```

```
!=============================================================
*ELEMENTGROUP
   2    0    0                    Girder of the model
   1    0    1
   1  29000       0.030  24.7       2370      4.0  4.0  2.0    11.0    0.3
   1    1   1000000   1000000
   1         1        11             1        1    1
   2        11        15             1        1    1
   3        17         5             1        1    1
   4         3        12             1        1    1
   5        12        16             1        1    1
   6        18         7             1        1    1
!=============================================================
*ELEMENTGROUP
   2    0    0                    Rigid Links of the model
   2    0    1
   1  29000       0.030 1000000    1000000    4.0  4.0  2.0
   2  29000       0.030 1000000    1000000    4.0  4.0  2.0
   1    1   1000000   1000000
   1         8        10             1        1    1
   2        10         6             1        1    1
   3         5         9            2        1    1
   4         9         7            2        1    1
!=============================================================
*ELEMENTGROUP
   4    0    0                    Hinges in the Panel
   2
   1  5285230      0.000  11127    11127     1.000E+00    3    0
   2  156032       0.030  1314     1314      1.000E+00    3    0
   1         9        10             1
   2         9        10             2
!=============================================================='
*ELEMENTGROUP
   4    0    0                    Plastic hinges in the girders
   2
   1  1.E+14       1E-14  1.102E+4 1.102E+4  1.000E+00    3    0
   2  3.26E+5      0.030  1.196E+3 1.196E+3  1.000E+00    3    0
   1        15        17             1
   2        15        17             2
   3        16        18             1
   4        16        18             2
!=============================================================
*RESULTS
NSD    011
NSV    011
NSA    011
E      011
!=============================================================================
*NODALOAD
 test
S     500                        4
S    -500                        2
!=============================================================================
```

```
*PARAMETERS
OS       0    1    1
!=============================================================================
*STAT
N     test      -1.0
L 0.002381
D   2        4          .1         7
!=============================================================================
*STOP
```

Works Cited

American Institute of Steel Construction, Inc. Manual of Steel Construction Load and Resistance Factor Design Third Edition 2001.

American Institute of Steel Construction, Inc. Seismic Provisions for Structural Steel Buildings Third Edition 1997.

Becker, R. "Panel Zone Effect on the Strength and Stiffness of Steel Rigid Frames." Engineering Journal, AISC v12 n1 1975: 19-29.

Betero V. V., E. P. Popov, and H. Krawinkler. "Beam Column Sub-Assemblages Under Repeated Loading." Journal of the Structural Division, ASCE v98 nst5 May 1972: 1137-1159.

Challa, V., R. Murty, and J. F. Hall. "Earthquake Collapse Analysis of Steel Frames." Earthquake Engineering and Structural Dynamics v23 n11 November 1994: 1199-1218.

Charney, F. A. "BSSC Guide to Application of the 2000 NEHRP Recommended Provisions" Unpublished paper available from author, 2001: 22-28.

Charney, F. A. RAM XLinea Version 4.0 June 2000.

Charney, F. A. "Sources of Elastic Deformation in Laterally Loaded Steel Frame and Tube Structures." *Proceedings of the Fourth World Congress, Tall Buildings: 2000 and Beyond* Council on Tall Buildings and Urban Habitat 1990: 893-915.

Charney, F. A., and R. Johnson. "The Effect of Panel Zone Deformation on the Drift of Steel Framed Structures." Presented at the ASCE Structures Congress, New Orleans, September 1986.

Chi, B. and C. Uang. "Cyclic Response and Design Recommendations of RBS Moment Connections with Deep Columns" Journal of Structural Engineering, ASCE v128 n4 April 2002: 464-473.

El-Tawil, S. et al. “Inelastic Behavior and Design of Steel Panel Zones.” Journal of Structural Engineering, ASCE v125 n2 February 1999: 183-193.

Federal Emergency Management Agency (FEMA). Interim Guidelines: Evaluation, Repair, Modification and Design of Welded Steel Moment Frame Structures. FEMA-267 Report No. SAC-95-02, SAC Joint Venture, Sacramento, CA: 1995.

Federal Emergency Management Agency (FEMA). Interim Guidelines: Advisory No. 1. Supplement to FEMA-267 Report No. SAC-96-03, SAC Joint Venture, Sacramento, CA: 1996.

Federal Emergency Management Agency (FEMA). Recommended Seismic Design Criteria for New Steel Moment Frame Buildings FEMA-350 Federal Emergency Management Agency Washington D.C. 2000.

Federal Emergency Management Agency (FEMA). Recommended Seismic Evaluation and Upgrade Criteria for Existing Welded Steel Moment Frame Buildings FEMA-351 Federal Emergency Management Agency Washington D.C. 2000.

Federal Emergency Management Agency (FEMA). Recommended Post-Earthquake Evaluation and Repair Criteria for Welded, Steel Moment Frame Buildings FEMA-352 Federal Emergency Management Agency Washington D.C. 2000.

Federal Emergency Management Agency (FEMA). Recommended Specification and Quality Assurance Guidelines for Steel Moment Frame Construction for Seismic Applications FEMA-353 Federal Emergency Management Agency Washington D.C. 2000.

Federal Emergency Management Agency (FEMA). State of the Art Report on Base Metals and Fracture FEMA-355A Federal Emergency Management Agency Washington D.C. 2000.

Federal Emergency Management Agency (FEMA). State of the Art Report on Welding and Inspection FEMA-355B Federal Emergency Management Agency Washington D.C. 2000.

Federal Emergency Management Agency (FEMA). State of the Art Report on Seismic Performance FEMA-355C Federal Emergency Management Agency Washington D.C. 2000.

Federal Emergency Management Agency (FEMA). State of the Art Report on Connection Performance FEMA-355D Federal Emergency Management Agency Washington D.C. 2000.

Federal Emergency Management Agency (FEMA). State of the Art Report on Past Performance of Steel Moment-Frame Building in Earthquake FEMA-355E Federal Emergency Management Agency Washington D.C. 2000.

Federal Emergency Management Agency (FEMA). State of the Art Report on Performance Prediction and Evaluation FEMA-355F Federal Emergency Management Agency Washington D.C. 2000.

Fielding, D. J. and J. S. Huang. "Shear in Steel Beam Column Connections." Welding Journal v50 n7 July 1971: 313s-326s.

Foutch, D. A., and S. Yun. "Modeling of Steel Moment Resisting Frames for Seismic Loads" Journal of Constructional Steel Research v58 2002: 529-564.

Hibbitt, Karlsson and Sorensen. ABAQUS Version 6.2 2001.

International Code Council, Inc. 2000 International Building Code 2000.

Gilton, C. S. and C. Uang. "Cyclic Response and Design Recommendations of Weak-Axis RBS Moment Connections" Journal of Structural Engineering, ASCE v128 n4 April 2002: 452-463.

Horvilleur, J. F. and F. A. Charney. "The Effect of Beam-Column Joint Deformation on the Lateral Response of Steel Frame Building Structures." III Simposio Internacional Y VI Simposio Natcional de Estructuras de Acero Oaxaca Mexico November 1993: 269-303.

Jones, S. L., G. T. Fry, and M. D. Engelhardt. "Experimental Evaluation of Cyclically Loaded Reduced Beam Section Moment Connections" Journal of Structural Engineering, ASCE v128 n4 April 2002: 441-451.

Kim, K., and M. D. Engelhardt. "Development of Analytical Models for Earthquake Analysis of Steel Moment Frames." PMFSEL 95-2 Phil M. Ferguson Structural Engineering Lab University of Texas at Austin April 1995: 216 pages.

Kim, K., and M. D. Engelhardt. "Monotonic and Cyclic Loading Models for Panel Zones in Steel Moment Frames" Journal of Constructional Steel Research v58 2002: 605-635.

Kim, T. et al. "Cover-Plate and Flange-Plate Steel Moment Resisting Connections" Journal of Structural Engineering, ASCE v128 n4 April 2002: 474-482.

Kim, T. et al. "Experimental Evaluation of Plate-Reinforced Steel Moment Resisting Connections" Journal of Structural Engineering, ASCE v128 n4 April 2002: 483-491.

Krawinkler, H., V. V. Betero, and E. P. Popov. "Shear Behavior of Steel Frame Joints." Journal of the Structural Division, ASCE v101 n11 November 1975: 2317-2336.

Krawinkler, H. "Shear in Beam-Column Joints in Seismic Design of Frames." Engineering Journal, AISC v15 n3 1978: 82-91.

Krawinkler, H., and S. Mohasseb. "Effects on Panel Zone Deformations on Seismic Response." Journal of Constructional Steel Research v8 1987: 233-250.

Kunnath, S. K. and J. O. Malley. "Advances in Seismic Design and Evaluation of Steel Moment Frames: Recent Findings from FEMA/SAC Phase II Project" Journal of Structural Engineering, ASCE v128 n4 April 2002: 415-419.

Leger, P., P. Paultre, and R. Nuggihalli. "Elastic Analysis of Frames Considering Panel Zone Deformations." Computers and Structures v39 n6 1991: 689-697.

Liew, J. Y. R., and W. F. Chen. "Analysis and Design Considering Panel Joint Deformations." Journal of Structural Engineering, AISC v121 n10 October 1995: 1531-1540.

Lui, E. M., and W. Chen. "Analysis and Behavior of Flexibly Jointed Frames." Engineering Structures v8 n2 April 1986: 107-118

Mao, C. et al. "Effect of Local Details on Ductility of welded Moment Connections" Journal of Structural Engineering, AISC v127 n9 2001: 1036-1044.

Popov, E. P., N. R. Amin, J. C. Louie and R. M. Stephen. "Cyclic Behavior of Large Beam-Column Assemblies." Engineering Journal, AISC v23 n1 1986: 9-23.

Popov, E. P. "Panel Zone Flexibility in Seismic Moment Joints." Journal of Constructional Steel Research v8 1987: 91-118.

Popov, E. P. "Seismic Moment Connections for MRFs." Journal of Constructional Steel Research v10 1988: 163-198.

Popov, E. P., and Keh-Chyuan Tsai. "Performance of Large Seismic Steel Moment Connections Under Cyclic Loads." Engineering Journal, AISC v26 n2 1989: 51-60.

Popov, E. P. et al. "Full-scale beam-column connection tests" Experimental Investigations of Beam-Column Subassemblages Technical Report SAC 96-01, Part 2 Applied Technology Council, Redwood City, CA 1996.

Prakash, V., G.H. Powell and S. Campbell. Drain-2DX Version 1.10 1993.

Ricles, J. M. "Inelastic Cyclic Testing of Welded Unreinforced Moment Connections" Journal of Structural Engineering, ASCE v128 n4 April 2002: 429-440.

Ricles, J. M. et al. "Development and Evaluation of Improved Ductile Welded Moment Connections" Report No. SAC/BD-00/24, SAC Joint Venture, Sacramento, CA 2000.

Roeder, C. W., and D. A. Foutch. “Experimental Results for Seismic Resistant Moment Frame Connections.” Journal of Structural Engineering, ASCE v122 n6 June 1996: 581-588.

Schneider, S. P., C. W. Roeder, and J. E. Carpenter. “Seismic Behavior of Moment Resisting Frames: Experimental Study.” Journal of Structural Engineering, ASCE v119 n6 June 1993: 1885-1902.

Schneider, S. P., and A. Amidi. “Seismic Behavior of Steel Frames with Deformable Panel Zones.” Journal of Structural Engineering, ASCE v124 n1 January 1998: 35-42.

Schneider, S. P. and Itthinun Teeraparbwong. “Inelastic Behavior of Bolted Flange Plate Connections” Journal of Structural Engineering, ASCE v128 n4 April 2002: 492-500.

Sumner, E. A. and T. M. Murray. “Behavior of Extended End-Plate Moment Connections Subject to Cyclic Loading” Journal of Structural Engineering, ASCE v128 n4 April 2002: 501-508.

Wang, S. J. “Seismic Response of Steel Building Frames with Inelastic Joint Deformation” Ph.D. Dissertation, Department of Civil Engineering, Lehigh University, Bethlehem PA, 1988

Whittaker, A., A. Gilani, and V. V. Betero. “Evaluation of Pre-Northridge Steel Moment Resisting Frames.” Structural Design of Tall Buildings v125 n2 February 1998: 263-283.

VITA

William Martin (Marty) Downs was born on October 17, 1970 in Spencer WV, the son of Bill and Mary Downs. He spent the first sixteen years of his life in Mineral Wells, WV, after which his family move to Huntington, WV. He graduated from Huntington East High School in 1988.

After a brief, very unsuccessful first attempt at college, Marty joined the U.S. Army where he served as a Satellite Communications System Repairer for six years. During this time, he was stationed in Augusta, GA; Augsburg, GE and Paso Robles, CA. Upon completion of his military service, he enrolled in Cuesta College, in San Luis Obispo, CA, to complete the first two years of his engineering education. Once completed, Marty was accepted at California Polytechnic State University of San Luis Obispo where he fulfilled his requirements for a Bachelor of Science degree in civil engineering in December 2000. The weekend following his graduation, he married his soul-mate Pamela Fuller Downs. They then moved to Virginia where Marty began his graduate studies in structural engineering at Virginia Tech in January 2001.

In January 2003, Marty will begin employment for Simpson Manufacturing where he will serve in the capacity of research engineer at Simpson Strong-Tie's new earthquake-engineering laboratory in Stockton, CA. For a copy of PANELS.exe, Marty can be reached at marty_downs@yahoo.com.